Synthesis of Metal-Modified B_{12} Derivatives by $CoCp_2$-Mediated Reconstitution of Secocorrins

---

Dissertation

zur

Erlangung der naturwissenschaftlichen Doktorwürde
(Dr. sc. nat.)

vorgelegt der

Mathematisch-naturwissenschaftlichen Fakultät

der

Universität Zürich

von

Lucas Prieto González-Posada

aus

Spanien

Promotionskommission

Prof. Dr. Roger Alberto (Vorsitz)
PD Dr. Felix Zelder (Leitung)
Prof. Dr. David Tilley
Prof. Dr. Fabio Zobi

Zürich, 2017

“No hay cuestiones agotadas sino hombres agotados en las cuestiones.” (There are no used up questions but men exhausted with them.)

Santiago Ramón y Cajal

Table of content

Abstract

The unique structure, outstanding reactivity and essential biochemical functions of vitamin B_{12} have spanned a century of groundbreaking chemical, biological and medical research. The central cobalt ion of B_{12} is the most reactive site of the nutrient. Thus, the aim of this thesis is the replacement of cobalt by other metals, leading to a new class of B_{12}-related derivatives: metbalamins. These metal-modified B_{12} derivatives keep the cobalamin framework intact but are expected to have altered physicochemical and catalytic properties. Therefore metbalamins are promising antivitamin B_{12} candidates for the development of antiproliferative or antimicrobial agents.

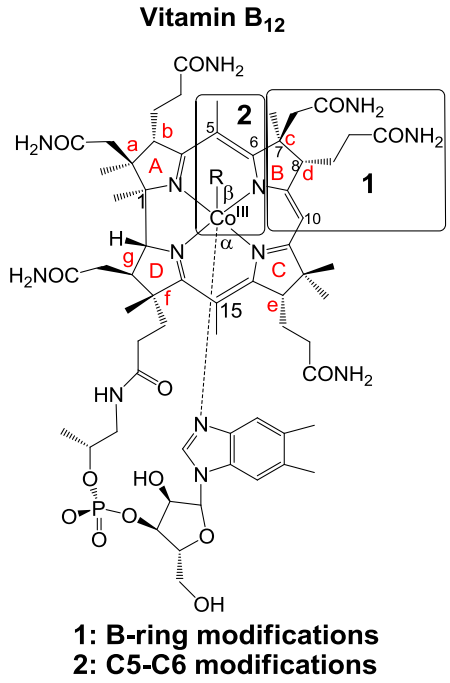

Although metbalamins can be obtained by complex biosynthetic procedures, their total and partial synthesis has not been reported yet. Indeed, all attemps to demetallate the intact corrin macrocycle led to destruction of the B_{12} scaffold. Hence, efforts during this work focused on the demetallation and corrin reconstitution of ring-opened secocorrinoids, leading to novel metbalamin derivatives.

Demetallation and corrin reconstitution experiments were applied on two classes of compounds: 5,6- and 7,8-*seco*-corrinoids. First, the opened B-ring of 7,8-*seco*-corrinoids was reconstituted in a rapid, stereospecific and quantitative reaction. This reaction was triggered by cobaltocene ($CoCp_2$), introduced as a new one-electron reducing agent for the formation of C-C bonds (C7-C8). Due to the presence of a redox sensitive Co^{III} ion, cyanide was used as a metal-ion protecting group to achieve ligand-centered chemoselectivity. Subsequently, B_{12} was reconstituted in three steps, completing the first reversible route for the synthesis of ring-opened "complete" secocorrins. The structure of the reconstituted vitamin was determined by X-ray crystallography and the biological function of reconstituted B_{12} and other route intermediates was evaluated with microbiologically using *L. Leichmannii*. Importantly one of the new B_{12} derivatives showed promising antivitamin B_{12} activity.

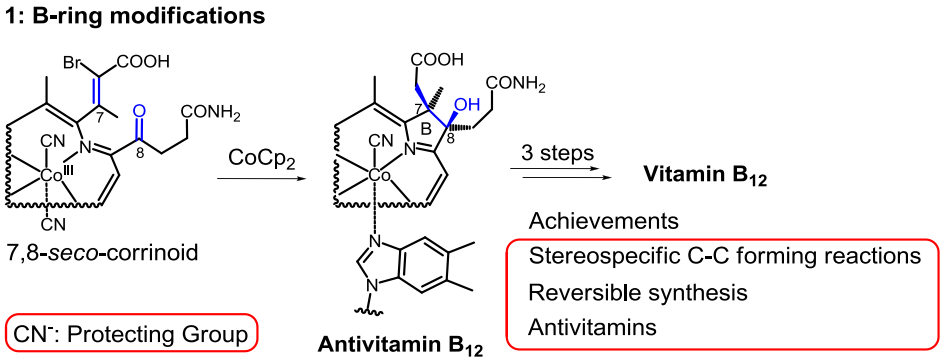

The second route focused on the demetallation and ring reconstitution of 5,6-*seco*-corrinoids. Herein, a straightforward method to simultaneously reconnect the opened macrocycle and remove the cobalt from the corrin cavity is presented. In this reaction and in contrast to the former strategy, $CoCp_2$ was used as both metal and ligand reducing agent. Thus, Co^{III} was reduced to Co^{II} and a C-C bond between a ketone (C5) and a lactam (C6) was formed. Subsequently, cyanide was employed as decomplexating agent for the extraction of the labile Co^{II} ion from the corrin cavity, obtaining a metal-free ring-closed B_{12} derivative. Metal ions like Ni^{II} were inserted in the corrin macrocycle, accessing a new family of B_{12} derivatives: 5,6-diolmetbalamins. These unprecedented metal-modified B_{12} derivatives were fully characterized by UV-Vis, HR-MS and extensive 1D and 2D NMR studies.

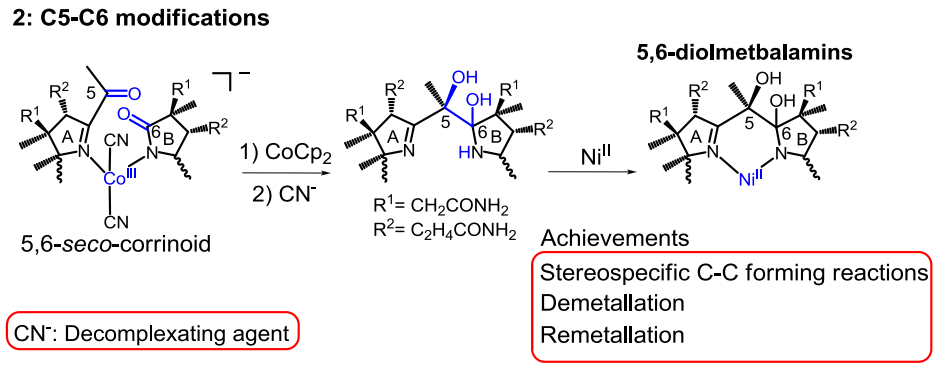

In summary, this thesis presents a chemical route for the synthesis of metal-modified B_{12} derivatives from secocorrins. The demetallation of 5,6-*seco*-corrinoids was achieved by reducing the inert Co^{III} to a more labile Co^{II} center with $CoCp_2$ and using cyanide as decomplexating agent Importantly, $CoCp_2$ was employed as a new versatile one-electron reducing agent for the formation of C-C bonds in the reconstitution of ring-opened 5,6- and 7,8-*seco*-corrinoids.

Zusammenfassung

Die einzigartige Struktur, Reaktivität und biochemische Funktion von Vitamin B_{12} inspiriert Naturwissenschaftler seit über einem Jahrhundert zu bahnbrechender chemischer, biologischer und medizinischer Forschung. Die Reaktivität von B_{12} hängt entscheidend vom zentral komplexierten Kobaltion ab. Daraus ergibt sich die Zielsetzung dieser Doktorarbeit: der Austausch besagten Kobalts durch ein anderes Metall, was zu einer neuen Klasse von B_{12}-Derivaten führt: Metbalaminen. Von diesen wird erwartet, dass sie trotz intaktem molekularen Gerüst veränderte physicochemische und katalytische Eigenschaften besitzen. Aus diesem Grund sind Metbalamine vielversprechende Kandidaten sogenannter Antivitamin B_{12} Verbindungen für die Entwicklung antiproliferativer oder antimikrobialer Reagenzien.

Vitamin B_{12}

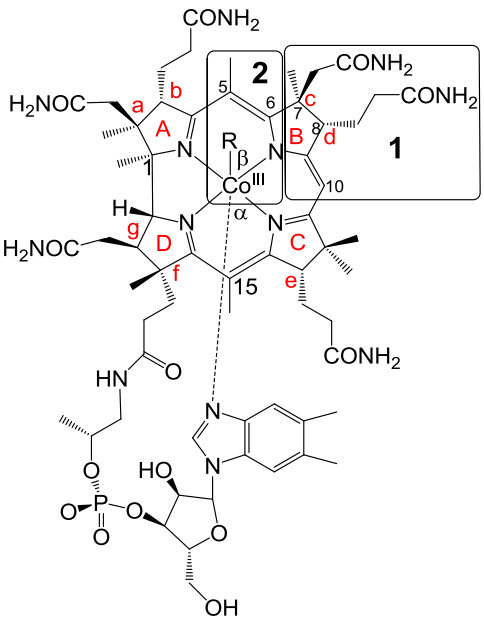

1: B-Ring Modifikationen
2: C5-C6 Modifikationen

Metbalamine können auf äusserst komplexem biosynthetischem Wege hergestellt werden. Ihre chemische Synthese jedoch stellt ein über Jahrzehnte verfolgtes, aber bislang unerreichtes Ziel dar. Sämtliche Versuche, den intakten Corrinring zu demetallieren, führten bislang zur Degradierung der molekularen Struktur. Folglich fokussiert sich die vorliegende Arbeit auf die Demetallierung und Rekonstituierung von Corrin-geöffneten Secocorrinoiden, mit dem Ziel der Herstellung neuartiger Metbalaminderivative.

Demetallierungs- und Rekonstituierungsexperimente wurden auf zwei Klassen von B_{12}-Ausgangsverbindungen angewandt: 5,6- und 7,8-*seco*-Corrinoiden. Zunächst wurde das B-Ring-geöffnete 7,8-*seco*-Corrinoid mittels einer schnellen, stereospezifischen und quantitativen Reaktion rekonstituiert. Diese Reaktion wurde durch Cobaltocen ($CoCp_2$) initiiert, welches als ein-Elektron-Reduktionsmittel zur C7-C8-Bindungsbildung agierte. Um die ligand-zentrierte Chemoselektivität in Gegenwart des redox-sensitiven Co^{III}-Ions zu gewährleisten, wurde Cyanid als Schutzgruppe eingesetzt. Anschliessend

wurde B_{12} in drei Stufen rekonstituiert, was die erste reversible Methode zur Synthese von Ring-geöffneten «vollständigen» Secocorrinoiden darstellt. Die Struktur des rekonstituierten B_{12} wurde durch Röntgenstrukturanalyse nachgewiesen. Die biologische Funktion sowohl des rekonstituierten B_{12} wie auch dessen Zwischenprodukte wurde in mikrobiologischen Tests mit *L. Leichmannii* getestet. Hierbei offenbarte ein neues B_{12} Derivat vielvesprechende Antivitamin-Aktivität.

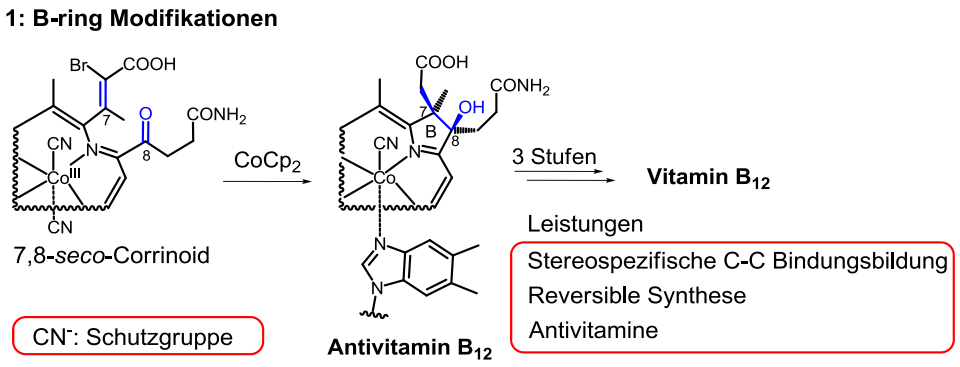

Die zweite Syntheseroute konzentrierte sich auf die Demetallierung und Rekonstitution von 5,6-*seco*-Corrinoiden. Von besonderem Interesse ist hierbei die entwickelte Methode, sowohl den bislang unerreichten Ringschluss des geöffneten Makrozyklus, als auch die Entfernung des Kobaltions simultan durchzuführen. Im Gegensatz zur früheren Strategie, wurde Cobaltocen als Metall- und Ligandenreduktionsmittel eingesetzt, was sowohl zur Reduktion von Co^{III} zu Co^{II}, als auch zur C-C-Bindungsbildung zwischen dem Keton-C5 und dem Lactam-C6 führte. Anschliessende Dekomplexierung des nun labilen Co^{II} und Remetallierung durch Metallionen wie Ni^{II} führte zu einer präzedenzlosen Klasse von B_{12}-Derivaten: 5,6-Diolmetbalaminen. Letztere wurden mittels UV-Vis, HR-MS, sowie ausführlichen 1D- und 2D NMR Untersuchungen umfänglich charakterisiert.

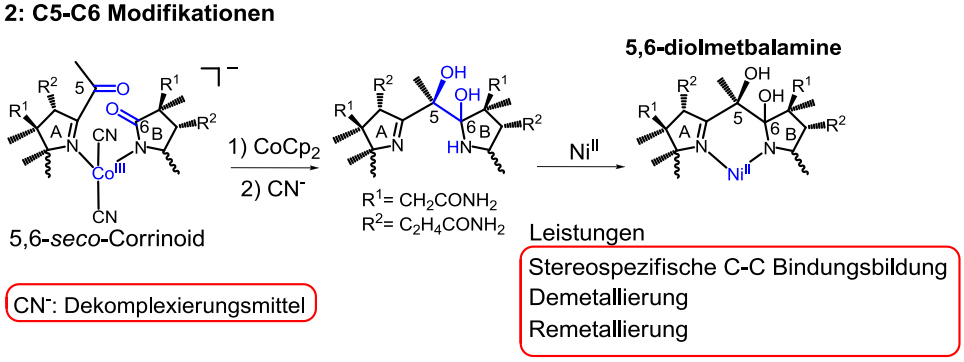

Die vorliegende Arbeit präsentiert eine chemische Methode zur Synthese einer neuen Klasse von Metall-modifizierten B_{12}-Derivaten aus Secocorrinoiden. Die Demetallierung von 5,6-*seco*-Corrinoiden wurde durch die Reduktion von inertem Co^{III} zu labilerem Co^{II} mittels Cobaltocen und anschliessender Dekomplexierung durch Cyanid erreicht. Die vielfältige Anwendbarkeit von Cobaltocen als Reduktionsmittel wurde des weiteren in der C-C-Bindungsbildung in der Rekonstitution sowohl von 5,6- als auch 7,8-*seco*-Corrinoiden nachgewiesen.

Acknowledgement

I would like to start by thanking PD Dr. Felix Zelder for more than four years of ideas, experiments, discussions, failures and success together. Thank you for being always reachable and for believing in my potential to take over such an ambitious project. Thank you for the motivation during the unavoidable periods of failure and for the recognition whenever I would approach you with a new color in my flask.

I want to thank Prof. Dr. Roger Alberto for his enthusiasm in this project and his useful feedback in each meeting.

I am thankful to Prof. Dr. David Tilley and Prof. Dr. Fabio Zobi for agreeing to be in my committee.

A big thank you goes to the multiple members of the Zelder group during the last years for making the lab a pleasant place to stay. In this lab, I found a long-lasting PhD colleague and an amazing friend in Dr. Marjorie Sonnay (the future is ours!) and I inherited extraordinary results from Dr. René Oetterli (who I wish to thank for his supervision and patience in my early days). When I arrived I teamed up with the "panda-approved" Master students Philipp Pfingstag and Balz Aebli. Later I "grew up" to supervise and share great moments with my own Master students Dominik Bernasconi and Klara Schuette. I shall not forget to thank our guests Lara Pestrin and Gesara Bimashofer for their help reproducing some of my synthesis. Last but not least, I want to wish the best luck to the new generation of bright PhD students in the group: Prerna Yadav and Christopher Brenig.

A well-deserved thank you to the UPLC-MS crew for all the efforts and the patience in those days we spent figuring out very imaginative solutions to maintenance issues. In this regard, I would like to express my deepest gratitude to Dr. Marjorie Sonnay and Dr. Sebastian Imstepf for spending those weeks of August setting up the UPLC columns and methods. After that it was time for Giuseppe Meola and me to keep things running and I am very grateful to Giusi for his flexibility and effective work. And if something was beyond our reach, we were lucky to have the immense know-how of Dr. Ferdinand Wild and Hanspeter Stalder.

I am thankful to Prof. Dr. Bernhard Spingler for measuring my challenging crystals, the Bigler group for HR-MS measurements and Dr. Thomas Fox for recording the most meaningful NMR spectra.

I want to thank Prof. Dr. Helmut Brandl for training me to perform microbiological assays. He was an extremely engaged scientist and he would never hesitate to give you a hand whenever needed. I am sure the group will miss your good mood whenever they will need to pipette some compounds on certain bacteria.

I have had the opportunity to attend very interesting conferences during these years and I need to thank SCNAT/SCS, SBIC and the CMSZH Graduate School for funding those adventures. Additionally, I must thank the CMSZH for the useful soft-skills courses and the unforgettable Retreats. I learned a lot from organizing the CMSZH Retreat 2016 and I want to thank all the members of that year's orga team (Matteo Croce, Elena Alberti, Angelo Frei, Marco Etter, Marianthi Zampakou).

I want to acknowledge the dozens of students I supervised during these years. From general chemistry to inorganic synthesis and from practical courses to exercises. Seeing your fast progress was a source of motivation and pride.

I need to thank express my gratitude to the friends I found along these years, who have turned Zurich into home. Thank you Angelo Frei for playing friendship on a Kobe Beef level, thank you Cristina Mari for being the irreplaceable and exclusive saffron that brings the risotto to completion, thank you Manon Briand for a slow-cooked friendship with a classy French touch. So many memories in "fikas", dobars, barbecues, dinners… with the ones like Giusi, Äxl (hermano!), Tony (gallu!), Robin, Giuliana, Riccardo (Skorpor!), Severin (Schönä!), Tobi, Michi, Immi, Anna, Anu, Mai, Karla, Bachmann and Evelyne (Brest team!), Seraina, Faustine, Nuria and of course the Italian crew.

Thank you to my parents for their full unconditional support, even if that support means distance. Servus and thanks to my Erasmus friends (Carmen, Nuria, Marta, Andrés, Marianne, Federicca) for keeping the Vienna spirit alive over the years and for the meetings in different parts of the world. Thank you to my friends in Spain for keeping

me anchored to my roots and for asking me “when are you finally coming here?” every second week. In this group I have to mention Cristina Prieto as the friend that shares a parallel “trospid” universe with me, Silvia Vázquez as the charismatic listener and producer of the best voice messages and Tania Morán as the spontaneous friend that could arrange any plan in 20 seconds without stress.

Abbreviation list

AcOH	acetic acid
Ado	5‘-deoxyadenosyl
ATP	adenosine triphosphate
Cbi	cobinamide
Cbl	cobalamin
COSY	correlation spectroscopy
d	doublet
ddH_2O	double distilled water
Dmbz	dimethylbenzimidazol
DNA	desoxyribonucleic acid
DMF	dimethylformamide
dTMP	deoxythymidine monophosphate
EDC·HCl	*N*-(3-dimethylaminopropyl)-*N’*-ethylcarbodiimide hydrochloride
equiv	equivalent
ESI-MS	electron spray ionization mass spectrometry
HR-ESI-MS	high resolution electron spray ionization mass spectrometry
FH_4	tetrahydrofolate
HCl	hydrochloric acid
HC	haptocorrin
HMBC	heteronuclear multiple-bond correlation spectroscopy
HPLC	high performance liquid chromatography
HSQC	heteronuclear single-quantum correlation spectroscopy
IF	intrinsic factor
IR	infrared spectroscopy
H_2SO_4	sulfuric acid
m	multiplet
MCM	methyl malonyl coenzyme A mutase
MB	methylene blue
MeOH	methanol
MetH	methionine synthase
MS	mass spectrometry

NMR	nuclear magnetic resonance
Py	Pyridine
RNR	ribonucleotide reductase
ROESY	rotating frame overhauser effect spectroscopy
s	singlet
SAM	*S*-adenosylmethionine
t	triplet
t_R	retention time
TC	transcobalamin
TFA	trifluoroacetic acid
THF	tetrahydrofuran
TEMPO	2,2,6,6-tetramethylpiperidinoyloxyl
TLC	thin layer chromatography
TRIS	tris(hydroxymethyl)aminomethane
UPLC	ultra performance liquid chromatography
UV-Vis	ultraviolet-visible spectroscopy
W	watt

1. Introduction

1.1. A century of vitamin B_{12}: a revolutionary molecule

In a world adapting to a new post Great War era, the Professor of Sanitary Engineering George C. Whipple was not aware that the experiments he was carrying out were laying the foundation for the discovery of one of the most complex and intriguing molecules in Nature.[1-3] His pioneering studies on the therapeutic effects of a liver diet on anemic dogs marked the start of a century of intensive research around the active component present in liver that could heal anemia. Indeed, during the Roaring Twenties pernicious anemia was still a fatal disease and the urge to find an effective treatment against it led George R. Minot and William P. Murphy to apply Whipple's advances on human patients. They demonstrated that the daily ingestion of large amounts of cooked calf or beef liver (between 120 and 240 g) guaranteed a prompt and long-lasting remission of their patients' anemia.[4,5] Thanks to "their discoveries concerning liver therapy in cases of anemia"; Whipple, Minot and Murphy were awarded the Nobel Prize in Physiology and Medicine in 1934.

Despite the successful clinical use of liver for treating pernicious anemia, the active substance responsible for the therapeutic effect remained a mystery for decades after Whipple's first efforts. It was not until 1948 that Folkers at Merck and Smith at Glaxo simultaneously isolated red crystalline needles of the anti-pernicious anemia factor, which they called vitamin B_{12}.[6-10] Attracted by the extraordinary properties of this substance, numerous chemists and crystallographers started working on the structural elucidation of vitamin B_{12}. Soon the community realized about the structural complexity of this molecule and only after years of work, Dorothy C. Hodgkin solved the structure of vitamin B_{12} in 1956.[11] Her "determinations by X-ray techniques of the structures of important biochemical substances" were worth the Noble Prize in Chemistry in 1964.

The unprecedented structure of vitamin B_{12} earned the attention of brilliant chemists. Establishing a bold collaboration during the 1960s, Albert Eschenmoser and Robert B. Woodward accomplished the total synthesis of vitamin B_{12} in almost 11 years of work and employing more than 100 coworkers on the project.[12-14] The ambitious enterprise remains as one of the classics of total synthesis and in 1965; Woodward was also awarded the Nobel Prize in Chemistry "for his outstanding achievements in the art of organic synthesis".

Being a millestone in organic chemistry, the total synthesis of vitamin B_{12} involves more than 70 synthetic steps and is therefore not a realistic method for the high scale production of the nutrient. In this regard, microbiologists played a crucial role establishing methods for the industrial production of vitamin B_{12} from bacterial fermentation.[15,16] Early microbiological studies discovered that vitamin B_{12} belongs to a family of structurally related naturally-occuring compounds called corrinoids.[17] Importantly, in 1958 Barker and coworkers isolated a corrinoid containing an organometallic Co-C bond with coenzyme activity in the bacterium *Clostridium tetanomorphum*.[18]

Having found the first organometallic coenzyme, enzymologists joined the vitamin B_{12} fever. Soon it was realized that the biological role of vitamin B_{12} as an enzymatic cofactor was widespread and present in almost all forms of life.[19-21] Additionally, the reactivity of coenzyme B_{12} is dominated by its structure as a coordination compound and involves elegant ligand exchange reactions with varying mechanisms in the different enzymes where vitamin B_{12} is involved.[22] In this context, vitamin B_{12} became a pivotal point for the development of bioinorganic chemistry since the second half of the 20th century.[23,24]

Almost 100 years after Whipple's experiments, the chemistry and biochemistry of vitamin B_{12} are well explored.[22-26] However, recent fundamental discoveries on the enzymatic activity of B_{12} together with the potential medicinal, sensing and catalytic B_{12}-based applications keep the thrill around this natural product.[27-32] Its beautiful complexity and unique properties guarantee that vitamin B_{12} will hold a special place in scientific research also in the 21st century.

1.2. Structure and electronic properties

B_{12} turned to be a substance of frightening complexity (Lord Todd).

Vitamin B_{12}, B_{12} or Cbl (Figure 1) possesses one of the most sophisticated structures of all monomeric natural products.[11] The core of this octahedral complex is occupied by a Co^{III} ion, coordinated by four nitrogen atoms in all the equatorial positions that belong to a tetrapyrrolic macrocycle called corrin. This unique macrocycle belongs to the family of porphyrinoids and has two important particularites: a) the pyrrol subunits A and D are directly connected over a C-C bond and b) corrinoids have a chromophore with 14 delocalized π-electrons over 13 carbon atoms.[33] The corrin macrocycle is completed with eight peripheral methyl groups (two at the *meso* positions C5 and C15 and six connected to the pyrrol rings) and seven amide side chains. One of this amide side chains contains a propan-2-ol, a phosphate, a ribose and a dimethylbenzimidazole base (Dmbz). These three subunits form the so-called "loop", a molecular switch that can reversibly coordinate the Co^{III} ion through its lower α axial position.[34] Thus, two possible configurations (base-on/base-off) are established, a fundamental equilibrium for the transport, cellular uptake and reactivity of the vitamin within enzymes.[35] On the upper β axial position, several ligands can coordinate the metal center depending on the biological role of vitamin B_{12}.[23]

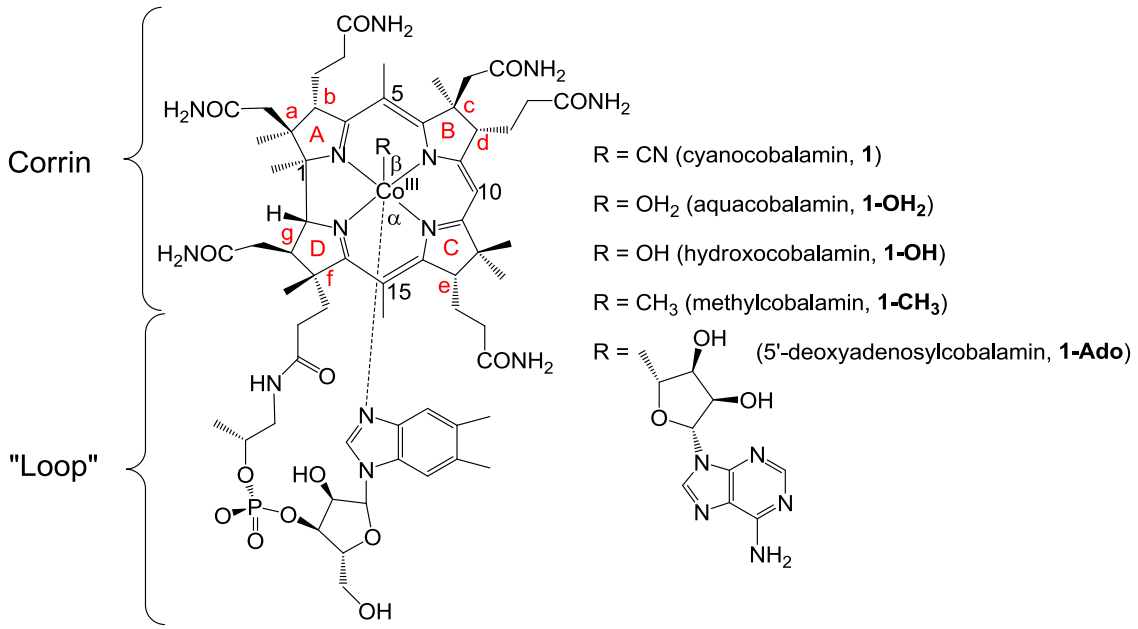

Figure 1. Structure of vitamin B_{12}.

Natural porphyrinoids have been named "pigments of life" due to their intense coloration.[36] Vitamin B_{12} is indeed an intensely red crystalline compound mostly due to the presence of 14 π-delocalized electrons in the corrin macrocycle. In fact, the π-π* corrin electronic transitions dominate the absorption spectra of Cbls. In general, three main distinctive bands are found: the α and β bands (between 600 and 450 nm) and the γ band (350-370 nm) (Figure 2).[22] Additionally, the aromatic system of the Dmbz ligand gives raise to absorption bands between 275-290 nm. The energy and intensity of all π-π* bands (α, β, γ, Dmbz) are influenced by the Co^{III} center and the presence of different α (base-on/base-off configuration) and β axial ligands (e.g. **1**, **1-OH$_2$**, **1-CH$_3$**, **1-Ado**).[37] Therefore, UV-Vis spectroscopy is a valuable source of information regarding structural features of vitamin B_{12} derivatives such as the π–system and the axially coordinating ligands.

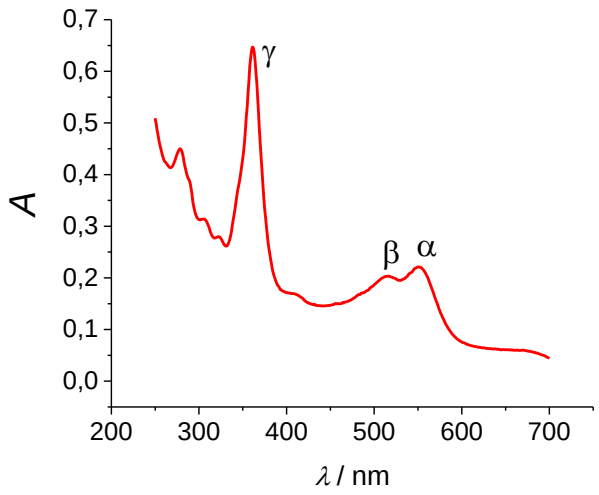

Figure 2. UV-Vis spectrum of cyanocobalamin (**1**).

B_{12} is the only vitamin containing a metal center and its presence is not arbitrary. Indeed the redox reactivity of this coordination compound within biological systems is normally metal-centered.[22] Cobalt can undergo oxidation and reduction reactions that influence the geometry of the whole complex (Scheme 1).[23,38] Thus, when the octahedral d^6 Co^{III} from B_{12} is reduced; d^7 Co^{II} square-pyramidal or d^8 Co^{I} square-planar complexes are formed.

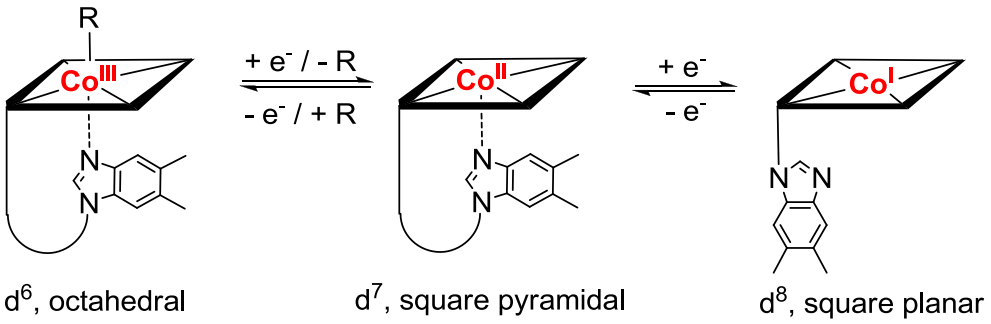

Scheme 1. Redox chemistry, electronic configurations and coordination geometries of Cbls. Charges are omitted for clarity.

1.3. Transport

The presence of B_{12} cofactors is essential for the metabolism of microorganisms and animals.[22] However, Cbls can only be synthesized by certain bacteria and therefore, animals need to take up this nutrient from their diet and subsequently transport it to their cells.[39,40] In humans, the recommended daily intake of vitamin B_{12} is 2-3 µg.[41] These minute amounts of B_{12} are delivered to our cells using a complex uptake pathway that involves transporting proteins with excellent selectivity, affinity and binding properties towards B_{12} in its base-on configuration (K_{on} = 10^7-10^8 $M^{-1}s^{-1}$, K_d = 10^{-15} M) (Figure 3).[35,41] These proteins are haptocorrin (HC, saliva and gastric fluids), intrinsic factor (IF, gastric fluid) and transcobalamin (TC, vascular endothelium).[35,40,42] Once cobalamin is released in human cells, the nutrient is metabolized to one of the two biologically active forms of B_{12}: adenosylcobalamin (**1-Ado**) or methylcobalamin (**1-CH_3**). The formation of the two organometallic cofactors is completed by the enzyme CblC, which catalyzes the dissociation of the single bond between cobalt and the corresponding upper β axial ligand i.e. cyanide.[43] A homolytic cleavage of the β axial ligand to form cob(II)alamin followed by alkylation with adenosyltriphosphate (ATP) achieves the synthesis of **1-Ado**. Conversely, a cob(I)alamin is required for the formation of **1-CH_3**. Indeed, the Co^I supernucleophile can bind a methyl group from S-adenosylmethionine (SAM).[44] Both **1-Ado** and **1-CH_3** fulfill different roles within human metabolism and unravel different types of reactivity that demonstrate the versatility of Cbls within enzymes.

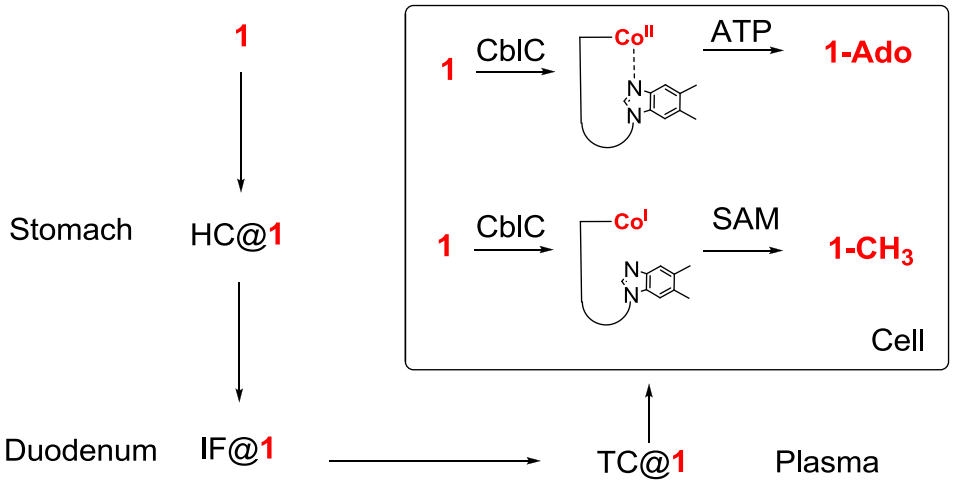

Figure 3. Human uptake pathway of vitamin B_{12}.[35,39-41]

1.4. Enzymology

Cbls participate in many metabolic reactions amongst different forms of life. The main classes of enzymes that profit from corrinoid cofactors are dehalogenases, methyl transferases, dehydratases, mutases, a deaminase and a ribonucleotide reductase.[35] Within these enzymes, different biologically active corrinoids are used, mostly methylcobalamin (**1-CH$_3$**) or adenosylcobalamin (**1-Ado**).[45,46] The chemistry of B_{12} within enzymes is so diverse that this molecule has been called "nature's most beautiful cofactor".[47] Indeed, a single molecule can act as a nucleophile, electrophile or participate in radical reactions due to the powerful redox chemistry at the cobalt center that normally involves the exchange of the β axial ligand.[22,48] In these enzymatic processes, the lower α axial position anchors the coenzyme to the corresponding enzymatic binding pocket. Thus, once base-on cobalamins have been transported into cells, they can adopt two different configurations within enzymes: either they stay in a base-on form or they switch to a base-off / histidine-on configuration (Figure 4). In the latter, the cobalt center is coordinated to a histidine residue of the corresponding enzyme.[46]

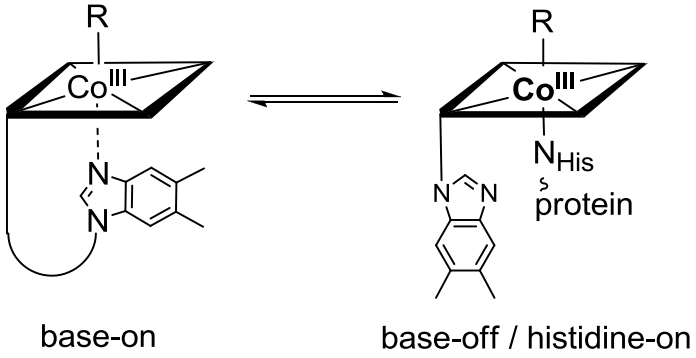

Figure 4. Configurations of vitamin B_{12} within enzymes.[46]

Two B_{12}-dependent enzymes are necessary for human metabolism: methylmalonyl coenzyme A mutase (MCM) and methionine synthase (MetH). In both enzymes, cobalamins adopt a base-off / histidine-on configuration.[45,46] However, the chemistry of both B_{12} cofactors largely differs.

1.4.1. Methyl malonyl coenzyme A mutase (MCM)

The main goal of this enzyme located in human mitochondria is to metabolize methyl malonyl coenzyme A into citric acid cycle intermediates. In this catalytic process, adenosylcobalamin (**1-Ado**) acts as a cofactor in the reversible transformation of (2*R*)-methylmalonyl-CoA to succinyl-CoA.[22] The interconversion follows a radical mechanism involving **1-Ado**.[45] First, the organometallic bond of coenzyme B_{12} is homolitically cleaved, leading to a pentacoordinate Co^{II}-containing Cbl and a 5'-deoxyadenosyl radical (Scheme 2, A). Subsequently, this radical abstracts one H from (2*R*)-methylmalonyl-CoA (Scheme 2, B, left), leading to 5'-deoxyadenosyl and a radical species that undergoes an intramolecular 1,2-rearrangement. Upon regeneration of the 5'-deoxyadenosyl radical, succinyl-CoA is formed (Scheme 2, B, right).

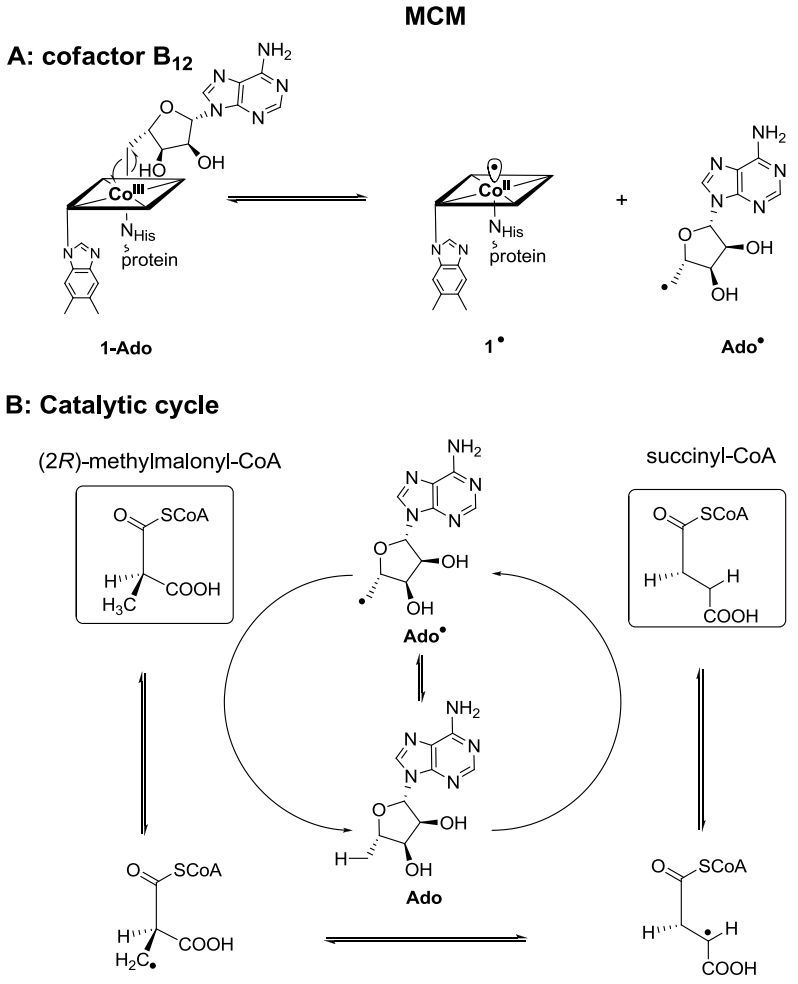

Scheme 2. **1-Ado** mediated isomerization of (2*R*)-methylmalonyl-CoA to succinyl-CoA within MCM.

1.4.2. Methionine synthase (MetH)

This enzyme is a cytosolic methyl transferase that catalyses the conversion of homocysteine into methionine using methylcobalamin (**1-CH$_3$**) as cofactor (Scheme 3).[22,46] To achieve the synthesis of methionine, the peripheral thiolate of homocysteine attacks the β axial methyl ligand of **1-CH$_3$** following an S_N2 mechanism. This reaction leads to methionine and a square planar cob(I)alamin, the latter being a supernucleophile that, in a subsequent reaction, withdraws a methyl group from methyltetrahydrofolate (CH_3-H_4-FH_4) to regenerate the Cbl cofactor.

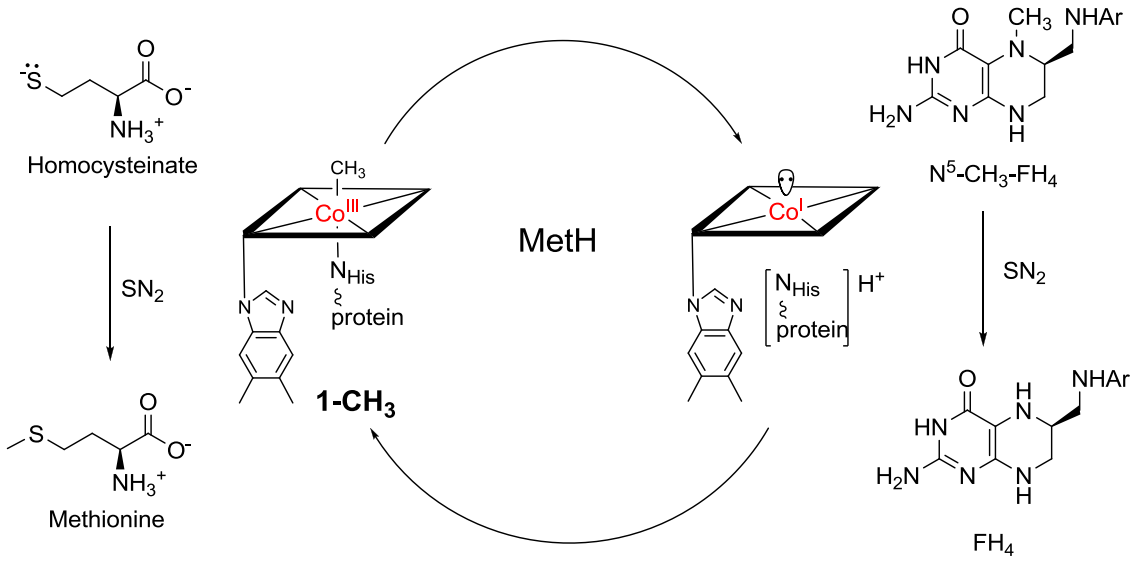

Scheme 3. **1-CH$_3$** mediated enzymatic methylation of homocysteine to methionine within MetH.

This single catalytic reaction is the link between several metabolic processes, since four essential biomolecules (vitamin B_{12}, homocysteine, methionine and folate) are involved in the enzyme. The interruption of this reaction originates a metabolic blockage with serious implications for human health (methylfolate trap).[49,50] The two most common causes for such a blockage are a) mutations affecting methionine synthase enzymatic activity, b) vitamin B_{12} deficiency.[51]

1.5. Clinical significance

As mentioned in section **1.1.**, vitamin B_{12} turned out to be an essential nutrient to avoid pernicious anemia. Knowing that this natural product was involved in the production of red-blood cells, it was not until its enzymatic roles were discovered and several clinical studies were performed that the importance of vitamin B_{12} was fully understood. Indeed, vitamin B_{12} deficiency leads to deteriorated neurophyschiatric and hematological conditions.[52-54]

The metabolic reactions where vitamin B_{12} is involved show the importance of this cofactor.[22,25] Taking methionine synthase as an example (see section **1.4.2.**, Scheme 3), the regeneration of methylcobalamin within this enzyme involves the synthesis of tetrahydrofolate, a necessary precursor for the synthesis of dTMP. Thus, vitamin B_{12} is indirectly involved in the synthesis of DNA nucleobases and is therefore essential for cell replication.[55] While the correlation of vitamin B_{12} with cell growth demonstrates why the deficiency of this nutrient causes serious medical conditions, this close relationship also explains why fast-proliferating cells (like those in tumors or sites of bacterial proliferation) increase their B_{12} consumption to fuel their uncommon growth.[39,56] This fact reveals a dangerous downside to this nutrient: while essential for healthy individuals, under certain clinical conditions B_{12} can turn into a threat.

1.6. Medicinal applications

The extraordinary chemistry and enzymology of vitamin B_{12} has attracted the attention of scientists over decades. Research in this field includes not only the characterization of the natural product and its biochemical functions, but also the potential use of (modified) Cbls as diagnostic or therapeutic agents.[28,29,49,57,58] In this regard, the unique chemistry of vitamin B_{12} offers attractive possibilities to develop new versatile drugs with novel modes of action.

1.6.1. Trojan horse/ biovector

A widely explored approach includes the use of vitamin B_{12} as a biovector to transport a given drug specifically to its target.[29,56,59] The introduction of a bulky foreign group in vitamin B_{12} needs to be carefully adressed, since its uptake pathway is specifically designed for the unique structure of this nutrient. Indeed, B_{12} transporting proteins tightly enclose the vitamin, leaving only two positions of the cobalamin scaffold unprotected: the upper axial ligand and the 5'-OH group of the ribose moiety at the "loop".[40,60,61] As a consequence, multiple organic and inorganic drugs, radiopharmaceuticals and diagnostic agents or fluorescence markers have been conjugated to these two sites (Figure 5).[61-66]

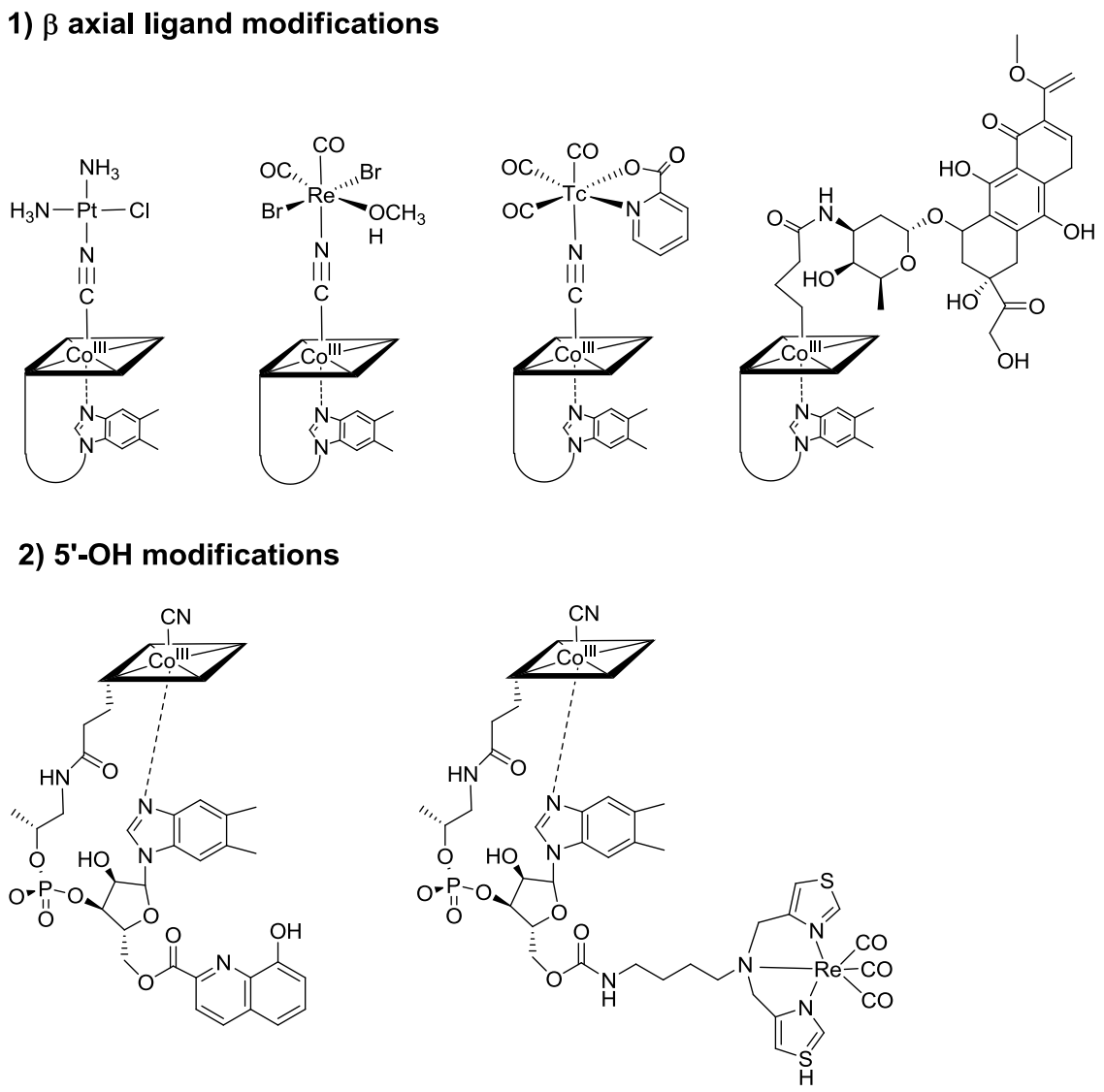

Figure 5. Examples of vitamin B_{12}-drug conjugates. [61-66]

1.6.2. Antivitamins

Although vitamins are essential nutrients, their effects can be harmful under certain clinical conditions. In those cases, the use of antivitamins as "molecules that diminish or abolish the action of a vitamin" is desirable.[67] Two main approaches for the inhibition of vitamin effects can be envisaged: 1) transform the nutrient into a structurally inactive species; 2) inhibit its biosynthesis, transport or enzymatic activity.[28]

As explained in section **1.5.**, vitamin B_{12} supports the growth of fast-proliferating tumor cells or bacterial infections.[39] In those cases, a temporary inhibition of B_{12} enzymatic processes would have beneficial antiproliferative effects. A promising approach for the impairment of B_{12}-dependent catalytic processes is the synthesis of non-functional surrogates of vitamin B_{12} with higher affinity for those enzymes than the natural product. These molecules could be antivitamins B_{12} and their rational design should take into consideration that:

a) The structure of the antivitamin should resemble that of vitamin B_{12} as much as possible. The antivitamin should compete with B_{12} for the binding sites of the involved transporting proteins and enzymes. Since these biomolecules are optimized for hosting the very specific structure of B_{12}, designing an antivitamin with a higher affinity for B_{12} dependent proteins and enzymes is often a big problem.
b) The reactivity within B_{12} dependent enzymes should be inhibited or modified in a way that the targeted enzymatic process is inhibited.

Research in this area has been intense since the 1960s and multiple candidates have been synthesized.[28,49,57] The potential antivitamins B_{12} include 1) corrin-modified, 2) "loop"-modified, 3) β axial ligand-modified and 4) metal-modified B_{12} derivatives (Figure 6). In the studies performed during 1960s-1970s, the antivitamin candidates were often evaluated using microbiological assays with *Lactibacillus leichmannii*, *Ochromonas malhamensis* and *Escherichia coli*.[49] Back then, a common indicator for the assessment and comparison of the antivitamin activity of different candidates is the inhibition index (I.I), defined as required ratio of inhibitor to vitamin needed to reduce bacterial growth by 50%. Nowadays, IC50 or specific *in vivo* studies are often employed.[68-70] According to all these indexes, subtle modifications of the basic Cbl framework are tolerated by B_{12} transporting proteins and/or dependent enzymes. Thus,

the presence of bromide as an electron-withdrawing group at C10 (I.I = 9; Figure 6, top left)[49,71], an artificial peptide "loop" (IC50 = 2 μM on *L. leichmannii*; Figure 6, top right)[68,72], a non-natural ethinyl axial ligand (14% inhibition of tumor growth in mice, Figure 6, bottom left)[73] or a different metal center in the corrin cavity i.e. rhodium (I.I = 8, Figure 6, bottom right)[74] achieve a remarkable competition with B_{12} cofactors and in turn inhibition of cell growth.

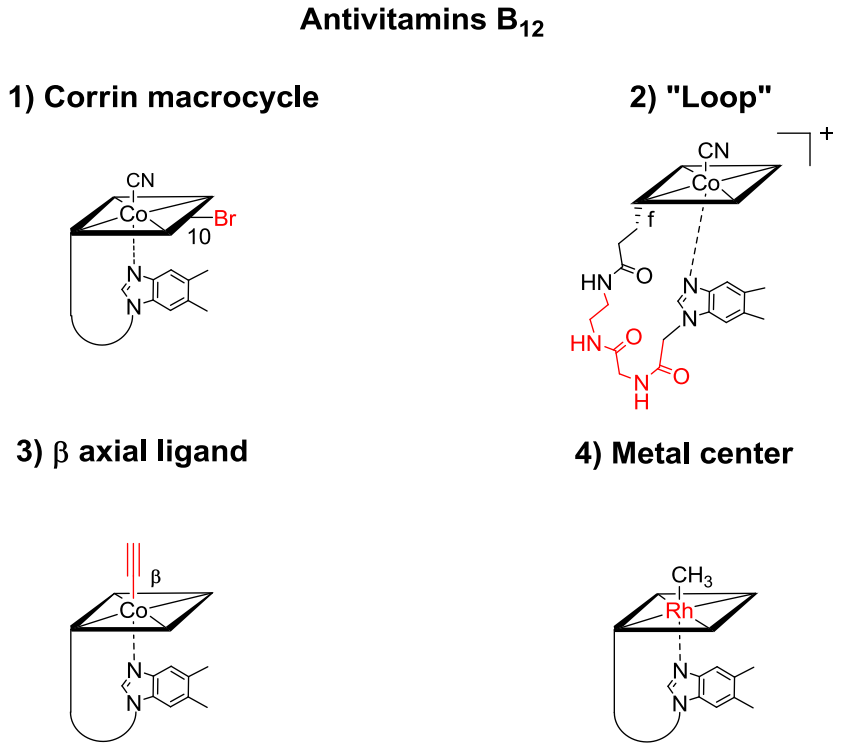

Figure 6. Modified B_{12} derivatives with antivitamin activity.[49,68,71,73,74]

Another interesting class of antivitamins B_{12} includes a series of yellow pigments called "stable yellow corrinoids".[75] Tested in patients suffering from anemia during the 1960s, one of these compounds (pigment I, isolated from *Aerobacter aerogenes*) showed only 8% of activity compared to B_{12}.[76] While the bioactivity and spectroscopic properties of these compounds differs from those of vitamin B_{12} (one broad absorption band at 450-480 nm instead of the common α and β bands), their exact structure remains a mistery.[23] Nowadays, it is known that "stable yellow corrinoids" are obtained by chemical means when Co^{II}-corrinoids are reoxidated to Co^{III}-corrinoids. The altered electronic properties of these yellow corrinoids have their origin in the disruption of the

π-electronic system of the corrin macrocycle (the double bond at C5-C6 is a remarkably reactive position).[77-79]

The development of new synthetic procedures for the selective modification of the Cbl scaffold will guarantee better access to promising known and new antivitamin B_{12} candidates as potential therapeutic agents with new modes of action. In spite of the difficulties lying ahead of us, the need for new drugs with novel modes of action has put antivitamins B_{12} back in the spotlight.[28,57]

1.7. Metbalamins

Metbalamins are vitamin B_{12} derivatives containing other metals than cobalt. Metbalamins with a modified metal center and an intact corrin ligand are excellent antivitamin B_{12} candidates (as already mentioned in section **1.6.2.**)[49,74], as their structure only differs in one single atom compared to Cbl. However, the metal center is the main actor in B_{12} dependent catalytic processes (see section **1.4.**).[22] Thus, the two main requisites for the design of an antivitamin are fulfilled: structurally related B_{12} derivatives which are catalytically inactive.

Ever since the interest in vitamin B_{12} chemistry exploded after Hodgkin's structural determination of the molecule,[11] the extraction and replacement of the metal center within this coordination complex has attracted the attention of numerous scientists.[28,57] While the idea is simple, the realization of it has been proven an extremely puzzling question. Unexpectedly, the synthesis of metbalamins ended up being one of the holy grails of bioinorganic chemistry.

1.7.1. Biosynthetic approaches towards metbalamins

Unidentified cobalt-free corrinoids were first isolated from photosynthetic bacteria in 1966 by Perlman and Toohey.[80,81] Following this finding, in 1971 Koppenhagen and Pfiffner discovered that the bacterium *Chromatium* was able to produce α-5,6-(dimethylbenzimidazoyl)hydrogenobamide in the presence of 5,6-dimethylbenzimidazole.[82] Thus, Cu^{II}, Zn^{II} and Rh^{III} were incorporated to the complete corrin scaffold (Figure 7).[82,83] Additionally, further studies by Koppenhagen on the coordination chemistry of the octahedral complex cyanorhodibalamin led to the exchange of the β axial ligand, thus affording analogues of organometallic B_{12} coenzymes (5'-deoxyadenosylrhodibalamin and methylrhodibalamin).[74] The metal-modified derivatives with an intact corrin macrocycle preserved the typical α, β and γ bands of B_{12} UV-Vis spectra (i.e. 345, 477 and 503 nm for aquarhodibalamin and 345, 485 and 514 nm for cyanorhodibalamin) and were tested as antivitamins in microbiological assays with *L. leichmannii*. Satisfyingly, it was found that the descobaltocorrin α-5,6-(dimethylbenzimidazoyl)hydrogenobamide and metbalamins (Cu, Zn, Rh-containing corrinoids) successfully antagonize vitamin B_{12} (Figure 7).[49] Furthermore, rhodibalamins with different axial ligands were tested on both

L. leichmannii and *E. coli*, demonstrating that a) the nature of the β axial ligands also affects their bioactivity and b) the antivitamin activity of a compound is specific for each organism.[74] For example, methylrhodibalamin is the most effective antagonist against *L. leichmannii* (I.I = 8, figure 7) while 5'-deoxyadenosylrhodibalamin is more effective as *E. Coli* inhibitor (I.I = 52, figure 7).

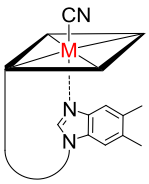

M	I.I (*L. Leichmannii*)
H	42
Cu	16
Zn	17
Rh	65

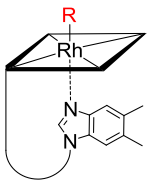

R	I.I (*L. Leichmannii*)	I.I (*E.Coli*)
H_2O	228	81
Cl	242	162
CH_3	8	272
5'-Ado	139	52

Figure 7. Antivitamin activity of metbalamins (left) and rhodibalamins with different β axial ligands (right).

In spite of the promising bioactivity of the studied metbalamins, research on this field vanished during the 1980s. Most probably, the loss of interest was related to the tedious and extremely low-yielding biosynthetic methods employed for the obtention of metbalamins. Only recently metbalamins earned renewed attention as an alternative biosynthesis of 5'-deoxyadenosylrhodibalamin was described (Scheme 4).[84] The new route was established around the construction of plasmids containing cloned amplified genes from B_{12}-producing bacteria (*Rhodobacter capsulatus SB1003*, *Brucella melitensis 16M*, *Methanosarcine barkeri* and *Citrobacter freundii*).

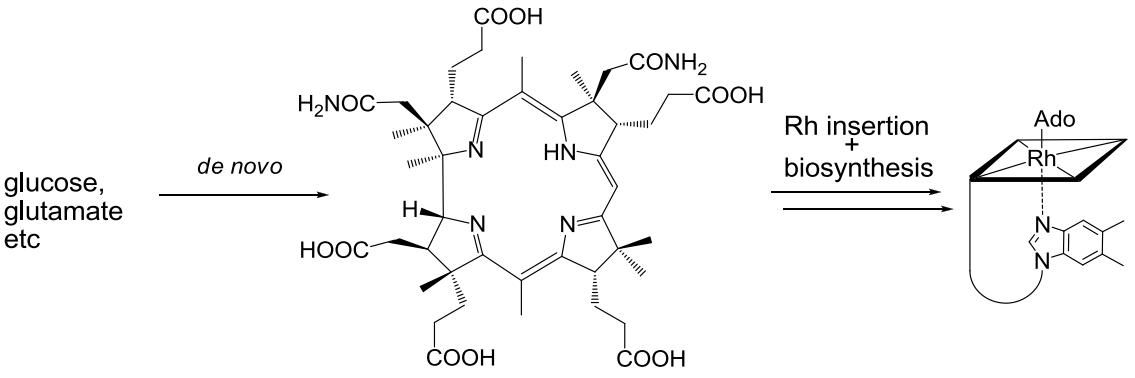

Scheme 4. Biosynthetic production of 5'-deoxyadenosylrhodibalamin.[84]

1.7.2. Synthetic approaches towards metbalamins

"No synthetic corrin would as yet exist without recourse to metal templates… converting the organic chemists involved in this work to genuine admirers of the depth, potentials and wonders of transition metal chemistry." (A. Eschenmoser)

The demetallation of vitamin B_{12} by chemical means remains unsolved and represents the most fascinating mistery around B_{12} chemistry.[22] Renowned chemists have tackled this question, yet no efficient method has managed to remove the stunningly stable Co^{III} center from the intact corrin macrocycle. However, some steps towards this ambitious goal have been achieved and will be summarized in this section.

In the context of the total synthesis of vitamin B_{12},[12,14] the use of metal templates played an essential role to arrange the proximity of reaction centers (steric strain), activate organic ligands electronically or protect organic sites against alkylation agents.[85] Importantly, two key coupling reactions that allowed the formation of the corrin macrocycle are completed in the presence of metals: 1) the connection of the pyrrolic A/B fragments through a methylene bridge by sulfide contraction utilizes a Zn^{II} center[86] and 2) the photochemical formation of a direct C-C bond between A/D fragments is completed in high yields (> 95%) when Pd^{II} coordinates the equatorial macrocycle (Scheme 5).[85,87]

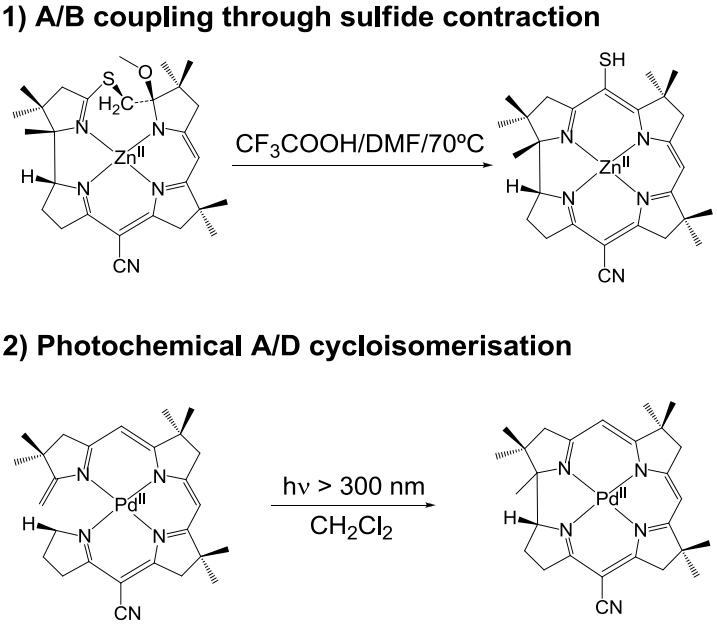

Scheme 5. Ring-closure reactions of artificial Zn^{II} and Pd^{II}-containing corrins.[85-87]

Seminal work by Eschenmoser during the 1960s describes the coordination chemistry of model artificial corrinoids, showing that different metal centers can be incorporated to ring-opened secocorrins.[85] For example, cyclization of a secocorrinoid containing an iminoester on the A-ring and an imine on the B-ring (Scheme 6, left) can only be achieved in the presence of a metal template (i.e. Co, Ni or Pd). In that case, a base ($^{t}BuO^{-}$) catalyzes the deprotonation of a peripheral methylene, rendering the double bond on C5-C6 more nucleophilic (Scheme 6, middle) and completing the corrin formation (Scheme 6, right).

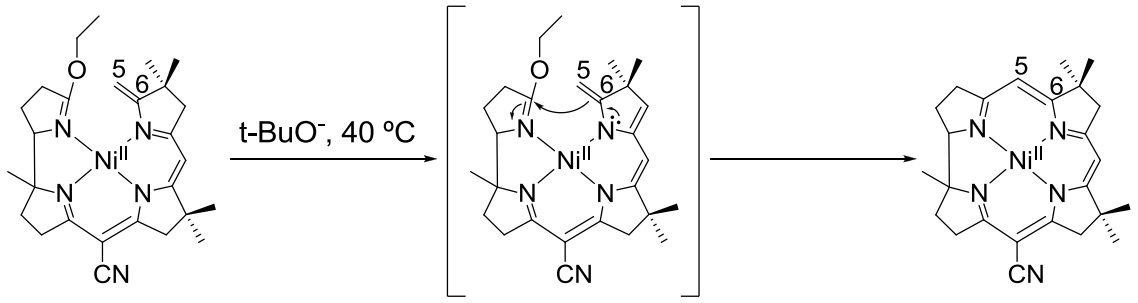

Scheme 6. Ni^{II}-templated ring closure of an artificial secocorrinoid.[85]

Interestingly, when the metal ions are surrounded by a complete ring-closed corrin (Scheme 6, right), demetallation proved to be an extremely challenging task, most likely due to the kinetic stabilization offered by the macrocyclic chelation.[85] While chemical procedures to demetallate various porphyrinoid macrocycles are well-established, the application of those methods to (model) corrins has led mostly to the destruction of the corrin system. Only in 1983, Eschenmoser proposed the first chemical method to demetallate a cobalt-containing model corrin compound, based on the use of 1,3-propanedithiol as a decomplexating agent in the presence of concentrated HCl (Scheme 7).[88] However, the model compound lacks all peripheral side chains from B_{12}.

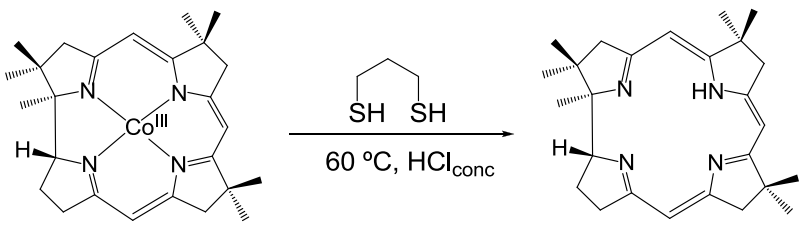

Scheme 7. Demetallation of an artificial cobalt-containing corrin.[88]

In the quest of more realistic B_{12} model compounds, Werthemann implemented the synthesis of dicyanocobyrinic acid heptamethylester, ('cobester') by acid-catalyzed methanolysis of the vitamin (Scheme 8).[89] In this compound, all amide side chains of B_{12} are replaced by methyl ester groups, rendering the corrinoid hydrophobic and thus making it a versatile tool for synthetic investigations of vitamin B_{12}.

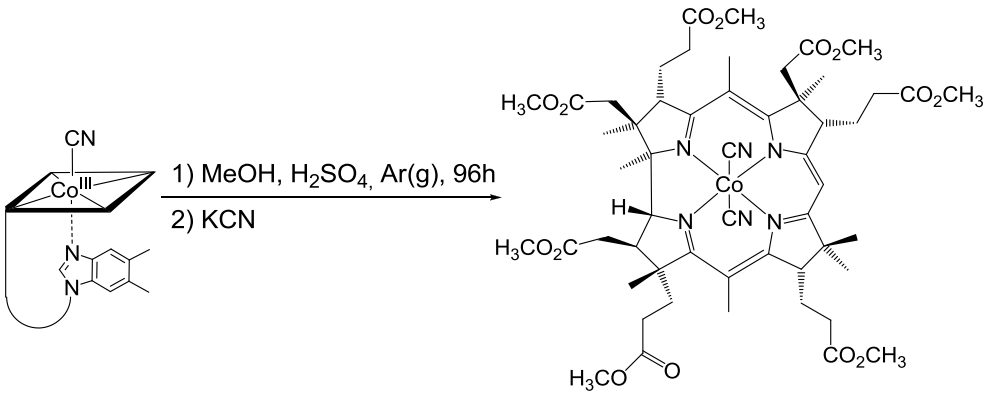

Scheme 8. 'Cobester' synthesis.[89]

With this model compound of vitamin B_{12} in hand, its demetallation was attempted using Eschenmoser's conditions (1,3-propanedithiol, HCl_{conc}). Unfortunately, cobalt could not be extracted from the corrin macrocycle. Curiously, the synthesis led only to the unexpected obtention of 5,15-bisnorcobester (Scheme 9, right).[90]

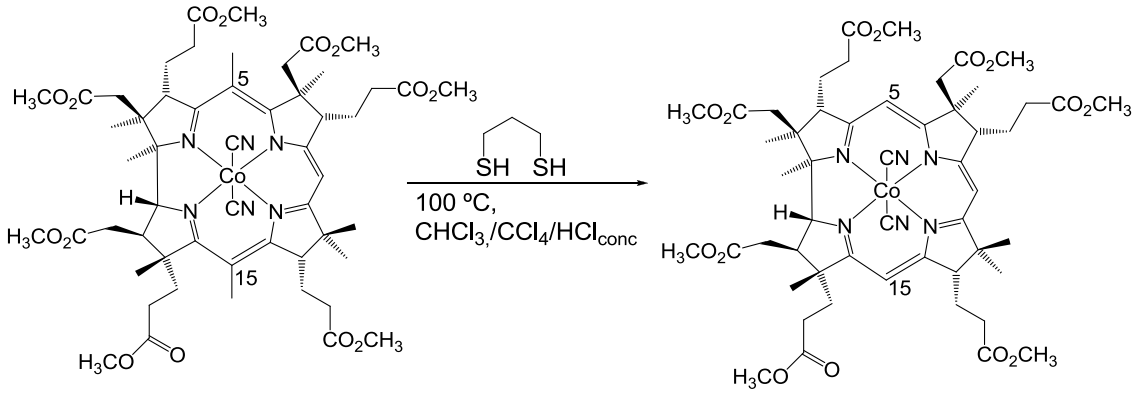

Scheme 9. Synthesis of 5,15-bisnorcobester. [90]

Assuming the improbable extraction of cobalt from "complete" ring-closed corrin systems, efforts diverted towards ring-opened secocorrinoids. Inhoffen and coworkers developed in 1979 a method to cleave the corrin macrocycle of 10-bromocobester (Scheme 10, top).[91] Through ozonolysis, the double bond at positions C5 and C6 was replaced by keto and lactam moieties respectively. Later, the reaction conditions were optimized by Kräutler and Stepanek, who introduced a photochemical method for the synthesis of dioxo and tetraoxocorrinoids.[92,93] In this method, light-induced singlet oxygen ($^1O_2{}^*$) was used to cleave the corrin macrocycle of cobester (Scheme 10, bottom).[93,94] $^1O_2{}^*$ can attack the delocalized π-electronic system at positions C5-C6 and/or C14-15 in a spin-allowed reaction, yielding two structural isomers: dicyano-14,15-dioxocobester and dicyano-5,6-dioxocobester.

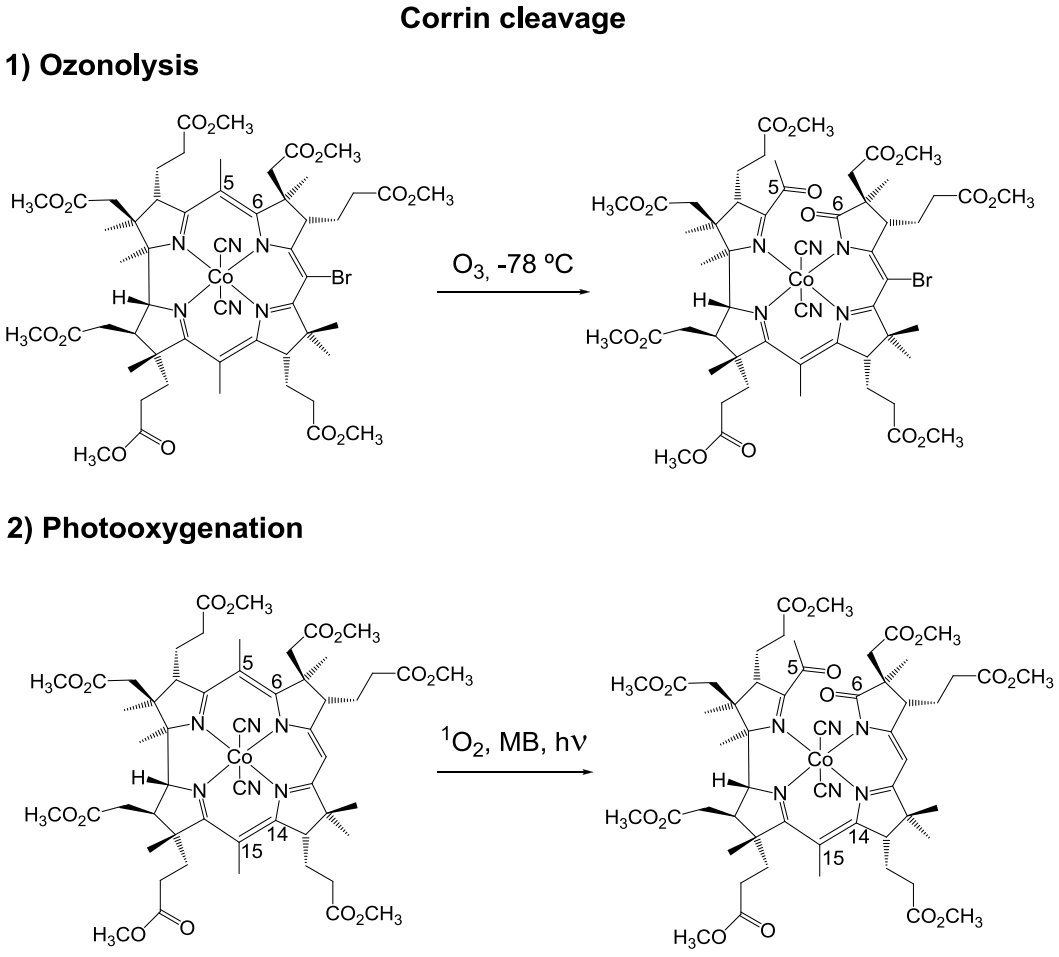

Scheme 10. Synthesis of dioxocobester derivatives by ozonolysis[91] (top) and photooxygenation[92] (bottom). Only the 5,6-dioxocobester isomers are shown.

As it was the case with ring-opened corrin models lacking peripheral side chains (Scheme 6, left), the demetallation of ring-opened 'cobester' derivatives was feasable. Herein, dicyano-10-bromo-5,6-dioxocobester (Scheme 11, top) was demetallated using NaSH as decomplexating agent.[91] Subsequently, different metals (Rh, Pd) were inserted in the oxidized metal-free macrocycle.[95] Unfortunately, all attempts to reconstitute the corrin macrocycle with other metals than cobalt failed (Scheme 11, bottom).

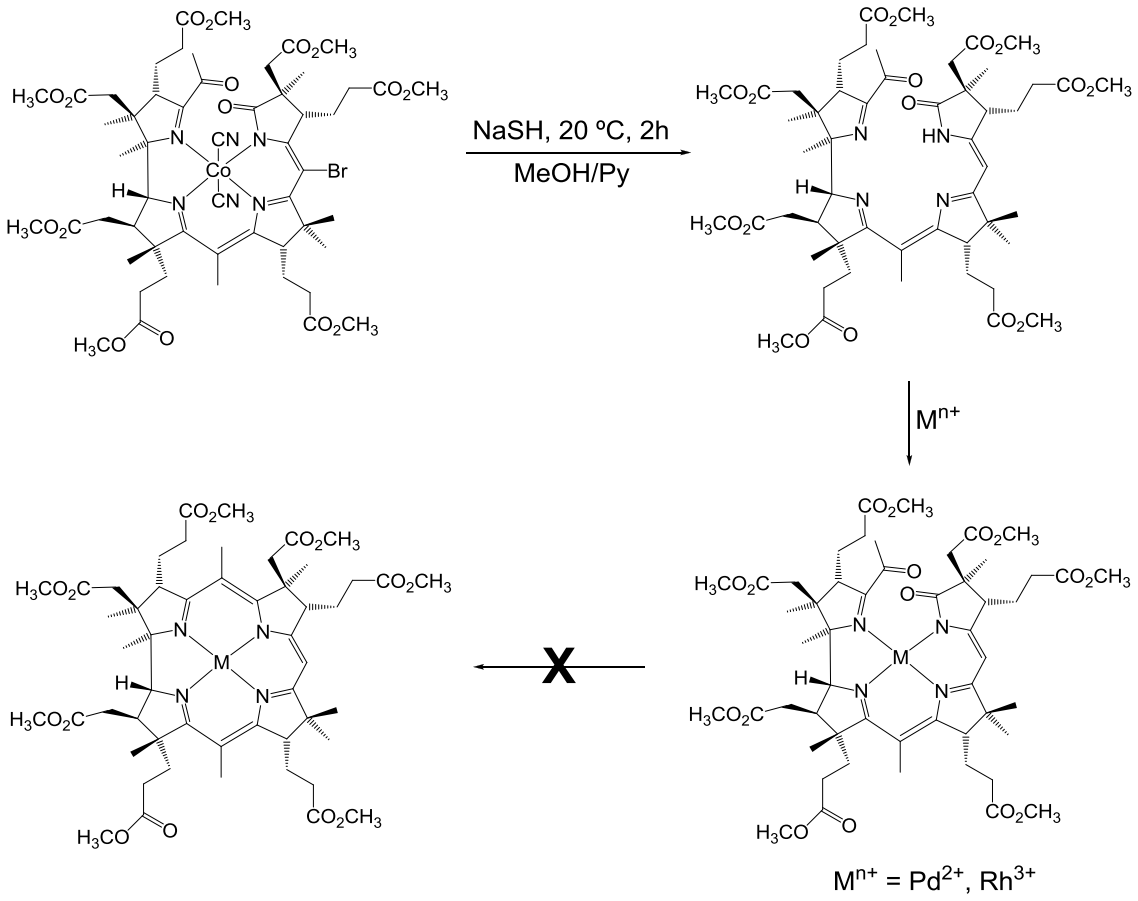

Scheme 11. Synthesis of the dioxopalladibester and dioxorhodibester. [95]

As it was the case with Eschenmoser's artificial corrinoids (see Schemes 6 and 7), the demetallation and complete corrin reconstitution of 'cobester' derivatives was only achieved when this hydrophobic compound was lacking a peripheral side-chain. Under pyrolytic conditions, a double bond between positions C7-C8 of 'cobester' originates, eliminating the c-side chain and forming the so-called 'pyrocobester'(Scheme 12, top middle).[96] After photooxygenolysis, the cobalt center could be extracted from this product using P_4S_{10} (Scheme 12, bottom right). Later Ni^{II} was inserted and Inhoffen and

coworkers stated that the oxidized nickel-containing corrin macrocycle could be reconstituted under McMurry conditions, affording ‘pyronibester’ (Scheme 12, bottom left).[97]

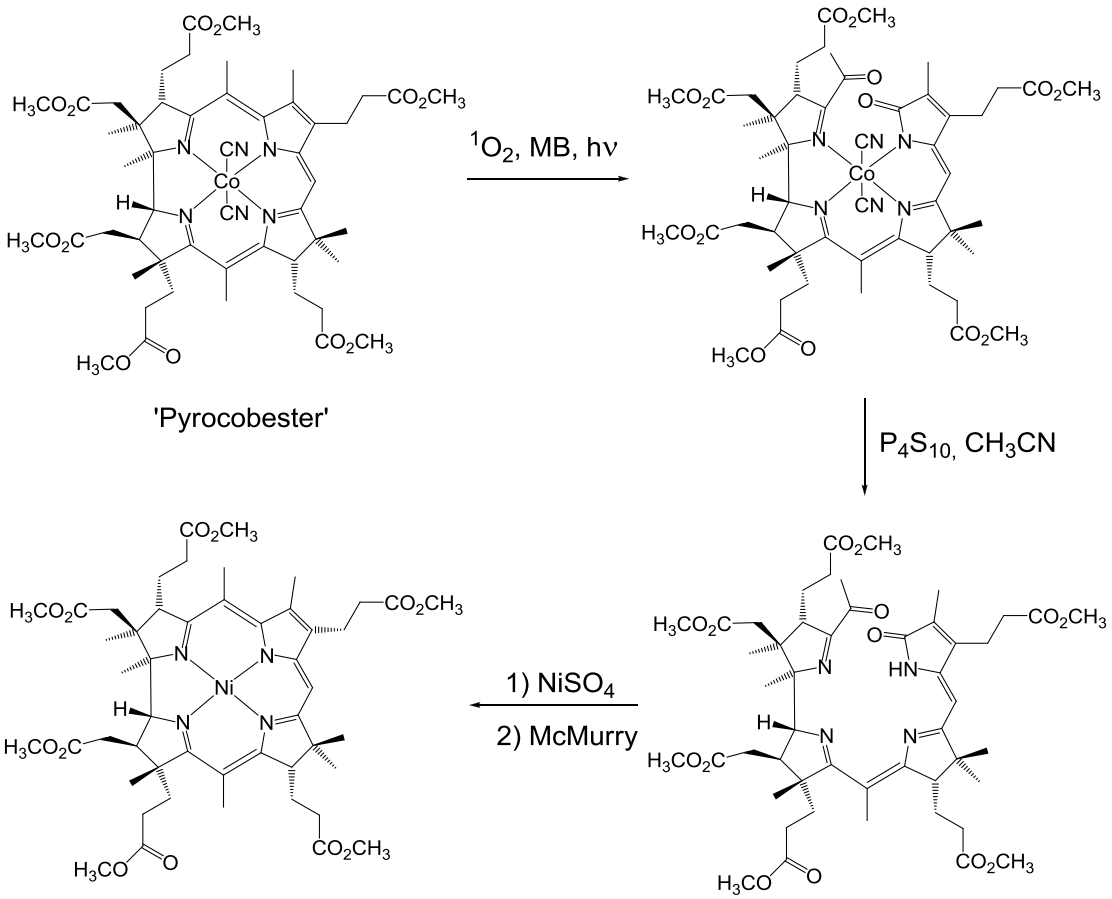

Scheme 12. Synthesis of ‘pyronibester’ from ‘pyrocobester’.[97]

Although hydrophobic models of corrins lacking the c-side chain and containing nickel instead of cobalt were synthesized in the 1980s, the obtention of metbalamins remains elusive. Striving to push forward this ambitious goal, the Zelder group started working on the complex topic of the chemical (semi)synthesis of metbalamins from vitamin B_{12}. Thus, the first chemical demetallation of a complete corrinoid was reported in 2010.[94] Concretely, cobalt was removed from the oxidized dicyano-5,6,14,15-tetraoxocobalamin using ethyleneglycol as decomplexating agent and thus obtaining two bicyclic fragments (A/D and B/C) as products of the reaction (Scheme 13).

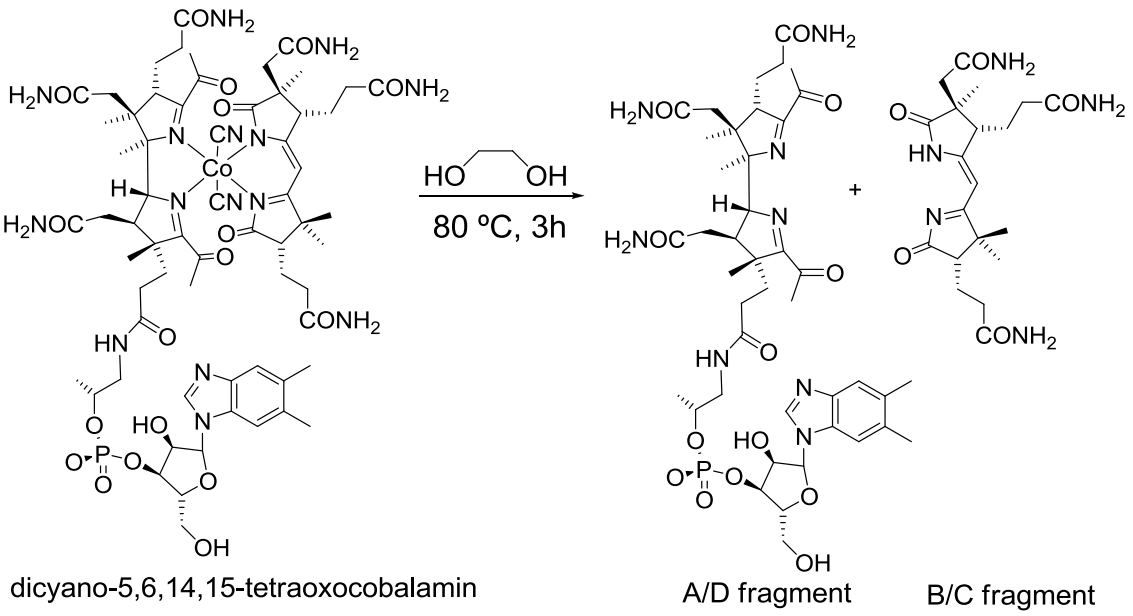

Scheme 13. Synthesis of the bicyclic A/D and B/C corrin fragments from dicyano-5,6,14,15-tetraoxocobalamin.[94]

Subsequent problems in the reconnection of the two independent fragments led to a change in the strategy. During his PhD thesis, Dr. René Oetterli worked on the demetallation of dicyano-14,15-dioxocobalamin, establishing a new method to obtain metal-free B_{12} derivatives (Scheme 14): the electrochemical reduction of the kinetically inert Co^{III} center to a more labile Co^{II} ion was followed by demetallation of the reduced species using an excellent σ-donor as decomplexating agent (KCN).[98] Thus, 14,15-dioxo-H-balamin was obtained and served as template to coordinate different metal ions to the disrupted corrin macrocycle (Ni, Pd, Cu etc).

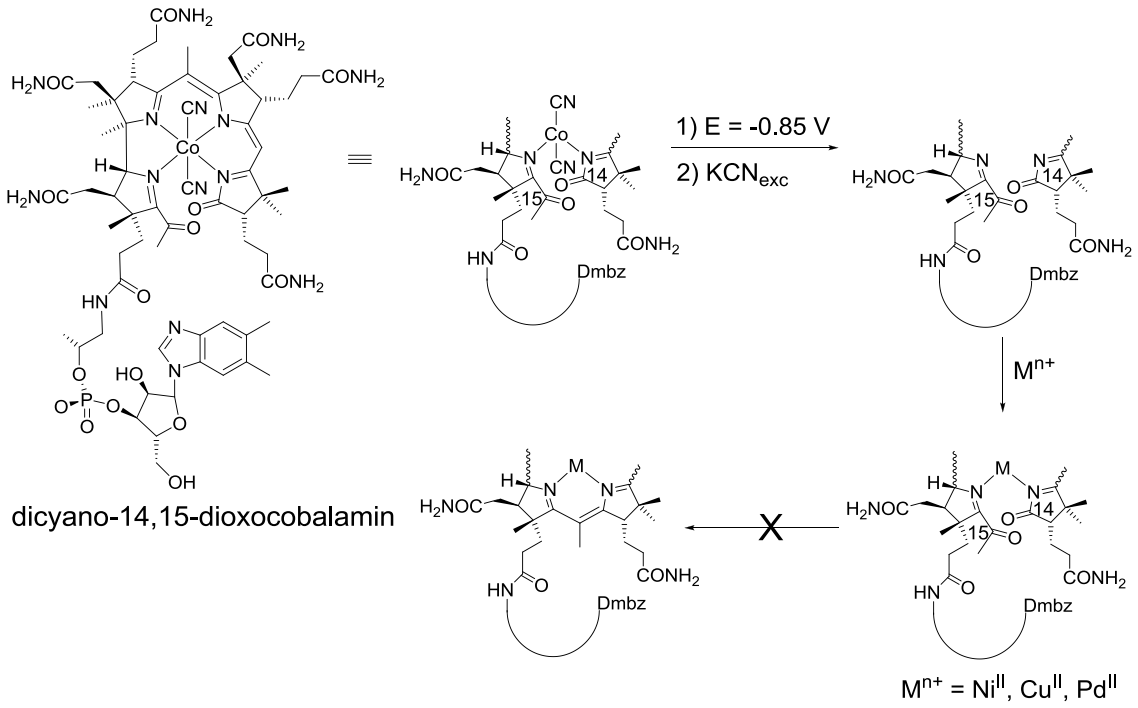

Scheme 14. Synthesis of 14,15-dioxometbalamins.[98]

Unfortunately, the attemps to reconstitute the original corrin macrocycle in 14,15-*seco*-corrins were unfruitful. Nevertheless, the commendable progress achieved in the last years and the group's experience in this project provide a solid ground for the goals of the present thesis.

2. Objective

The goal of this PhD thesis was to establish a chemical route towards metbalamins, vitamin B_{12} derivatives containing different metal centers than cobalt. Since cobalt is the main actor in B_{12}-dependent catalytic processes, its replacement gives access to a new family of B_{12} derivatives with modified physicochemical properties. Hence metbalamins are excellent candidates of antivitamins B_{12}, molecules that diminish or abolish the action of B_{12}-dependent enzymes. Given the involvement of B_{12} in cell-growth processes amongst many forms of life, important medicinal applications for metbalamins can be envisaged as antibiotics and antiproliferative agents in cancer therapy.

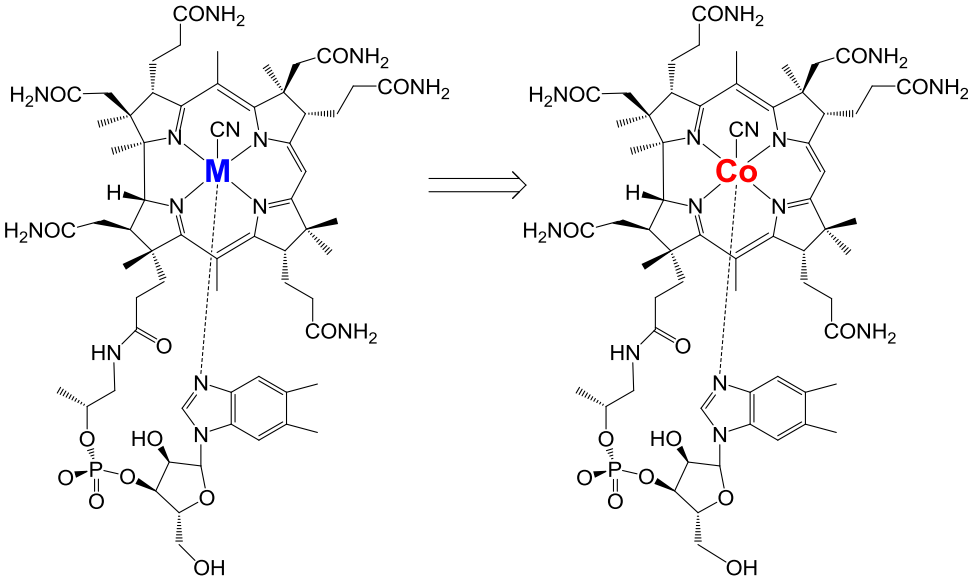

For decades, the extraction of the cobalt center from the intact corrin macrocycle has not been achieved without destruction of the corrin ligand. Therefore, this work aims to develop a chemical route towards metbalamins from ring-opened B_{12} derivatives. Herein, the main challenges of this work are to:

- Demetallate ring-opened secocorrinoids.
- Introduce new metals in the ring-opened corrin cavity.
- Reconstitute the original corrin macrocycle.

3. Results and discussion

3.1. Reconstitution of the corrin macrocycle of B-ring modified 7,8-*seco*-corrinoids

This section describes investigations of B-ring opened B_{12} derivatives as potential precursors for the synthesis of metbalamins. Particularly, it was found that the corrin macrocycle of halogen-containing 7,8-*seco*-corrinoids is efficiently reconstituted under reducing conditions. Quantitative conversion was achieved with the one-electron reducing agent cobaltocene ($CoCp_2$) and chemoselectivity was obtained by the unprecedented use of cyanide as an inorganic protecting group for the metal center (Co^{III}). In the absence of cyanide, competitive metal (Co^{III}) and ligand (corrin) reduction processes lead to the formation of several products, including two novel corrinoids with an altered delocalized π-electronic system.

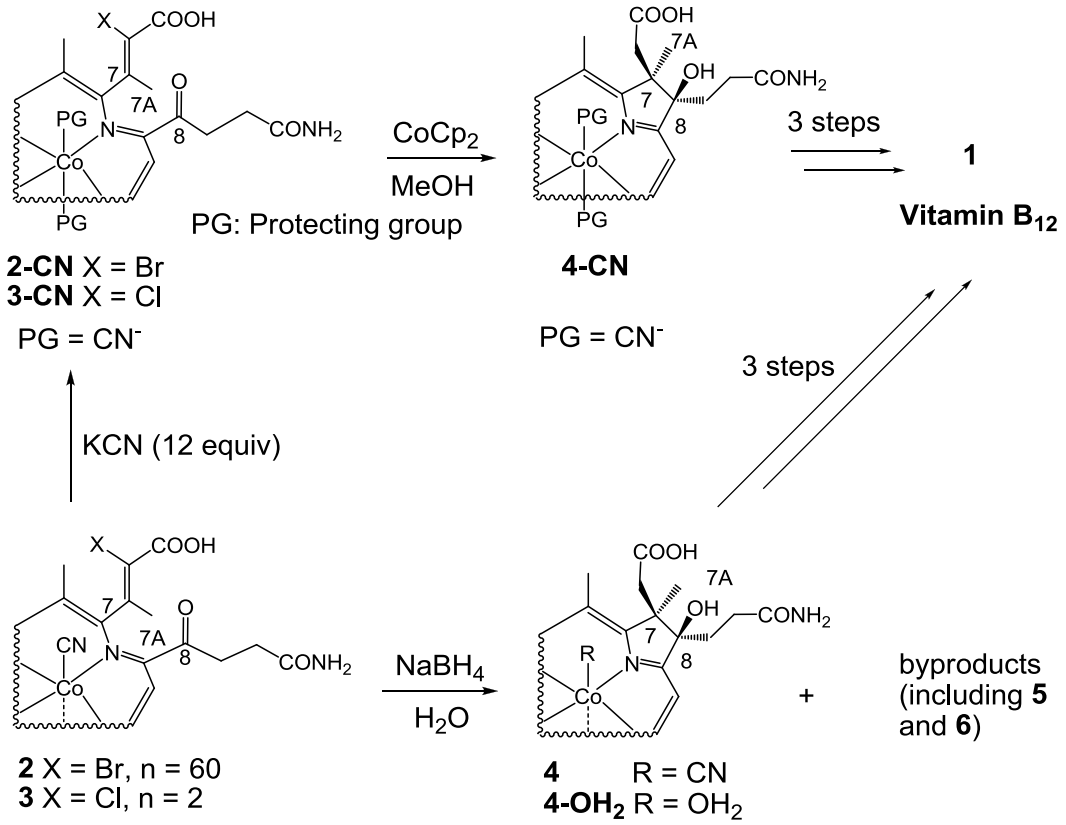

Scheme 15. Reductive B-ring reconstitution of **2** and **3** with $CoCp_2$ (top) and $NaBH_4$ (bottom).

3.1.1. Reconstitution of the B-ring using $NaBH_4$ as reducing agent

Two green 7,8-*seco*-corrinoids (**2** and **3**, Scheme 15) with an interrupted corrin macrocycle at the B-ring were synthesized in quantitative yields by Dr. René Oetterli in our group.[98,99] Interested in the potential utility of 7,8-*seco*-corrinoids as metbalamin precursors, the reactivity of **2** and **3** regarding a) corrin repair and b) metal exchange was extensively studied.

As a starting point, it was investigated if 7,8-*seco*-corrinoids **2** and **3** could be repaired to an intact macrocycle. Previous studies by Kräutler *et al.* demonstrated that the original π-system of a blue 7,8-*seco*-corrinoid was reconstituted under reducing conditions (Scheme 16).[100]

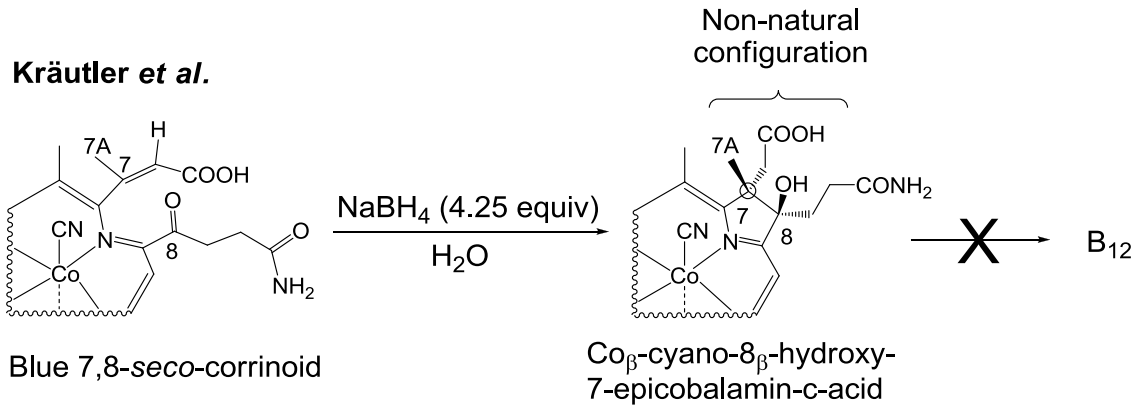

Scheme 16. Ring-closure of a blue 7,8-*seco*-corrinoid with $NaBH_4$.[100]

Inspired by this work, the reconstitution of the B-ring of **2** and **3** was attempted using the reducing agent $NaBH_4$ (Scheme 15, bottom). The addition of 1.5 equiv of $NaBH_4$ to a milimolar aq. sln. of **2** or **3** at 23 ºC led to an immediate colour change from green to dark red. UPLC analysis of the reaction mixture after 1 h indicated complete conversion of the starting material (Figure 8). From the crude mixture, two compounds (**4**, **5**) were isolated by preparative HPLC and fully characterized and a third product (**6**) was identified and its structure was tentatively assigned based on UPLC-MS analysis.

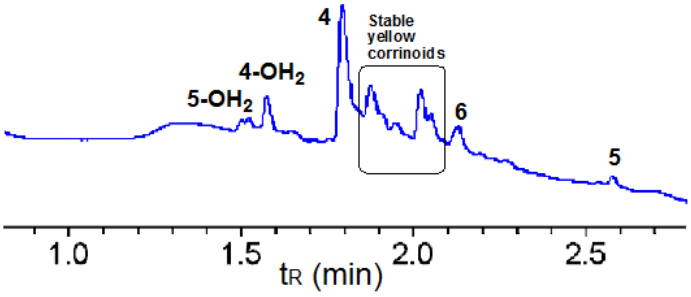

Figure 8. UPLC trace (Method 1, see Materials and Methods) of the reaction mixture of **2** and $NaBH_4$ after 1 h (see Scheme 15, bottom).

The main fraction (**4**, Figure 8) contained a red corrinoid with typical values for α, β and γ UV-Vis bands of B_{12} derivatives with an intact corrin macrocycle (551, 517 and 360 nm respectively, figure 9). MS analysis of the purified fraction suggested the presence of a single product with m/z = 1372.6 $[M+H]^+$. Based on both spectra, the formation of Co_β-cyano-8-hydroxy-cobalamin-c-acid (**4,** Scheme 15, middle) is proposed. Notably, the presence of an axial cyanide ligand in **4** (ϑ = 2137 cm^{-1}) suggests that Co^{III} was not reduced to Co^{II} upon addition of $NaBH_4$ and only a ligand-centered reduction (corrin reconstitution) took place for most of the starting material. Due to the use of an excess of $NaBH_4$ (1.5 equiv), a small fraction of the green 7,8-*seco*-corrinoids (**2** or **3**) was apparently not only reduced at the ligand site but also at the metal center. Thus, after reoxidation of this fraction with air, Co_β-aqua-8-hydroxy-cobalamin-c-acid (**4-OH$_2$**, m/z = 673.6 $[M-H_2O]^{2+}$) was also obtained. Indeed, when a larger excess of $NaBH_4$ is employed (5 equiv) **4-OH$_2$** becomes the main product of the reaction, being easily converted to **4** by addition of a stoichiometric amount of KCN.

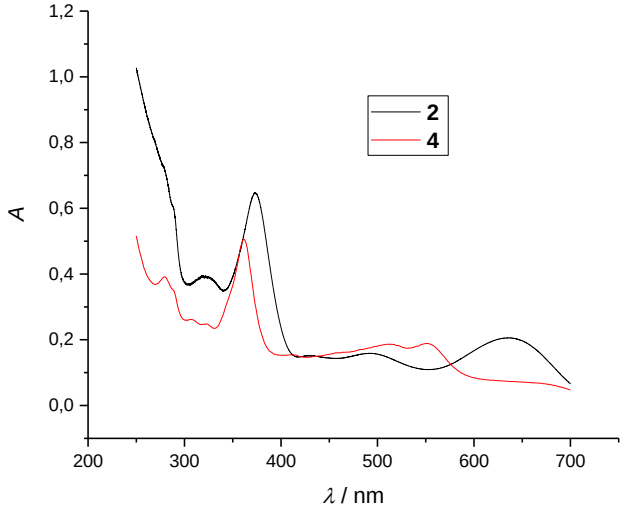

Figure 9. UV-Vis spectra of **2** (black line, H_2O, c = 5.1 x 10^{-5} M) and **4** (red line, H_2O, c = 1.6 x 10^{-5} M).

In order to investigate the mechanism of the reductive ring-closure, the reaction was also performed using deuterated sodium borohydride or deuterated solvents (Scheme 17). Surprisingly, the addition of $NaBD_4$ to **2** in H_2O leads to no change in the mass spectrum of **4** (m/z = 1372.6, $[M+H]^+$), indicating that no hydride from the reducing agent is incorporated into the corrin scaffold. Thus, a tentative radical mechanism in which $NaBH_4$ provides an electron to form a ketyl radical at C8 (**Y**) is proposed. The suggested reactive intermediate **Y** is rapidly coupled to C7 in a C-C forming reaction between the radical at C8 and the double bond at C7-C71. If the bromide group is eliminated as a $Br^{\cdot}$ radical, a short-lived carbene intermediate at C71 (**Z**) can be originated and rapidly converted to **4** in protic media. Conversely, the use of $NaBH_4$ in heavy water (D_2O) leads to the formation of a bideuterated ring-closed product (**[D$_2$]4**, m/z = 1374.6, $[M-H+2D]^+$), supporting the assumption that two D from the solvent are incorporated at C71 in **[D$_2$]4**.

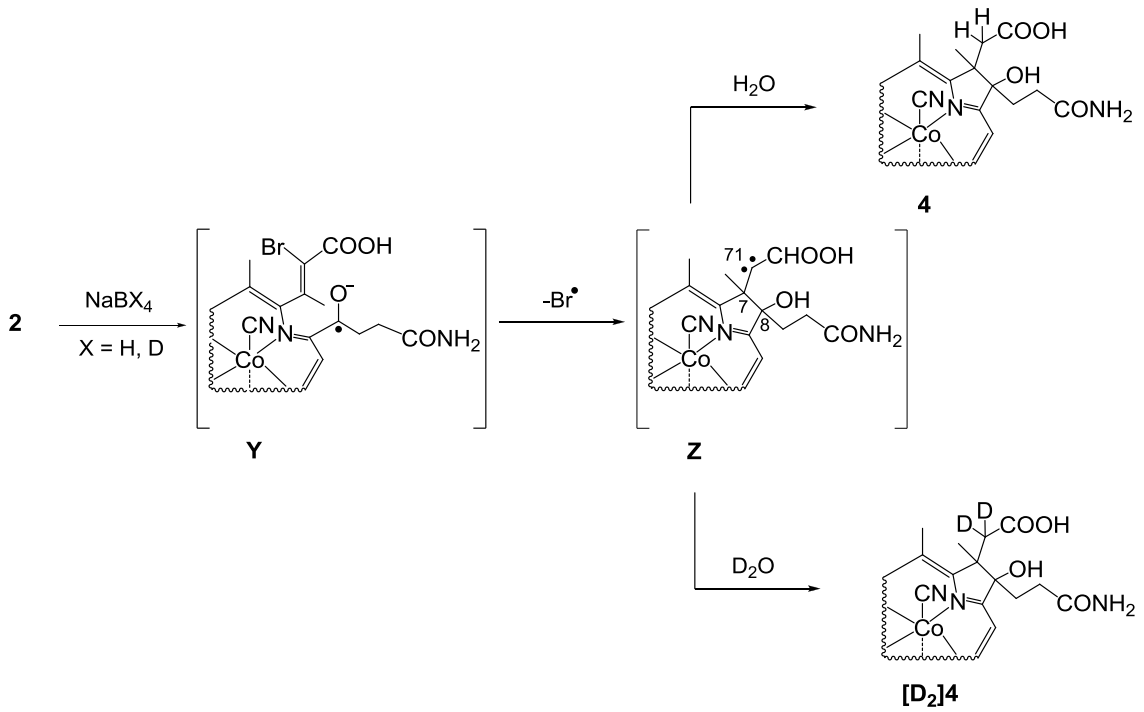

Scheme 17. Proposed mechanism of the radical ring-closure reaction of **2** to **4** with tentative intermediates **Y** and **Z**.

While **4** is the main product (33% yield) obtained in the $NaBH_4$-promoted B-ring closure reaction described above, several byproducts with different electronic properties are formed and can be isolated by HPLC (Figure 8). Most of these fractions are complex mixtures of "stable yellow corrinoids".[76-79] It was assumed that the presence of these compounds was only related to redox processes occurring at the metal center and not a consequence of the reductive B-ring reconstitution. Therefore, these compounds were not studied in more detail. However, two minor blue (**5**) and green (**6**) colored fractions with unusual electronic properties for corrinoids were isolated and identified.

5 is a by-product isolated in 6% yield in the described reduction of **2** and **3** with $NaBH_4$ (Scheme 15, middle). In agreement with the measured mass spectrum (m/z = 1225.6 $[M+H]^+$), ^{13}C NMR analysis (figure 10, section **6.3.**) confirmed that **5** is Co_β-cyano-Δ^7-dehydro-7-decarboxymethyl-8-decarboxyethyl-cobalamin, a corrinoid that lacks the b- and c-side chains at the B-ring. Comparison of the ^{13}C spectra of **5** and vitamin B_{12} (**1**) revealed excellent agreement between the chemical shifts of both molecules except for the B-ring signals. Indeed, the C71 ,C72, C81, C82 and C83 signals of the b- and c- side chains are missing, C7 is now a quaternary carbon

(δ = 150.9 ppm, $\Delta\delta_{C7}$ = 96.7 ppm) and C8 becomes a tertiary carbon (δ = 74.2, $\Delta\delta_{C8}$ = 16.0 ppm). Additionally, C6 and C9 are shifted upfield by 12.4 and and 11.7 ppm respectively. These shifts are explained by an increase of the electronic density around the B-ring due to the presence of an additional double bond at C7-C8. As a consequence of the new double bond, the conjugated π-system of the corrin macrocycle is extended and **5** has an intense blue color (λ_{max} = 622.9 nm, log ε = 4.1).

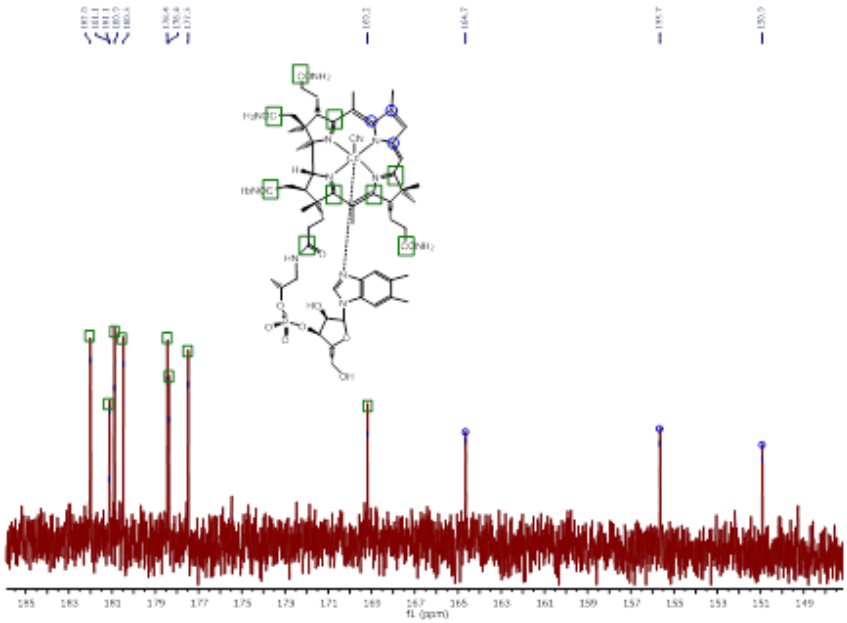

Figure 10. ^{13}C NMR spectrum of **5**. Quaternary carbons are marked in green (A-, C-, D-rings and side chains) and blue (B-ring).

A green by-product (**6**, Figure 8) was also identified within the reaction mixture of the ring-closure reaction with $NaBH_4$ (1.5 equiv). Mass spectrometry studies revealed the presence of a mixture of m/z = 1269.6 $[M\text{-}H_2O]^+$ and m/z = 1296.6 $[M+H]^+$ that was quantitatively converted to m/z = 1296.6 $[M+H]^+$ upon addition of an excess of KCN (Figure 11). With this data and having characterized **5** as a B_{12} derivative lacking the b- and c- side chains, the structure of the new green compound **6** was tentatively assigned assigned as Co$_\beta$-cyano-Δ^7-dehydro-7-decarboxymethyl-cobalamin. A possible mechanism for the conversion of green 7,8-*seco*-corrinoids **2** and **3** into **6** involves the reduction of the ketone at C8 to an alcoholate with $NaBH_4$ (Scheme 18, left) and a subsequent [2+2] cycloaddition between the alcoholate moiety and the double bond at C7-C71 (Scheme 18, middle).

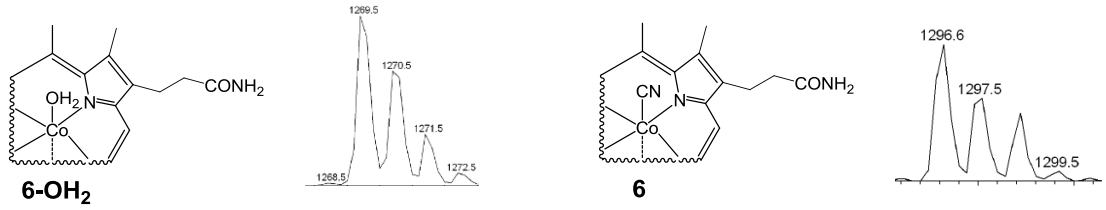

Figure 11. Experimental MS isotopic pattern of **6-OH$_2$** and **6**.

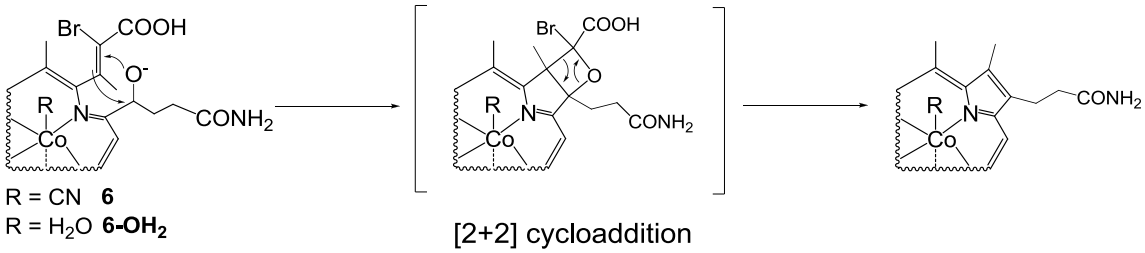

Scheme 18. Proposed mechanism for the formation of **18**.

5 and **6** represent the first examples of "complete" corrinoids with missing side chains reported so far. Until now, such compounds have only been studied using hydrophobic models of vitamin B_{12} (i.e. 'pyrocobester, see section **1.7.2.**).[96] Recent work by Kräutler has described the redox chemistry of such modified corrin derivatives.[101] Remarkably, **5** and **6** were obtained at 23 ºC, highlighting that heat is not the only possible driving force to form these compounds.

The transformation of 7,8-*seco*-corrinoids to **4** was achieved in 33% yields using $NaBH_4$ for triggering a ligand-centered reduction. However, the Co^{III} center is partially reduced under these conditions leading to the formation of several side-products. Aiming to improve chemoselectivity in the reductive B-ring closure and to protect the Co^{III} center against reduction, other reducing agents were tested.

3.1.2. Reconstitution of the B-ring using cobaltocene: cyanide as inorganic protecting group

As described in section **3.1.1.** (Scheme 17), a plausible mechanism for the corrin reconstitution of 7,8-*seco*-corrinoids **2** and **3** involves the formation of a radical at C8. According to this assumption, the main stimulus needed to initiate the reaction is the donation of one electron to the secocorrinoids **2** or **3** at their C8 position. Therefore, the one-electron reducing agent cobaltocene ($CoCp_2$) was applied to **2** or **3** as an alternative to $NaBH_4$.

When 2 equiv of $CoCp_2$ (E = -0.750 V vs. Ag^+/AgCl in MeOH)[102] were added to **2** under inert atmosphere a metal-centered reduction (Co^{III} to Co^{II}) was observed. If the reaction mixture was bubbled with air after 30 min of reduction, **2-OH$_2$** (m/z = 711.72391 $[M]^{2+}$, m/z_{calc}: 711.72340) was obtained (Scheme 19, top). Surprisingly, a partial reduction of the corrin ligand was only observered if the reaction mixture was stirred for 120 min in the presence of $CoCp_2$, leading to **4-OH$_2$** after reoxidation with air (Scheme 19, bottom). The observed reactivity differs notably from the ligand-centered reduction of 7,8-*seco*-corrinoids **2** and **3** when $NaBH_4$ was used (section **3.1.1.**).

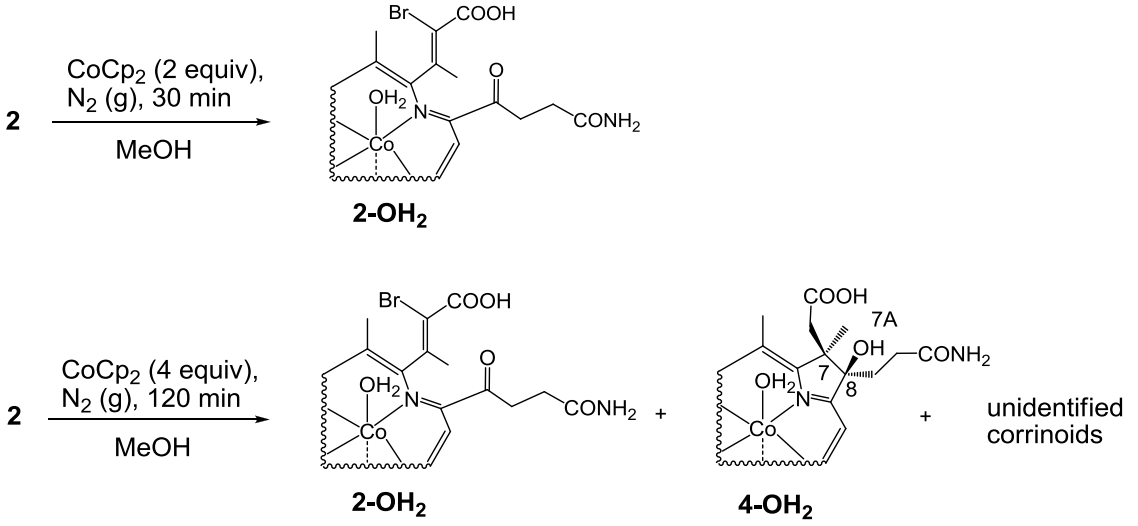

Scheme 19. Metal-centered reduction of **2** with $CoCp_2$.

Aiming for a chemoselective corrin reconstitution between C7 and C8, a protecting group for the Co^{III} center at **2** was envisaged. The coordination of a second axial cyanide is a straightforward reversible process that lowers the reduction potential of Co^{III} by up to 400 mV.[38,103] Indeed, when $CoCp_2$ is added to **2-CN** under the same reaction conditions as described above, an immediate colour change from dark green to violet was observed (Scheme 20). UPLC-MS analysis revealed quantitative conversion to **4-CN** (t_R = 1.7 min, 1372.5 $[M\text{-}CN+H]^+$). After deprotecting the Co^{III} center under slightly acidic conditions (pH 6), **4** was obtained in quantitative yields. This reaction represents the first example in which inorganic cyanide is used as a protecting group in natural product synthesis.

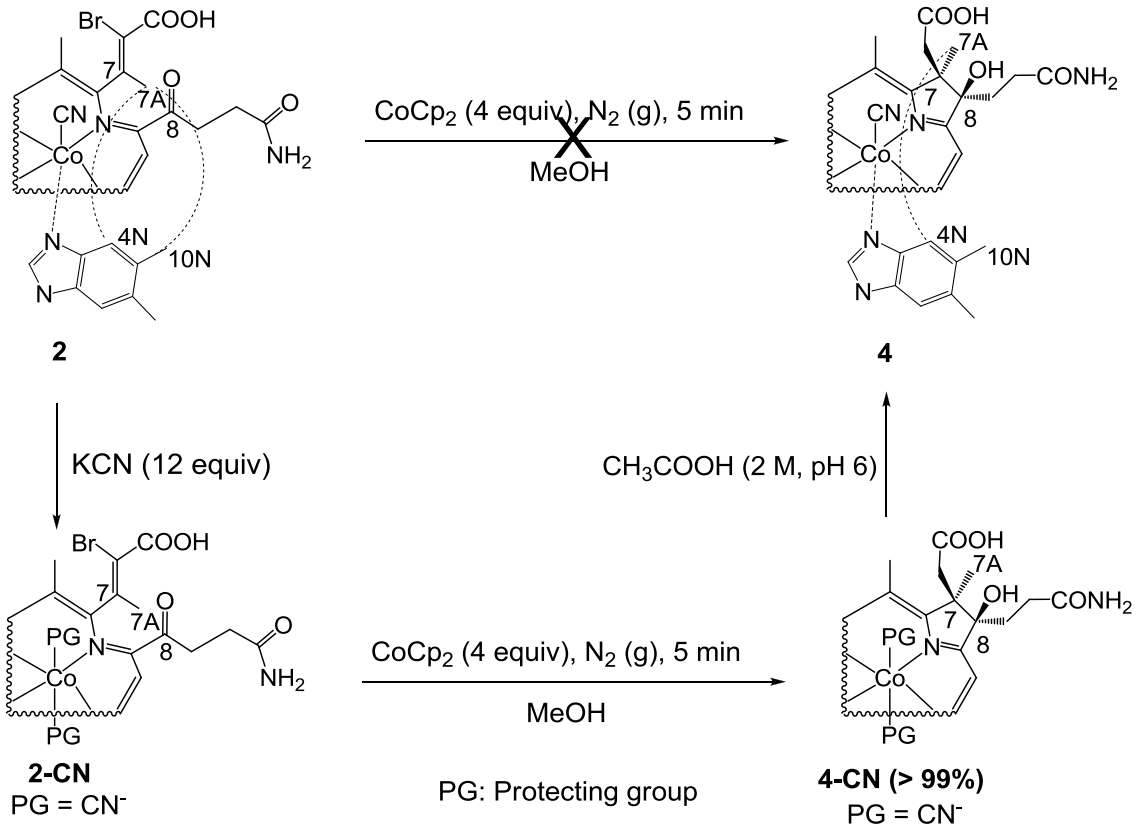

Scheme 20. Synthesis of **4-CN** from **2-CN**. Dotted lines in **2** and **4** indicate ^1H-^1H ROESY correlations.

3.1.3. Stereochemistry of Co$_\beta$-cyano-8-hydroxy-cobalamin-c-acid (4)

The orientation of the corrin side chains is fundamental for the biological activity of corrinoids.[22,100] In order to determine the stereochemistry of the c- and d-side chains in **4**, 1D and 2D NMR studies were performed (see section **6.3.**). Remarkably, C7A (δ = 1.87 ppm) showed a through-space ^{1}H-^{1}H ROESY correlation with C4N (δ = 6.45 ppm), demonstrating that the side chains at C7 have the same orientation as in natural Cbls (Scheme 20).

This orientation of the peripheral groups at C7 and C8 was confirmed by the reactivity of **4**: intramolecular esterification between the carboxylic acid at C72 and the alcohol group at C8 was completed overnight in quantitative yields, forming a new product (m/z = 1354.6 $[M+H]^+$) that contains a c-lactone on the B-ring . For steric reasons, such an esterification is only possible if both groups (carboxylic acid at C72 and alcohol at C8) are oriented towards the same side of the molecule. The spectra of this c-lactone containing compound were compared to those of Co$_\beta$-cyanocobalamin-c-lactone (**7**), a well-known oxidation product of vitamin B_{12}. Indeed, UPLC coinjections (Figure 12) as well as ^{1}H and ^{13}C NMR studies (Figure 13) revealed that **7** can also be synthesized from 7,8-*seco*-corrinoids **2** and **3**. In turn, this means that the peripheral groups at C8 are also oriented as observed in vitamin B_{12} and thus Co$_\beta$-cyano-8$_\beta$-hydroxy-cobalamin-c-acid (**4**) was formed.

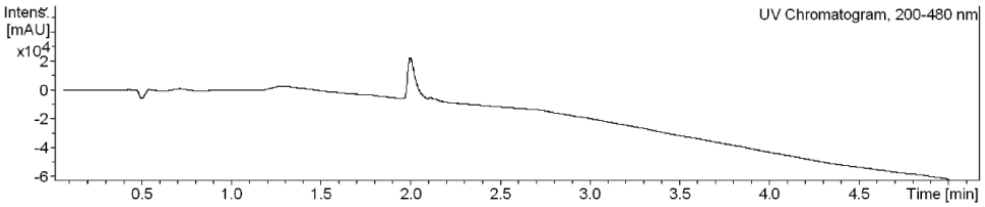

Figure 12. UPLC coinjection of **7** synthesized a) from vitamin B_{12} (**1**) and b) from green secocorrinoids (**2** or **3**).

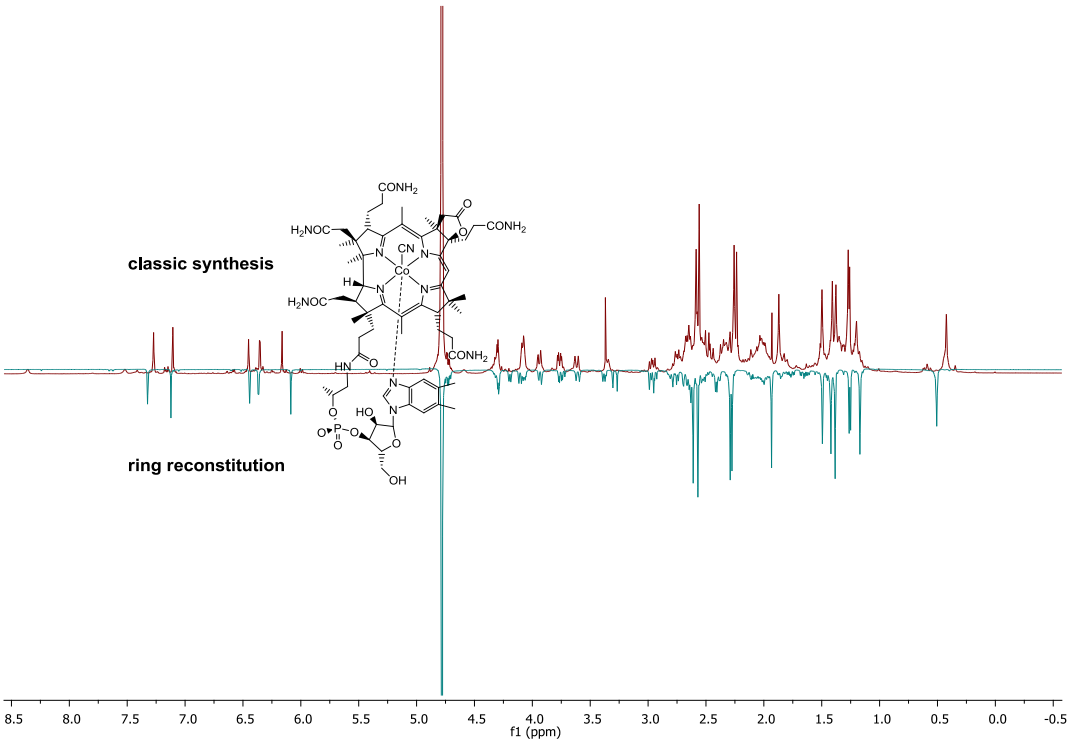

Figure 13. ^{1}H NMR spectra of **7** synthesized from B_{12} (red) or from **2** or **3** (green).

3.1.4. Ring-closure experiments with rearranged green secocorrinoids

A rearrangement of the methyl group C7A and the halogen atom at C71 occurs when **2** or **3** are stirred at 23 ºC in an aq. soln. (Scheme 21), according to crystallographic and spectroscopic data (NMR, UV-Vis) collected by Dr. René Oetterli.[98]

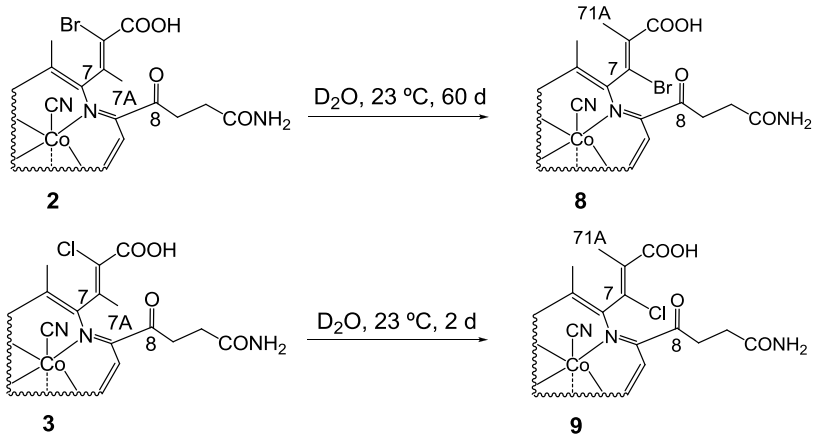

Scheme 21. Rearrangement of **2** and **3** to **8** and **9**.

The optimized reaction conditions for the reductive B-ring closure of 7,8-*seco*-corrinoids (see section **3.1.1.** and **3.1.2.**) were also applied to **8** and **9**. Thus, when $NaBH_4$ was added to **8** or **9** an immediate colour change from green to red showed the reconstitution of the corrin macrocycle. Importantly, UPLC-MS analysis after 1 h (Figure 14) showed the formation of a single corrinoid with either a cyano (**10**, m/z = 687.3 $[M+2H]^{2+}$) or an aqua upper axial ligand (**10-OH$_2$**, 673.5 $[M-H_2O+2H]^{2+}$). Addition of stoichiometric amounts of KCN led to the formation of a new product (**10)** in quantitative yields. Contrary to the reactivity of **2** and **3**, the reductive ring-closure of **8** and **9** in the presence of $NaBH_4$ yielded a single product. As expected, **10** was also obtained in quantitative yields when $CoCp_2$ was applied to the cyanide-protected species **8-CN** or **9-CN**. However, when a soln. of **10** was stirred overnight at pH 2, UPLC-MS studies showed no significant changes in t_R or exact mass, demonstrating that no intramolecular esterification took place between C72 and the OH group at C8 in **10**. This observation points towards a different orientation of the B-ring peripheral groups in **10** compared to **4**.

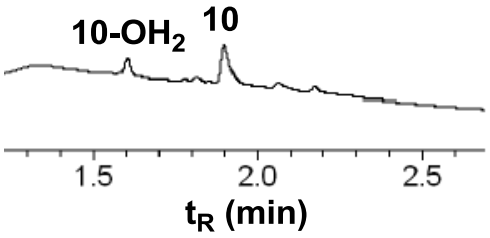

Figure 14. UPLC trace (Method 1, see Materials and Methods) of reaction mixture after 1 h.

In order to determine a) the orientation of the peripheral groups at the B-ring and b) the position of the methyl group C7A (C71A in **8** and **9**) after the reductive ring closure, 1D and 2D NMR studies were conducted with the new compound (**10**). According to ^{1}H NMR analysis, the methyl group corresponding to C7A in **4** (δ = 1.87 ppm) is shifted upfield in **10** (δ = 1.35 ppm, $\Delta\delta$ = 0.52 ppm). Additionally, ^{1}H-^{13}C HMBC analysis of **10** showed correlations between C7A and C6, C7, C71 and C8, demonstrating that this –CH_3 is still located on C7 (Scheme 22). Since no other major changes were found in the ^{1}H or ^{13}C spectra of **10** in comparison to **4**, it was concluded that the stereocenter at the c-side chain has now an unnatural configuration, with the methyl group bound directly to C7 but pointing to the upper side of the corrin. This means the methyl group C71A at the rearranged 7,8-*seco*-corrinoids **8** and **9** migrates back to C7 under reducing conditions and is oriented to the upper side of the corrin macrocycle (C7A, Scheme 22, right). The lack of reactivity of **10** under acidic conditions hints towards a hydroxyl group at C8 oriented towards the β face of the corrin. Therefore, this group cannot undergo intramolecular esterification with the α oriented carboxylic acid at C72 due to steric hindrance. Thus, Co$_\beta$-cyano-8$_\beta$-hydroxy-7-epicobalamin-c-acid (**10**) originated (Scheme 22, right).

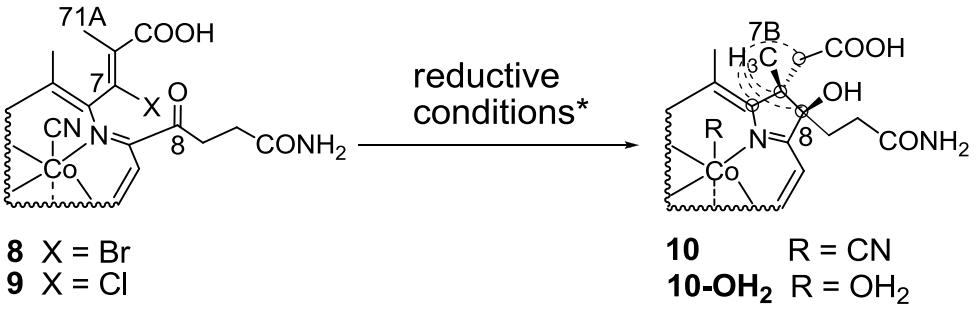

8 X = Br
9 X = Cl

10 R = CN
10-OH$_2$ R = OH$_2$

*$NaBH_4$ in H_2O or $CoCp_2$ in MeOH as described in **1.1.** and **1.2.** respectively

Scheme 22. Synthesis of **10** from **8** or **9**. Dotted lines represent ^{1}H-^{13}C HMBC correlations.

3.1.5. Demetallation experiments with 7,8-*seco*-corrinoids

The reversible procedures to cleave and repair the corrin macrocycle between C7 and C8 in quantitative yields represent a straightforward route for the synthesis of modified secocorrinoids. Such routes are highly desirable in the context of this thesis since 1) distortion of the corrin macrocycle is a valid approach to demetallate corrinoids[85,94] and 2) it has been demonstrated in section **3.1.2.** that the reductive reconstitution of 7,8-*seco*-corrinoids is independent of the metal center and could therefore be transferred to secocorrinoids containing other metals than cobalt.

In order to specifically reduce the metal center while keeping the corrin ligand intact, $CoCp_2$ was used as a reducing agent for the base-on compound **2**. As a general approach, solns. of **2** were reduced for 20-30 min under inert atmosphere to afford a Co^{II}-containing 7,8-*seco*-corrinoid (**2**$^{\bullet}$, Scheme 23, middle) lacking the upper axial cyanide ligand. When UPLC-MS analysis confirmed the formation of the reduced form of **2**, a decomplexating agent was added (Scheme 23). Reaction conditions for this step and products are summarized in Table 1.

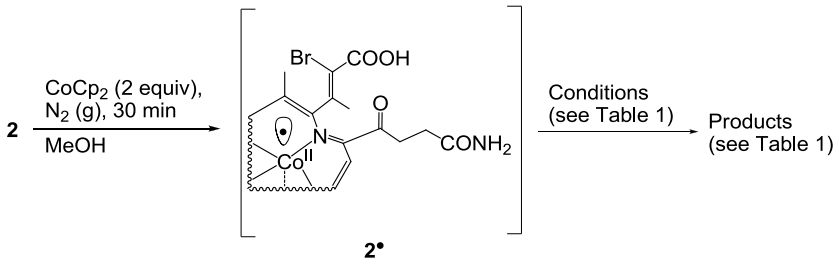

Scheme 23. General approach for the demetallation trials of **2**•.

Conditions	Products
2) EDTA, 105 ^{0}C, 3h, MeOH	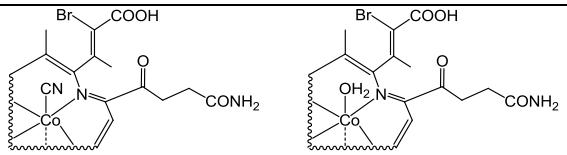 **2** **2-OH$_2$**
2) EDTA, 0.05% TFA, 105 ^{0}C, 3h, MeOH	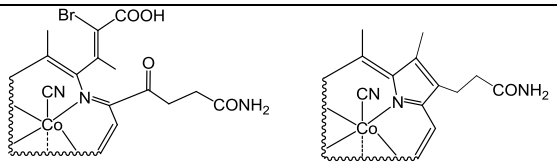 **2** **6**
2) EDTA, 0.05% TFA, 105 ^{0}C, 6h, MeOH	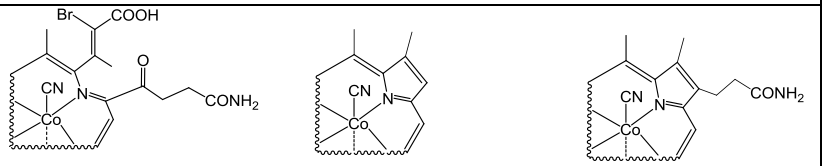 **2** **5** **6**
2) 80 ºC, 3h, ethylene glycol	Complex mixture
2) 78 ºC, 1h, H_2SO_4 conc	Complex mixture

Table 1. Reaction conditions tested and products of the attempted demetallation of **2**.

Unfortunately, no metal-free corrinoids were identified and the only products observed by UPLC-MS were either starting material or side-products from the metal and ligand reduction. Even though the B-ring is opened and cobalt is reduced to the more labile Co^{II} state, **2*** posesses an extended π-system that heavily protects the metal centre against demetallation. On the other hand, it is noteworthy that the presence of some acid (0.05 % TFA) at high temperatures (105 ºC) favors the formation of blue and green corrinoids **5** and **6**.

3.1.6. Stereospecific reconstitution of vitamin B_{12}

The quantitative synthesis of **7** allowed the stereospecific reconstitution of vitamin B_{12} within two steps: 1) a reductive lactone opening with $NaBH_4$ and 2) a primary amide formation with NH_4Cl and *N*-(3-dimethylaminopropyl)-*N'*-ethylcarbodiimide hydrochloride (EDC·HCl) as coupling reagent (Scheme 24).[104] All in all, a stereospecific reconstitution of vitamin B_{12} from green 7,8-*seco*-corrinoids **2** and **3** was achieved in four steps.

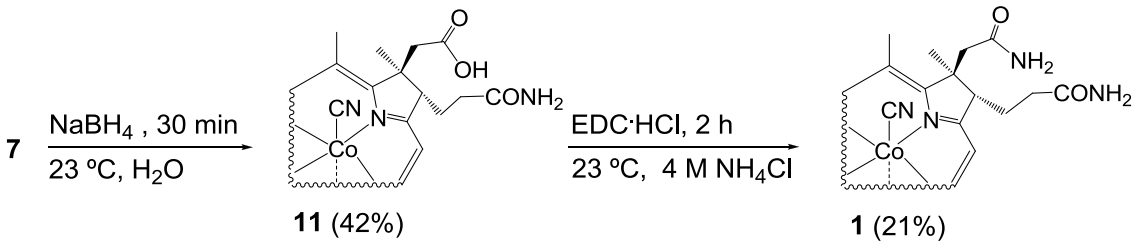

Scheme 24. Conversion of **7** to B_{12} (**1**) in two steps.

The structures of these two last compounds (**11** and **1**) were elucidated by X-ray diffraction analysis. Single crystals were grown by vapour diffusion of acetone into **11** or **1** (1 mM). As the crystals were weakly diffracting on a molybdenum source and X-ray fluorescence was observed when using copper radiation, both crystals were finally measured with the help of a gallium source by Prof. Bernhard Spingler and Dr. Markus Neuburger (University of Basel). As anticipated by previous spectroscopic data, the orientation of all stereocenters is identical to those observed in naturally occurring B_{12} (Figure 15).

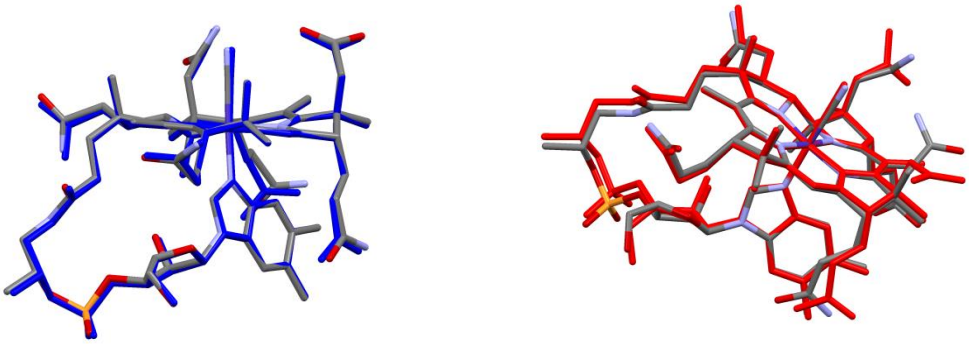

Figure 15**.** *Left*: overlay of the X-ray structures of **1** (blue) and **11** (normal element colours). *Right*: overlay of **1** (normal element colours) and a reference structure of vitamin B_{12} (red).

As described in section **3.1.1.**; when the ring closure reaction was performed with $NaBH_4$ in deuterated solvents, bideuterated **[D$_2$]-4** was obtained as main product and transformed in **[D$_2$]-7** overnight under acidic conditions (pH 2). Following the same synthetic route described above in Schemes 17 and 24, bideuterated B_{12} (**[D$_2$]-1**) was obtained (m/z = 1357.6 $[M-H+2D]^+$). Compared to **1**, the ^{1}H NMR spectrum of **[D$_2$]-1** differs only in the absence of a duplet at δ = 2.2 ppm and a slightly flater multiplet at δ = 2.0 ppm, plausible peaks for the missing CH_2 group at C81 (Figure 16).

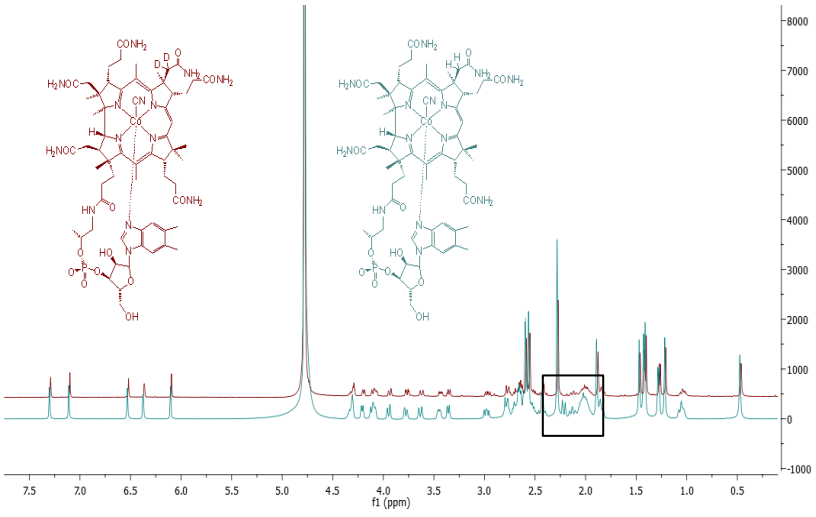

Figure 16. Overlapped ^{1}H NMR spectra of **1** (green) and **[D$_2$]-1** (red). The only differences between both spectra are highlighted.

In conclusion, a reversible four-step route for the stereospecific reconstitution of vitamin B_{12} (**1**) from B-ring opened 7,8-*seco*-corrinoids **2** and **3** was developed (Scheme 25).[105] These green secocorrinoids were previously synthesized in a two-step route according procedures developed earlier in our group.[98,99] The whole six-step route from **1** represents a promising approach for exploring B-ring modified B_{12} derivatives. The ring-closure step of the corrin macrocycle is a potential source of numerous chemical modifications of vitamin B_{12} with modified electronic properties (Scheme 15). Furthermore, procedures were optimized until the corrin macrocycle could be disrupted to a secocorrinoid and reconstituted in quantitative yields and without the use of time-consuming purification techniques. These synthetic methods are unprecedented in the normally low-yielding vitamin B_{12} chemistry and could therefore facilitate the production of new modified corrinoids for catalytic, sensing and medicinal applications.

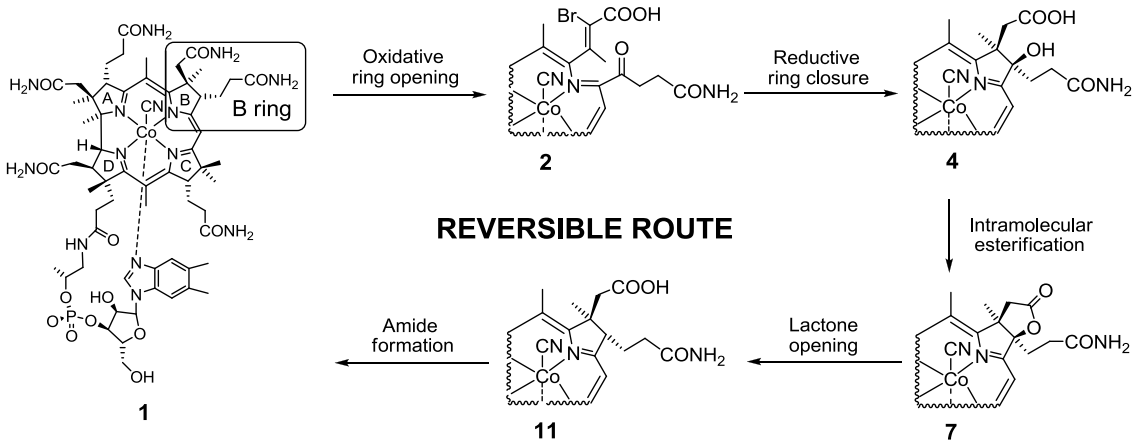

Scheme 25. Six-step reversible route for the cleavage and reconstitution of the corrin macrocycle of B_{12}.

3.2. Synthesis of metbalamins from 5,6-*seco*-corrinoids

This chapter summarizes efforts to synthesize metbalamins from dicyano-5,6-*seco*-corrinoids (Scheme 26). First, dicyano-5,6-dioxocobalamin (**13**) was obtained from the photooxygenation of B_{12} described in section **1.7.2.** (see Scheme 10). Subsequently, chemical and electrochemical methods to demetallate **13** were implemented based on the extraction of labile Co^{II} ions from the corrin cavity using cyanide as decomplexating agent. Next, reconstitution of the corrin macrocycle was partially achieved under reductive conditions. Remarkably, both steps (demetallation and corrin reconstitution) were later combined in a one-step reaction that led to a metal-free vitamin B_{12} derivative with a single C-C bond at C5-C6 (**23**). Finally, insertion of Ni^{II}, Cu^{II} and Zn^{II} in the metal-free corrin cavity of 5,6-diol-H-balamin was achieved under mild conditions, leading to the synthesis of novel 5,6-diolmetbalamins (**22**, **24**, **25**, **26**).

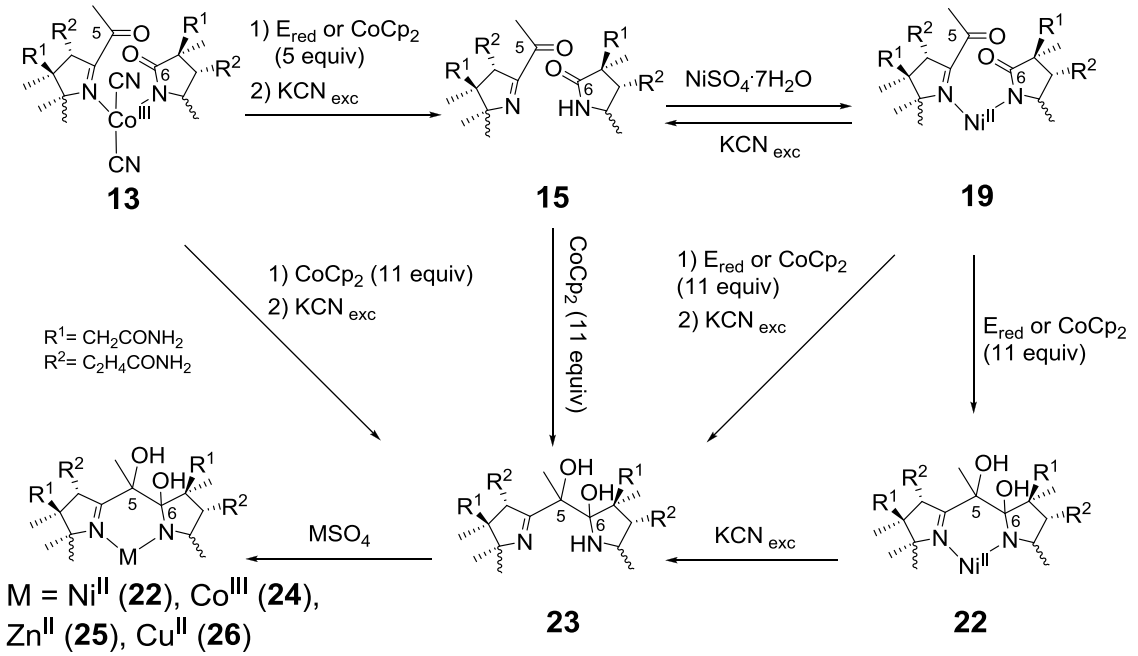

Scheme 26. Multi-step route for the synthesis of 5,6-diolmetbalamins (M = Ni^{II}, Cu^{II}, Zn^{II}). Charges are omitted for clarity.

3.2.1. Reactivity of 5,6-*seco*-corrinoids under reducing conditions: demetallation

As described in section **1.7.**, the photooxygenation of the corrin macrocycle can be applied to B_{12}, obtaining two dioxoisomers: dicyano-14,15-dioxocobalamin (**12**, Scheme 27, top) and dicyano-5,6-dioxocobalamin (**13**, Scheme 27, bottom). Since previous work in the group achieved the demetallation of **12** to form 14,15-dioxo-H-balamin (**14**, Scheme 28), it was envisaged to adapt this reaction for **13** and thus build a route towards metbalamins using 5,6-dioxocobalamins. Based on previous studies[71,99,106] and experiences described in chapter **1** of this thesis, the "northern" side of the corrin macrocycle has an enhanced reactivity for reversible modifications of its structure compared to the "southern" side. Therefore, 5,6-dioxocobalamins are potential starting materials for the synthesis of metbalamins.

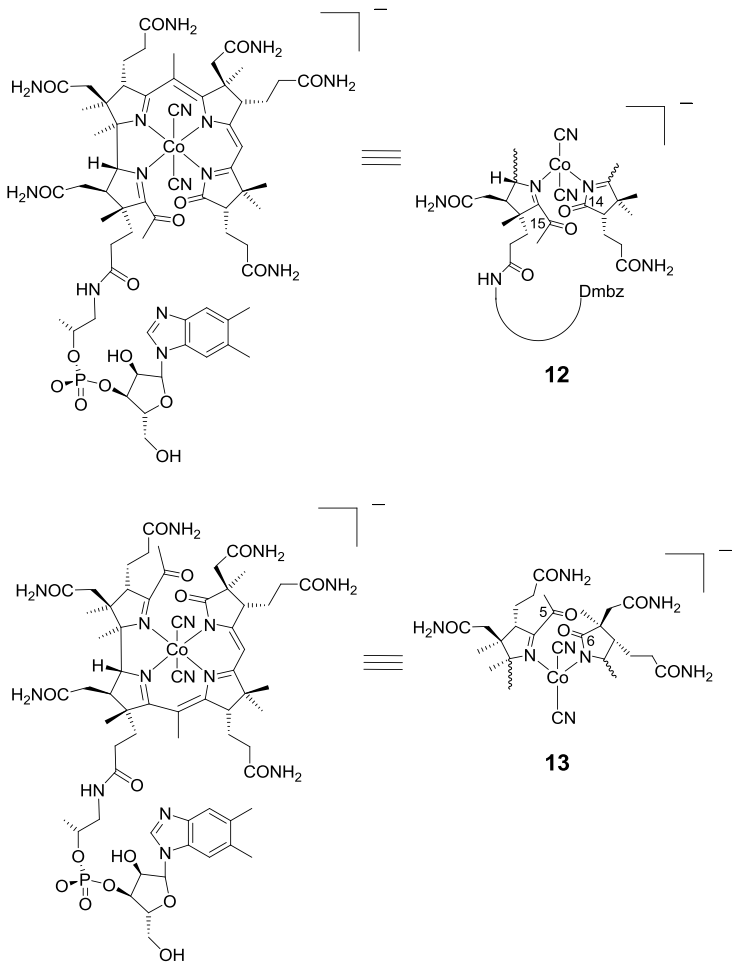

Scheme 27. Structure and schematic representation of dicyano-14,15-dioxocobalamin (**12**) and dicyano-5,6-dioxocobalamin (**13**).

Earlier studies: "southern" face modifications

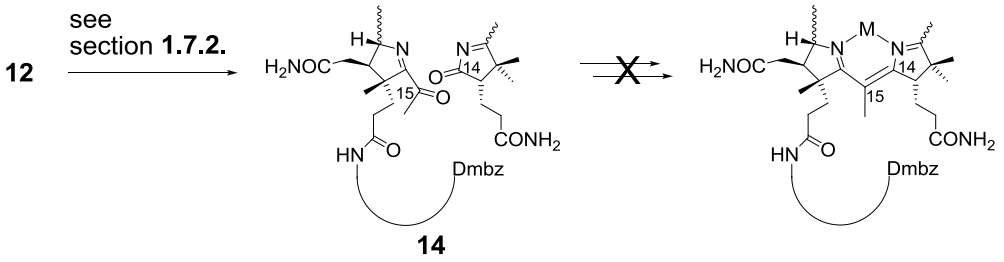

This work: "northern" face modifications

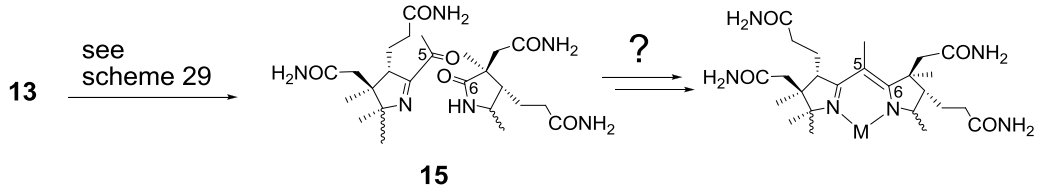

Scheme 28. Demetallation of dioxocobalamins **12** and **13**. Charges are omitted for clarity.

Accordingly, the first goal of this project was to develop a reproducible method to demetallate **13**. Based on earlier experiences with **12** (see section 1.7.2.), the metal center was first reduced from the inert Co^{III} to a more labile Co^{II} oxidation state and subsequently extracted from the corrin macrocycle by adding a decomplexating agent.[99] The electrochemical reduction was optimized adapting voltage, pH, temperature and time. The best reaction conditions were found when a voltage of -0.90 V (vs. Ag/AgCl 3M) was applied to an electrolyte soln. (0.1 M TRIS pH 8.1) containing **13** (0.8 mM) for 2 h at 50 ºC. Subsequently an excess of KCN (100 equiv) was added to the reduced soln. containing intermediate **A** (Scheme 29) and cobalt was instantly removed from the core of the macrocycle, obtaining 5,6-dioxo-H-balamin (**15,** Scheme 29, right) in 22% yield, as observed by the rapid color change of the soln. from dark brown to pale yellow.

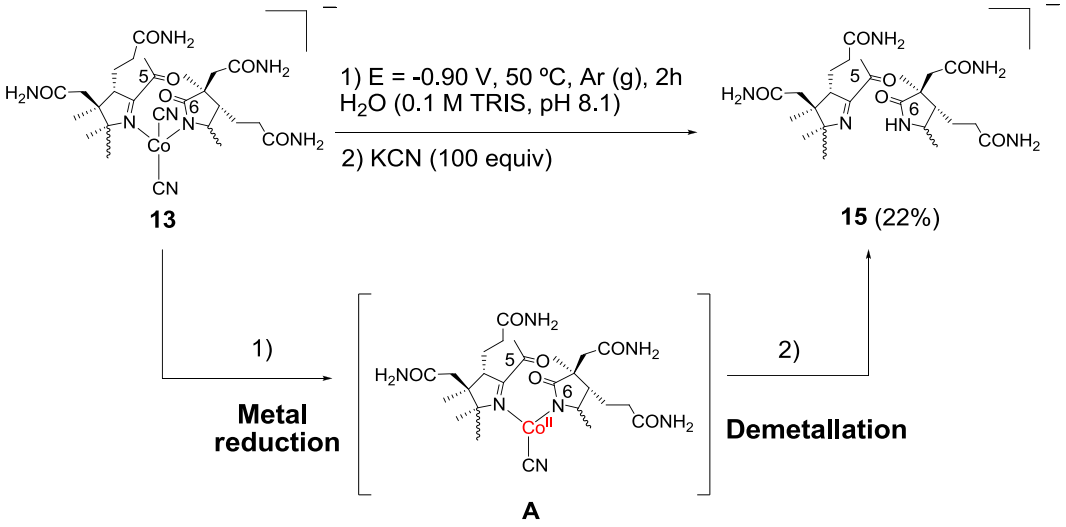

Scheme 29. Electrochemical demetallation of **13**.

The metal-free compound **15** is a yellow corrinoid with an absorption maximum at 379 nm (log ε = 3.9) at pH 7 (Figure 17). MS analysis of **15** shows a single peak at m/z = 1302.63042 $[M]^-$ (m/z_{calc} = 1302.62933) (Figure 17) and its ^1H NMR spectrum typical for a base-off corrinoid (Figure 18). This data confirms that the extraction of the cobalt ion from **13** to form **15** causes no change in the delocalized π-electronic system of the secocorrin macrocycle. Surprisingly, **15** is highly stable in soln. at pH 10 (no significant change in its structure is found after 1 month according to UPLC-MS analysis). However, **15** degrades to undetermined side products after some minutes at pH 2, the main one with m/z = 1285.6 $[M]^-$.

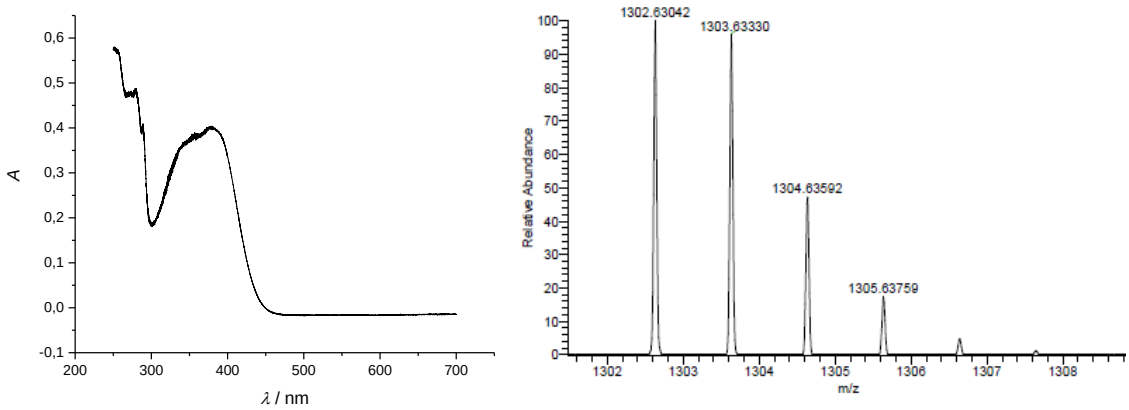

Figure 17. UV-Vis (H_2O, c = 4.5 x 10^{-5} M) and HR-MS spectra of **15**.

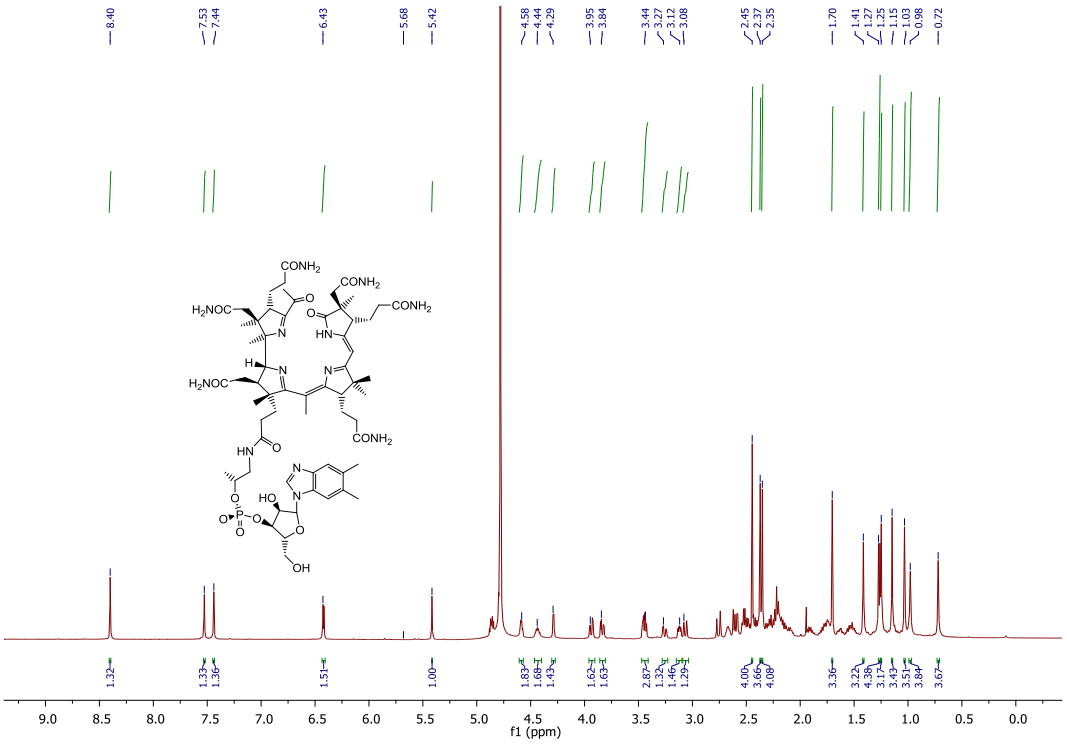

Figure 18. ^{1}H NMR spectrum of **15**.

3.2.2. Reactivity of 5,6-*seco*-corrinoids under reducing conditions: reconstitution of the corrin

The reactivity of 5,6-*seco*-corrinoid **13** was also studied by electrochemical means without addition of an excess of KCN as decomplexating agent. As described before (section **3.2.1.**), when the reduction of **13** was performed at E = -0.90 V for 2 h only the Co^{III} center was reduced, while the equatorial ligand remained unaltered according to spectroscopic data. However, when a slightly more negative voltage (E = -1.00 V vs Ag/AgCl 3M) was applied for a longer reaction time (> 2.5 h), additional reduction of the secocorrin ligand took place (Scheme 30). 16 equiv of KCN were subsequently added and HPLC purification under slightly acidic conditions (pH 5) yielded a lemon-yellow product with a broad band at 455 nm (logε = 3.8, Figure 19). The main band was shifted bathochromically by 18 nm (λ_{max} = 473 nm, Figure 19) upon addition of an excess of KCN (100 equiv), indicating the coordination of a second axial cyanide ligand. These absorption values are typical for cobalt-containing "stable yellow corrinoids" with an altered π-electronic system at the equatorial macrocycle due to the

presence of a single bond between C5-C6.[107] This assumption was also supported by UPLC-MS analysis (m/z = 1387.6 $[M]^-$), indicating the formation of aquacyano-5,6-diolcobalamin (**16,** Scheme 30). A plausible mechanism for the C-C bond formation at the "northern" face of the corrin ligand involves the reduction of the two keto moieties at C5 and C6 to ketyl radicals (intermediate B, Scheme 30) and a subsequent coupling of both radicals. Unfortunately, no reproducible demetallation of **16** was achieved under reducing conditions, even after the addition of a large excess of KCN (> 100 equiv).

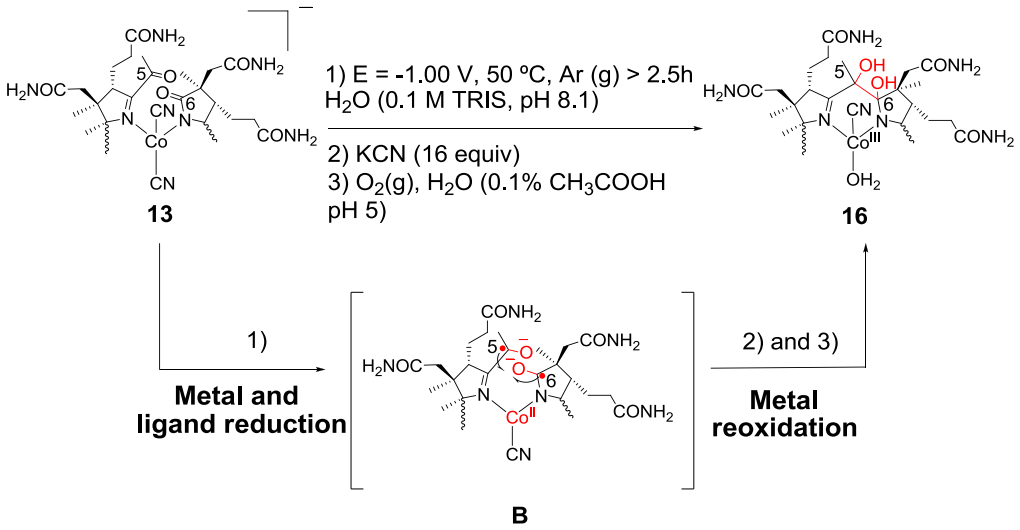

Scheme 30. Reductive ring closure of **13** to form **16**.

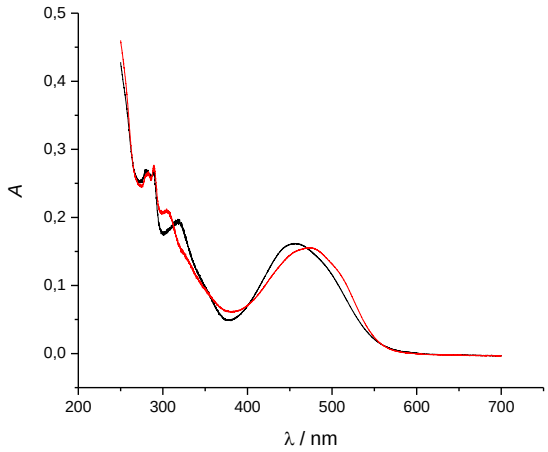

Figure 19. UV-Vis spectrum of **16** (black line) and **16-CN** (red line) (H_2O, c = 2.5 x 10^{-5} M).

3.2.3. A base-on 5,6-dioxocobalamin obtained by remetallation of 5,6-dioxo-H-balamin (15)

15 was stirred at 23 ºC under slightly basic conditions (H_2O, 0.1 M TRIS pH 8.1) in the presence of $CoSO_4 \cdot 7H_2O$ (5 equiv, Scheme 31, top). An immediate colour change from yellow to dark orange was observed and after 1 h, UPLC-MS analysis showed complete conversion to a cobalt-containing corrinoid with t_R= 3.5 min and m/z = 1360.6 $[M\text{-}OH_2]^+$ (Method 2, see Materials and Methods). ^{1}H NMR analysis of the crude mixture confirmed the formation of a single product with peaks corresponding to the Dmbz base (C2N, C4N and C7N) appearing at δ = 7.50, 7.43 and 7.39 ppm (Figure 20, top). The presence of the most downfield chemical shifts between 7 and 8 ppm is typical for base-on corrinoids.[108] According to this spectroscopic data, hydroxo-5,6-dioxocobalamin (**17**, Scheme 31) was obtained.

In order to compare the behavior of metal-free dioxoisomers **15** and **14** towards metallation, $CoSO_4 \cdot 7H_2O$ was also added to **14** under the same conditions described above (Scheme 31, bottom). In this case, the base-off corrinoid aquahydroxo-14,15-dioxocobalamin (**18**) was obtained according to ^{1}H NMR analysis (a Dmbz peak appears at δ = 9.9 ppm, Figure 20, bottom). This fact indicates a different chemical behavior of **14** and **15** upon cobalt insertion. Likely, when the cleavage occurs at a site spatially close to the f-side chain (C14-C15) unfavorable steric interactions hinder the coordination of the "loop" to the Co^{III} center. As a result, only in the "upper" oxidized corrinoid **17** the Dmbz base is able to coordinate a Co^{II} center through the lower axial position of the octahedral complex forming a corrinoid with a base-on configuration. Importantly, access to base-on corrinoids is an important requirement for transporting B_{12} surrogates with modified catalytic activity into cells (see section **1.3.**).[22,25,68]

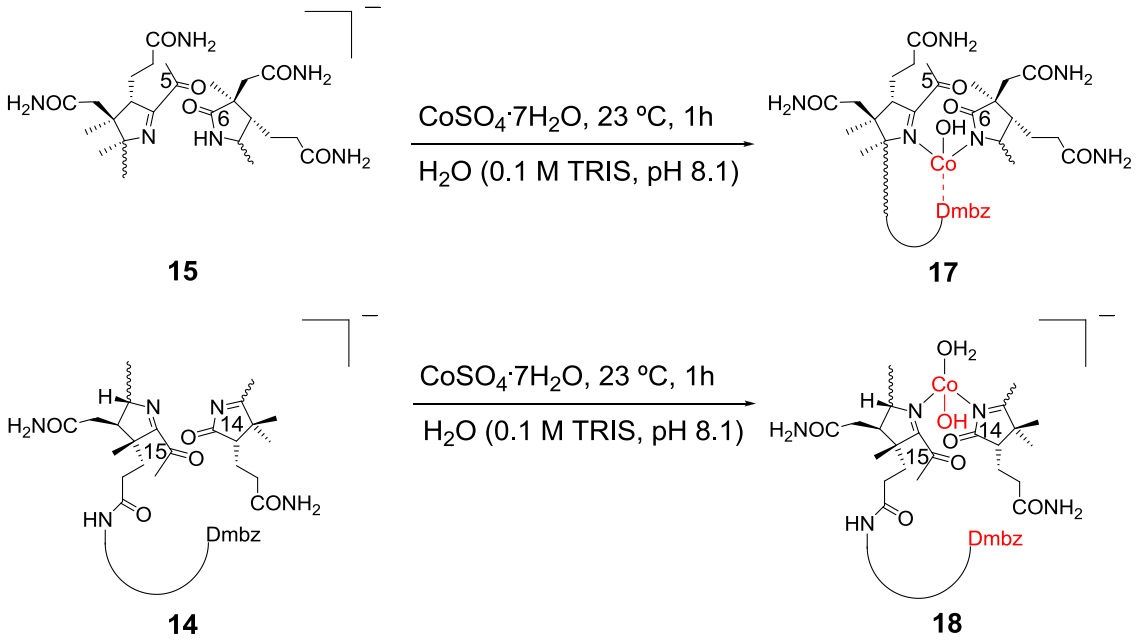

Scheme 31. Synthesis of base-on **17** and base-off **18**.

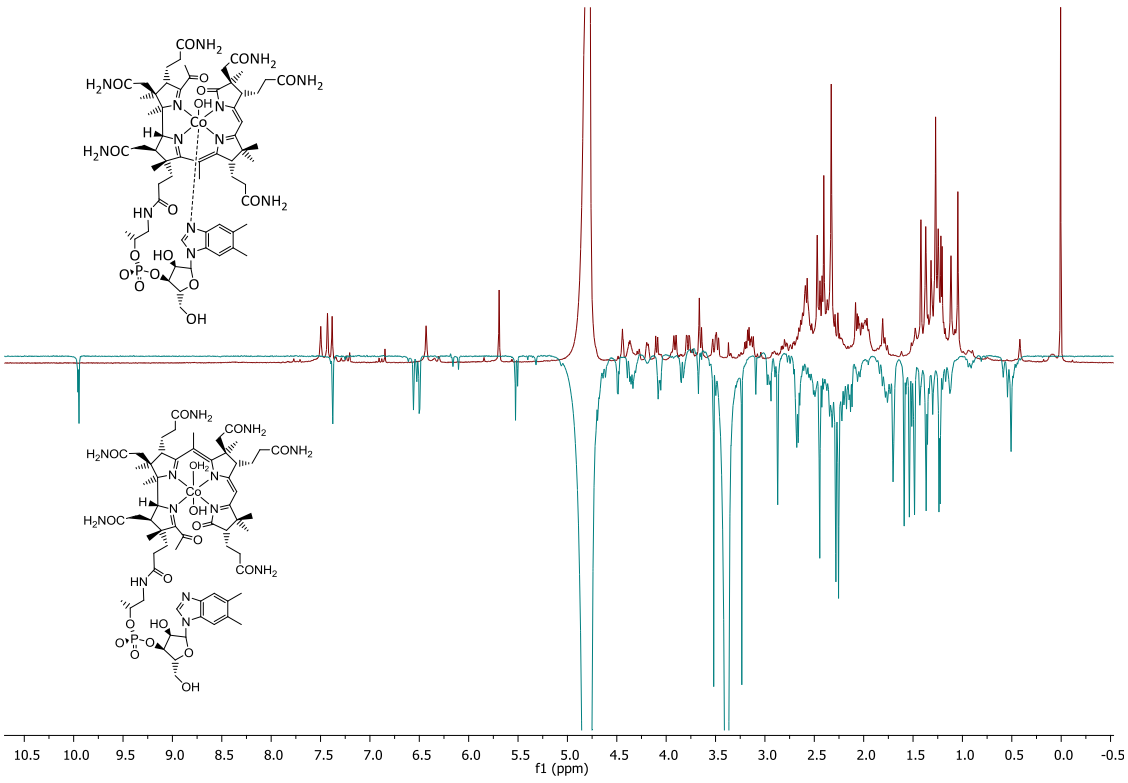

Figure 20. ^{1}H NMR of base-on **17** (top) vs ^{1}H NMR of base-off **18** (bottom).

3.2.4. Synthesis of dioxometbalamins

Having observed the straight forward incorporation of Co^{II} into **15**, the same method was tested with Ni^{II}. Satisfyingly, quantitative conversion to 5,6-dioxonibalamin (**19**) was observed within 1 h (Scheme 32), as confirmed by a batochromic shift of the main UV-Vis band to from 379 to 447 nm (logε = 3.8) and by HR-MS analysis (m/z = 680.78633, m/z_{calc} = 680.78543 $[M+2H]^{2+}$). ^{1}H NMR analysis proved that **19** is a diamagnetic complex (Figure 21), which in turn means a Ni^{II} complex with a square-planar d^8 configuration was formed. As expected for this geometry and in contrast to **17**, **19** is a base-off compound (δ_{Dmbz} = 8.36, 7.48 and 7.43 ppm). These results highlight that the corrin cavity of **15** is a suitable macrocyclic ligand for the incorporation of other metal ions than cobalt. Remarkably, quantitative conversion of **15** to Ni^{II}-containing **19** was completed using the same reaction conditions (time, temperature) as for the synthesis of Co^{III}-containing **17**. Compound **19** is stable under acidic (pH 2), neutral (pH 7) and basic conditions (pH 10). However, upon addition of an excess of KCN (100 equiv), **19** is partially demetallated over 30 min, as monitored by UV-Vis spectroscopy (Figure 22). Demetallation of **19** to **15** is quantitative after 48 h in the presence of KCN (pH 10), as observed by UPLC-MS (t_R = 2.5 min, m/z = 1302.6 $[M]^-$, Method 2, see Materials and Methods).

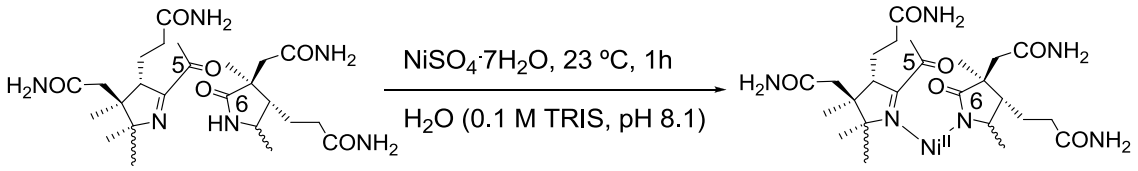

Scheme 32. Synthesis of **19**.

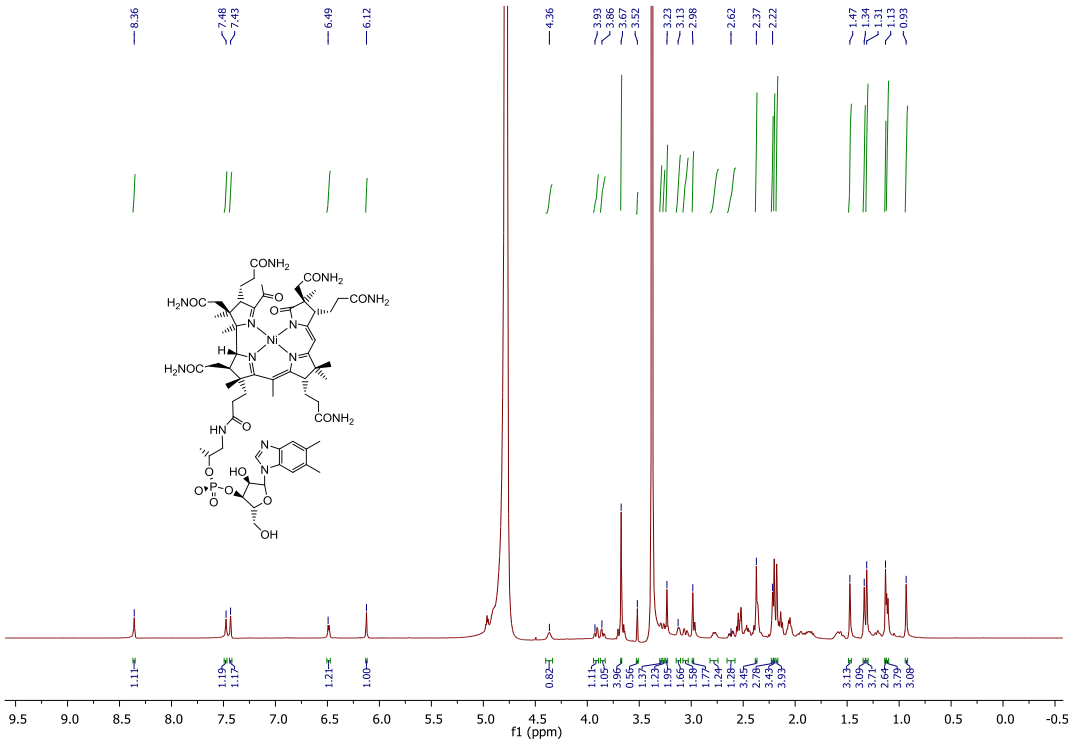

Figure 21. ^{1}H NMR spectrum of **19**.

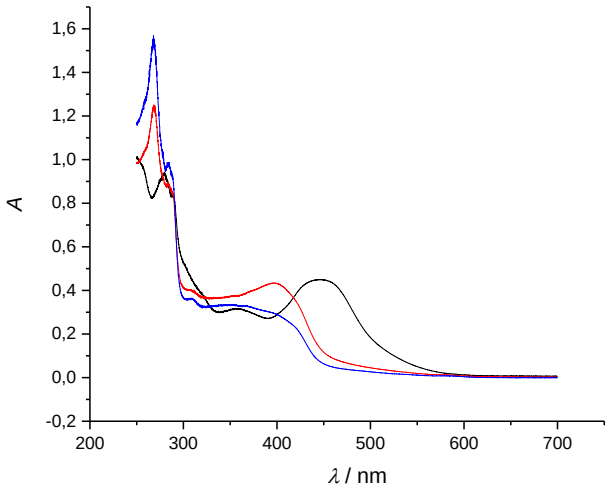

Figure 22. UV-Vis spectrum of **19** without KCN (black line) and with KCN (30 min, pH 10, red line; 48 h, pH 10, blue line).

After demonstrating that **15** is a suitable macrocyclic ligand for other metals than cobalt, 5,6-dioxozincbalamin (**20**) and 5,6-dioxocubalamin (**21**) were synthesized analogously (Scheme 33). **20** is a Zn^{II}-containg yellow compound (λ_{max} = 434 nm) with m/z = 1368.57403 $[M+H]^+$ (m/z_{calc} = 1368.57303) obtained in base-off configuration according to ^1H NMR analysis (δ_{Dmbz} = 8.73, 7.56, 7.37 ppm, Figure 23). While Ni^{II}-containing **19** could only be demetallated upon addition of an excess of KCN, Zn^{II} in **20** can be extracted from the corrin either with KCN (100 equiv) or in soln. at pH 2. The demetallation of **20** was indicated by hypsochromic shifts (Figure 22) in the UV-Vis spectrum. The coordination of Cu^{II} to form 5,6-dioxocubalamin (**21)** was observed by a batochromic shift in the UV-Vis spectrum (λ_{max} = 447 nm) but the paramagnetic nature of this complex hindered further structural studies by NMR.

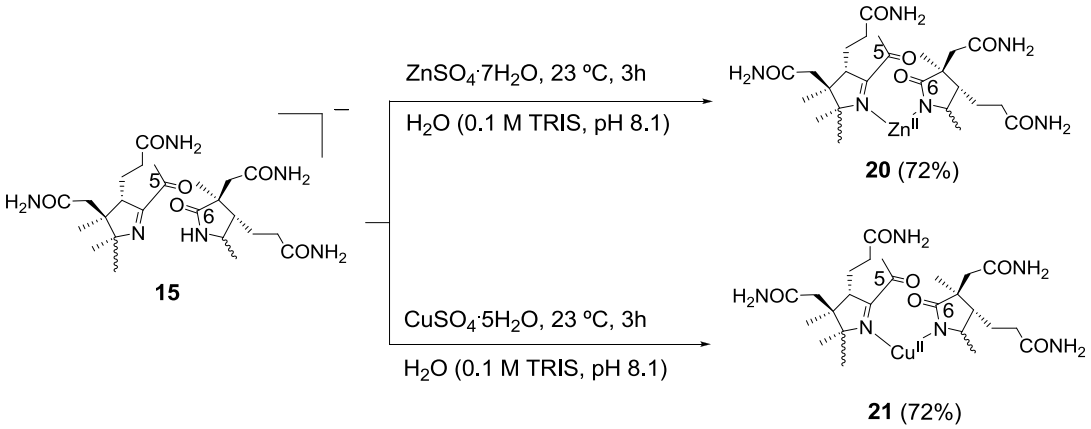

Scheme 33. Synthesis of **20** and **21**.

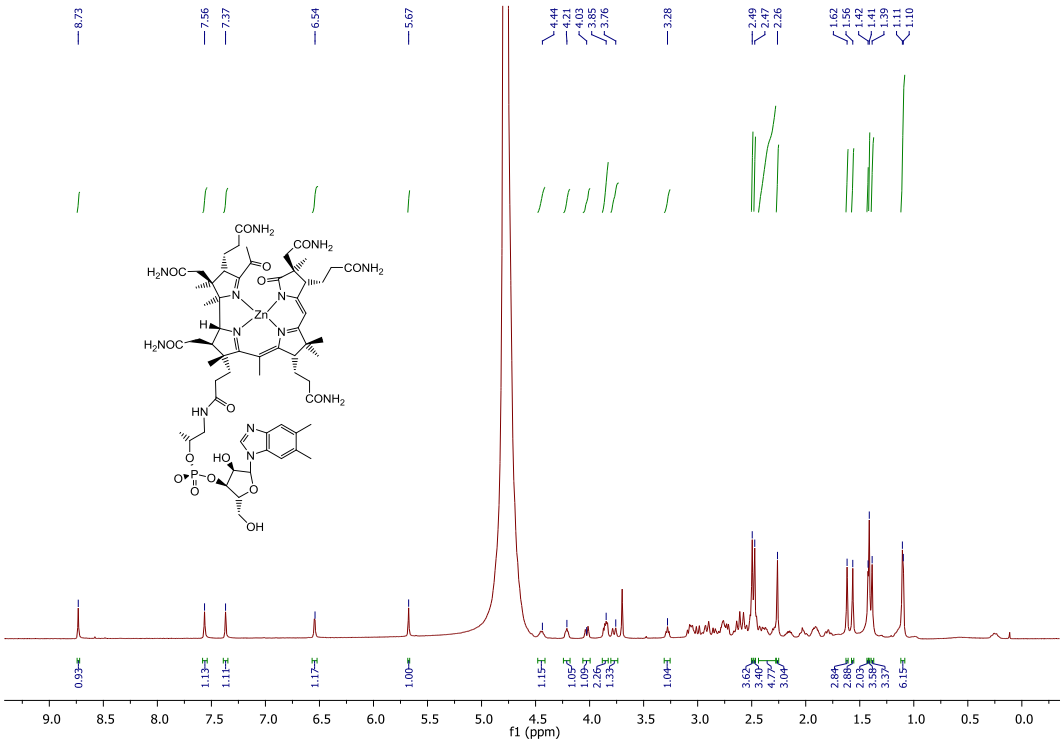

Figure 23. ^{1}H NMR spectrum of **20**.

3.2.5. Reactivity of 5,6-dioxonibalamin (19) under reducing conditions: demetallation and corrin reconstitution

The presence of a Ni^{II} ion allows **19** to resist harsh reaction conditions and provides a square planar geometry within the complex. It was envisaged that this geometry would allow the reconnection of positions C5 and C6 at the secocorrin. To achieve this goal, electrochemical reducing conditions (E = -1.00 V, 3h, see section **3.2.2.**) were applied to **19** (Scheme 34). Two main observations were made:

1) The metal ion is resistant to demetallation under reducing conditions. When a voltage of -1.00 V is applied to **19**, the soln. gradually gets a darker orange color. It is assumed that Ni^{II} can be reversibly reduced to Ni^{I}.
2) The ketone at C5 and the lactam at C6 in nickel-containing **19** are coupled under reducing conditions forming 5,6-diolnibalamin (**22,** m/z = 682.4 $[M+2H]^{2+}$), an analogous reaction to the formation of aquacyano-5,6-diolcobalamin (**16**). Concretely, three isomers of **22** were found in the reaction mixture (t_R = 2.4 min, 3.1 min and 3.5 min) according to UPLC-MS analysis (Figure 24, Method 2, see Materials and Methods), most likely due to the different possible orientations of the diol at C5-C6. As described in section **3.2.2.**, a pinacol-type reaction of C5 and C6 undergoing a radical C-C bond formation is envisaged (intermediate C, Scheme 34, middle).

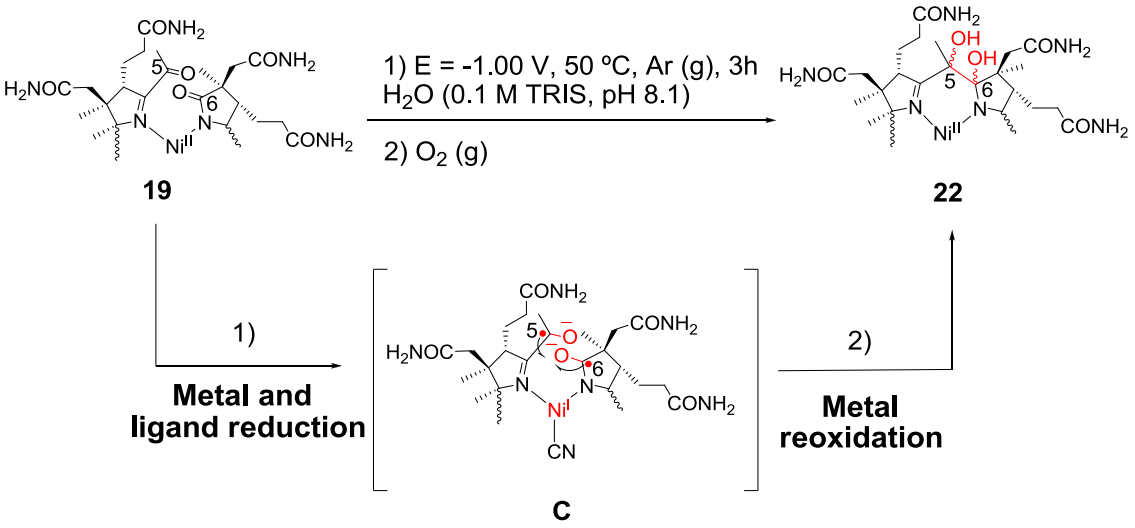

Scheme 34. Electrochemical synthesis of **22**.

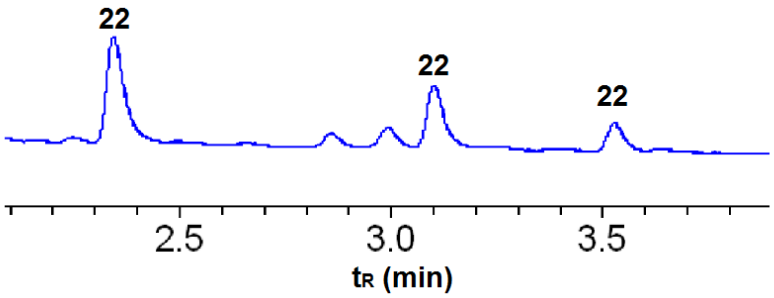

Figure 24. UPLC trace (Method 2, see Materials and Methods) of the crude mixture (see Scheme 34).

When an excess of KCN (100 equiv) was added to the reduced Ni^{I}-containing corrinoid, an immediate colour change from orange to yellow was observed (Scheme 35). UPLC-MS analysis revealed that out of the three nickel-containing isomers, the two most polar were quantitatively demetallated (Figure 25). This observation supports that labile Ni^{I}-corrinoids originate in this reaction, since such a fast demetallation is not observed with Ni^{II}-containing **19** (section **3.2.4.**). Thus, a ring-closed metal-free corrinoid (5,6-diol-H-balamin, **23**, m/z = 1304.6 $[M]^{-}$) was instantly synthesized. The metal-free isomers were isolated by preparative HPLC and analyzed by ^{1}H NMR, observing identical spectra for both compounds (Figure 26). With this data in hand, it is highly likely that the only difference between both isomers is the stereochemistry at C6.

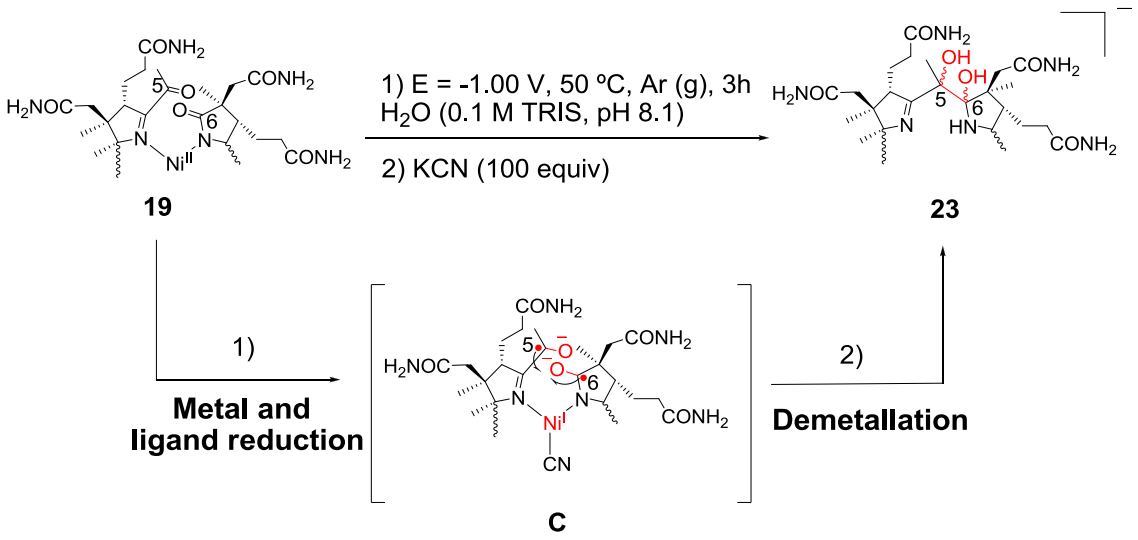

Scheme 35. Electrosynthesis of **23**.

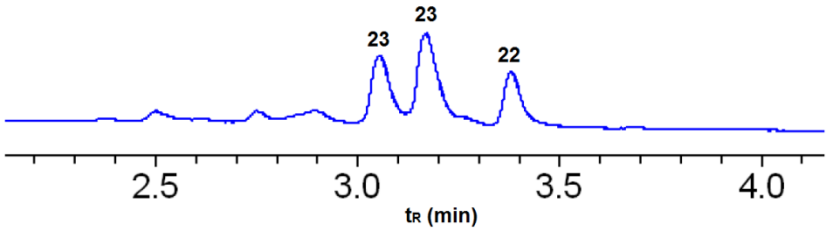

Figure 25. UPLC trace (Method 2, see Materials and Methods) of the crude mixture (see Scheme 35).

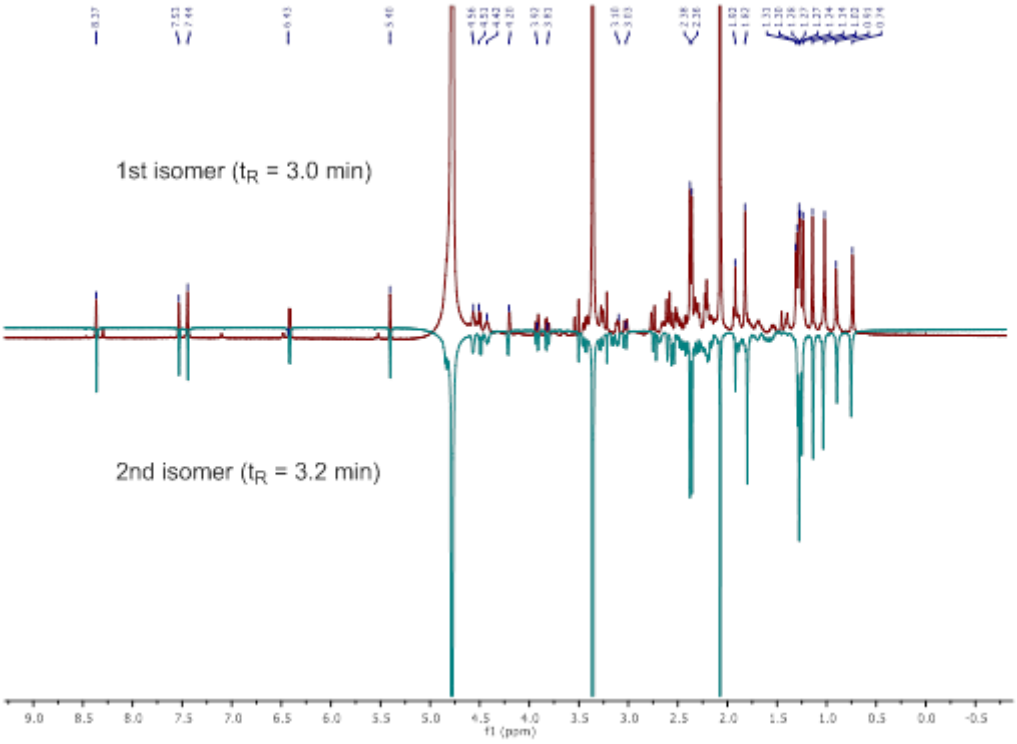

Figure 26. ^{1}H NMR spectrum of the first (t_R = 3.0 min) and second (t_R = 3.2 min) isomers of **23**.

In summary, the experiments described in sections **3.2.1.** to **3.2.5.** propose a 4-step route towards a ring-closed metal-free template of vitamin B_{12}. This route includes the following steps: a) photochemical cleavage of the corrin macrocycle, b) demetallation of an electrochemically reduced 5,6-dioxocobalamin, c) remetallation with Ni^{II} to a square-planar 5,6-dioxonibalamin and d) simultaneous C-C bond formation and demetallation to obtain the final product **23** (Scheme 36).

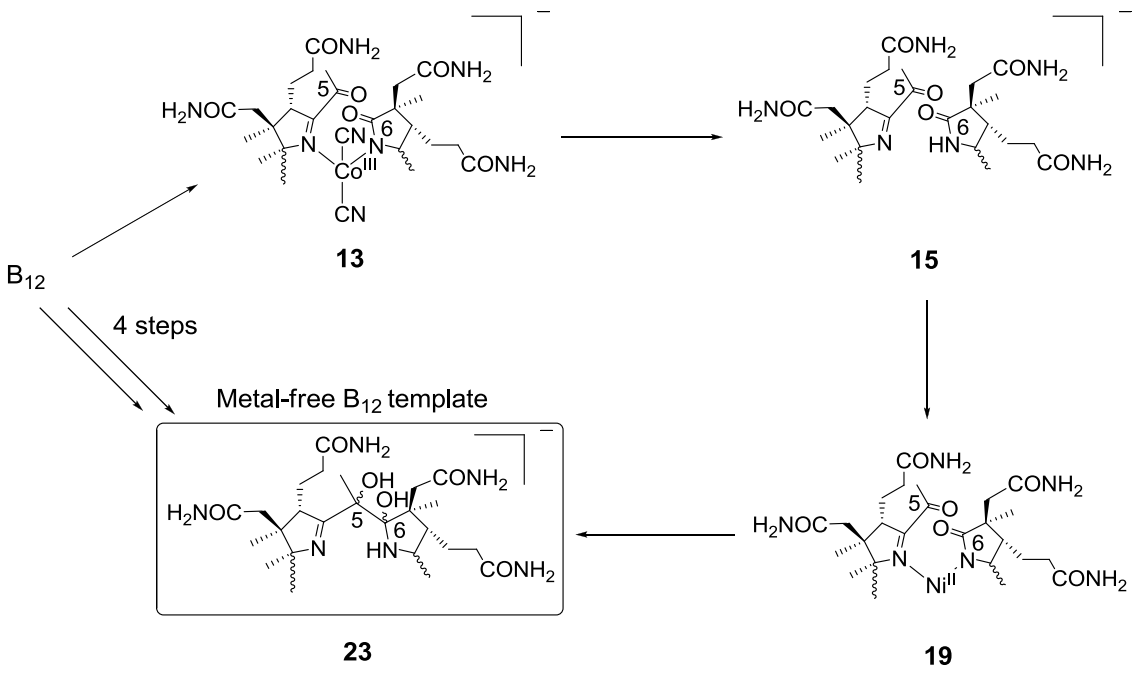

Scheme 36. 4-step route for the synthesis of **23** from vitamin B_{12}.

Even though this route achieves a reproducible synthesis of **23**, different isomers are obtained according to UPLC-MS analysis of the reaction mixture. Aiming for a stereospecific route involving less synthetic steps, further optimizations were pursued.

3.2.6. $CoCp_2$-mediated one-step synthesis of 5,6-diol-H-balamin from 5,6-dioxocobalamins

Seeking further developments in the synthesis of metal-free templates of vitamin B_{12}, a one-step demetallation and corrin reconstitution reaction starting from **13** to obtain **23** was envisaged. The prerequisites for such a simultaneous reaction are a) a metal reduction to labilize the cobalt center and b) a carbonyl reduction to complete a pinacol-type reaction. The latter step consists of a C-C bond formation similar to the one described in section **3.1.** of this work. Therefore, experiments with the one-electron reducing agent $CoCp_2$ were also performed with **13**.

The addition of $CoCp_2$ (5 equiv) to **13** caused an immediate color change of the soln. from blood-orange to dark red. After only 2 min, the addition of an excess of KCN (107 equiv) led to **15** (Scheme 37, path A). When a larger excess of $CoCp_2$ (11 equiv) was added to **13** in three portions over 20 min, not only the metal but also the corrin ligand was reduced at positions C5 and C6 (Scheme 37, path B). Thus, the main product obtained after the addition of cyanide was **23** (m/z = 1304.6 $[M]^-$, λ_{max} = 383 nm, log ε = 4.0). In this case, the reaction was stereospecific and only one isomer (t_R = 2.7 min) of the metal-free compound was obtained in 23% yields. ^{1}H NMR analysis of this isomer was compared to the spectrum of one of the isomers of **23** synthesized by electrochemical reduction (see section **3.2.5.**). The main difference in the spectrum is the change in the chemical shift of the methyl group at C51 ($\Delta\delta$ = 0.38 ppm, Figure 27), indicating a different orientation of C51 and therefore suggesting that the stereospecific synthesis yields a new isomer with different stereochemistry at C5. Subsequently, the ^{1}H NMR spectra of 5,6-diol-H-balamin (**23**) and 5,6-dioxo-H-balamin (**15**) were also compared: the two spectra are indeed very similar, showing only noticeable shifts for the methyl groups at C51 and C151, as expected for the different electronic environments of both compounds at the bridging *meso* positions of the corrin macrocycle (Figure 28).

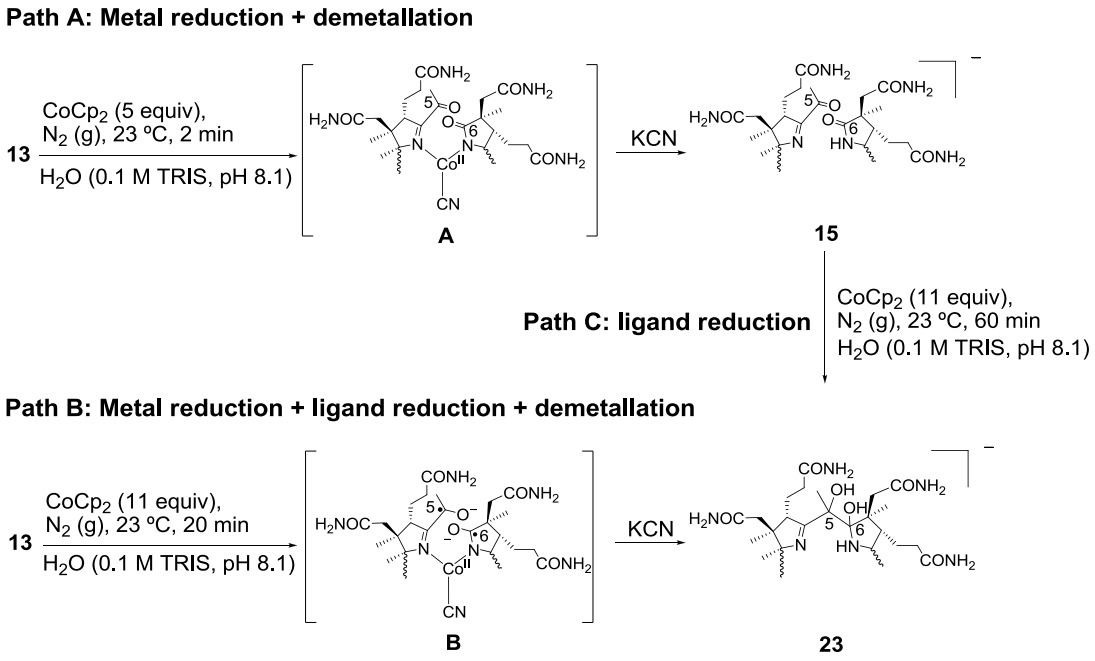

Scheme 37. Synthesis of **23** with $CoCp_2$ following a two-step (Path A + C) or a one-step (Path B) procedure.

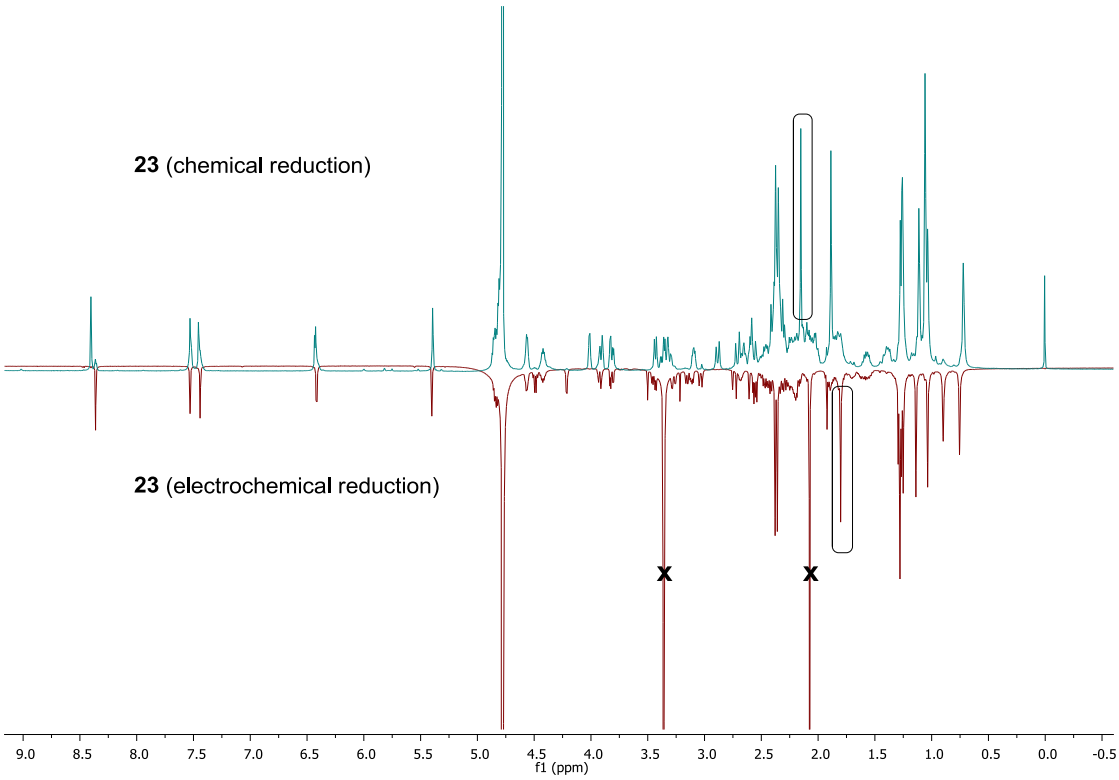

Figure 27. ^{1}H NMR spectra of **23** synthesized by chemical (top) or electrochemical (bottom) reduction. Peaks corresponding to C51 are highlighted.

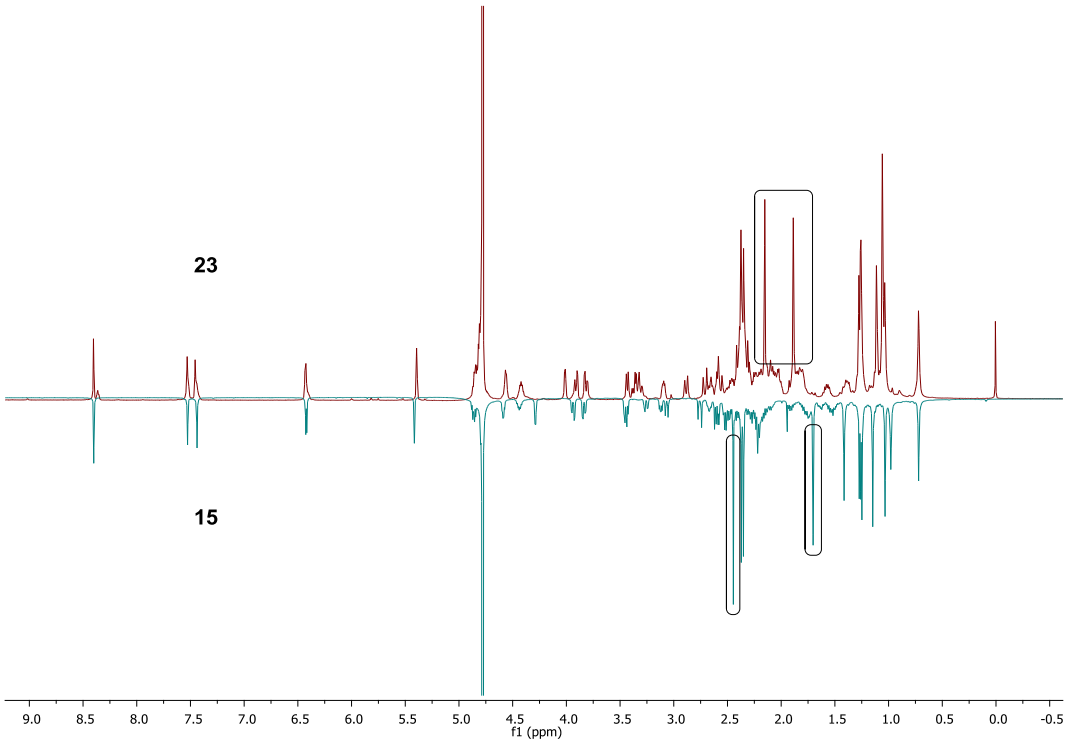

Figure 28. ^{1}H NMR spectra of **23** and **15**. Peaks corresponding to C51 and C151 are highlighted.

Having observed a metal-centered reduction in the one-step synthesis of **23** from **13**, experiments were conducted to determine whether the ligand reduction is dependent on the metal center. Consequently an excess of $CoCp_2$ (11 equiv) was added to the metal-free compound **15** in 3 portions (Scheme 37, Path C). After 1 h, UPLC-MS control experiments showed the formation of one single isomer of **23** (t_R = 2.7 min). Additionally, when this reaction was performed in the presence of an excess of the radical scavenger TEMPO (30 equiv), only starting material was found by UPLC-MS analysis of the mixture. These experiments demonstrate that the ring closure follows a pinacol-type radical mechanism, independent of the presence or absence of the metal center within the corrin cavity.

3.2.7. A base-on 5,6-diolcobalamin (24) obtained by remetallation of 5,6-diol-H-balamin (23)

Knowing that **15** can incorporate Co^{III} in its core and coordinate Dmbz through the lower axial position, analogous experiments were performed with **23**. Indeed, when **23** was stirred at 23 ºC in the presence of $CoSO_4 \cdot 7H_2O$ under slightly basic conditions (H_2O, 0.1 M TRIS, pH 8.1), the base-on derivative Co_β-hydroxo-5,6-diolcobalamin (**24**) was rapidly formed (around 90 min for full conversion of **23** to **24**), as shown by MS spectrometry (m/z = 1362.6 $[M\text{-}OH]^+$) and ^1H NMR analysis of the crude mixture (δ_{C4N} = 7.54 ppm, δ_{C7N} = 7.32 ppm, δ_{C2N} = 7.10 ppm, Figure 29).

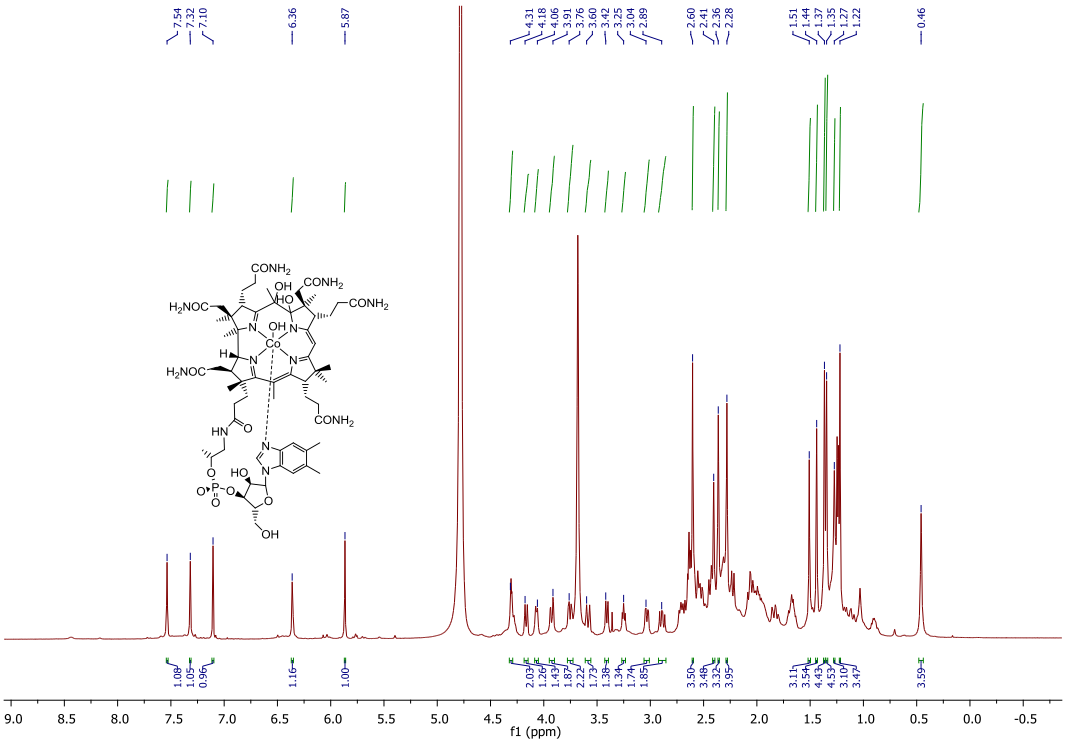

Figure 29. ^1H NMR spectrum of **24**.

In order to fully elucidate the structure of **24** and as an indirect way to gain additional insights into the structure of metal-free 5,6-diol-H-balamin (**23**) and other possible diolmetbalamins, thorough 2D NMR studies were performed (see section **6.3.**). The main conclusions of these studies are:

- A C-C bond is present between C5 and C6: ^1H-^{13}C HMBC show correlations of the methyl group at C51 with both C4 and C6.

- The compound possesses a base-on configuration with Dmbz being almost perpendicularly oriented to the C51-C151 axis of the molecule and only slightly tilted towards the A-ring: ^{1}H-^{1}H ROESY shows several Dmbz signals correlating with various peaks belonging to the corrin macrocycle. Thus, C4N correlates with all the lower oriented peripheral groups of the "northern" A-ring (C1A, C2A, C31). Additionally, C2N has a through-space correlation with the southern methyl group at C151.
- C51 is strongly shifted downfield according to ^{13}C NMR analysis (δ = 47.2 ppm, +28.9 ppm compared to **1-OH**) due to the presence of an –OH group at C5. In addition, C51 shows ^{1}H-^{1}H ROESY through space correlations with the methyl group C2A, demonstrating that this $-CH_3$ is oriented to the lower side of the corrin macrocycle.

3.2.8. Synthesis of diolmetbalamins

Having determined the structure of **24** and its stereochemistry at C5, other metals were incorporated in the metal-free corrin cavity of **23**. The same method used for the metallation of 5,6-dioxo-H-balamin (**15**) was applied for 5,6-diol-H-balamin (**23**). The partial corrin reconstitution at C5-C6 had no remarkable effect on the ability of **23** to coordinate other metals than cobalt. Thus, when **23** was stirred for 90 min at 23 ºC in the presence of $NiSO_4{\cdot}7H_2O$, quantitative conversion to 5,6-diolnibalamin (**22,** Scheme 38) was observed by UV-Vis spectroscopy (λ_{max} = 437 nm, log ε = 3.8) and HR-MS spectrometry (1360.56121 $[M-H]^-$, m/z_{calc} = 1360.56468). UPLC analysis revealed that only one isomer was synthesized (t_R = 3.1 min) with square-planar geometry and base-off configuration according to ^{1}H NMR analysis (δ_{Dmbz} = 8.34, 7.45, 7.39 ppm, Figure 30).

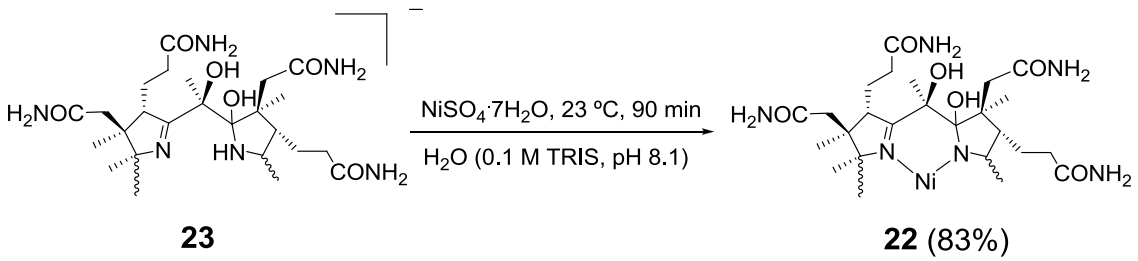

23 **22** (83%)

Scheme 38. Synthesis of **22**.

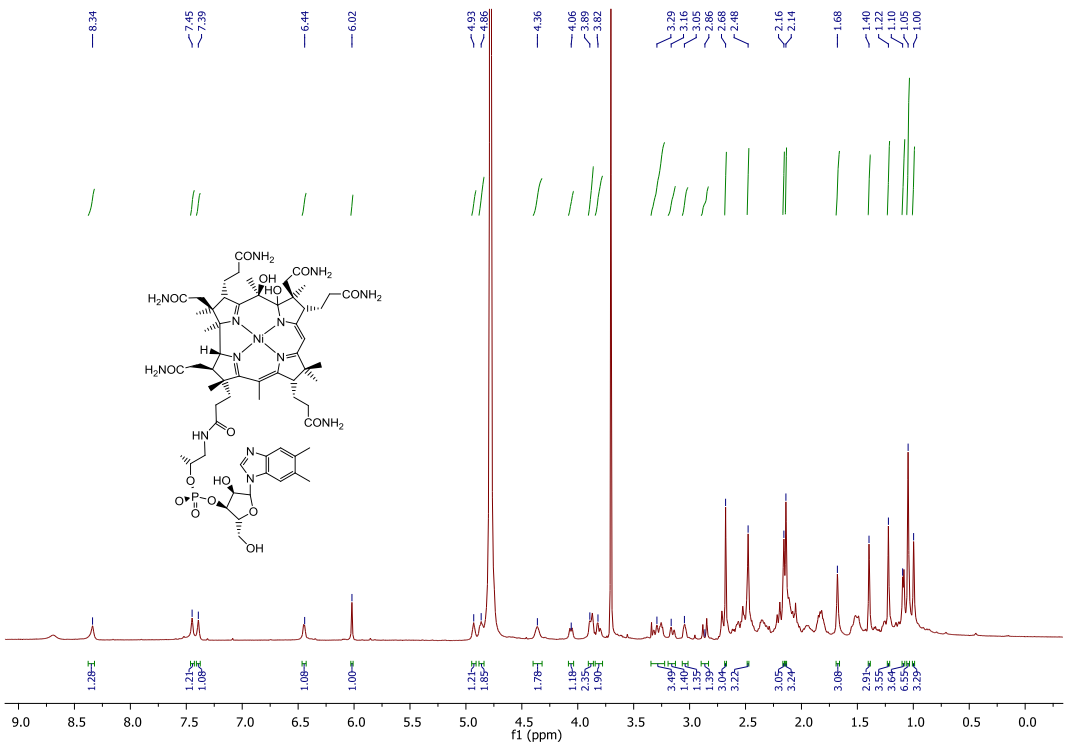

Figure 30. ^{1}H NMR spectrum of **22**.

Analogously, 5,6-diol-zincbalamin (**25**) was synthesized by adding $ZnSO_4{\cdot}7H_2O$ to a stirred soln. of **23** at 23 ºC (Scheme 39), as confirmed by UV-Vis spectroscopy (λ_{max} = 438 nm, log ε = 3.9) and HR-MS spectrometry (m/z = 1368.57403 $[M+H]^+$, m/z_{calc} = 1368.57303). ^{1}H NMR analysis shows the most downfield singlet signal at δ = 8.17 ppm and the most upfield triplet at δ = 0.72 ppm (Figure 31), ambiguous chemical shifts with values between those of base-off 5,6-diolnibalamin (**22**, δ = 8.34 and 1.00 ppm, Figure 30) and base-on hydroxo-5,6-diolcobalamin (**24,** δ = 7.54 and 0.46 ppm, Figure 29). Additionally, these values differ significantly from those of 5,6-dioxozincbalamin (**20**, δ = 8.73 and 1.00 ppm, Figure 23) and the pattern for the Dmbz UV-Vis bands of **25** differs from those of base-off diol compounds like **23** (Figure 32). Subsequently and knowing that the coordination of the Dmbz base in vitamin B_{12} is a pH dependent equilibrium, UV-Vis spectra of **25** were recorded at different pH values. At neutral conditions the Dmbz bands appear at 283 and 289 nm. No significant changes in the shape or intensity of these bands were observed when the compound was dissolved in a strongly basic (pH 12) soln. When a soln. of **25** was acidified (pH 1), the Zn^{II} ion left the macrocycle leading to **23** as observed for the zinc-containing dioxocompound **20**. As UV-Vis measurements could not determine the

configuration of **25**, ^{1}H-^{1}H ROESY analysis was done under neutral conditions. Indeed the spectrum revealed through-space correlations between two peripheral methyl groups and Dmbz signals, pointing towards a base-on configuration of this compound (see section **3.2.7.** and **6.3.**). Further NMR and/or crystallographic studies will be needed to confirm the formation of a base-on diolmetbalamin.

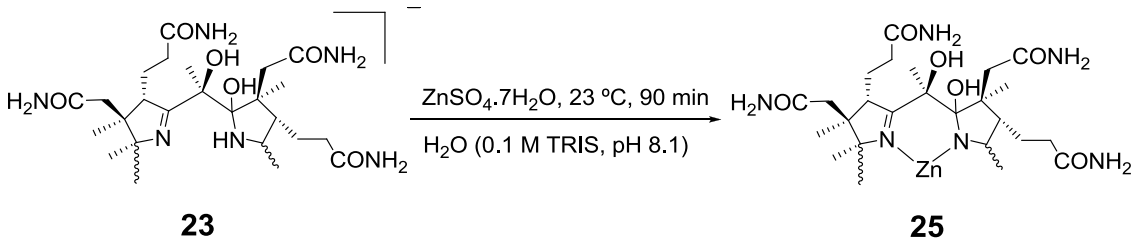

23 **25**

Scheme 39. Synthesis of **25**.

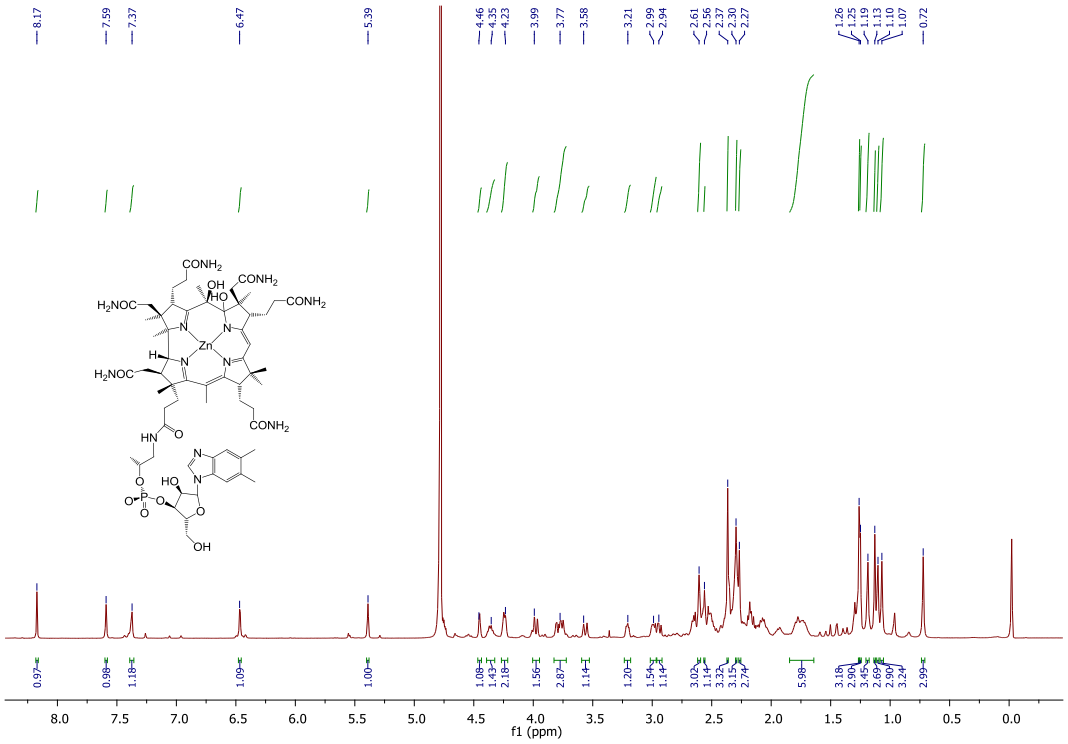

Figure 31. ^{1}H NMR spectrum of **25**.

In the presence of $CuSO_4{\cdot}5H_2O$, **23** was converted to 5,6-diolcubalamin (**26,** Scheme 40) as detected by UV-Vis spectroscopy (λ_{max} = 439 nm, log ε = 3.9) and HR-MS spectrometry (m/z = 1365.55327 $[M-H]^-$, m/z_{calc} = 1365.55327). Like the

Cu^{II}-containing dioxoderivative **21**, **26** is a paramagnetic complex and thus NMR studies could not be efficiently conducted.

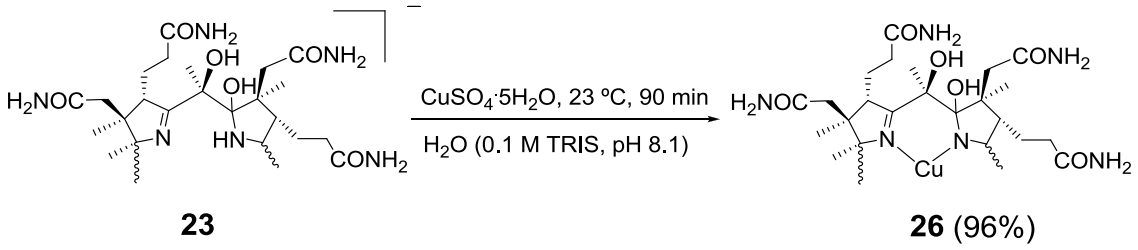

23 **26** (96%)

Scheme 40. Synthesis of **26**.

The synthesized diolmetbalamins (**22**, **25**, **26**) were obtained in quantitative yields and the coordination of Ni^{II}, Zn^{II} and Cu^{II} was completed under the same reaction conditions as for the synthesis of cobalt-containing **24**. The main difference between **24** and diolmetbalamins **22**, **25** and **26** lies in the lability of the latter compounds within the corrin macrocycle. Thus, when a strong σ–donor like KCN (100 equiv) was added to a soln. of **22**, **25** or **26**; the three diolmetalamins were transformed into **23** (Figure 32), as observed for the dioxometbalamins described in section **3.2.4**.

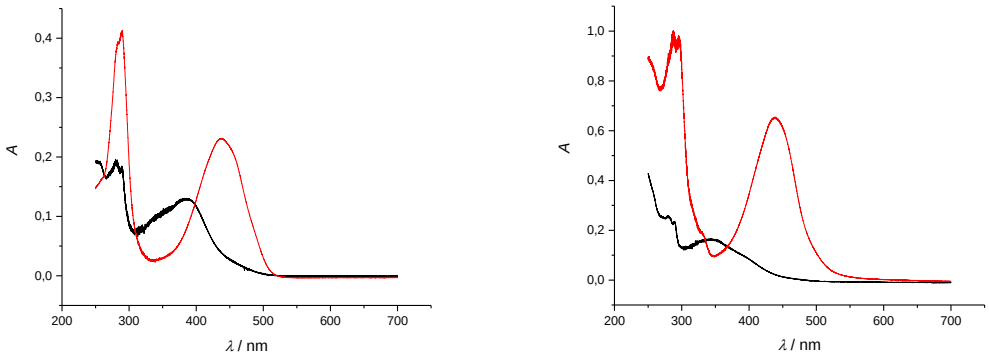

Figure 32. Left: UV-Vis spectrum of **25** without KCN (red line, H_2O, c = 3.1 x 10^{-5} M) and with KCN (100 equiv, black line). Right: UV-Vis spectrum of **26** without KCN (red line, H_2O, c = 7 x 10^{-5} M) and with KCN (100 equiv, black line).

In summary, sections **3.2.6.** to **3.2.8.** describe a 2-step route for the synthesis of the metal-free B_{12} template 5,6-dioxo-H-balamin (**23**). The key point of the route is a one-step demetallation and corrin reconstitution at positions C5 and C6 using the one-electron reducing agent $CoCp_2$ (11 equiv). Advantageously, this reaction yields only one isomer of **23** (23%) as main product. The structure of metal-free **23** was indirectly determined by introducing cobalt in the corrin cavity, affording hydroxo-5,6-diolcobalamin (**24**). 1D and 2D NMR studies demonstrated the stereochemistry at C5 (methyl group is oriented to the lower side of the corrin) and showed that **24** posesses a base-on configuration. Therefore **24** is a good candidate for biological applications, since it could be transported in its base-on configuration but its modified electronic properties would change its reactivity within cells.[22,28] Aiming to extend the portfolio of potential candidates for B_{12} surrogates with modified enzymatic reactivity, other metals (Ni, Zn, Cu) were complexed with **23** in quantitative yields. However, the coordination of these metal ions was completely reversible upon addition of KCN and/or acids. Seeking to further stabilize other metal centers than cobalt within the corrin macrocycle, subsequent efforts were focused on the complete repair of the delocalized π-electronic system of the corrin.

3.3. Attemps of dioxo and diol elimination

In this section, endeavors to reconstitute the intact delocalized π-electronic system of the corrin macrocycle from "northern" face modified B_{12} derivatives (5,6-*seco*-corrinoids) are presented. The main strategy consisted on the reductive repair of 5,6-dioxo and 5,6-diol B_{12} derivatives containing either cobalt or nickel as metal centers (Scheme 41). Experiments included the use of a) classic reductive procedures in B_{12} chemistry (i.e. reductions with Zn/AcOH); b) methods implemented in this work (i.e. $CoCp_2$); and c) classic organic reactions for the formation of C-C and C=C bonds from diketones and diols (i.e. Mc Murry, Wolff-Kischner, SmI_2). Since many of the aforementioned reactions are often solvent-dependent, "incomplete" hydrophobic models of 5,6-*seco*-cobalamins and 5,6-*seco*-nibalamins were synthesized and screened for developing new corrin reconstitution reactions. Results highlight the inertness of the so-called "stable yellow corrinoids" with an interrupted electronic system at C5-C6 towards corrin repair. Although alternative methods for demetallating and forming a single C-C bond at positions C5 and C6 were found, a full repair of the corrin macrocycle was not achieved.

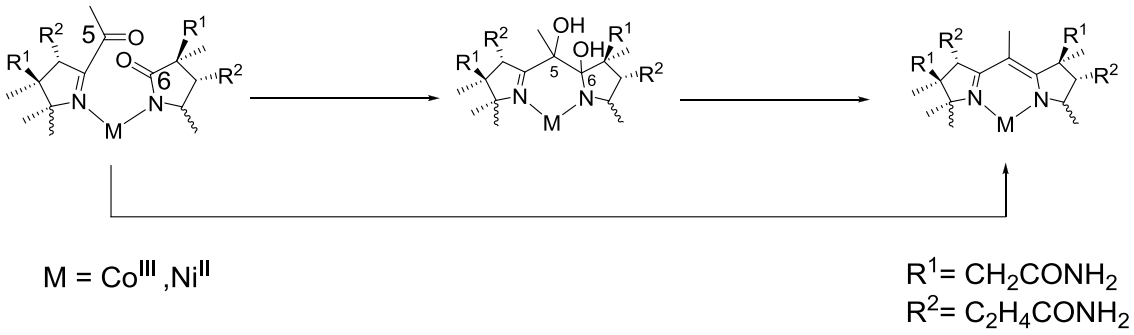

Scheme 41. Envisaged reconstitution of 5,6-*seco*-corrinoids containing Co^{III} or Ni^{II}.

3.3.1. Hydrophobic analogues of dioxo and diolmetbalamins

Due to the solvent dependency of some of the C-C and C=C bond forming reactions that will be described in section **3.3.**, the synthesis of hydrophobic B_{12} derivatives was envisaged. One of the main hydrophobic B_{12} models available is 'cobester' (**27-CN**, Scheme 42, see section **1.7.2.**).[89] Photooxygenolysis of **27-CN** (Scheme 42, see section **1.7.2.**) led to secocorrins dicyano-14,15-dioxocobester (dicyano-14,15-dioxocobyrinic acid heptamethyl ester, **28**) and dicyano-5,6-dioxocobester (dicyano-5,6-dioxocobyrinic acid heptamethyl ester, **29**).[92,109]

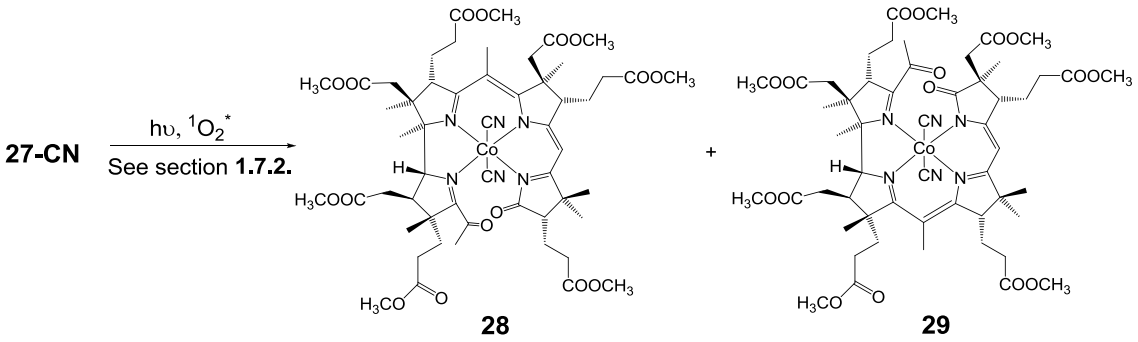

Scheme 42. Synthesis of **28** and **29**.

Aiming to extend the library of available hydrophobic Cbls to B_{12} derivatives containing other metals than cobalt, modifications of Werthemann's procedures to synthesize 'cobester' were applied to dioxo and diolB_{12} derivatives with other metals than cobalt. Within the synthesized metbalamins, those containing Ni^{II} as metal center are the most stable derivatives under acidic conditions (see section **3.2.**). Therefore, hydrophobic models of Ni^{II}-containing B_{12} derivatives were envisaged.

The first studies were conducted with the "southern" modified 14,15-dioxonibalamin (**30**).[98] The methanolysis of **30** at 80 ºC under acidic conditions led to the replacement of the amide side chains by methyl ester groups (Scheme 43). Optimal conversion was found after 120 h, with 14,15-dioxonibyrinic acid heptamethyl ester (14,15-dioxonibester, **31**, m/z = 1067.5 6 $[M+H]^+$) being the main product according to UPLC-MS analysis. According to this spectrum, two main byproducts were identified in the crude mixture: 14,15-dioxonibyrinic acid pentamethyl ester (m/z = 1039.5 $[M+H]^+$) and 14,15-dioxonibyrinic acid hexamethyl ester (m/z = 1053.5 $[M+H]^+$). Compound **31**

was subsequently isolated in 57% yield by flash chromatography (t_R = 3.6 min). Contrary to "complete" Ni^{II} dioxocorrinoids (**19**, **30**), ^1H NMR analysis of **31** showed broad unresolved peaks that point towards a paramagnetic species. Thus, it was assumed that the replacement of all side chains affected the planarity of the secocorrin. These observations are in agreement with the geometry of synthetic Ni^{II} corrinoids lacking all peripheral side chains, as determined by X-ray crystallography.[110]

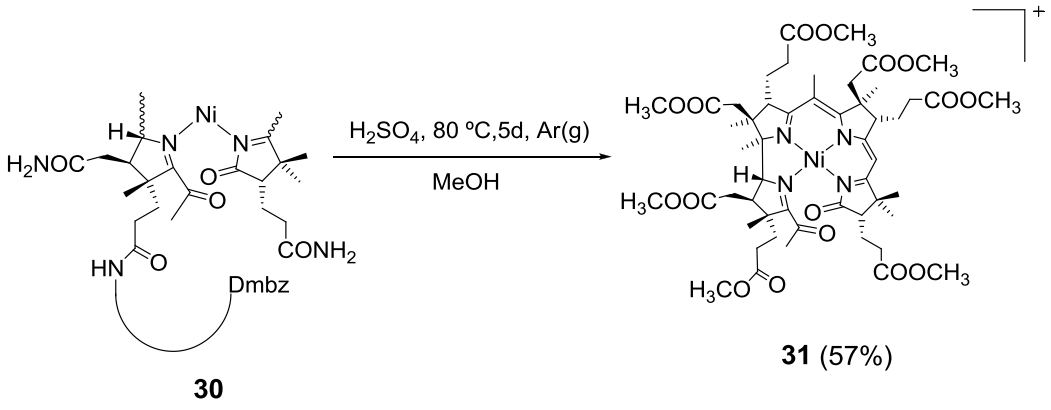

30 **31** (57%)

Scheme 43. Synthesis of **31**.

Having established the optimal temperature, pH, and reaction time for the synthesis of **31**, these conditions were transferred to the "northern" modified and more reactive isomer 5,6-dioxonibester (**32**, Scheme 44). The reaction progressed in a similar way as for the "southern" oxidized derivative **31** and after 120 h, 5,6-dioxonibyrinic acid heptamethyl ester (5,6-dioxonibester, **32**, m/z = 1067.5 6 $[M+H]^+$) was identified as the main product of the crude mixture. Again, small fractions of 5,6-dioxonibyrinic acid pentamethyl ester (m/z = 1039.5 $[M+H]^+$) and 5,6-dioxonibyrinic acid hexamethyl ester (m/z = 1053.5 $[M+H]^+$) were found. Isolation of **32** from these side products proved to be a demanding task and for our synthetic purposes (synthesis of nibalamins with an intact corrin macrocycle) fractions containing small amounts of penta and hexasubstituted dioxonibesters were employed.

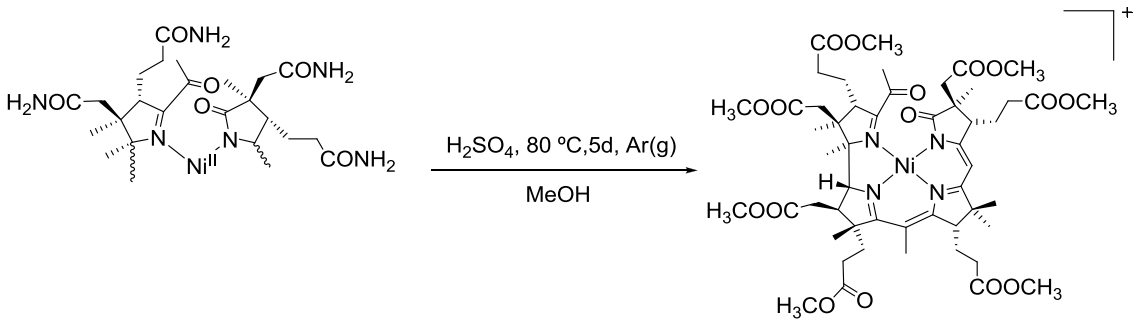

19 **32**

Scheme 44. Synthesis of **32**.

The described reaction conditions were also transferred to 5,6-diolnibalamin (**22,** Scheme 44). After 120 h, 5,6-diolnibyric acid heptamethyl ester (5,6-diolnibester, **33**, m/z = 1069.5 $[M+H]^+$) was the main product of the crude mixture, finding also 5,6-diolnibyric acid hexamethyl ester (m/z = 1055.5, $[M+H]^+$) and 5,6-diolnibyric acid pentamethyl ester (m/z = 1041.5, $[M+H]^+$) as side products. Attemps to purify **33** by flash chromatography or preparative HPLC failed and the crude mixture was further used for synthetic studies.

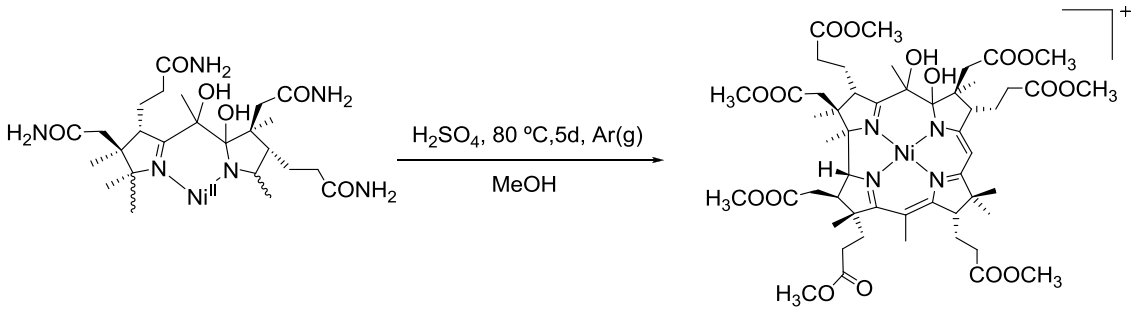

22 **33**

Scheme 45. Synthesis of **33**.

The synthesis of dioxo and diolnibester derivatives with high temperatures (80 ºC), long reaction times (5 days) and under acidic conditions (pH < 1) demonstrated that metal ions greatly stabilize the corrin macrocycle. Under milder conditions (pH 2, rt, overnight), the metal-free 5,6-dioxo-H-balamin (**15**) degrades as described in section **3.2.1.** When Ni^{II} is present in the corrin cavity, the equatorial macrocycle remains intact under the harsh reaction conditions described above and only the amide side chains are slowly replaced by methyl ester groups. With hydrophobic Cbl and nibalamin derivatives in hand, endeavors were focused on reconstituting the original π-electronic system of the corrin macrocycle.

3.3.2. Attemps to reconstitute the corrin macrocycle of 5,6-*seco*-cobalamins and 5,6-*seco*-nibalamins

a) Reduction with Zn/AcOH

Gossauer and coworkers have extensively studied the structure and reactivity of hydrophobic "stable yellow corrinoids".[77-79,107] Concretely, their work led to the reductive reconstitution of 'cobester' (**27-CN**) from a yellow 'cobester' derivative with a corrin macrocycle containing a single bond at C5-C6, a hydroxy group at C5 and a hydrogen substituent at C6 (**34**, Scheme 46, left).[77] They proposed a reductive ring reconstitution in which cobalt plays a fundamental role. Indeed, a metal-centered reduction to obtain Co^{I} is completed in the presence of Zn/AcOH. The subsequent reoxidation of Co^{I} to Co^{III} pushes two electrons into the A/B methylene bridge, achieving the formation of a double bond at positions C5-C6 and thus restoring the original delocalized π-electronic system of the corrin macrocycle. Inspired by that work, Zn was added to a soln. of aquacyano-5,6-diolcobalamin (**16**, Scheme 46, right) in acetic acid under a N_2(g) atmosphere. However, only complex mixtures were observed by UPLC-MS, most likely due to the presence of a hydroxy group at C6 instead of a hydrogen.

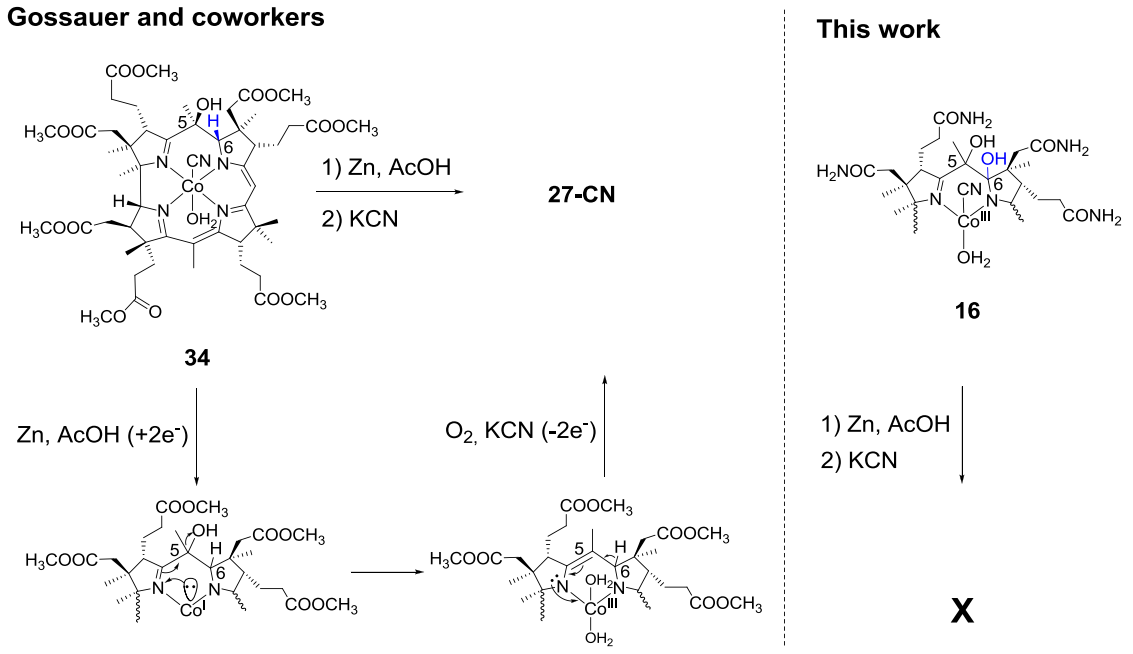

Scheme 46. *Left*: reconstitution of **27-CN** from **34.** *Right*: unsuccessful reconstitution of **16** under the same reaction conditions.

b) McMurry approach

The use of low-valent titanium reagents for coupling carbonyl or diol functionalities into olefins (Scheme 47) has been widely used in organic synthesis during decades.[111,112] Despite the versatility of this reaction and its numerous applications, McMurry couplings are highly solvent-dependent and not always reproducible. Within our Cbl framework, one of the main synthetic constraints is the choice of solvent: vitamin B_{12} is only soluble in polar solvents like H_2O and alcohols of short chain (methanol, ethanol). To overcome this limitation, McMurry experiments were conducted either in aprotic polar solvents (DMF) or mixtures of apolar solvents (Py:dioxane 1:1) that partially dissolve B_{12} derivatives at high temperatures. Alternatively, test reactions were performed with hydrophobic derivatives of B_{12} (cobester and nibester derivatives described in section **3.3.1.**) that are soluble in solvents typically employed for McMurry reactions (i.e. THF).

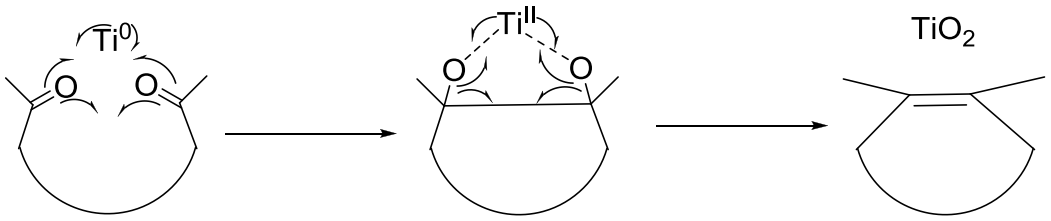

Scheme 47. General mechanism for McMurry couplings.

Knowing that the harsh reaction conditions normally required for McMurry couplings could affect the corrin macrocycle, preliminary studies were conducted with vitamin B_{12}. When **1** was added to a mixture containing low-valent Ti at 100 ºC in either DMF or pyridine:dioxane (1:1) for 45 min, a metal-centered reduction of the Co^{III} ion was observed but the corrin macrocycle remained intact. Thus, aquacobalamin (**1-OH$_2$**) was obtained as the main product after reoxidation of the crude with air according to MS analysis (m/z = 664.9 $[M\text{-}OH_2]^{2+}$, Scheme 48, top). If the same reaction conditions were applied for 90 min, the corrin macrocycle still remained unaltered but the "loop" was partially cleaved, leading to mixtures of **1-OH$_2$** and diaquacobinamide (**OH$_2$-Cbi**) after reoxidation (Scheme 48, bottom).

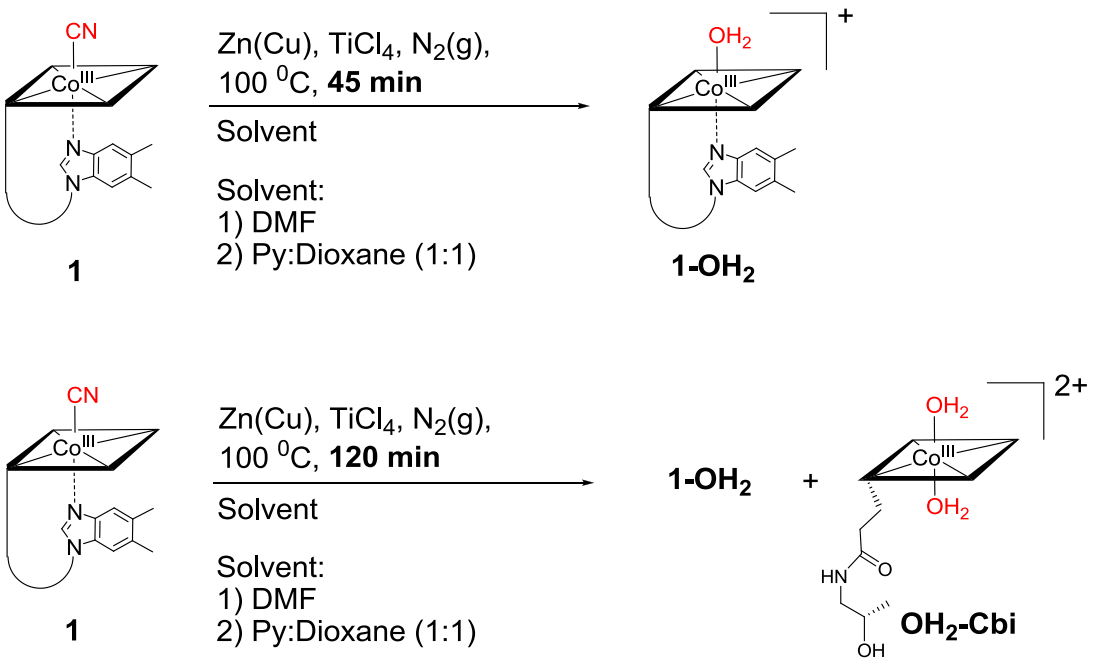

Scheme 48. Reactivity of **1** under McMurry conditions.

Once the stability of the corrin macrocycle under McMurry conditions was evaluated, the reaction was applied to 5,6-*seco*-cobalamins. As described in section **3.1.** and **3.2.**, the "northern" face of the corrin macrocycle displays an enhanced reactivity towards reconstitution. However, when dicyano-5,6-dioxocobalamin (**13**) or aquacyano-5,6-diolcobalamin (**16**) were treated with low-valent Ti in DMF or dioxane:pyridine (1:1), the reactivity of the equatorial macrocycle led to complete destruction of the corrin after 90 min, according to UPLC-MS measurements. Analogous attempts with 5,6-diolnibalamin (**25**) using shorter reaction times (45 min) yielded similar results (Scheme 49).

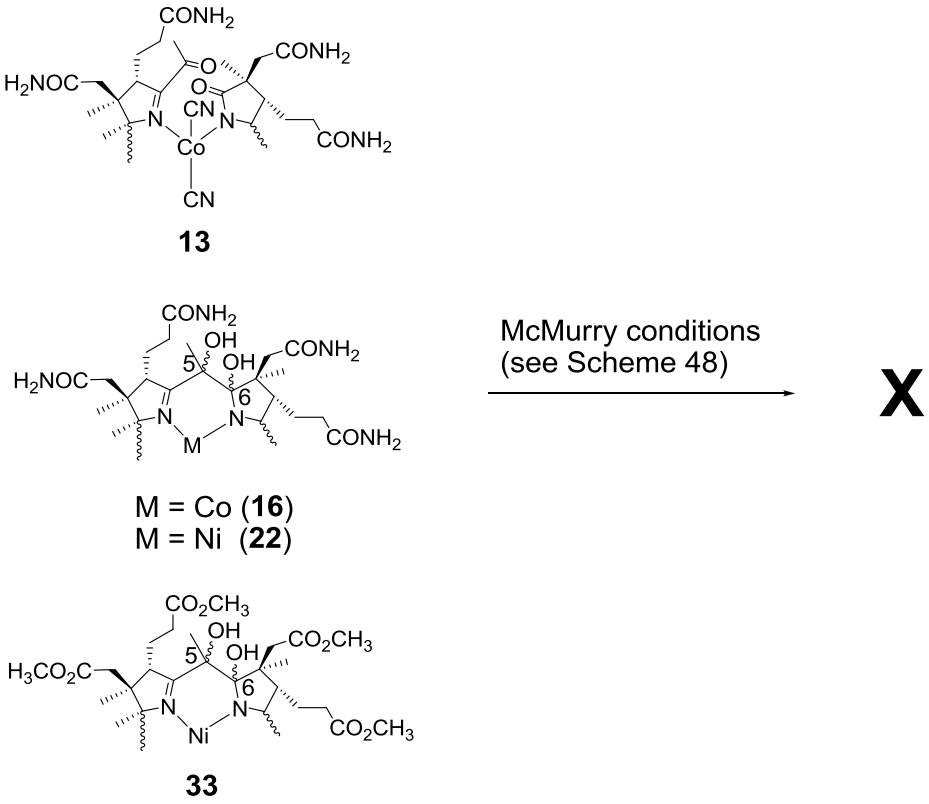

Scheme 49. Treatment of **13**, **16** and **22** and **33** under McMurry conditions. Charges are omitted for simplicity.

Taking into account the solvent dependency of the attempted McMurry ring closure, preliminary studies were conducted with a hydrophobic derivative of vitamin B_{12} containing Ni^{II} as a metal ion: 5,6-diolnibester (**33**). UV-Vis spectroscopy indicated that no changes took place in the corrin macrocycle even after 6 h, with a main band at 433 nm that remained unaltered throughout the reaction. Indeed, MS analysis showed no significant differences between the starting material and the crude mixture.

In summary, the use of McMurry conditions with B_{12} derivatives leads exclusively to reduction of the metal center but leaves the (seco)corrin macrocycle unaltered. Additionally, when harsh reaction conditions typical of this method are applied the equatorial ligand is eventually destroyed.

c) Combined $CoCp_2$ and McMurry approach

Inspired by the effectiveness of $CoCp_2$ to form C-C bonds within 7,8- and 5,6-*seco*-corrins (as described in sections **3.1.2.** and **3.2.6.**), the formation of a double bond between C5-C6 in a one-step reaction was attemped by combining $CoCp_2$ with low-valent Ti. It was envisaged that a) addition of $CoCp_2$ would connect C5 and C6 by a single C-C bond and b) low-valent Ti would provide the necessary reducing conditions to eliminate the diol moiety at C5-C6 (Scheme 50).

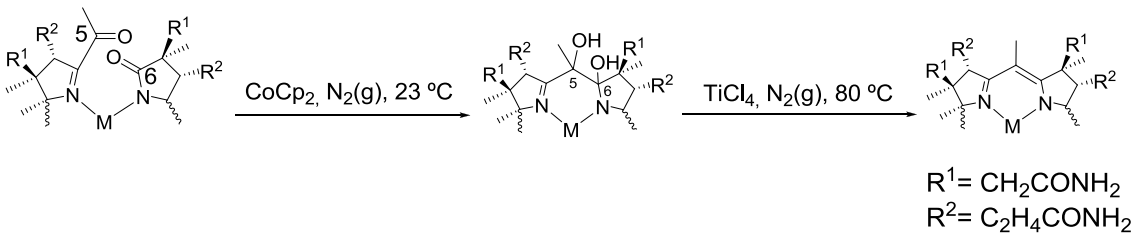

Scheme 50. General approach for the combined use of $CoCp_2$ and low-valent Ti.

Control experiments were performed with vitamin B_{12} (**1**). $CoCp_2$ (6 equiv) was added to a soln. of **1** in MeOH under inert atmosphere at 23 ºC. After 30 min, $TiCl_4$ (11 equiv) was added to the reduced mixture and temperature was set at 80 ºC for 45 min. UPLC-MS analysis revealed that this method is harmless for the intact corrin macrocycle, triggering only a quantitative metal-centered reduction to **1-OH$_2$** (m/z = 664.9 $[M\text{-}OH_2]^{2+}$). Therefore, the same reaction conditions were applied to dicyano-5,6-dioxocobalamin (**13**). Surprisingly, 5,6-diol-H-balamin (**23**) was the main product obtained in the reaction as indicated by UPLC-MS (m/z = 1304.6 $[M]^-$), even if no KCN was added to the reaction mixture as decomplexating agent (Scheme 51). $CoCp_2$ reacted as expected reducing Co^{III} to Co^{II} and forming a C-C bond between C5 and C6. On the other hand, the addition of $TiCl_4$ did not lead to the desired diol elimination but achieved the removal of the reduced cobalt center.

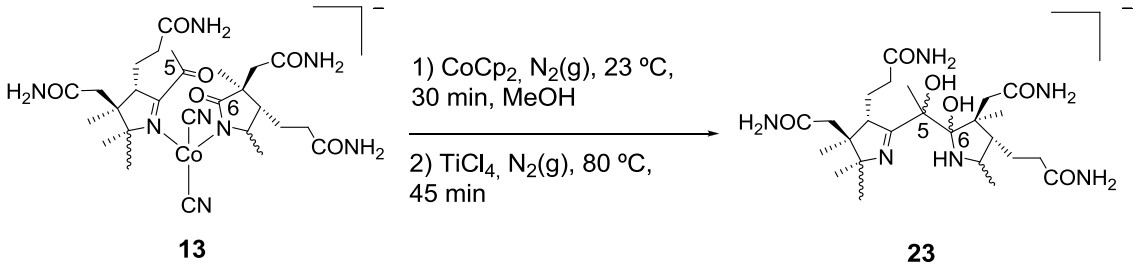

Scheme 51. Synthesis of **23** from **13** using $CoCp_2$ and $TiCl_4$.

With this unexpected reactivity and assuming solvents play an important role in low-valent Ti-mediated couplings, experiments were conducted with hydrophobic cobester derivatives in THF. As expected, control experiments with 'cobester' (**27-CN**) confirmed the stability of the intact corrin macrocycle under such reaction conditions. Again, the only reactivity observed was a partial reduction of the Co^{III} center to form diaquacobester (**27-OH_2**, Scheme 52, top). In this case, the reduction of **27-CN** to **27-OH_2** was not quantitative most likely due to the presence of additional axial cyanide that lowers the reduction potential of the Co^{III} center (see section **3.1.2.**). When dicyano-5,6-dioxocobester (**29**) was treated analogously, the only remarkable change is also a partial metal-centered reduction to yield diaqua-5,6-dioxocobester (**29-OH_2**, Scheme 52, bottom). In this case, no demetallation of **29** was observed.

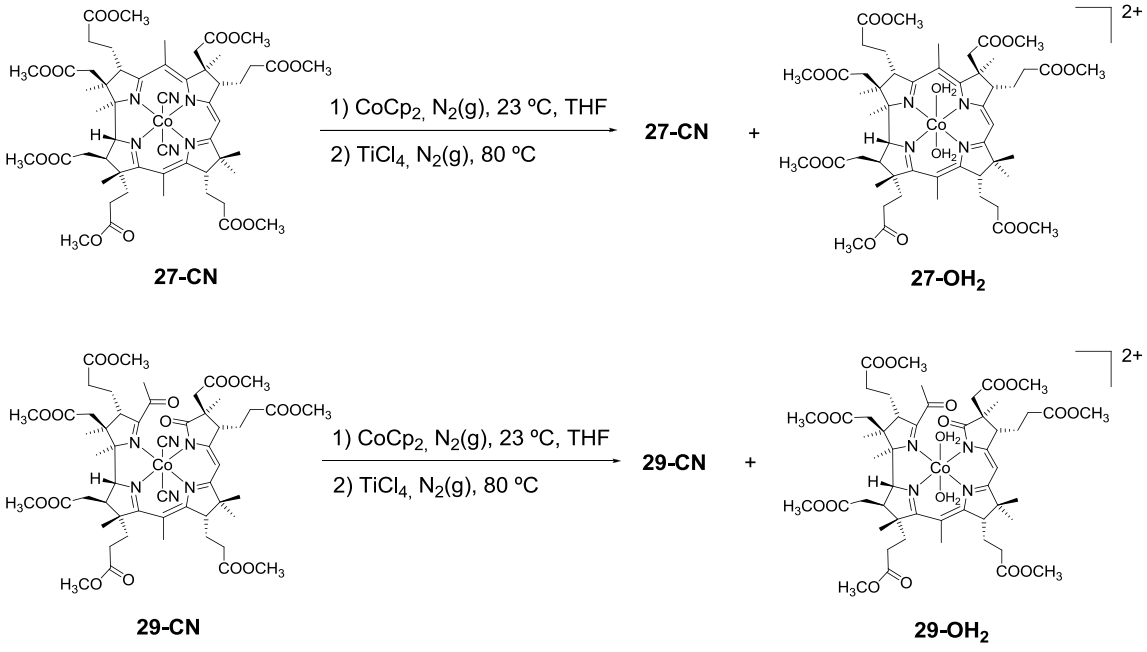

Scheme 52. Reactivity of **27-CN** and **29-CN** under the described reduction conditions.

d) SmI_2

Since the discovery of SmI_2 by Kagan in the 1970s, extensive synthetic applications of this reducing agent have been developed.[113,114] This versatile reagent can complete one and two-electron reduction processes and was therefore considered as a suitable candidate for performing reductive ring-closing experiments. Additionally, several of these SmI_2-mediated reactions were performed in advantageous solvent systems for our Cbl derivatives, like mixtures of H_2O:THF.[114]

Preliminary studies showed that the addition of SmI_2 (0.1 M in THF) to a soln. of **1** in THF:H_2O (5:1) was able to reduce the Co^{III} center while leaving the corrin macrocycle unaltered. Consequently, SmI_2 is also a convenient reducing agent for synthesizing **1-OH$_2$**. When SmI_2 (4.2 equiv) was applied to dicyano-5,6-dioxocobalamin (**13**) under the same reaction conditions, a specific metal-centered reduction was found (Scheme 53). The addition of an excess of KCN (11 equiv) to the reduced soln. after different reaction times (30 to 90 min) led to 5,6-dioxo-H-balamin (**15**, Scheme 53, Figure 33).

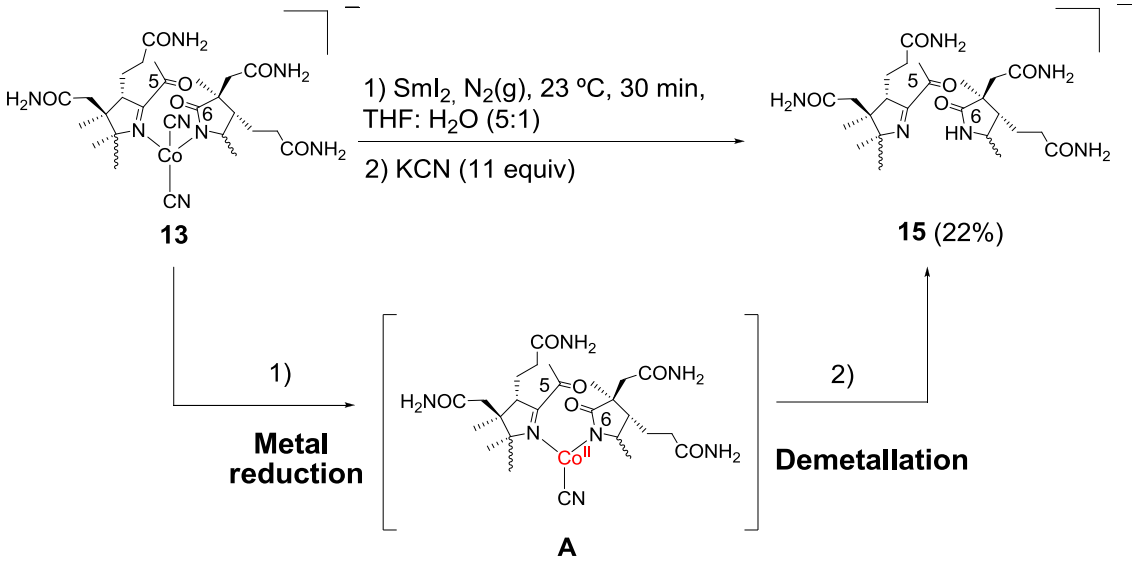

Scheme 53. Synthesis of **15** using SmI_2.

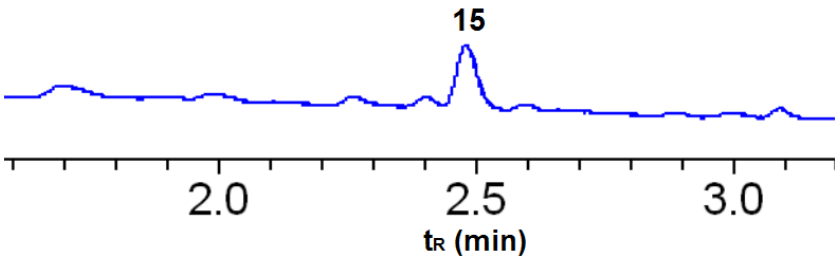

Figure 33. UPLC trace (Method 2, see Materials and Methods) of the reaction crude (see Scheme 53).

Observing a metal-centered reactivity, the feasibility of SmI_2 as reducing agent for the corrin ligand at positions C5 and C6 was tested. For this purpose, 12 equiv of SmI_2 were added stepwise in three portions over 15 min to a soln. of **13** under inert conditions (analogous conditions as in the ring reconstitution with $CoCp_2$ described in section **3.2.6.**). Unfortunately, no further reactivity of the corrin macrocycle was observed and **15** remained the main product of the reaction when an excess of KCN was added to the reduced reaction mixture.

The reducing agent was tested in a purely organic solvent (THF) with hydrophobic 5,6-dioxonibalamin (**32**) and in the presence of LiCl as Lewis acid to increase the reducing power of SmI_2.[115] Under these conditions, the addition of SmI_2 (9 equiv) to **32** achieves the pinacol coupling of the carbonyl moieties at C5 and C6 to form 5,6-diolnibalamin (**33**) in 5 h as observed by MS analysis (m/z = 1069.5 $[M+H]^+$). As it was the case in previous experiments (see section **3.2.**), no further reactivity than the formation of **33** was found.

All in all, SmI_2 proved to be a useful reducing agent for metal-centered reductions and the formation of single C-C bonds. This reactivity is in line with that of $CoCp_2$ (see sections **3.1.** and **3.2.**) but does not allow to complete any further step towards the synthesis of metbalamins.

e) Wolff-Kischner

The Wolff-Kischner reduction was considered as a possible way to close the ring in 5,6-*seco*-corrinoids.[116,117] For this purpose, it was envisaged to first convert the keto moiety at C5 into a hydrazine and then evict an N_2 group forming a carbene at C5. This reactive intermediate would then reconnect C5 and C6, due to the spatial proximity and the preorganization of both atoms.

Attempts to form a hydrazone at C5 or C15 of **12** or **13** with p-toluensulfonyl hydrazide showed negliglible conversion of the starting material, most likely due to steric hindrance. Therefore, the less bulky acetohydrazide was employed. The reaction was tested on the "southern" oxidized corrinoid **12**, obtaining the best results using a slightly acidic aqueous solvent system (pH 5.2) and refluxing the reaction mixture for 4 h. Under such conditions, aquacyano-14-oxo-15-acetohydrazonecobalamin (**34**, m/z = 1441.5 $[M-H]^-$, Scheme 54) was obtained as main product in the crude mixture according to UPLC-MS analysis. Attaching acetohydrazone to **12** caused an expansion of the π-delocalized system around the D-ring. The additional electrons at **34** affected its UV-Vis spectrum, finding a main band (λ_{max} = 472 nm, log ε = 4.0) accompanied by a prominent shoulder (λ_{max} = 530 nm, log ε = 3.9). The presence of a hydrazone was further confirmed by ^{13}C NMR: 64 signals were found for this product (two more than in the starting material **12**) that correspond to a new quaternary and a new primary carbon from the acetohydrazone moiety (figure 34).

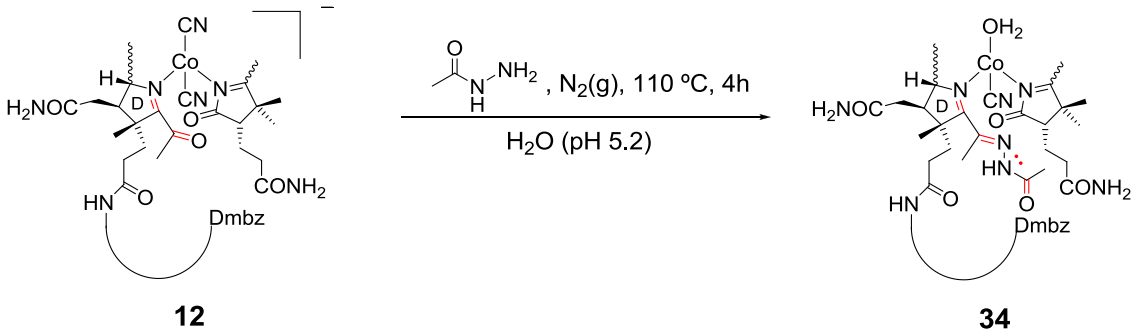

Scheme 54. Synthesis of **34**. Delocalized electrons at the D-ring of **12** and **34** are marked in red.

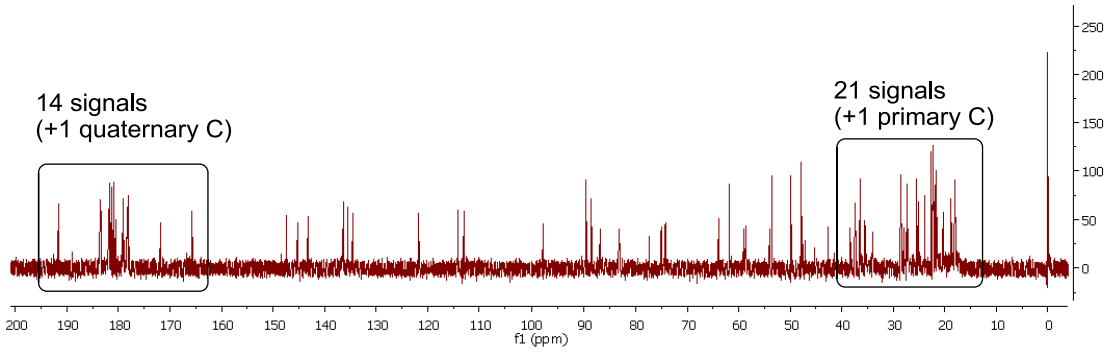

Figure 34. ^{13}C NMR spectrum of **34**.

The optimized reaction conditions were transferred to the "northern" oxidized corrin macrocycle **13**. Due to the enhanced reactivity of the upper part of the corrin macrocycle, quantitative conversion to aquacyano-5-acetohydrazone-6-oxocobalamin (**35**, m/z = 1441.5 $[M-H]^-$) was achieved within 30 min according to UPLC-MS analysis (Scheme 55).

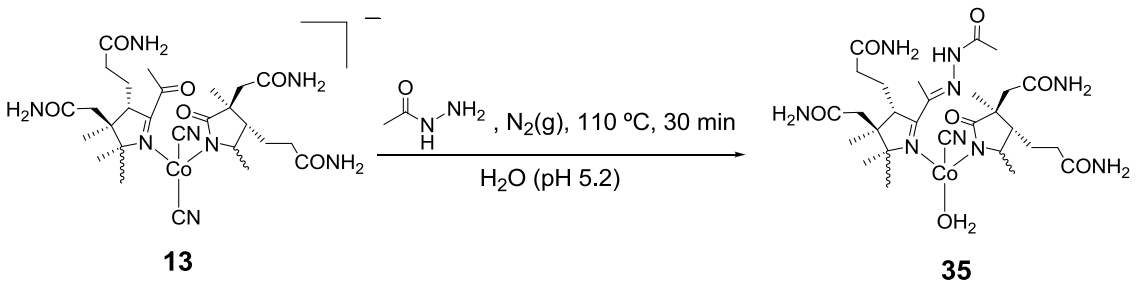

13 **35**

Scheme 55. Synthesis of **35**.

From the numerous procedures that have been developed during the last decades to form a carbene from a hydrazone via liberation of N_2, those with mild conditions and compatible solvents were tried on **35** (Scheme 56). Cram's modification of the reaction[118] with potassium terbutoxide in DMSO at 25 ºC was explored but no color change was observed in the soln. after 72 h (λ_{max} = 458 nm). Inspired by Caglioti's work,[119] a hydride donor ($NaBH_4$) was added to a soln. of **35** under inert atmosphere and at 23 ºC. Reduction of the Co^{III} center to Co^{II} was observed by MS as the axial cyanide was lost forming **35-OH$_2$** (m/z = 1416 $[M-OH_2]^-$) but no ligand reactivity was found. Encouraged by previous successful experiences on corrin modifications with $CoCp_2$ (see sections **3.1.** and **3.2.**), this one-electron donor was also applied to **35** under

inert atmosphere and 23 ºC. However, similar results as with $NaBH_4$ were obtained in this case. As observed for 5,6-*seco*-cobalamins the addition of an excess of KCN after 2 min of reduction of **35** allowed the identification of the metal-free compound 5-acetohydrazone-6-oxo-H-balamin (**36**) by UPLC-MS.

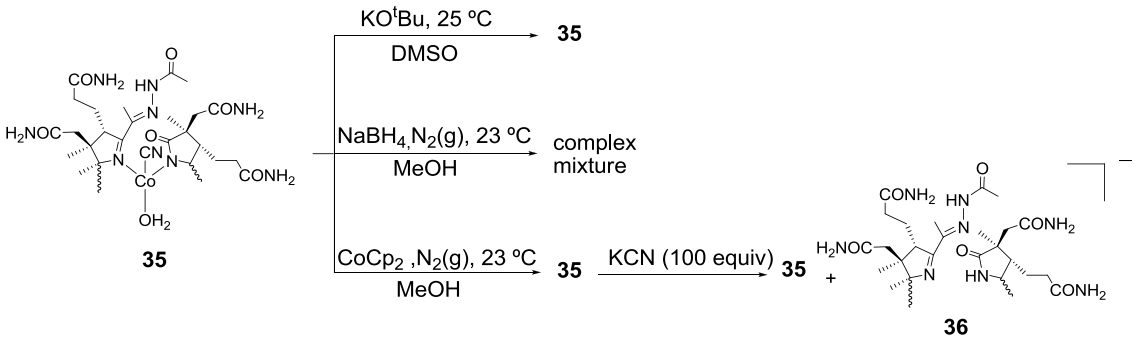

Scheme 56. Reactivity of **35** under basic and reducing conditions.

Remarkably, the synthesized hydrazone at C5 is a stable species that resists strong basic and reductive conditions and renders the "northern" side of the corrin macrocycle inert towards ring reconstitution reactions. The presence of an 8 delocalized π-electronic system between the D-ring and the hydrazone moiety might enhances the stability of **34** and **35**, rendering them inert towards carbene formation and hindering the second step of the Wolff-Kischner reaction.

3.4. Microbiological activity of B_{12} derivatives

One of the main goals of this work is the synthesis of B_{12} antagonists (antivitamins B_{12}) to inhibit B_{12} dependent enzymatic processes. In order to achieve this inhibition, either the transport of B_{12} into cells or the uptake of B_{12} into the corresponding enzymes must be impeded. Consequently, the ideal antivitamin B_{12} must have high affinity towards B_{12} transporting proteins, ideally in the range of the binding affinities for the natural product. Considering the structural complexity of this nutrient and the specificity of B_{12} transporting proteins and B_{12} dependent enzymes, subtle modifications of the Cbl framework were envisaged for accessing antivitamins B_{12}.

The biological activity of several antivitamin B_{12} candidates was evaluated with a microbiological assay using *L. Leichmanii*. This gram-positive bacterium is an internationally approved organism to assess the biological activity of vitamin B_{12} and modified B_{12} surrogates.[49,120] Indeed, the enzyme ribonucleotide reductase (RNR) in *L. Leichmanii* depends on cofactor B_{12} (Figure 35).[68] Thus, when a structurally related but catalytically inactive antivitamin B_{12} is able to compete with B_{12} for the corresponding binding pockets of RNR, the cellular growth of this organism is disrupted. Since *L. Leichmanii* grows forming long opaque filaments in its medium, the growth rate of this bacterium can be easily monitored by spectrophotometry (λ = 680 nm).

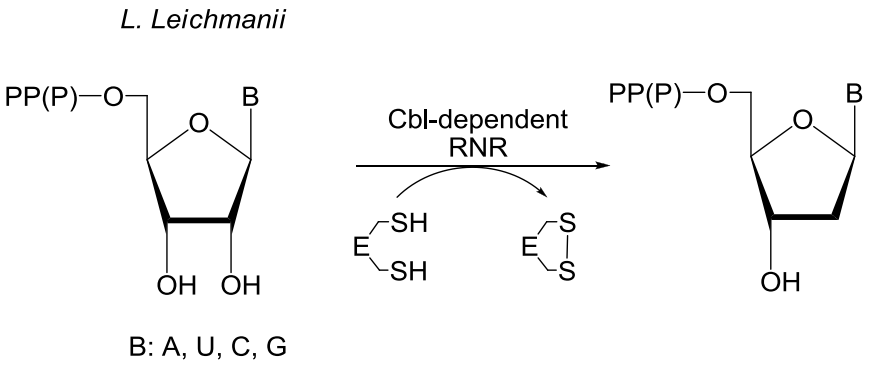

Figure 35. B_{12}-dependent enzymatic conversion of ribonucleotides to deoxyribonucleotides in *L. Leichmannii*.

3.4.1. Biological evaluation of B-ring modified vitamin B_{12} derivatives

As described in section **3.1.**, the reconstitution of B_{12} (**1**) from a green 7,8-*seco*-corrinoid (**2**) in 4 steps was implemented. In order to assess the consequences of structural modifications of Cbls on their bioactivity and searching for new antivitamins B_{12}, competitive assays between B_{12} and **4**, **7** and **11** were performed. In these studies, a 1000-fold excess of the antivitamin candidates was added to a bacterial medium containing 0.1 nM B_{12}.

As observed in Figure 36, competitive assays between B_{12} (**1**) and **4** or **7** demonstrate that both B_{12} derivatives are potent antagonists of the nutrient and can inhibit the growth of *L. Leichmannii* by 50% at 100 nM range. In turn this means **4** and **7** may compete with **1** for the transporting proteins or for the enzyme, most likely due to their structural similarity to the original B_{12} cofactor (both the corrin macrocycle and the stereochemistry of all side chains are identical to those of B_{12}). Indeed, it has been found that **4** and **7** diminish the expected catalytic activity from cofactor B_{12}.

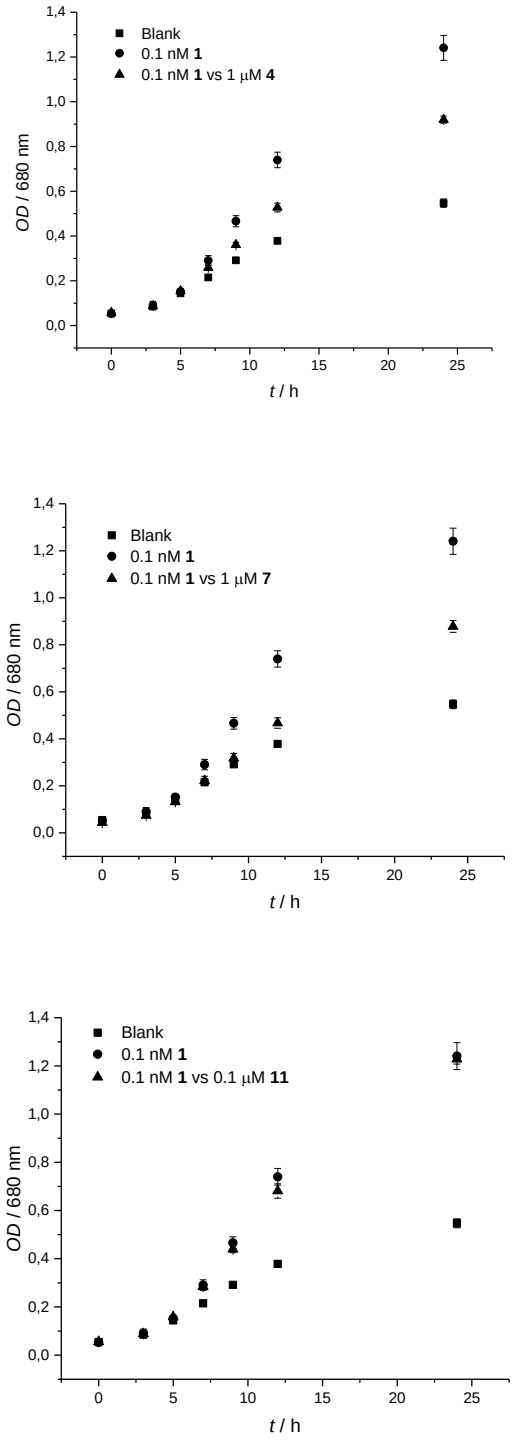

Figure 36. Growth of *L. Leichmannii* at 37 ºC (n = 3) in the presence of **1** and **4** (top), **1** and **7** (middle) as well as **1** and **11** (bottom).

3.4.2. Biological evaluation of reconstituted vitamin B_{12}

Having observed by X-ray crystallography that the final compound of the route is intact vitamin B_{12} (**1**, see section **3.1.6.**), the microbiological assay with *L. Leichmannii* was performed to prove that the biological activity of **1** remains intact independently of its origin (bacterial or chemical production). Concretely, a calibration curve with different concentrations of reconstituted B_{12} in bacterial media was elaborated (Figure 37). An increasing growth was found with concentrations from 0.05 nM to 1 nM, confirming that reconstituted B_{12} is an active nutrient for *L. Leichmannii*. As expected, the bacterial growth was identical when the same concentration of microbiologically produced B_{12} or chemically reconstituted B_{12} was added to two independent *L. Leichmannii* containing media.

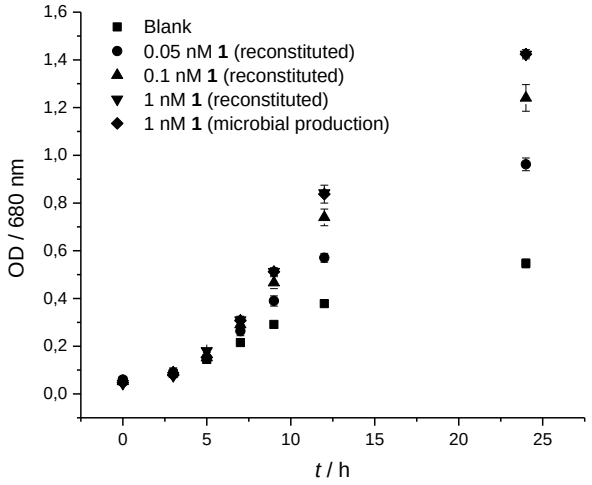

Figure 37. Growth of *L. Leichmannii* at 37 ºC (n = 3) with different concentrations of reconstituted B_{12} (0.05, 0.1, 1 nM) and microbially produced B_{12} (1 nM) .

4. Conclusions and outlook

The aim of this work was to establish chemical procedures for the synthesis of metbalamins starting from ring-opened secocorrinoids. To obtain metbalamins, it was envisaged to 1) demetallate, 2) remetallate and 3) reconstitute the corrin macrocycle of different ring-opened B_{12} derivatives. Herein, two complementary routes towards this goal are presented.

1) The 7,8-*seco*-corrin approach

The stereospecific reconstitution of vitamin B_{12} from artificial green 7,8-*seco*-corrinoids was completed in four steps. The key step of this route consists of a quantitative, fast and stereospecific ring closure reaction (Scheme 57). For completing this C-C bond formation reaction, $CoCp_2$ was introduced as a new reducing reagent and cyanide was used as inorganic protecting group to achieve a ligand-centered reduction. Even though no demetallation of 7,8-*seco*-corrinoids was achieved, this route represents the first reversible synthesis of B-ring opened B_{12} derivatives. Importantly, two route intermediates are antivitamins B_{12}, as shown by microbiological assays with *L. Leichmannii*.

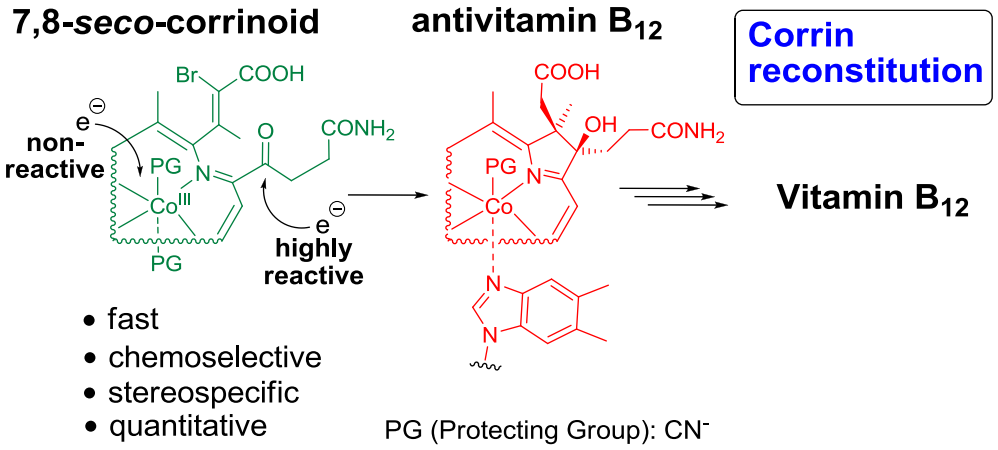

Scheme 57. Four-step synthesis of vitamin B_{12} from a 7,8-*seco*-corrinoid.

2) The 5,6-*seco*-corrin approach

The synthesis of metal-modified B_{12} derivatives was achieved in three steps. The crucial reaction in this project is the one-step demetallation and ring closure of dicyano-5,6-dioxocobalamin (Scheme 58, left). In this unprecedented method, $CoCp_2$ was used as metal and ligand reducing agent and KCN was employed for the extraction of cobalt. With 5,6-diol-H-balamin in hand, Ni^{II}, Zn^{II} and Cu^{II} were incorporated to the corrin cavity obtaining diolmetbalamins. These are a new family of compounds that only differ from B_{12} in its metal center and the presence of a diol moiety instead of a double bond at positions C5 and C6.

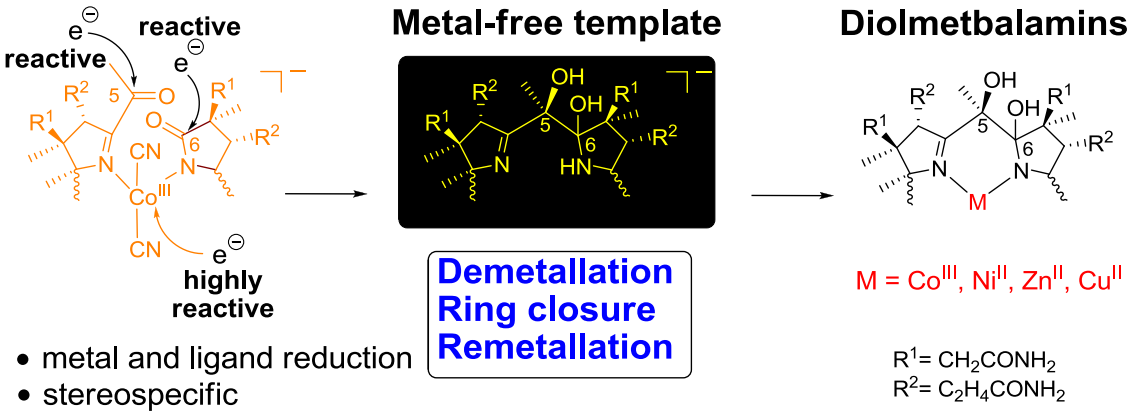

Scheme 58. Three-step synthesis of 5,6-diolmetbalamins.

In summary, two routes towards the synthesis of metbalamins from secocorrinoids are presented. In both approaches, the corrin macrocycle was reconstituted under reducing conditions using $CoCp_2$ as electron donor. However, the different electronic properties of 7,8- and 5,6-*seco*-corrinoids led to completely opposite results when cyanide was introduced. Indeed, while this ligand acted as a protecting group for the cobalt center in 7,8-*seco*-corrinoids, it behaved as a decomplexating agent for 5,6-*seco*-corrinoids and hence allowed the synthesis of 5,6-diol-metbalamins.

These results pose two major challenges to complete a chemical route towards metbalamins: 1) eliminate the diol moiety of 5,6-diolmetbalamins and 2) demetallate 7,8-*seco*-corrinoids.

5. List of compounds

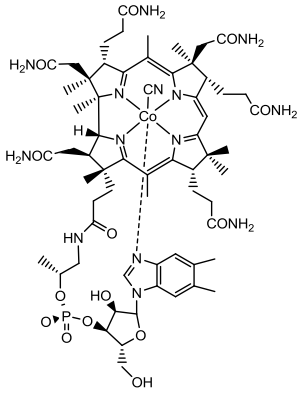

1

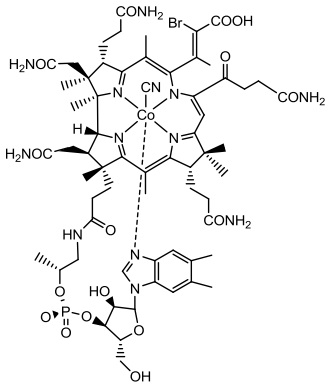

2

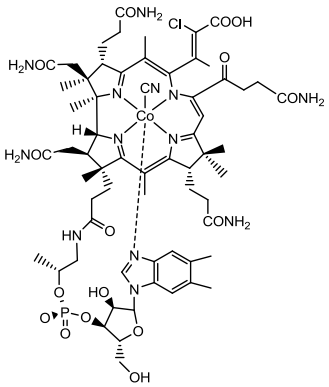

3

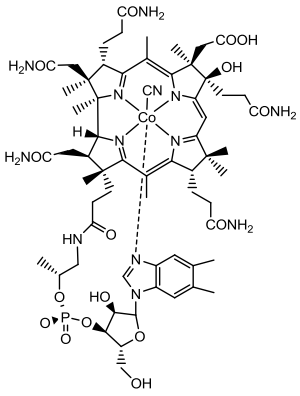

4

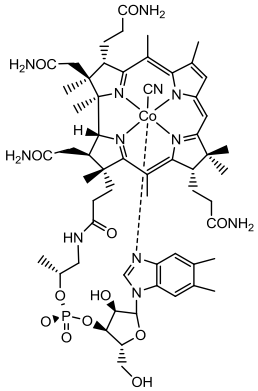

5

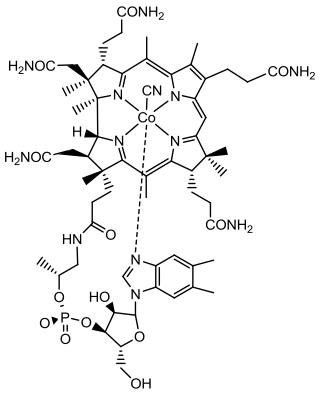

6

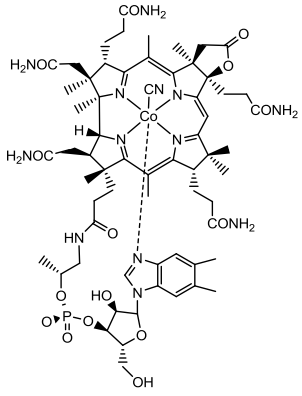

7

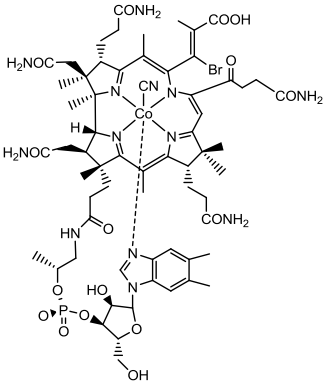

8

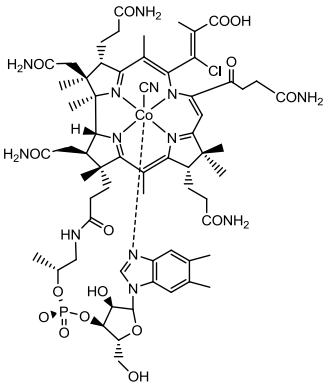

9

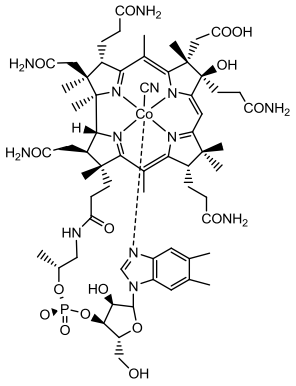

10

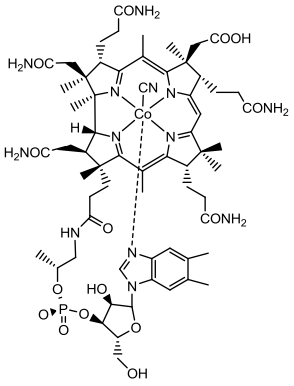

11

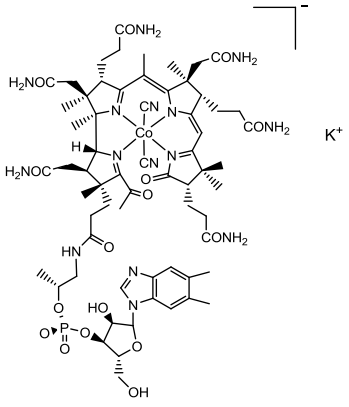

12

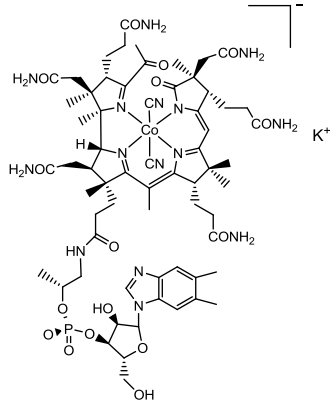

13

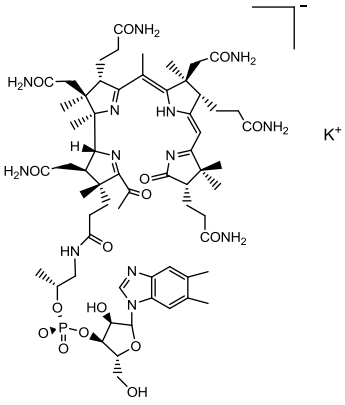

14

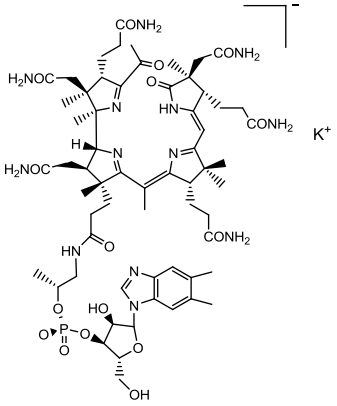

15

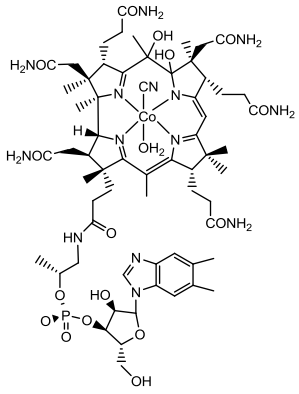

16

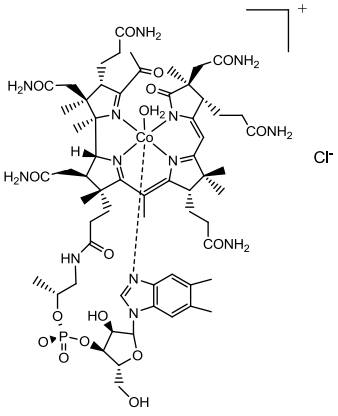

17

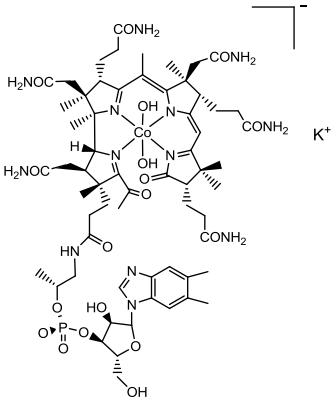

18

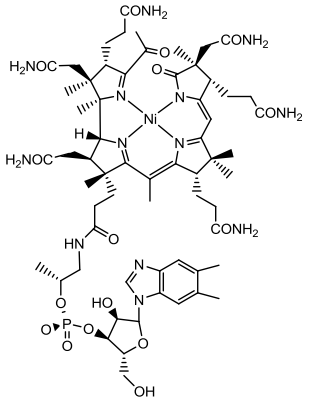

19

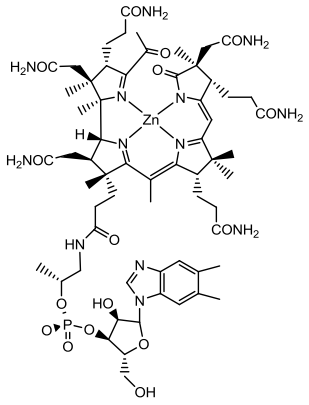

20

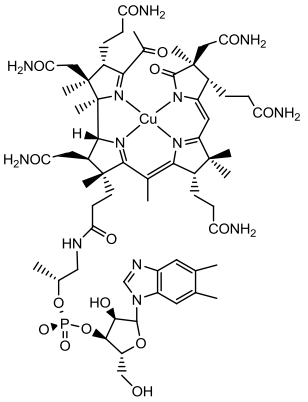

21

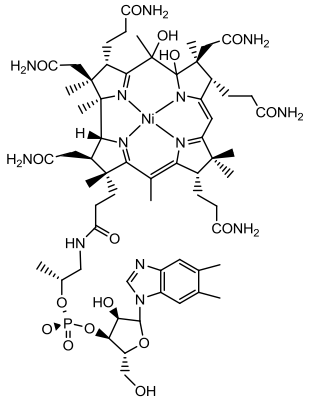

22

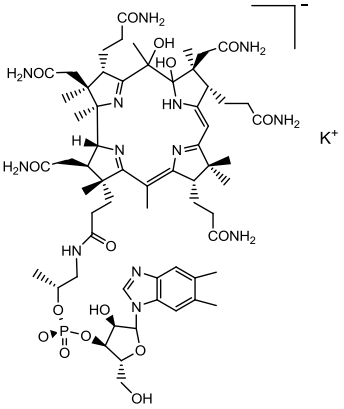

23

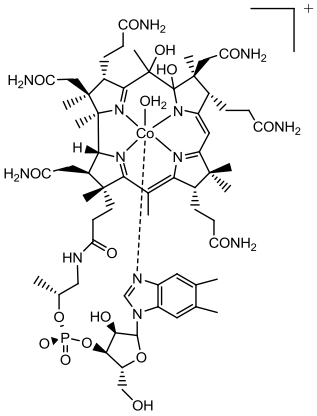

24

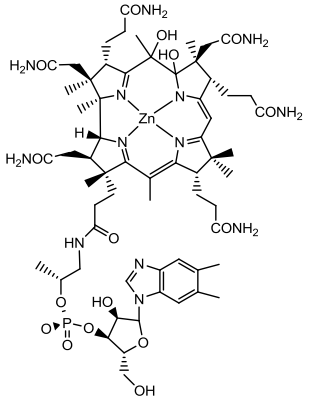

25

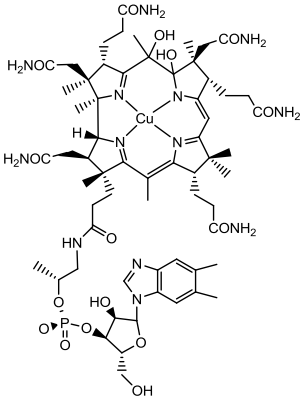

26

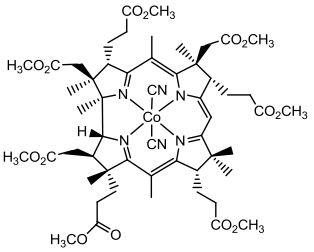

27

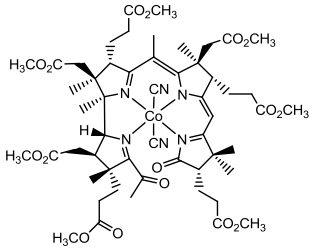

28

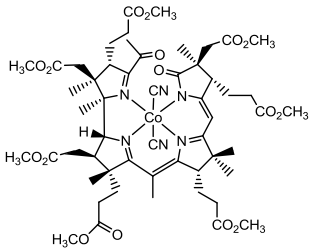

29

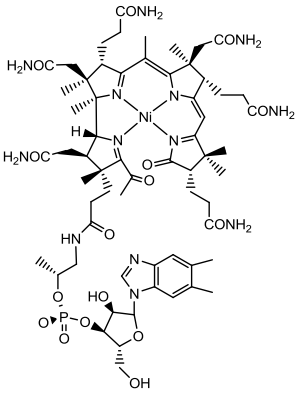

30

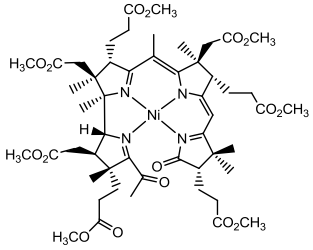

31

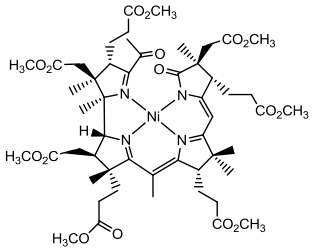

32

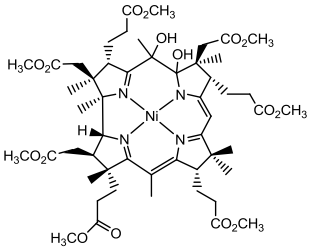

33

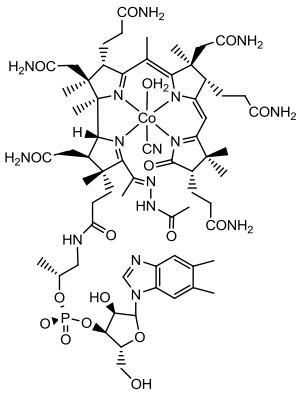

34

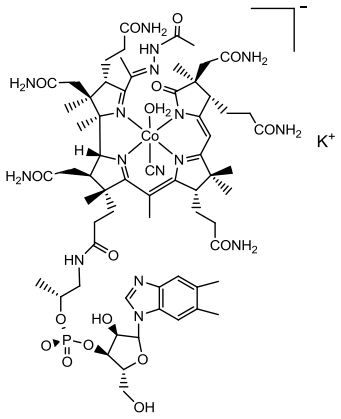

35

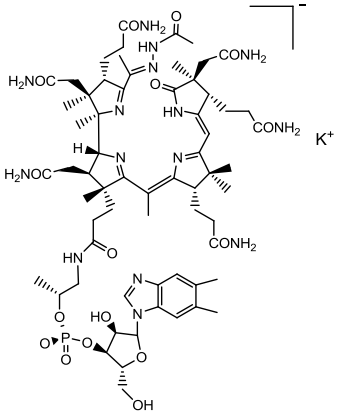

36

6. Experimental

6.1. Materials and Methods

Materials: Chemicals were of reagent grade quality or better, obtained from commercial suppliers and used without further purification. Vitamin B_{12} was a generous gift from DSM Nutritional products AG (Basel/Switzerland) and Prof. B. Jaun (retired ETH Zurich). All solvents were of reagent, analytical, HPLC or LC-MS grade respectively and obtained from commercial suppliers. Bidistilled water was used in all reactions. Millipore water was used in UPLC measurements.

UPLC: UPLC-MS spectra were recorded on an Acquity Waters system equipped with a PDA detector and an autosampler using an ACQUITY UPLC BEH C18 Gravity 1.7 μm (2.1 mm × 50 mm) reverse phase column. The UPLC system was connected to a Bruker Daltonics HCT ESI-MS spectrometer. A total volume of 1 μL of a sample soln. was analysed. All solvents used were of LC-MS grade.

- Method 1: A gradient (0 min 5% A, 0.5-2 min 30% A, 2-4 min 100% A, 4-5 min 100% A) of acetonitrile (solvent A) versus an aq. soln. of 0.1% HCOOH (solvent B) was applied using a flow rate of 0.3 mL/min.
- Method 2: A gradient (0 min 14% A, 0.5-4 min 20% B, 4-4.1 min 100% B, 4.1-5 min 100%A) of acetonitrile (solvent A) versus an aq. soln. of 0.1% HCOOH (solvent B) was applied using a flow rate of 0.3 mL/min.

Preparative HPLC: Separations were conducted on a *VWR LaPrep* system equipped with a PDA detector and Nucleosil C18 250/21 or Nucleosil C18 250/40 columns from Macherey-Nagel.

- Method 3: A gradient (0 min 25% C, 0.5-30 min 60% C, 30-30.1 min 100% C, 30.1-40 min 100% C) of MeOH (solvent C) versus an aq. soln. of 0.1% CF_3COOH (solvent D) was applied using a flow rate of 16 mL/min.

- Method 4: A gradient (0 min 25% C, 0.5-30 min 60% C, 30-30.1 min 100% C, 30.1-40 min 100% C) of MeOH (solvent C) versus an aq. soln. of 0.1% CH_3COOH (pH 5, solvent E) was applied using a flow rate of 16 mL/min.
- Method 5: A gradient (0 min 20% B, 0.5-30 min 26% B, 30-30.1 min 100% B, 30.1-40 min 100% B) of CH_3CN (solvent B) versus an aq. soln. of 0.1% CH_3COOH (pH 5, solvent E) was applied using a flow rate of 18 mL/min.
- Method 6: A gradient (0 min 20% B, 0.5-40 min 30% B, 40-40.1 min 100% B, 40.1-50 min 100% B) of CH_3CN (solvent B) versus an aq. soln. of 0.1% CH_3COOH (pH 5, solvent E) was applied using a flow rate of 18 mL/min.
- Method 7: CH_3CN (19%; solvent A) versus an aq. soln. of 0.1% CF_3COOH (solvent D) was applied for the iscratic elution using a flow rate of 40 mL/min.

ESI-MS: Spectra were recorded on a Bruker Daltonics HTC ESI-MS operated in the positive or negative mode. Injection rate 3 µL/min. Nebulizer P =10 psi, dry gas flow rate 5 L/min, gas T = 350 ºC. All solvents used were of LCMS grade.

HR-ESI-MS: Spectra were recorded on a Bruker maXis QTOF-MS instrument (Bruker Daltonics GmbH, Bremen, Germany). The samples were dissolved in MeOH and analyzed via continuous flow injection at 3 µL/min. The mass spectrometer was operated either in positive or negative ion mode with a capillary voltage of 4 kV, an endplate offset of –500 V, nebulizer pressure of 5.8 psig, and a drying gas flow rate of 4 L/min at 180°C. The instrument was calibrated with a sodium formate soln. (500µl H_2O: 500µl iPrOH: 20µl HCOOH: 20µl 0.1M $NaOH_{aq}$). The resolution was optimized at 30.000 FWHM in the active focus mode. The accuracy was better than 2 ppm in a mass range between *m/z* 118 and 1600.

Spectroscopy: UV-Vis spectra were recorded on a *Varian Cary 50* using quartz cells with a path length of 1 cm. Citation of λ_{max} (log ε) in nm. ^{1}H- and ^{13}C-NMR as well as 2D-NMR spectra were recorded on a 500 MHz *Oxford NMR AS 500* using a QNP probehead and *MestReNova 6.0.2* as evaluation tool. All spectra were recorded in D_2O at 300 K and TSP was used as a reference for all ^{13}C-NMR experiments.

Electrochemistry: Electrosynthesis was performed in a 50 mL five-necked round bottom flask containing three electrodes: a Pt-net (working electrode), a Pt wire

(counterelectrode) and an Ag/AgCl (3M) reference electrode. The electrodes were connected to AMEL Potentiostat Mod. 549 and compounds were dissolved in an electrolyte soln. (0.1 M TRIS in H_2O, pH 8.1).

Solid Phase Extraction: Chromafix C18ec columns were applied for solid phase extraction (SPE). The compounds were dissolved in water, transferred to the adsorbent, washed with water and eluted with MeOH.

Bacterial growth tests: B_{12} dependent *Lactobacillus leichmannii* was purchased (as strain DSMZ 20355, ATCC 7830) from the German Collection of Microorganisms and Cell Cultures (Braunschweig, Germany). For maintenance, stock cultures Lactobacillus were routinely grown overnight in Difco Microinoculum broth at 30 °C. The medium was centrifuged after 24 h (3 min x 5000 rpm), the supernatant was removed and the pellet was washed three times with sterile 0.9 % NaCl. Vitamin B_{12} Assay Medium (#82897; Fluka, Buchs, Switzerland) was prepared in 8 mL screw cap test tubes according to the supplier's instructions and sterilized (15 min at 121 °C). Dilutions of B_{12} were added to the medium using sterile filters (0.22 µm) followed by the addition of a 50 µL inoculum. All growth experiments were always performed in triplicates at 37 °C. Growth was monitored spectrophotometrically at 680 nm at time intervals of 2-3 h.

6.2. Experimental procedures

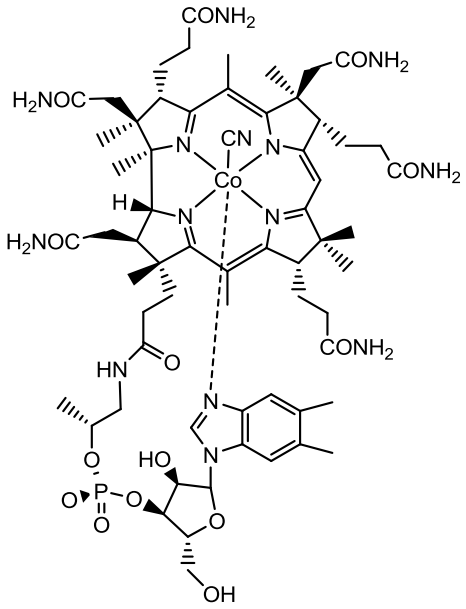

Cyanocobalamin (1): **11** (11 mg, 8 μmol, 1 equiv) was dissolved in NH_4Cl (4M; 4 mL) and EDC·HCl (150 mg, 780 μmol**,** 10 equiv) was added. The mixture was stirred overnight at 23 ºC, purified with solid phase extraction and then with preparative HPLC (Method 3). Lyophilization afforded **1** (2.3 mg, 2 μmol, 21%) as a red powder.

UV-Vis (H_2O, c = 1.3 x 10^{-5} M) λ /nm (logε) = 279 (4.4), 306 (4.3), 321 (4.1), 361 (4.5), 411 (4.0), 512 (4.0), 522 (4.1). **ESI-MS** (H_2O) m/z = 1355.6 $[M+H]^+$, 678.6 $[M+2H]^{2+}$ (m/z_{calc}: 1355.6). **HR-ESI-MS** (H_2O) m/z= 678.29106 $[M+2H]^{2+}$ (m/z_{calc}: 678.29098) **UPLC** (Method 1) t_R = 1.7 min. **^{1}H-NMR** (D_2O, 500 MHz) δ/ppm = 7.29 (s, 1H), 7.10 (s, 1H), 6.52 (s, 1H), 6.36 (d, J = 3.2 Hz, 1H), 6.09 (s, 1H), 4.28 (m, 2H), 4.20 (m, 1H), 4.07 (m, 2H), 3.92 (m, 1H), 3.76 (dd, J = 12.9, 3.9 Hz, 1H), 3.59 (d, J = 14.7 Hz, 1H), 3.41 (dd, J = 11.4, 5.3 Hz, 1H), 2.97-0.99 (m, 40H), 2.59 (s, 3H), 2.55 (s, 3H), 2.27 (s, 6H), 1.88 (s, 3H), 1.46 (s, 3H), 1.41 (s, 3H), 1.40 (s, 3H), 1.27 (d, J = 6.3 Hz, 3H), 1.21 (s, 3H), 0.46 (s, 3H). **^{13}C-NMR** (D_2O, 126 MHz) δ/ppm = 182.8, 181.6, 180.9, 180.6, 179.8, 179.6, 178.5, 178.4, 177.8, 177.5, 176.3, 168.8, 168.0, 144.5, 139.4, 137.9, 135.8, 132.7, 119.2, 114.2, 110.3, 106.8, 97.7, 89.8, 87.8, 84.9, 77.7, 75.7, 75.7, 71.5, 63.1, 61.9, 59.0, 58.4, 56.4, 54.2, 50.9, 50.0, 48.0, 45.6, 45.5, 41.7, 37.6, 37.3, 35.3, 34.9, 34.3, 34.2, 34.0, 30.8, 28.7, 28.7, 22.7, 22.6, 22.2, 22.1, 22.0, 21.9, 19.5, 18.5, 18.1, 17.9.

Co$_\beta$-cyano-71-bromo-7,8-*seco*-cobalamin (2): synthesized according to literature procedures.[98]

Co$_\beta$-cyano-71-chloro-7,8-*seco*-cobalamin (3): synthesized according to literature procedures.[98]

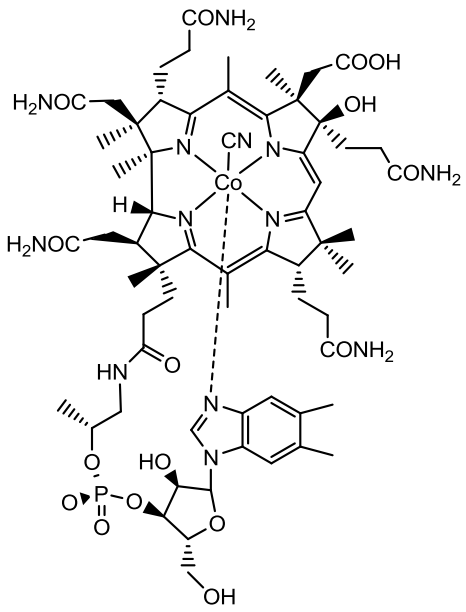

Co$_\beta$-cyano-8$_\beta$-hydroxy-cobalamin-c-acid (4): Method a: 7,8-*seco*-corrinoid **2** (38 mg, 26 μmol, 1 equiv) was dissolved in ddH_2O (2 mL) and $NaBH_4$ (1.5 mg, 39 μmol, 1.5 equiv) was added to the stirred soln. An immediate colour change from green to dark red was observed. The mixture was stirred for 45 min and then purified by solid phase extraction and preparative HPLC (Method 4). **4** was obtained as a red powder (12 mg, 9 μmol, 33%) after lyophilization.

Method b: 7,8-*seco*-corrinoid **2** (20 mg, 14 μmol, 1 equiv) and KCN (11 mg, 170 μmol, 12 equiv) were dissolved in MeOH (4 mL). The mixture was stirred for 30 min. Subsequently, the dark green soln. was purged with N_2(g) for 15 min and $CoCp_2$ (10 mg, 53 μmol, 4 equiv) was added in a nitrogen atmosphere. The mixture turned immediately violet. Quantitative conversion to Co$_{\alpha,\beta}$-dicyano-8$_\beta$-hydroxy-cobalamin-c-acid (**4-CN**) was observed within 5 min according to MS measurements (m/z = 1380.6 $[M]^-$). The pH of the soln. was adjusted to 6 with an aq. soln. of CH_3COOH (2 M) and stirred at 23 ºC for 1 h until the soln. turned red. Solvents were removed under reduced pressure. The red product **4** was dissolved in ddH_2O and purified with solid phase extraction. The solvent was evaporated and **4** was isolated in good yields (16 mg, 12 μmol, 86%) after lyophilization.

Note: When TEMPO (4 equiv) was added to the mixture immediately before the addition of $CoCp_2$, no colour change was observed and UPLC-MS analysis yielded a single peak at t_R = 2.2 min and m/z = 1450.4 $[M+H]^+$, corresponding to the starting material (**2**).

UV-Vis (H_2O, c = 1.6 x 10^{-5} M) λ / nm (logε) = 278 (4.3), 306 (4.1), 360 (4.5), 410 (3.9), 517 (4.0), 552 (4.0). **UPLC** (Method 1) t_R = 1.7 min. **ESI-MS** (H_2O) m/z = 1372.5 $[M+H]^+$ (m/z_{calc}: 1372.6). **HR-ESI-MS** m/z= 686.78065 $[M+2H]^{2+}$ (m/z_{calc}: 687.78279). **^{1}H NMR** (500 MHz, D_2O) δ/ppm = 7.27 (s, 1H), 7.10 (s, 1H), 6.45 (s, 1H), 6.35 (d, *J* = 3.2 Hz, 1H), 6.16 (s, 1H), 4.30 (dd, *J* = 10.4, 6.5 Hz, 3H), 4.08 (m, 4H), 3.95 (dd, *J* = 12.7, 2.3 Hz, 1H), 3.77 (dt, *J* = 12.4, 6.3 Hz, 2H), 3.62 (m, 2H), 3.36 (d, *J* = 6.6 Hz, 1H), 2.96-1.10 (m, 35 H), 2.58 (s, 3H), 2.56 (s, 3H), 2.25 (s, 3H), 2.23 (s, 3H), 1.86 (s, 3H), 1.50 (s, 3H), 1.41 (s, 3H), 1.38 (s, 3H), 1.26 (s, 3H), 1.21 (s, 3H), 0.59 (dd, *J* = 21.7, 9.6 Hz, 1H), 0.42 (s, 3H). **^{13}C NMR** (126 MHz, D_2O) δ/ppm = 182.8, 181.8 , 181.7, 180.9 , 180.5, 180.2, 179.4, 178.5, 178.4, 177.5, 176.7, 168.7, 166.4, 144.4, 139.5, 138.0, 135.9, 132.6, 119.0, 114.2, 109.4, 107.3, 95.4, 89.8, 88.4, 87.9, 84.7, 77.6, 75.7, 75.6, 71.5, 63.0, 62.0, 59.4, 57.4, 56.5, 51.1, 49.9, 48.0, 45.9, 45.5, 41.7, 37.6, 37.3, 36.1 , 35.3, 35.0, 34.2, 33.9, 31.7, 30.8, 28.8, 22.6, 22.1, 22.0, 21.8, 21.7, 20.0, 19.5, 18.6, 17.9.

Co$_\beta$-cyano-Δ^7-dehydro-7-decarboxymethyl-8-decarboxyethyl-cobalamin (5): 7,8-*seco*-corrinoid **2** (20 mg, 14 μmol, 1 equiv) was dissolved in ddH_2O (2 mL) and $NaBH_4$ (0.8 mg, 21 μmol, 1.5 equiv) was added to the stirred soln. at 23 ºC. An immediate color change from green to dark red was observed. The mixture was stirred for 45 min and then purified by solid phase extraction and preparative HPLC (Method 3), yielding **5** as a blue powder (1 mg, 1 μmol, 6%) after lyophilization. *Note*: The main product in this reaction was **4** (33%) and **6** was also obtained as a side-product.

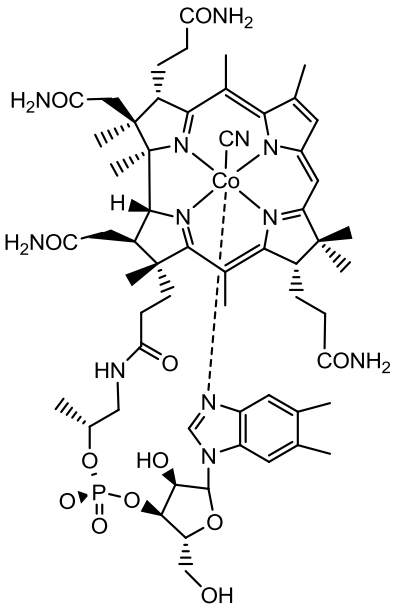

UV-Vis (H_2O, c = 2.5 x 10^{-5} M) λ / nm (logε) = 278 (4.4), 359 (4.4), 432 (3.9), 623 (4.1). **UPLC** (Method 1) t_R = 2.6 min. **ESI-MS** (H_2O) m/z = 1225.6 $[M+H]^+$ **(**m/z_{calc}: 1225.5). **HR-ESI-MS** m/z = 613.25401 $[M+2H]^{2+}$ (m/z_{calc}: 613.25387). **^{1}H NMR** (500 MHz, D_2O) δ/ppm = 7.06 (s, 1H), 6.99 (s, 1H), 6.44 (s, 1H), 6.28 (s, 1H), 5.87 (s, 1H), 4.70 (td, J = 8.8, 4.3 Hz,

1H), 4.31 (d, J = 8.5 Hz, 1H), 4.26 (d, J = 3.4 Hz, 1H), 4.16 (d, J = 6.3 Hz, 1H), 4.09 (d, J = 10.9 Hz, 2H), 3.96 (d, J = 11.1 Hz, 1H), 3.77 (dd, J = 12.9, 4.4 Hz, 1H), 3.65 (d, J = 14.4 Hz, 1H), 3.48 (d, J = 10.3 Hz, 1H), 2.94-1.71 (m, 19H), 2.72 (s, 6H), 2.68 (s, 3H), 2.28 (s, 3H), 1.92 (s, 3H), 1.50 (s, 3H), 1.42 (s, 3H), 1.35 (s, 3H), 1.28 (d, J = 6.3 Hz, 3H), 1.20 (s, 3H), 0.42 (s, 3H). **^{13}C NMR** (126 MHz, D_2O) δ/ppm = 182.0, 181.1, 181.1, 180.9, 180.5, 178.4, 178.4, 177.5, 169.2, 164.7, 155.7, 150.9, 144.2, 139.2, 137.1, 135.8, 132.4, 118.5, 116.3, 113.9, 108.3, 95.5, 89.7, 89.1, 84.9, 78.7, 75.9, 75.5, 74.5, 71.5, 64.3, 63.4, 63.3, 62.0, 59.2, 56.7, 51.4, 50.3, 48.2, 44.7, 41.7, 37.6, 37.1, 35.8, 35.2, 34.2, 33.9, 30.9, 28.3, 23.6, 22.6, 22.3, 21.8, 19.3, 19.0, 18.8, 18.1, 14.8.

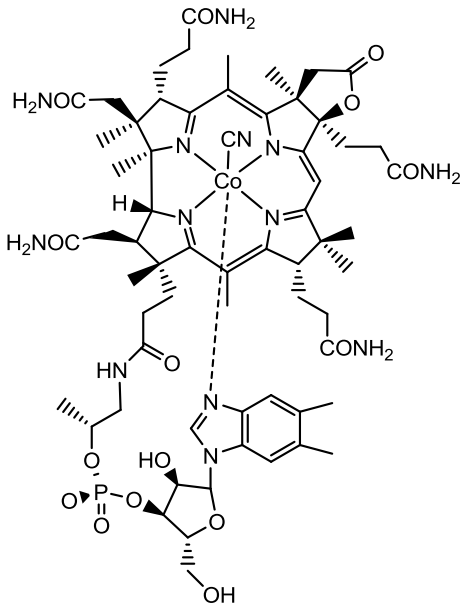

Co$_\beta$-cyanocobalamin-c-lactone (7): 7,8-*seco*-corrinoid **2** (20 mg, 14 μmol, 1 equiv) and KCN (11 mg, 170 μmol, 12 equiv) were dissolved in MeOH (4 mL). The mixture was stirred for 30 min. Subsequently, the dark green soln. was purged with N_2(g) for 15 min and $CoCp_2$ (10 mg, 53 μmol, 4 equiv) was added in a nitrogen atmosphere. The mixture turned immediately violet. Quantitative conversion to Co$_{\alpha,\beta}$-dicyano-8$_\beta$-hydroxy-cobalamin-c-acid (**4-CN**) was observed within 5 min according to MS measurements (m/z = 1380.6 $[M]^-$). The pH was adjusted to 3 with an aq. soln. of CH_3COOH (2 M) and stirred at 23 ºC and solvents were removed under reduced pressure. The crude was stirred overnight in an aq. soln. of CF_3COOH (0.1%, 3 mL), affording quantitative conversion to **7**. The red soln. was desalted with solid phase extraction. The solvents were removed under reduced pressure yielding **7** in good yields (16 mg, 12 μmol, 85%).

Alternatively, **7** was also synthesized according to literature procedures[121] in 91% yields starting from **1** and used as reference.

UV-Vis (H_2O, 1.8 x 10^{-5} M): λ / nm (logε) = 278 (4.3), 305 (4.2), 359 (4.5), 409 (3.9), 522 (4.0), 551 (4.0). **UPLC** (Method 1) t_R = 2.0 min. **ESI-MS** (H_2O): m/z = 1354.6 $[M+H]^+$, 677.9 $[M+2H]^{2+}$ (m/z_{calc}: 1354.5). **HR-ESI-MS** (H_2O): m/z = 677.77521 $[M+2H]^{2+}$ (m/z_{calc}: 677.77516). **^{1}H NMR** (D_2O, 500 MHz) δ/ppm = 7.32 (s, 1H), 7.12 (s, 1H), 6.44 (s, 1H), 6.37 (d, J = 3.2 Hz, 1H), 6.09 (s, 1H), 4.29 (m, 2H), 4.20 (dd, J = 8.9, 1.9 Hz, 1H), 4.09 (m, 2H), 3.93 (dd, J = 12.9, 2.4 Hz, 1H), 3.75 (dd, J = 12.9, 4.0 Hz, 1H), 3.61 (d, J = 14.4 Hz, 1H), 3.38 (d, J = 9.8 Hz, 1H), 3.31 – 3.26 (m, 1H), 3.00 – 2.92 (m, 2H), 2.85-1.15 (m, 35H), 2.61 (s, 3H), 2.57 (s, 3H), 2.29 (s, 3H), 2.27 (s, 3H), 1.93 (s, 3H), 1.49 (s, 3H), 1.42 (s, 3H), 1.38 (s, 3H), 1.26 (d, J = 6.3 Hz, 3H), 1.17 (s, 3H), 0.50 (s, 3H). **^{13}C NMR** (D_2O, 126 MHz): δ/ppm = 183.0, 182.5, 182.2, 180.8, 180.5, 179.1, 178.8, 178.5, 178.4, 177.4, 169.8, 168.6,165.1, 144.7, 139.7, 138.1, 136.1, 132.9, 118.2, 114.7, 109.7, 108.6, 98.1, 94.6, 90.0, 88.00, 84.9, 78.4, 75.9, 75.7, 75.1, 71.6, 63.2, 62.1, 59.3, 56.5, 55.1, 51.7, 50.1, 45.5, 44.3, 41.8, 37.7, 37.2, 35.3, 35.1, 34.2, 33.6, 32.0, 31.6, 30.7, 28.8, 22.8, 22.3, 22.1, 21.9, 21.8, 21.8, 19.5, 19.1, 18.8, 18.0.

Co$_\beta$-7-bromo-71-methyl-7,8-*seco*-cobalamin (8): synthesized according to literature procedures.[98]

Co$_\beta$-7-chloro-71-methyl-7,8-*seco*-cobalamin (9): synthesized according to literature procedures.[98]

Co$_\beta$-cyano-8$_\beta$-hydroxy-cobalamin-epi-c-acid (10):

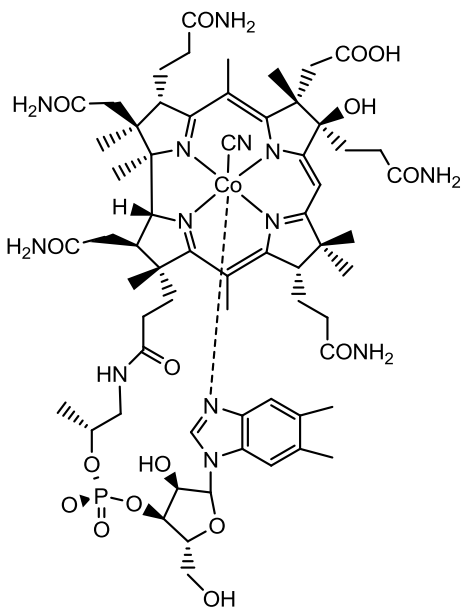

Method a: Rearranged 7,8-*seco*-corrinoid **8**[98] (13 mg, 9 μmol, 1 equiv) was dissolved in ddH_2O (2 mL) and $NaBH_4$ (1.5 mg, 39 μmol, 4 equiv) was added to the stirred soln. at 23 ºC. An immediate color change from green to dark red was observed. After 1 h, an aq. soln. of CF_3COOH (0.1%, 2 mL) was added and the mixture was stirred overnight at 23 ºC. The product was desalted by solid phase extraction and **10** was obtained as a red powder (11 mg, 8 μmol, 89 %) after lyophilization.

Method b: Rearranged 7,8-*seco*-corrinoid **8**[98] (14 mg, 10 μmol, 1 equiv) and KCN (16 mg, 244 μmol, 24 equiv) were dissolved in MeOH (3 mL). The mixture was stirred for 30 min. Subsequently, the dark green soln. was purged with N_2(g) for 15 min and $CoCp_2$ (8 mg, 42 μmol, 4 equiv) was added in a nitrogen atmosphere. The mixture turned violet within seconds. Quantitative conversion to Co$_{\alpha,\beta}$-dicyano-8$_\beta$-hydroxy-7-epicobalamin-c-acid (**10-CN**) was observed within 5 min according to MS measurements. The pH of the soln. was adjusted to 3 with an aq. soln. of CF_3COOH (0.5%) and stirred at 23 ºC overnight. Solvents were removed under reduced pressure. The red product **10** was dissolved in ddH_2O and purified with solid phase extraction. The solvent was evaporated and **10** was isolated in good yields (12 mg**,** 9 μmol, 89 %) after lyophilization.

UV-Vis (H_2O, 1.8 x 10^{-5} M): λ / nm (logε) = 278 (4.4), 287 (4.4), 361 (4.5), 410 (3.7), 519 (4.0), 550 (4.0). **UPLC** (Method 1) t_R = 1.9 min. **ESI-MS** (H_2O) m/z = 1372.6 $[M+H]^+$ (m/z$_{calc}$: 1372.6). **^{1}H NMR** (D_2O, 500 MHz) δ/ppm = 7.27 (s, 1H), 7.08 (s, 1H), 6.42 (s, 1H), 6.35 (d, J = 2.9 Hz, 1H), 6.01 (s, 1H), 4.30 (dd, J = 10.3, 6.5 Hz, 3H), 4.17 (d, J = 7.2 Hz, 1H), 4.07 (t, J = 9.0 Hz, 3H), 3.92 (m, 2H), 3.77 (dd, J = 12.7, 3.4 Hz, 2H), 3.63 (m, 3H), 3.35 (d, J = 8.0 Hz, 2H), 3.18 (m, 2H), 2.96 (dd, J = 14.3, 9.5 Hz, 2H), 2.77-1.13 (m, 15H), 2.58 (s, 3H),

2.56 (s, 3H), 2.25 (s, 6H), 1.48 (s, 3H), 1.40 (s, 3H), 1.38 (s, 3H), 1.35 (s, 3H), 1.25 (s, 3H), 1.20 (s, 3H), 0.43 (s, 3H). **^{13}C NMR** (D_2O, 126 MHz): δ/ppm = 182.8, 182.1, 181.6, 180.7, 180.3, 179.9, 179.4, 178.3, 178.2, 177.4, 174.5, 168.5, 166.9, 144.2, 139.3, 137.8, 135.7, 132.5, 118.8, 114.1, 109.2, 107.1, 94.7, 89.6, 87.7, 86.9, 84.5, 77.5, 75.5, 75.4, 71.3, 62.9, 61.7, 59.0, 57.4, 56.2, 50.9, 49.7, 47.8, 45.3, 43.8, 41.6, 37.3, 37.1, 35.8, 35.1, 34.8, 34.0, 33.8, 31.5, 30.6, 28.8, 22.4, 21.9, 21.8, 21.7, 21.5, 21.1, 19.3, 18.6, 18.3, 17.7.

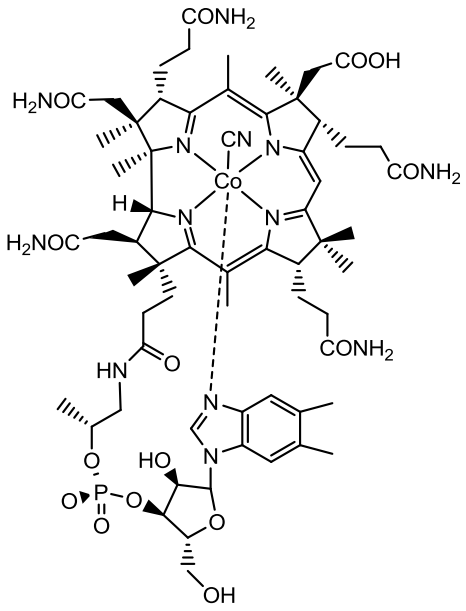

Coβ-cyanocobalamin-c-monocarboxylic acid (11): **7** (16 mg, 12 μmol, 1 equiv) was dissolved in ddH_2O (2 mL). $NaBH_4$ (1.4 mg, 38 μmol, 3 equiv) was added and the red soln. was stirred for 20 min at 23 ºC. Afterwards a second portion of $NaBH_4$ (1.4 mg, 38 μmol, 3 equiv) was added and the resulting mixture was stirred for further 20 min at 23 ºC. The product was subsequently purified with solid-phase extraction. The solvent was evaporated under reduced pressure and **11** was isolated by preparative HPLC (Method 3), affording **11** (6.5 mg, 5 μmol, 42%) as a red powder after lyophilization.

Alternatively, **11** was synthesized from **1** according to literature procedures in two steps and 44% yields. This compound was used as a reference.[104]

UV-Vis (H_2O, c = 1.8 x 10^{-5} M): λ /nm (logε) = 279 (4.3), 305 (4.1), 323 (4.1), 361 (4.5), 410 (3.9), 516 (4.0), 551 (4.0). **UPLC** (Method 1) t_R = 1.8 min. **ESI-MS** (H_2O) m/z = 1356.5 $[M+H]^+$, 678.9 $[M+2H]^{2+}$ (m/z_{calc} : 1356.6). **HR-ESI-MS** (H_2O): m/z = 678.78326 $[M+2H]^{2+}$ (m/z_{calc} = 678.78299). **^{1}H-NMR** (D_2O, 500 MHz) δ/ppm = 7.29 (s, 1H), 7.10 (s, 1H), 6.51 (s, 1H), 6.36 (s, 1H), 6.09 (s, 1H), 4.29 (s, 3H), 4.12 (m, 3H), 4.08 (d, J = 12.1 Hz, 3H), 3.93 (d, J = 12.1 Hz, 2H), 3.77 (m, 2H), 3.62 (d, J = 14.0 Hz, 2H), 3.48 (dd, J = 10.9, 5.0 Hz, 2H), 3.34 (d, J = 10.0 Hz, 2H), 2.97 (dd, J = 14.2, 9.3 Hz, 2H), 2.80-0.99 (m, 28 H) 2.58 (s, 3H), 2.56 (s, 3H), 2.27 (s, 6H), 1.87 (s, 3H), 1.46

(s, 3H), 1.42 (s, 3H), 1.39 (s, 3H), 1.26 (d, J = 6.1 Hz, 3H), 1.19 (s, 3H), 0.46 (s, 3H). **^{13}C-NMR** (D_2O, 126 MHz) δ/ppm = 182.8, 181.7, 181.0, 180.6, 179.9, 179.8, 178.6, 178.5, 177.6, 177.3, 176.4, 168.8, 168.4, 144.7, 139.6, 137.9, 135.9, 132.8, 120.5, 119.3, 118.1, 114.3, 109.9, 106.9, 97.6, 89.9, 87.9, 84.8, 77.8, 75.9, 75.8, 71.7, 63.2, 62.0, 59.3, 57.9, 56.5, 53.5, 50.9, 50.0, 45.6, 44.6, 41.8, 37.7, 37.4, 35.4, 35.1, 34.5, 34.3, 34.1 30.9, 28.9, 22.7, 22.2, 22.1, 22.0, 21.9, 21.9, 19.6, 18.7, 18.2, 18.0.

Dicyano-14,15-dioxocobalamin (12): synthesized according to literature procedures.[98]

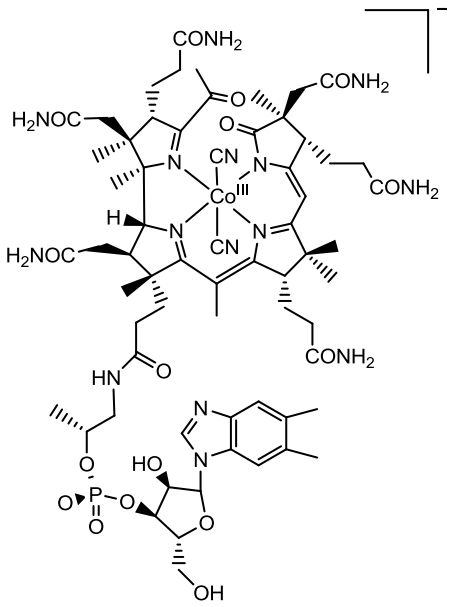

Dicyano-5,6-dioxocobalamin (13): The photooxigenation of B_{12} was performed with modifications based on the procedure described by Kräutler and Stepánek.[93,94] Vitamin B_{12} (240 mg, 177 μmol, 1 equiv), KCN (14 mg, 215 μmol, 1.2 equiv) and the photosensitizer MB (7 mg, 22 μmol, 0.1 equiv) were dissolved in O_2(g)-saturated CH_3OD (8 mL). The mixture was irradiated with a 250 W halogen lamp and bubbled with O_2(g) (1 bubble per second) for 8 h. The solvent was subsequently removed under reduced pressure and the crude was purified by preparative HPLC (Method 7), obtaining dicyano-5,6-dioxocobalamin (66 mg, 47 μmol, 27%) as a blood-orange powder after lyophilization.

UV-Vis (H_2O, c = 4.5 x 10^{-5} M): λ /nm (logε) = 278 (3.7), 285 (3.7), 318 (3.5), 356sh (3.2), 465 (3.4). **UPLC** (Method 2) t_R = 2.3 min. **ESI-MS** (H_2O) m/z = 1412.6 $[M]^-$, (m/z_{calc}: 1412.6). **^{1}H-NMR** (D_2O, 500 MHz) δ/ppm = 8.41 (s, 1H), 7.57 (s, 1H), 7.49 (s, 1H), 6.44 (d, J = 4.7 Hz, 1H), 5.87 (s, 1H), 4.86 (dt, J = 7.7, 5.3 Hz, 2H), 4.62 (d, J = 3.0 Hz, 1H), 4.43(dd, J = 10.9, 5.8 Hz, 1H), 3.95 (dd, J = 12.6, 2.5 Hz, 1H), 3.85 (dd, J = 12.7, 4.2 Hz, 1H), 3.77 (d, J = 10.2 Hz, 1H), 3.72 (dd, J = 6.7, 4.0 Hz, 1H), 3.46 (dd, J = 14.3, 3.3 Hz, 1H), 3.33 (dd, J =

14.1, 5.6 Hz, 1H), 3.12 (dd, J = 7.7, 3.4 Hz, 1H), 2.98 (m, 2H), 2.71-1.12 (m, 40H) 2.42 (s, 3H), 2.40 (s, 3H), 2.12 (s, 3H), 1.71 (s, 3H), 1.33 (s, 6H), 1.30 (d, J = 6.3 Hz, 3H), 1.21 (s, 3H), 1.16 (s, 3H), 0.91 (s, 3H). **^{13}C NMR** (D_2O, 126 MHz) δ/ppm = 201.0, 191.9, 190.1, 186.4, 181.1, 181.0, 180.8, 180.3, 178.7, 178.2, 177.7, 177.6, 163.7, 145.4, 143.2, 136.3, 135.3, 134.5, 121.6, 120.3, 118.0, 114.0, 90.3, 88.5, 86.1, 77.6, 77.0, 75.0, 74.9, 73.9, 63.8, 62.0, 61.7, 56.4, 51.8, 51.00, 49.6, 47.6, 44.6, 44.2, 44.2, 42.5, 42.5, 37.1, 36.6, 35.9, 35.2, 34.6, 34.4, 29.5, 28.7, 26.8, 24.7, 22.6, 22.2, 22.0, 21.5, 21.3, 20.6, 20.2, 19.1, 17.7.

14,15-dioxo-H-balamin (14): synthesized according to literature procedures.[98]

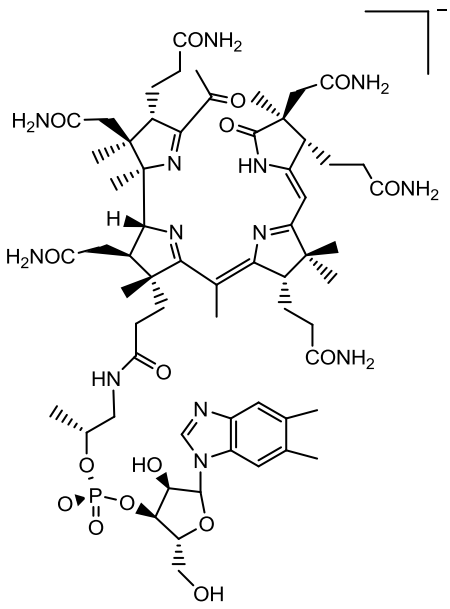

5,6-dioxo-H-balamin (15):

Method a, electrosynthesis: 13 (40 mg, 28 μmol, 1 equiv) was dissolved in ddH_2O (0.1 M TRIS in H_2O, pH 8.1, 35 mL), which was added to the electrochemical reactor (see Materials and Methods). The soln. was purged with N_2(g) for 15 min. A reducing potential (E = -0.9V vs. Ag/AgCl 3M) was applied at 50 ºC and the soln. turned gradually darker. The voltage was turned off after 2 h and an excess of KCN (200 mg, 3 mmol, 107 equiv) was immediately added to the brown soln., which turned bright orange within 1 min. The crude was stirred at 23 ºC for 30 min and then purified by solid phase extraction and preparative HPLC (Method 5). **15** (8 mg, 6 μmol, 22%) was obtained as a yellow powder after lyophilization.

Method b, chemical synthesis: 13 (18 mg, 13 μmol, 1 equiv) was dissolved in ddH_2O (0.1 M TRIS in H_2O, pH 8.1, 3 mL) and the soln. was purged with N_2(g) for 15 min. $CoCp_2$ (12 mg, 63 μmol, 5 equiv) was added to the blood orange soln. in a nitrogen atmosphere and the soln. turned brown within seconds. After 2 min an excess of KCN

(93 mg, 1.4 mmol, 107 equiv) was added at once. The soln. turned dark yellow within 1 min and was stirred in the presence of cyanide for 30 min. The crude was subsequently purified with solid phase extraction and preparative HPLC (Method 5), thus affording **15** (3.5 mg, 3 μmol, 27%) as a yellow powder after lyophilization.

UV-Vis (H_2O, c = 4.5 x 10^{-5} M): λ /nm (logε) = 280 (4.0), 289 (4.0), 379 (3.9). **UPLC** (Method 2) t_R = 2.5 min. **ESI-MS** (H_2O) m/z = 1302.7 $[M]^-$, (m/z_{calc} : 1302.6). **HR-ESI-MS** (H_2O) m/z= 1302.63042 $[M]^-$ (m/z_{calc}: 1302.62933). **^{1}H-NMR** (D_2O, 500 MHz) δ/ppm = 8.40 (s, 1H), 7.53 (s, 1H), 7.44 (s, 1H), 6.43 (d, J = 4.5 Hz, 1H), 5.42 (s, 1H), 4.58 (dd, J = 8.2, 4.1 Hz, 2H), 4.44 (m, 2H), 4.29 (d, J = 3.7 Hz, 1H), 3.95 (dd, J = 12.6, 2.9 Hz, 2H), 3.84 (dd, J = 12.6, 4.2 Hz, 2H), 3.44 (m, 3H), 3.27 (dd, J = 14.1, 3.3 Hz, 1H), 3.12 (dd, J = 8.4, 4.9 Hz, 1H), 3.08 (d, J = 12.9 Hz, 1H), 2.77-1.45 (m, 33H), 2.45 (s, 3H), 2.37 (s, 3H), 2.35 (s, 3H), 1.70 (s, 3H), 1.41 (s, 3H), 1.27 (s, 3H), 1.26 (s, 3H), 1.25 (s, 3H), 1.15 (s, 3H), 1.03 (s, 3H), 0.98 (s, 3H), 0.72 (s, 3H). **^{13}C-NMR** (D_2O, 126 MHz) δ/ppm = 206.3, 192.9, 186.3, 182.4, 182.0, 181.8, 181.4, 181.1, 180.4, 180.1, 179.3, 177.8, 172.5, 154.0, 145.3, 142.9, 136.3, 135.4, 134.5, 121.6, 118.9, 113.9, 91.8, 88.5, 86.7, 86.2, 84.2, 77.0, 75.1, 75.0, 73.9, 63.8, 59.9, 57.8, 52.9, 51.9, 51.8, 51.5, 50.3, 48.3, 44.4, 44.2, 43.0, 41.9, 38.2, 37.6, 36.2, 35.8, 34.2, 30.6, 30.4, 29.0, 25.9, 24.3, 22.6, 22.2, 22.0, 21.4, 21.3, 20.7, 20.0, 19.6.

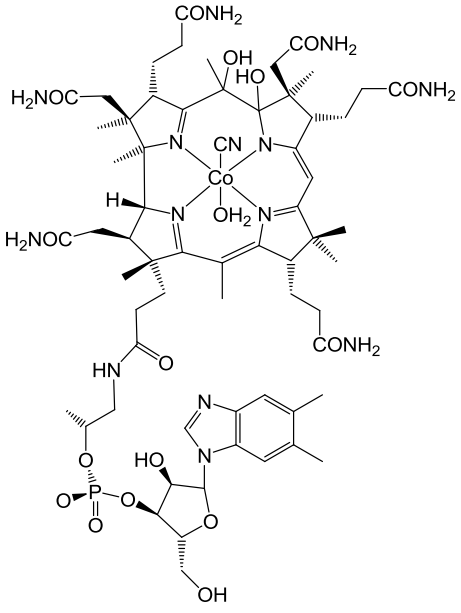

Aquacyano-5,6-diolcobalamin (16): 13 (42 mg, 29 μmol, 1 equiv) was dissolved in ddH_2O (0.1 M TRIS in H_2O, pH 8.1, 35 mL) and was subsequently added to an electrochemical reactor (see Materials and Methods). The soln. was purged with N_2(g) for 15 minutes. A reducing potential (E = -1.0 V vs. Ag/AgCl 3M) was applied at 50 ºC and the soln. turned gradually darker. The voltage was stopped after 4 h and an excess of KCN (30 mg, 461 μmol, 16 equiv) was immediately added to the brown soln., which turned blood-orange within 2 min. The crude was stirred at 23 ºC for 5 min and then purified by solid phase

extraction and preparative HPLC (Method 5). **16** (8 mg, 6 μmol, 22%) was obtained as a yellow powder after lyophilization.

UV-Vis (H_2O, c = 7.3 x 10^{-5} M): λ /nm (logε) = 283 (4.0), 290 (4.0), 320 (3.9), 455 (3.8). **UPLC** (Method 2) t_R = 3.0 min. **ESI-MS** (H_2O) m/z = 1387.7 $[M]^-$,(m/z_{calc} : 1387.6). **HR-ESI-MS** (H_2O) m/z = 695.29359 $[M+2H]^{2+}$ (m/z_{calc}: 695.29372). **^{1}H-NMR** (D_2O, 500 MHz) δ/ppm = 9.25 (s, 1H), 7.70 (s, 1H), 7.66 (s, 1H), 6.62 (d, J = 5.3 Hz, 1H), 6.06 (s, 1H), 4.31 (m, 2H), 4.02 (d, J = 8.7 Hz, 1H), 3.93 (d, J = 10.1 Hz, 2H), 3.83 (dd, J = 12.6, 3.9 Hz, 2H), 3.45 (s, 1H), 3.37 (m, 2H), 3.28 (d, J = 4.6 Hz, 3H), 2.98 (d, J = 17.6 Hz, 1H), 2.91 (s, 1H), 2.79-1.05 (m, 23H), 2.46 (s, 3H), 2.35 (s, 3H), 1.51 (s, 3H), 1.47 (s, 3H), 1.39 (s, 3H), 1.27 (s, 3H), 1.23 (s, 3H), 1.21 (d, J = 3.1 Hz, 3H), 1.21 (s, 3H), 1.11 (s, 3H).

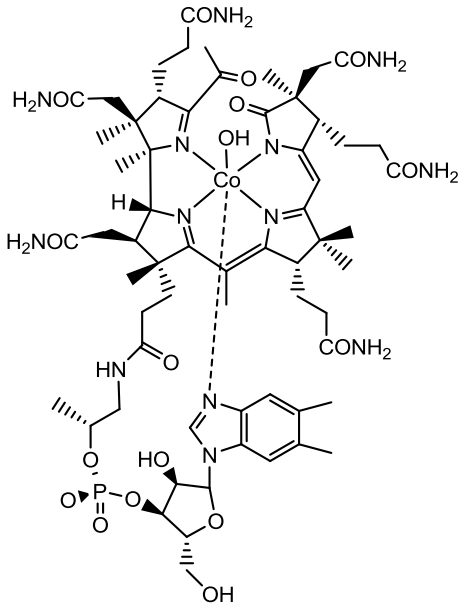

Co$_\beta$-hydroxo-5,6-dioxocobalamin (17): 15 (4 mg , 3 μmol, 1 equiv) was dissolved in ddH_2O (0.1 M TRIS, pH 8.1, 3 mL) and $CoSO_4 \cdot 7H_2O$ (4 mg, 14 μmol, 5 equiv) was added at 23 ºC. The mixture was stirred for 1 h and purified with solid phase extraction. **17** was obtained as an orange powder (3.3 mg, 2.4 μmol, 79%) after lyophilization.

UV-Vis (H_2O, c = 1.0 x 10^{-5} M): λ /nm (logε) = 280 (4.4), 463 (4.0). **UPLC** (Method 2) t_R = 3.5 min. **ESI-MS** (H_2O) m/z = 1360 $[M-OH_2]^+$, 681.0 $[M-OH_2]^{2+}$ (m/z_{calc} : 1360.6). **^{1}H-NMR** (D_2O, 500 MHz) δ/ppm = 7.49 (s, 1H), 7.42 (s, 1H), 7.37 (s, 1H), 6.42 (d, J = 2.9 Hz, 1H), 5.68 (s, 1H), 4.44 – 4.42 (m, 1H), 4.18 (d, J = 8.3 Hz, 1H), 4.09 (d, J = 9.8 Hz, 1H), 3.90 (d, J = 12.8 Hz, 1H), 3.77 (dd, J = 12.9, 4.0 Hz, 1H), 3.50 (s, 1H), 3.21 (s, 2H), 2.85-0.89 (m, 27H), 2.46 (s, 3H), 2.40 (s, 3H), 2.32 (s, 6H), 1.41 (s, 3H), 1.36 (s, 3H), 1.26 (s, 3H), 1.23 (s, 3H), 1.20 (d, J = 6.4 Hz, 3H), 1.11 (s, 3H), 1.04 (s, 3H).**^{13}C-NMR** (D_2O, 126 MHz) δ/ppm = 210.0,

198.0, 184.4, 182.3, 181.7, 181.5, 181.0, 180.3, 179.7, 178.8, 177.9, 177.9, 177.8, 167.6, 146.3, 145.6, 141.7, 137.7, 135.4, 133.6, 123.6, 114.3, 109.3, 98.1, 91.8, 89.9, 84.9, 81.5, 76.2, 75.8, 75.7, 72.3, 63.4, 61.1, 57.1, 55.5, 52.8, 50.9, 50.9, 50.6, 47.6, 46.4, 45.2, 42.9, 37.6, 37.0, 34.6, 34.5, 33.9, 33.7, 33.5, 30.5, 28.8, 24.9, 22.6, 22.3, 21.9, 21.6, 20.2, 18.9, 18.7, 18.5, 16.5.

Dihydroxo-14-15-dioxocobalamin (18): synthesized according to literature procedures.[98]

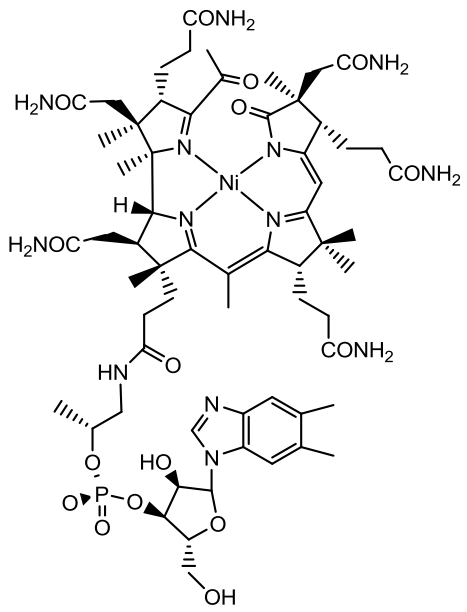

5,6-dioxonibalamin (19): 15 (8 mg , 6 μmol, 1 equiv) was dissolved in ddH_2O (0.1 M TRIS, pH 8.1, 3 mL) and $NiSO_4 \cdot 6H_2O$ (9 mg, 34 μmol, 6 equiv) was added at 23 ºC. The mixture was stirred for 1 h and purified with solid phase extraction. **19** was obtained as an orange powder (7 mg, 5 μmol, 84%) after lyophilization.

UV-Vis (H_2O, c = 2.5 x 10^{-5} M): λ /nm (logε) = 279 (4.3), 289 (4.3), 448 (4.0). **UPLC** (Method 2) t_R = 2.6 min. **ESI-MS** (H_2O) m/z = 1360.6 $[M+H]^+$, 681.0 $[M+2H]^{2+}$ (m/z_{calc} for $C_{62}H_{88}N_{13}NiO_{16}P$:1360.6). **HR-ESI-MS** (H_2O): m/z = 680.78633 $[M+2H]^{2+}$ (m/z_{calc} for $C_{62}H_{90}N_{13}NiO_{16}P$: 680.78543), 691.77731 $[M+Na]^{2+}$ (m/z_{calc} for $C_{62}H_{89}N_{13}NaNiO_{16}P$: 691.77640), 702.76837 $[M+2Na]^{2+}$. **^{1}H-NMR** (D_2O, 500 MHz) δ/ppm = 8.36 (s, 1H), 7.48 (s, 1H), 7.43 (s, 1H), 6.49 (d, J = 5.3 Hz, 1H), 6.12 (s, 1H), 4.35 (d, J = 15.0 Hz, 1H), 3.92 (dd, J = 12.4, 2.7 Hz, 1H), 3.85 (dd, J = 12.5, 4.1 Hz, 1H), 3.67 (s, 4H), 3.29 (d, J = 3.6 Hz, 1H), 3.26 (d, J = 3.5 Hz, 1H), 3.23 (s, 2H), 3.14 – 3.10 (m, 1H), 3.05 (d, J = 11.8 Hz, 1H), 2.98 (s, 2H), 2.82 – 2.74 (m, 1H), 2.65-1.00 (m, 22 H), 2.37 (s, 3H), 2.22 (s, 3H), 2.20 (s, 3H), 2.18 (s, 3H), 1.47 (s, 3H), 1.34 (s, 3H), 1.31 (s, 3H), 1.13 (s, 3H), 1.11 (d, J = 6.4 Hz, 3H), 0.93 (s, 3H). **^{13}C-NMR** (D_2O, 126 MHz) δ/ppm = 201.4, 194.6, 185.6, 185.1, 180.9, 180.6, 178.7, 178.5, 178.0, 177.8, 177.7, 176.8, 165.8, 144.7, 143.5, 135.0, 134.6,134.5, 134.4, 121.5, 114.0, 110.5, 97.8, 89.6, 88.5, 78.6, 78.0,

75.5, 75.1, 64.5, 64.4, 64.3, 62.2, 59.7, 55.3, 52.7, 51.8, 51.7, 50.6, 49.0, 47.0, 46.3, 43.3, 43.1, 36.9, 35.9, 35.8, 34.4, 34.2, 32.5, 29.7, 27.2, 25.3, 23.3, 22.9, 22.4, 22.2, 21.1, 21.0, 20.9, 18.9, 17.1.

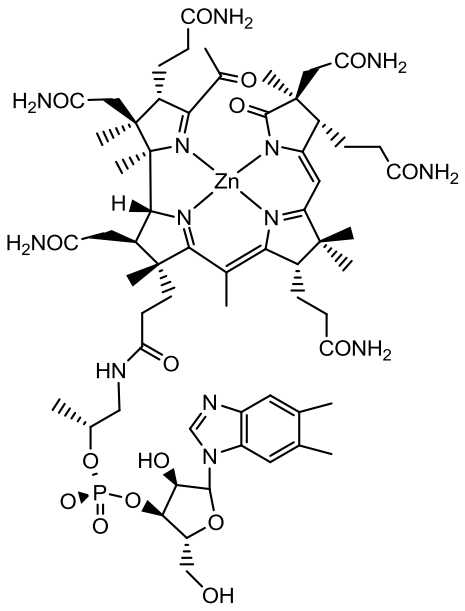

5,6-dioxozincbalamin (20): 15 (3 mg , 2 μmol, 1 equiv) was dissolved in ddH_2O (0.1 M TRIS, pH 8.1, 2 mL) and $ZnSO_4 \cdot 5H_2O$ (3.5 mg, 12 μmol, 6 equiv) was added at 23 ºC. The mixture was stirred for 3 h and purified with solid phase extraction. **20** was obtained as a yellow powder (2.5 mg, 1.8 μmol, 90%) after lyophilization.

UV-Vis (H_2O, c = 1.2 x 10^{-5} M): λ /nm (logε) = 288 (4.7), 433 (4.4). **ESI-MS** (H_2O) m/z = 1365.6 $[M+H]^+$ (m/z_{calc} for $C_{62}H_{89}O_{16}N_{13}PZn$ = 1365.6 $[M+H]^+$). **^{1}H-NMR** (D_2O, 500 MHz) δ/ppm = 8.73 (s, 1H), 7.56 (s, 1H), 7.37 (s, 1H), 6.54 (d, J = 3.3 Hz, 1H), 5.67 (s, 1H), 4.45 (d, J = 6.7 Hz, 1H), 4.21 (s, 1H), 4.03 (d, J = 12.7 Hz, 1H), 3.85 (dd, J = 12.3, 6.0 Hz, 2H), 3.77 (d, J = 14.3 Hz, 1H), 3.28 (t, J = 6.9 Hz, 1H), 3.10-1.05 (m, 31 H), 2.49 (s, 3H), 2.47 (s, 3H), 2.26 (s, 3H), 1.62 (s, 3H), 1.56 (s, 3H), 1.42 (s, 2H), 1.41 (s, 3H), 1.39 (s, 3H), 1.11 (s, 3H), 1.10 (s, 3H). **^{13}C-NMR** (D_2O, 126 MHz) δ/ppm = 199.7, 196.9, 192.3, 184.7, 182.1, 181.0, 180.9, 180.7, 180.67, 179.2, 178.9, 178.0, 176.9, 170.2, 146.5, 138.6, 138.2, 137.0, 134.7, 120.4, 114.0, 111.3, 95.4, 87.0, 86.5, 84.4, 76.3, 75.5, 75.0, 73.4, 65.4, 63.9, 63.7, 57.4, 55.4, 54.0, 51.6, 51.2, 48.7, 46.8, 45.0, 42.2, 37.7, 36.9, 36.9, 36.9, 36.6, 35.5, 31.8, 30.0, 28.9, 26.1, 24.5, 23.1, 22.5, 22.3, 21.9, 20.9, 20.7, 19.7, 18.9, 17.7.

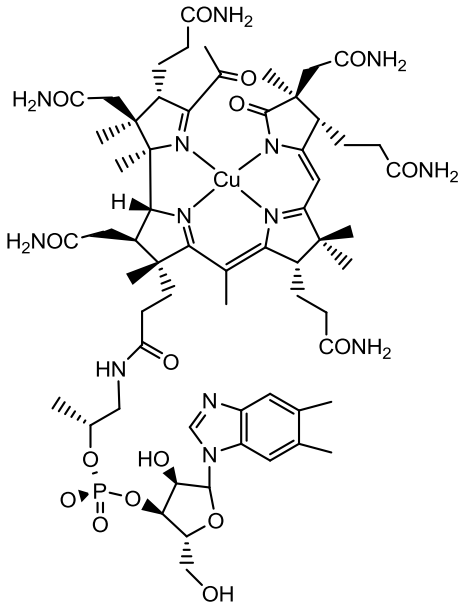

5,6-dioxocubalamin (21): 15 (2 mg , 1.5 μmol, 1 equiv) was dissolved in ddH_2O (0.1 M TRIS, pH 8.1, 2 mL) and $CuSO_4 \cdot 5H_2O$ (2 mg, 8 μmol, 5 equiv) was added at 23 ºC. The mixture was stirred for 3 h and purified with solid phase extraction. **21** (1.5 mg, 1.1 μmol, 72%) was obtained as an orange powder after lyophilization.

UV-Vis (H_2O, c = 4.2 x 10^{-5} M): λ /nm (logε) = 290 (4.3), 301 (4.2), 447 (4.1). **UPLC** (Method 2) t_R = 3.0 min. **ESI-MS** (H_2O) m/z = 1365.6 $[M+H]^+$ (m/z_{calc} : 1365.6). **HR-ESI-MS** (H_2O): m/z = 683.28191 $[M+2H]^{2+}$ (m/z_{calc}: 683.28256).

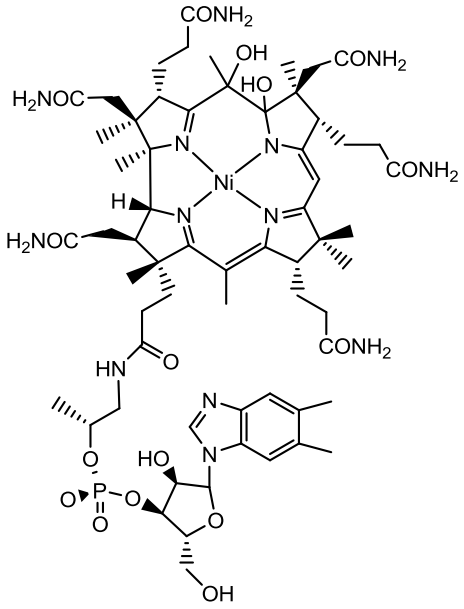

5,6-diolnibalamin (22):

Method a: 19 (6 mg, 4 μmol, 1 equiv) was dissolved in ddH_2O (0.1 M TRIS, pH 8.1, 30 mL) that was subsequently added to an electrochemical reactor (see materials and methods). The soln. was purged with N_2(g) for 15 min. A reducing potential (E = -1.0 V vs. Ag/AgCl 3M) was applied at 50 ºC and the soln. turned gradually darker. The voltage was swichted off after 4 h and the crude was stirred at 23 ºC for 30 min in the presence of air. The crude mixture was then purified by solid phase extraction and preparative HPLC (Method 6), obtaining 3 isomers of **19** as orange powders after lyophilization.

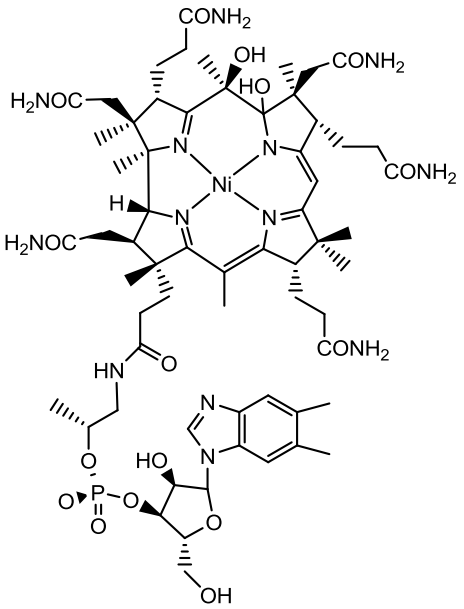

Method b: 23 (2.5 mg**,** 1.8 μmol, 1 equiv) was dissolved in ddH_2O (0.1 M TRIS, pH 8.1, 2 mL) and an excess of $NiSO_4 \cdot 7H_2O$ (17 mg, 60 μmol, 33 equiv) was added. The mixture was stirred for 90 min at 23 ºC and the product was purified using solid phase extraction. **22** (2 mg, 1.5 μmol, 83%) was obtained as an orange powder.

Analytical data referred to the isomer obtained by Method b. **UV-Vis** (H_2O, c = 3.2 x 10^{-5} M): λ /nm (logε) = 280 (4.0), 290 (4.0), 437 (3.8). **UPLC** (Method 2) t_R = 3.1 min. **ESI-MS** (H_2O) m/z = 1360.5 $[M-H]^-$, 1398.5 $[M+Cl]^-$ (m/z_{calc} : 1360.6 $[M-H]^-$ 1398.5 $[M+Cl]^-$). **HR-ESI-MS** (H_2O): m/z = 1360.56121 $[M-H]^-$ (m/z_{calc}: 1360.56468). **^{1}H-NMR** (D_2O, 500 MHz) δ/ppm = 8.34 (s, 1H), 7.45 (s, 1H), 7.39 (s, 1H), 6.45 (s, 1H), 6.02 (s, 1H), 4.93 (s, 1H), 4.86 (s, 2H), 4.36 (s, 2H), 4.06 (d, J = 9.5 Hz, 1H), 3.89 (d, J = 10.8 Hz, 2H), 3.82 (d, J = 9.4 Hz, 2H), 3.29 (m, 3H), 3.16 (d, J = 13.8 Hz, 1H), 3.05 (s, 1H), 2.86 (d, J = 17.3 Hz, 1H), 2.70-0.86 (m, 36 H), 2.68 (s, 3H), 2.48 (s, 3H), 2.16 (s, 3H), 2.14 (s, 3H), 1.68 (s, 3H), 1.40 (s, 3H), 1.22 (s, 3H), 1.10 (d, J = 5.9 Hz, 3H), 1.05 (s, 6H), 1.00 (s, 3H). **^{13}C-NMR** (D_2O, 126 MHz) δ/ppm = 202.2, 188.7, 186.3, 180.8, 180.7, 180.6, 179.6, 178.5, 177.9, 177.9, 177.8, 176.8, 165.4, 144.8, 143.5, 139.0, 135.3, 134.7, 121.5, 114.0, 110.8, 97.3, 89.0, 88.4, 81.3, 79.1, 78.5, 75.5, 75.4, 74.6, 73.1, 64.4, 63.6, 62.4, 55.2, 51.8, 50.6, 46.5, 46.5, 45.6, 43.3, 43.1, 36.9, 36.0, 35.6, 35.1, 35.0, 34.1, 32.3, 29.2, 28.2, 25.0, 23.3, 23.2, 22.4, 21.9, 21.1, 21.0, 19.2, 19.1, 18.9, 17.6.

5,6-diol-H-balamin (23):

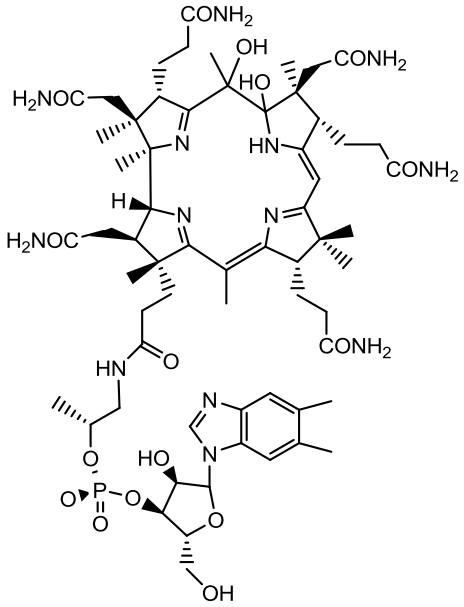

Method a (from 19): 19 (8 mg, 6 μmol, 1 equiv) was dissolved in ddH_2O (0.1 M TRIS, pH 8.1, 30 mL) that was subsequently added to an electrochemical reactor (see materials and methods). The soln. was purged with N_2(g) for 15 min. A reducing potential (E = -1.0 V vs. Ag/AgCl 3M) was applied at 50 ºC and the bright yellow soln. turned gradually darker. The voltage was stopped after 4 h and an excess of KCN (26 mg, 400 μmol, 100 equiv) was added. The mixture was stirred for 30 min at 23 ºC in the presence of air. The product was purified by solid phase extraction and preparative HPLC (Method 6), obtaining 3 isomers of **19** as orange powders after lyophilization.

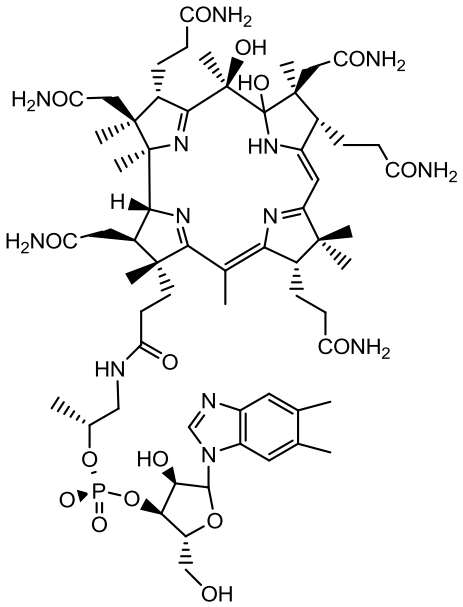

Method b (from 13): **13** (57 mg, 40 μmol, 1 equiv) was dissolved in ddH_2O (0.1 M TRIS, pH 8.1, 7 mL) and the soln. was purged with N_2 (g) for 15 min. $CoCp_2$ (83 mg, 439 μmol, 11 equiv) was added under a nitrogen atmosphere in three portions over 15 min at 23 ºC. The reduced mixture was stirred for other 5 min and then an excess of KCN (200 mg, 3 mmol, 107 equiv) was added at once. The soln. turned brighter within 1 min and was further stirred for 30 min. The crude was subsequently purified with solid phase extraction and preparative HPLC (Method 5), thus affording **23** (12 mg, 9 μmol, 23%) as a yellow powder after lyophilization.

Method c (from 15): 15 (8 mg, 6 μmol 1 equiv) was dissolved in ddH_2O (0.1 M TRIS, pH 8.1, 7 mL), and the mixture was purged with N_2(g) for 15 min. $CoCp_2$ (14 mg, 74 μmol, 12 equiv) was added to the yellow soln. in three portions over 1 h in a N_2(g) atmosphere at 23 ºC. The mixture was stirred at 23 ºC for additional 30 min. $CoCp_2$ was filtered off and the crude mixture was purified using solid phase extraction and preparative HPLC (Method 5). **23** (1.6 mg, 1.2 μmol, 20%) was afforded as a yellow powder after lyophilization.

Note: When TEMPO (30 equiv) was added to a soln. of **15** in ddH_2O (0.1 M TRIS, pH 8.1):MeOH (2:1, 3 mL) before adding $CoCp_2$, UPLC-MS analysis yielded a single peak at t_R = 2.6 min and m/z = 1302.6 $[M]^-$, corresponding to the starting material **15**.

Analytical data refered to the isomer synthesized by Methods b and c. **UV-Vis** (H_2O, c = 7.7 x 10^{-5} M): λ /nm (logε) = 279 (4.1), 288.0 (4.0), 383.0 (4.0). **UPLC** (Method 2) t_R = 2.7 min. **ESI-MS** (H_2O) m/z = 1304.6 $[M]^-$,(m/z_{calc} : 1304.6). **HR-ESI-MS** (H_2O) m/z= 1304.63348 $[M]^-$ (m/z_{calc}: 1304.64498). **^{1}H-NMR** (D_2O, 500 MHz) δ/ppm 8.41 (s, 1H), 7.53 (s, 1H), 7.45 (s, 1H), 6.43 (d, J = 4.9 Hz, 1H), 5.43 (s, 1H), 4.57 (d, J = 3.2 Hz, 1H), 4.41 (m, 2H), 4.08 (d, J = 4.2 Hz, 1H), 3.92 (dd, J = 12.5, 2.6 Hz, 1H), 3.81 (dd, J = 12.6, 4.2 Hz, 1H), 3.56 (d, J = 7.5 Hz, 1H), 3.33 (m, 3H), 3.11 (dd, J = 8.2, 5.0 Hz, 1H), 2.85-1.00 (m, 35H), 2.86 (d, J = 13.7 Hz, 1H), 2.71 (d, J = 16.3 Hz, 1H), 2.65 (d, J = 5.9 Hz, 3H), 2.57 (m, 2H), 2.37 (s, 3H), 2.35 (s, 3H), 2.18 (s, 3H), 1.91 (s, 3H), 1.27 (s, 3H), 1.26 (s, 3H), 1.12 (s, 3H), 1.11 (s, 3H), 1.06 (s, 6H), 0.78 (s, 3H).**^{13}C-NMR** (D_2O, 126 MHz) δ/ppm = 193.8, 184.9, 182.2, 182.1, 181.9, 181.2, 181.1, 180.6, 179.5, 177.8, 145.5, 143.1, 136.3, 135.3, 134.7, 121.7, 119.6, 113.8, 91.3, 88.2, 86.6, 85.3, 84.3, 77.1, 77.1, 75.2, 75.1, 73.8, 73.8, 72.9, 72.6, 63.9, 59.5, 52.8, 51.6, 51.3, 50.6, 48.3, 47.7, 47.5, 44.8, 44.5, 44.4, 41.2, 38.4, 37.3, 36.2, 35.8, 34.3, 31.1, 30.7, 29.2, 29.1, 26.1, 24.0, 22.6, 22.2, 22.1, 21.5, 20.8, 19.8, 19.7.

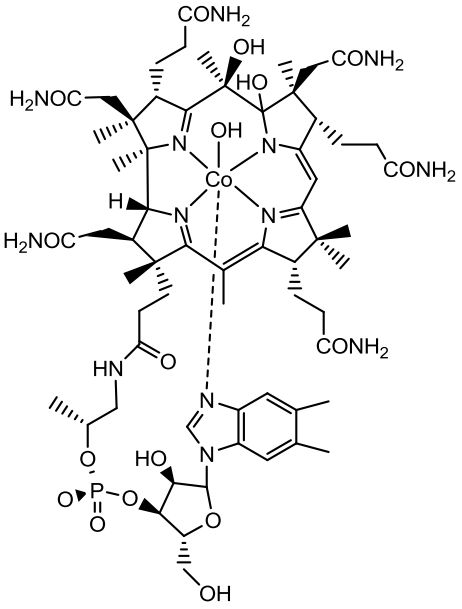

Co$_\beta$-hydroxo-5,6-diolcobalamin (24): 23 (12 mg, 9 μmol, 1 equiv) was dissolved in ddH_2O (0.1 M TRIS, pH 8.1, 3 mL) and the soln. was purged with N_2(g) for 15 min. $CoSO_4 \cdot 7H_2O$ (20 mg, 71 μmol, 8 equiv) was added to the yellow soln. in a nitrogen atmosphere and in the absence of light. The mixture was stirred for 90 min at 23 ºC and purified with solid phase extraction. **24** (11 mg, 8 μmol, 88%) was obtained as an orange powder.

UV-Vis (H_2O, c = 6.6 x 10^{-5} M): λ /nm (logε) = 280 (4.0), 288 (4.0), 359.(3.5), 456 (3.5). **UPLC** (Method 2) t_R = 3.7 min. **ESI-MS** (H_2O) m/z = 1362.5 $[M\text{-}OH]^+$ (m/z_{calc} : 1362.6). **HR-ESI-MS** (H_2O) m/z = 682.29026 $[M\text{-}OH+2H]^{2+}$ (m/z_{calc} : 682.29218). **^{1}H-NMR** (D_2O, 500 MHz) δ/ppm = 7.54 (s, 1H), 7.32 (s, 1H), 7.10 (s, 1H), 6.36 (d, J = 2.9 Hz, 1H), 5.87 (s, 1H), 4.30 (dd, J = 10.5, 6.8 Hz, 2H), 4.17 (d, J = 10.7 Hz, 1H), 4.07 (m, 1H), 3.92 (d, J = 10.9 Hz, 2H), 3.75 (dd, J = 12.8, 3.5 Hz, 2H), 3.58 (d, J = 14.3 Hz, 2H), 3.41 (d, J = 10.5 Hz, 1H), 3.25 (m, 1H), 3.03 (dd, J = 11.7, 3.3 Hz, 2H), 2.89 (dd, J = 14.3, 9.6 Hz, 2H), 2.60 (s, 3H), 2.41 (s, 3H), 2.36 (s, 3H), 2.28 (s, 3H), 1.51 (s, 3H), 1.44 (s, 3H), 1.37 (s, 3H), 1.35 (s, 3H), 1.27 (s, 3H), 1.22 (s, 3H), 0.46 (s, 3H). **^{13}C-NMR** (D_2O, 126 MHz) δ/ppm = 202.2, 186.5, 182.5, 182.4, 182.3, 180.9, 180.1, 179.0, 178.5, 177.7, 177.4, 168.3, 160.8, 146.1, 140.8, 138.3, 136.9, 132.8, 121.3, 119.7, 114.8, 108.9, 97.5, 90.4, 85.2, 85.1, 81.5, 77.8, 75.8, 75.5, 71.6, 63.4, 63.2, 62.6, 61.8, 55.8, 53.5, 52.2, 52.0, 51.3, 48.1, 47.2, 46.6, 46.0, 42.0, 37.7, 37.5, 35.5, 34.8, 34.7, 34.5, 33.8, 30.6, 30.2, 29.0, 22.9, 22.1, 22.0, 21.7, 19.5, 19.0, 16.6.

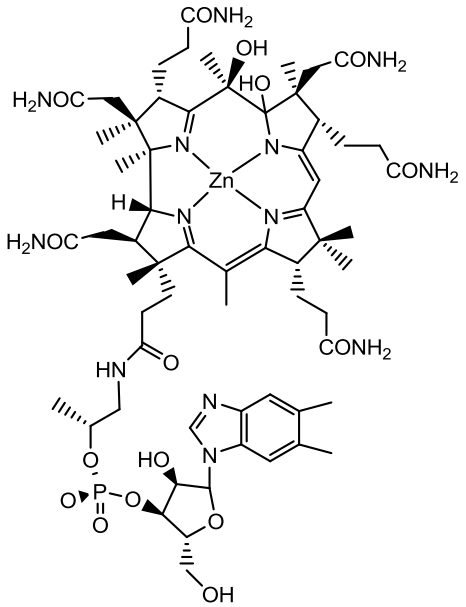

5,6-diolzincbalamin (25): **23** (11 mg, 8 μmol, 1 equiv) was dissolved in ddH_2O (0.1 M TRIS, pH 8.1, 3 mL) and an excess of $ZnSO_4 \cdot 7H_2O$ (25 mg, 87 μmol. 11 equiv) was added in the absence of light. The mixture was stirred for 90 min at 23 ºC and the product was purified using solid phase extraction. **25** (10 mg, 8 μmol, 87%) was obtained as a yellow powder.

UV-Vis (H_2O, c = 3.1 x 10^{-5} M): λ /nm (logε) = 283 (4.1), 289 (4.1), 438 (3.9). **UPLC** (Method 2) t_R = 3.6 min. **ESI-MS** (H_2O) m/z = 1368.6 $[M+H]^+$. **HR-ESI-MS** (H_2O) m/z = 1368.57403 $[M+H]^+$ (m/z_{calc}: 1368.57303). **^{1}H-NMR** (D_2O, 500 MHz) δ/ppm = 8.17 (s, 1H), 7.59 (s, 1H), 7.37 (s, 1H), 6.47 (d, J = 2.7 Hz, 1H), 5.39 (s, 1H), 4.45 (d, J = 3.3 Hz, 1H), 4.35 (dd, J = 14.7, 6.5 Hz, 1H), 4.23 (d, J = 7.2 Hz, 2H), 3.99 (d, J = 12.8 Hz, 2H), 3.73(m, 3H), 3.58 (d, J = 14.3 Hz, 1H), 3.21 (m, 1H), 2.99 (m, 1H), 2.94 (m, 1H), 2.66-0.95 (m, 24 H), 2.56 (s, 1H), 2.37 (s, 3H), 2.30 (s, 3H), 2.27 (s, 3H), 1.26 (s, 3H), 1.25 (s, 3H), 1.19 (s, 3H), 1.13 (s, 3H), 1.10 (s, 3H), 1.07 (s, 3H), 0.72 (s, 3H). **^{13}C-NMR** (D_2O, 126 MHz) δ/ppm = 198.5, 192.8, 184.4, 183.3, 181.9, 181.4, 181.1, 180.9, 179.9, 178.6, 177.8, 177.8, 170.6, 145.5, 140.3, 137.6, 136.6, 133.0, 120.4, 113.7, 110.9, 93.1, 89.2, 84.8, 76.9, 76.1, 75.5, 74.0, 73.4, 72.0, 64.7, 63.6, 56.6, 53.3, 52.7, 51.3, 50.0, 48.6, 48.2, 44.9, 44.8, 42.0, 37.1, 36.1, 36.0, 35.5, 35.2, 32.4, 29.4, 29.1, 26.8, 26.1, 22.3, 22.3, 21.9, 21.8, 21.8, 21.7, 21.5, 20.2, 18.8, 18.6.

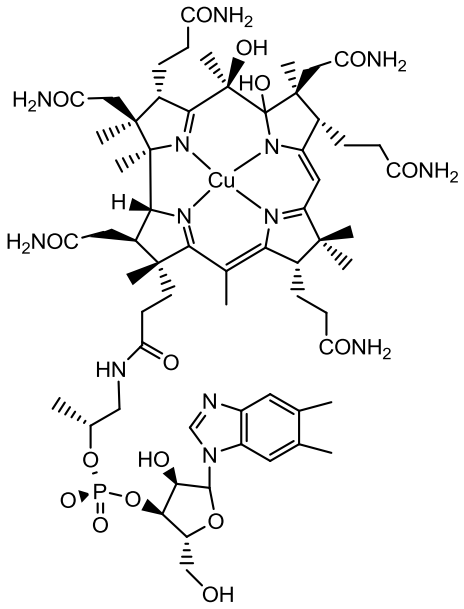

5,6-diolcubalamin (26): 23 (1 mg, 0.7 μmol, 1 equiv) was dissolved in ddH_2O (0.1 M TRIS, pH 8.1, 2 mL) and an excess of $CuSO_4 \cdot 5H_2O$ (10 mg, 40 μmol, 57 equiv) was added. The mixture was stirred for 90 min at 23 °C and the product was purified using solid phase extraction. **26** (1 mg, 0.7 μmol, 96%) was obtained as an orange powder.

UV-Vis (H_2O, c = 7.4 x 10^{-5} M): λ /nm (logε) = 287 (4.1), 295 (4.1), 439 (3.9). **UPLC** (Method 2) t_R = 3.6 min. **ESI-MS** (H_2O) m/z = 1365.6 $[M-H]^-$ (m/z_{calc} = 1365.6). **HR-ESI-MS** (H_2O) m/z = 1365.55327 $[M-H]^-$ (m/z_{calc} : 1365.55893 $[M-H]^-$).

Dicyanocobyrinic acid heptamethyl ester ('cobester', 27-CN): synthesized according to literature procedures.[89]

Dicyano-14,15-dioxo-cobyrinic acid heptamethyl ester (14,15-dioxocobester, 28): synthesized according to literature procedures.[92]

Dicyano-5,6-dioxo-cobyrinic acid heptamethyl ester (5,6-dioxocobester, 29): synthesized according to literature procedures.[92]

14,15-dioxonibalamin (30): synthesized according to literature procedures.[98]

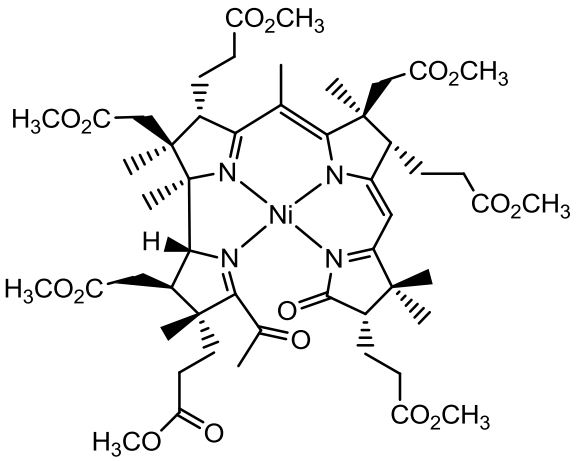

14,15-dioxonibyrinic acid heptamethyl ester (14,15-dioxonibester, 31): 14,15-dioxonibalamin (**30**, 18 mg, 13 μmol, 1 equiv) was dissolved in MeOH (10 mL) and the soln. was purged with N_2(g) for 15 min. The flask was cooled to 0 ºC and H_2SO_4 (250 μL, 98%) was added. The acidic soln. was then refluxed at 85 ºC under inert atmosphere for 120 h, after which the crude was cooled to 23 ºC and diluted with ddH_2O (30 mL). The product was subsequently extracted with CH_2Cl_2 (3x20 mL), the organic phase was washed with brine (2x20 mL), dried with Na_2SO_4 and and the solvent was removed under reduced pressure. The product was isolated by flash chromatography (CH_2Cl_2:MeOH 98:2 to 90:10) and 14,15-dioxonibester (8 mg, 7.5 μmol, 57%) was obtained as an orange powder after lyophilization.

UV-Vis (H_2O, c = 6.2 x 10^{-5} M): λ /nm (logε) = 359 (3.3), 452 (3.6). **UPLC** (Method 1) t_R = 3.6 min. **ESI-MS** (H_2O:MeOH 1:1) m/z = 1067.6 $[M+H]^+$ (m/z_{calc} = 1067.4). **HR-ESI-MS** (MeOH) m/z = 1067.43762 $[M+H]^+$ (m/z_{calc} : 1067.43700 $[M+H]^+$).

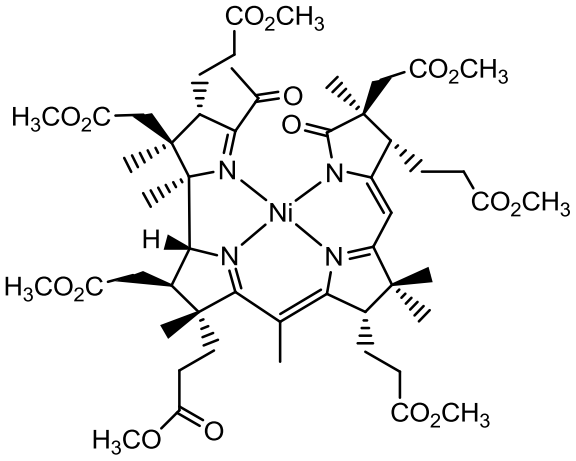

5,6-dioxonibyrinic acid heptamethyl ester (5,6-dioxonibester, 32): 5,6-dioxonibalamin (**19**, 5 mg, 4 μmol, 1 equiv) was dissolved in MeOH (3 mL) and the soln. was purged with N_2(g) for 15 min. The flask was cooled to 0 ºC and H_2SO_4 (65 μL, 98%) was added. The acidic soln. was then refluxed at 85 ºC under inert atmosphere for 120 h, after which the crude was cooled to 23 ºC and diluted with ddH_2O (10 mL). The product was subsequently extracted with CH_2Cl_2 (3x10 mL), the organic phase was washed with brine (2x10 mL) and dried with Na_2SO_4. The solvent was removed under reduced pressure. The crude was used for synthetic purposes without further purification.

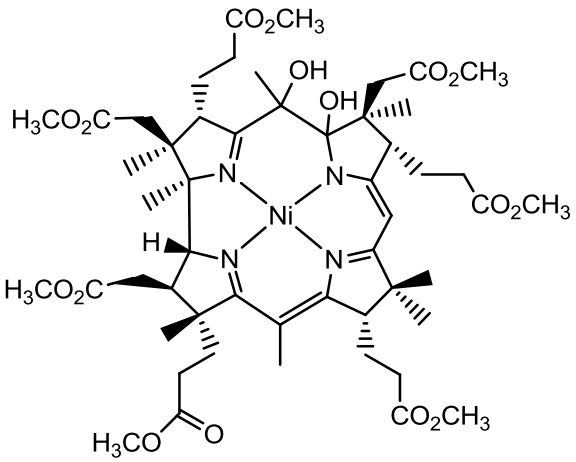

5,6-diolnibyrinic acid heptamethyl ester (5,6-diolnibester, 33): 5,6-diolnibalamin (**22**, 5 mg, 4 μmol, 1 equiv) was dissolved in MeOH (4 mL) and the soln. was purged with N_2(g) for 15 min. The flask was cooled to 0 ºC and H_2SO_4 (65 μL, 98%) was added. The acidic soln. was then refluxed at 85 ºC under inert atmosphere for 120 h, after which the crude was cooled to 23 ºC and diluted with ddH_2O (10 mL). The product was subsequently extracted with CH_2Cl_2 (3x10 mL), the organic phase was washed with brine (2x10 mL) and dried with Na_2SO_4. The solvent was removed under reduced pressure. The crude was used for synthetic purposes without further purification.

Aquacyano-14-oxo-15-acetohydrazonecobalamin (34): **12** (50 mg, 35 μmol, 1 equiv) was dissolved in ddH_2O (0.1 % CH_3COOH, pH 5.2) and the soln. was purged with N_2(g) for 15 min. Acetohydrazide (40 mg, 540 μmol, 15 equiv) was added to the stirred soln. under a nitrogen atmosphere and the mixture was heated to 110 ºC. After 4 h the crude was cooled to 23 ºC and desalted by solid phase extraction. The product was purified by preparative HPLC (Method 5) and **36** (7.5 mg, 5 μmol, 15%) was obtained as a blood-orange powder after lyophilization.

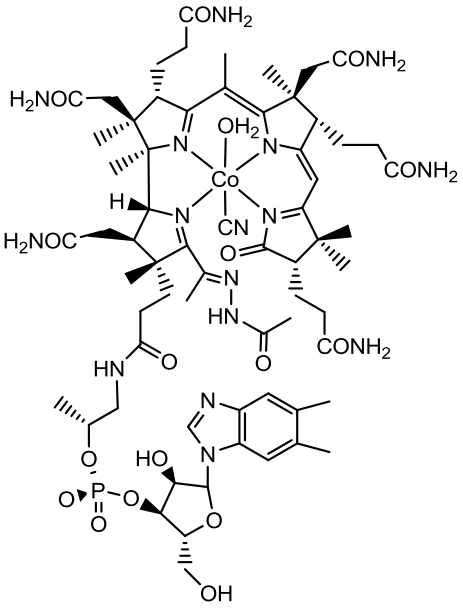

UV-Vis (H_2O, c = 2.3 x 10^{-5} M): λ /nm (logε) = 280 (4.5), 288 (4.4), 321 (4.2), 472 (4.0), 530ish (3.9). **UPLC** (Method 2) t_R = 2.2 min. **ESI-MS** (H_2O) m/z = 1441.5 $[M-H_2O+H]^+$ (m/z_{calc} = 1441.6). **^{1}H-NMR** (D_2O; 500 MHz) δ/ppm = 8.13 (s, 1H), 7.32 (s, 1H), 7.23 (s, 1H), 6.16 (d, J = 2.9 Hz, 1H), 5.44 (s, 1H), 4.46 (m, 2H), 4.36 (d, J = 3.3

Hz, 1H), 4.15 (t, J = 4.9 Hz, 1H), 3.65 (m, 1H), 3.57 (t, J = 8.5 Hz, 1H), 3.14 (m, 1H), 3.02 (m, 1H), 2.89 (m, 1H), 2.55-1.89 (m, 28 H) 2.16 (s, 6H), 2.05 (s, 3H), 2.00 (s, 3H), 1.74 (s, 3H), 1.44 (s, 3H), 1.14 (s, 3H), 1.08 (s, 3H), 1.05 (d, J = 6.2 Hz, 3H), 1.01 (s, 3H), 0.99 (s, 3H), 0.28 (s, 3H). **^{13}C-NMR** (D_2O, 126 MHz) δ/ppm = 191.6, 183.5, 183.4, 181.8, 181.3, 180.9, 180.5, 179.1, 179.0, 178.2, 178.0, 178.0, 171.8, 165.7, 147.3, 145.2, 143.2, 136.3, 135.4, 134.5, 121.7, 114.0, 112.9, 97.8, 89.7, 88.7, 86.9, 83.2, 77.4, 75.0, 74.2, 63.9, 61.8, 59.1, 58.5, 54.0, 53.5, 49.8, 47.9, 47.7, 47.0, 45.3, 42.6, 38.4, 37.4, 36.5, 35.6, 35.5, 33.9, 28.5, 28.0, 27.3, 27.2, 25.5, 25.2, 23.9, 22.7, 22.3, 22.1, 21.1, 21.6, 20.4, 18.8, 18.1.

Aquacyano-5-acetohydrazone-6-oxocobalamin (35): **13** (5 mg, 4 μmol, 1 equiv) was dissolved in ddH_2O (0.1 % CH_3COOH, pH 5.2) and the soln. was purged with N_2(g) for 15 min. Acetohydrazide (4 mg, 54 μmol, 15 equiv) was added to the stirred soln. under a nitrogen atmosphere and the mixture was heated to 110 ºC. After 30 min the crude was cooled to 23 ºC and desalted by solid phase extraction. The product was identified by UPLC-MS (m/z = 1441.5 [M-H_2O+H]$^+$) and used for synthetic purposes without further purification.

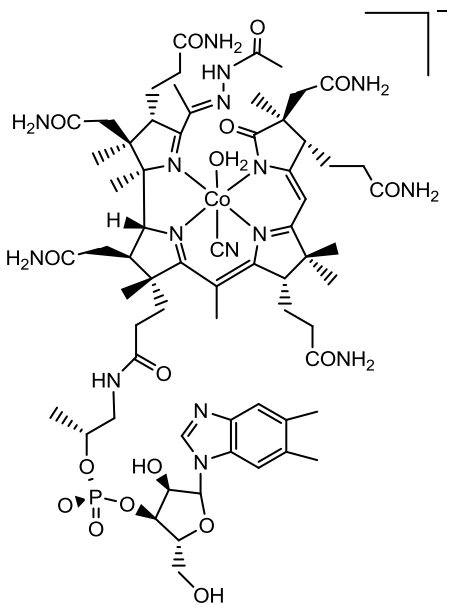

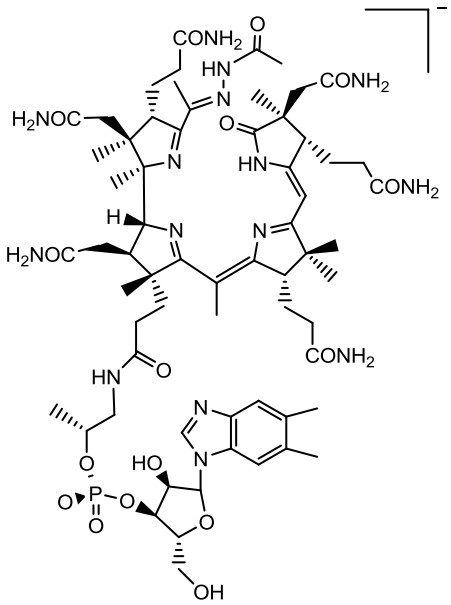

Aquacyano-5-acetohydrazone-6-oxo-H-balamin (36): **35** (2 mg, 1 μmol, 1 equiv) was dissolved in MeOH and the soln. was purged with N_2(g) for 15 min. $CoCp_2$ (1.5 mg, 8 μmol, 8 equiv) was added to the soln. in a nitrogen atmosphere and the soln. turned brown within seconds. After 2 min an excess of KCN (6.5 mg, 0.1 mmol, 100 equiv) was added at once. The product was identified by UPLC-MS (m/z = 1358.6 $[M-H]^-$).

6.3. NMR data

Co$_\beta$-cyano-8$_\beta$-hydroxy-cobalamin-c-acid (**4**):

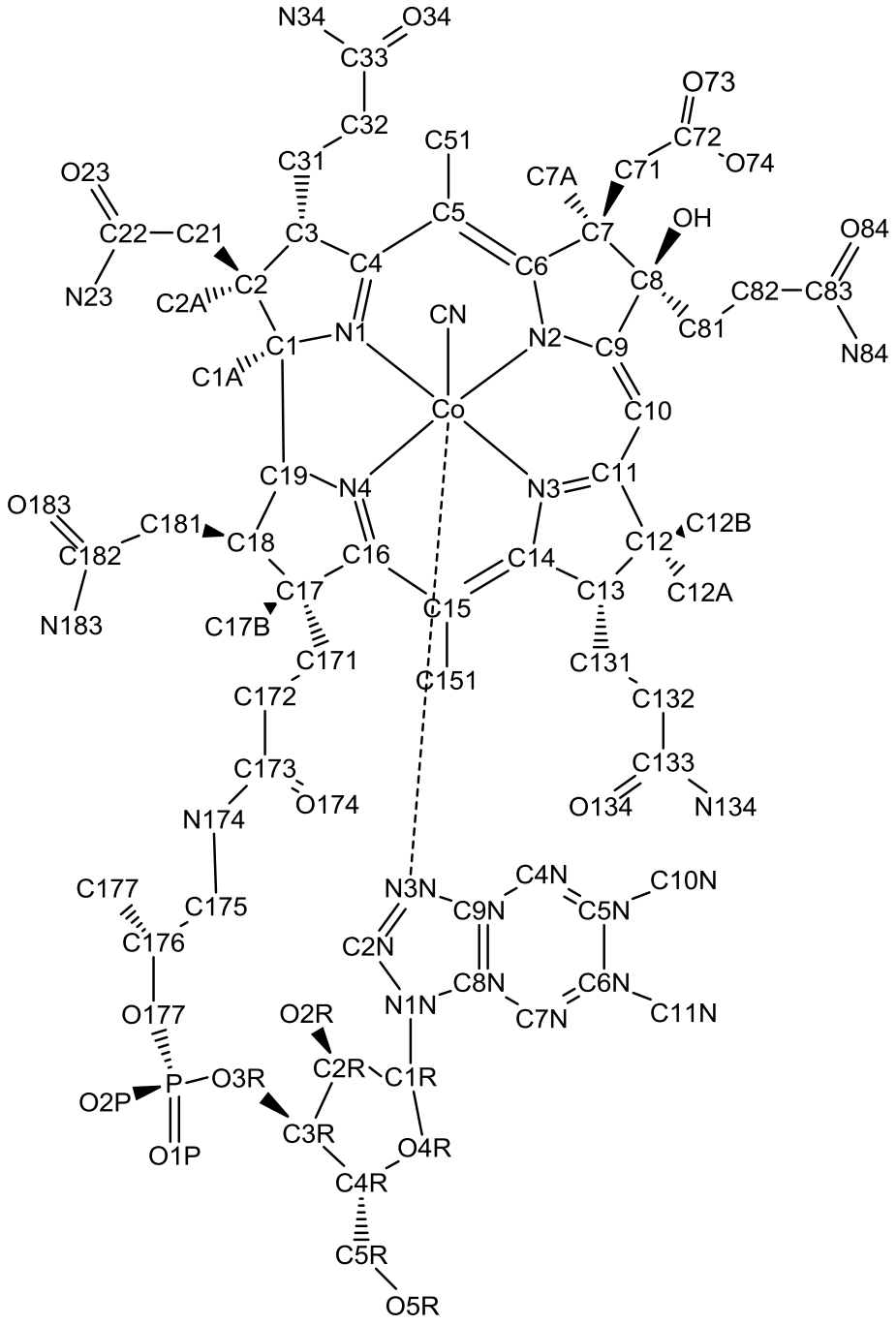

Figure 38. Atom numbering of **4**.

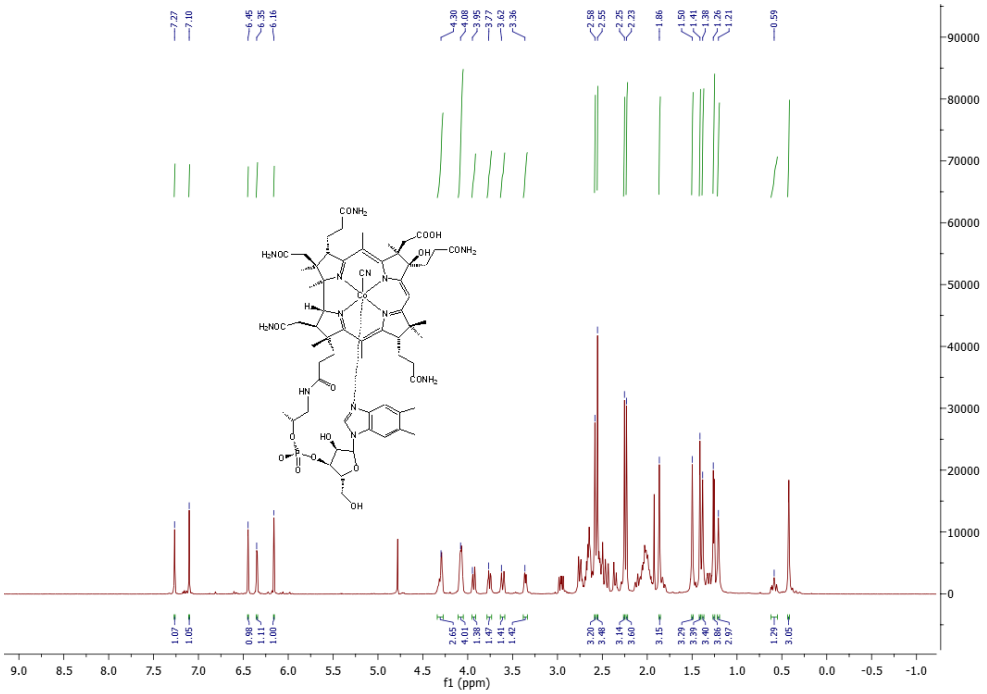

Figure 39. ^{1}H NMR spectrum of **4**.

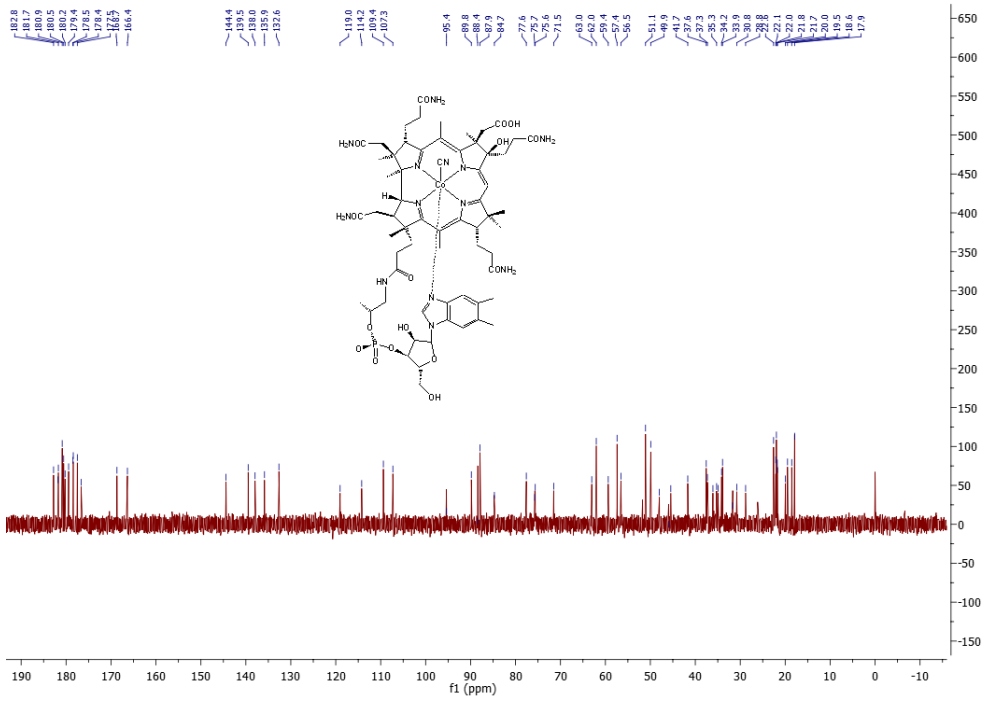

Figure 40**.** ^{13}C NMR spectrum of **4**.

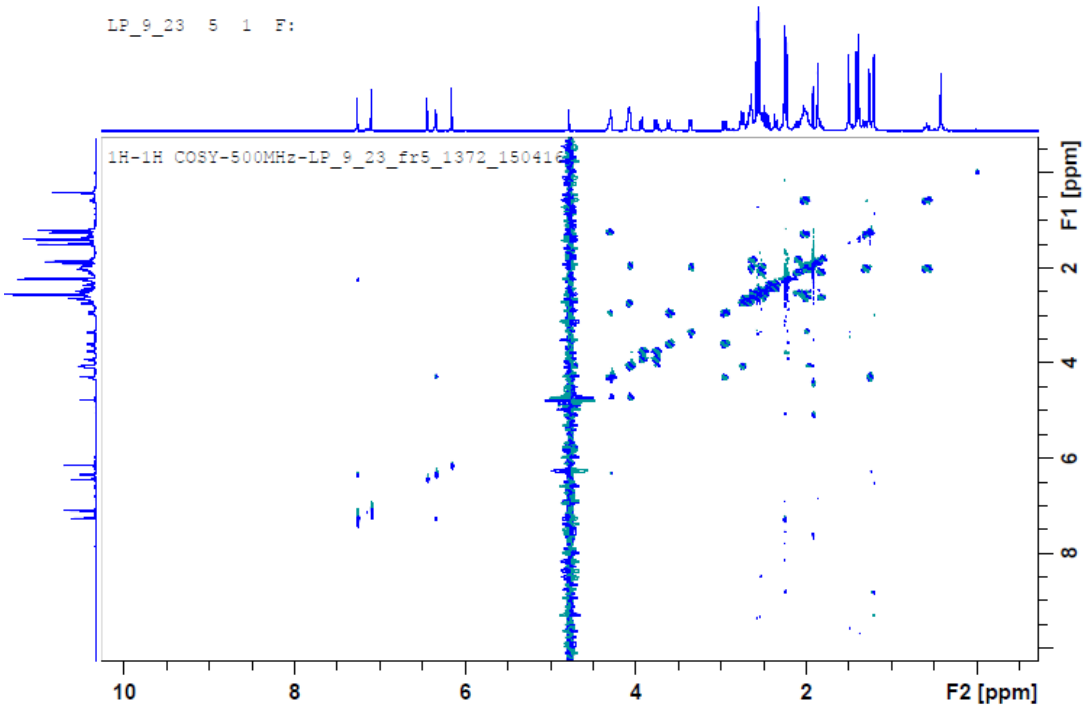

Figure 41. ^{1}H-^{1}H COSY spectrum of **4**.

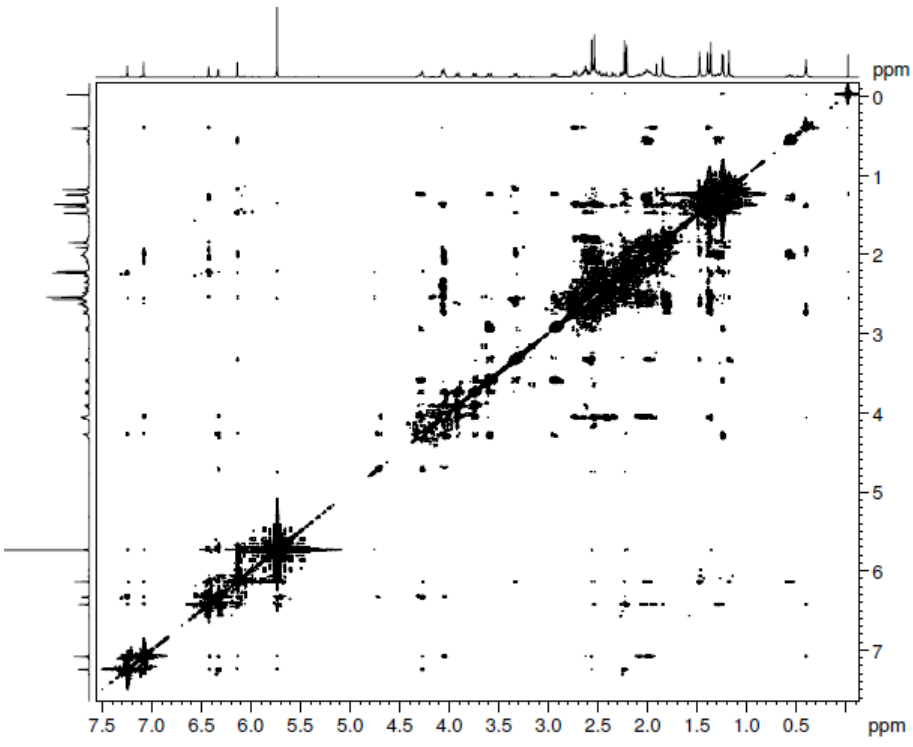

Figure 42. ^{1}H-^{1}H ROESY spectrum of **4**.

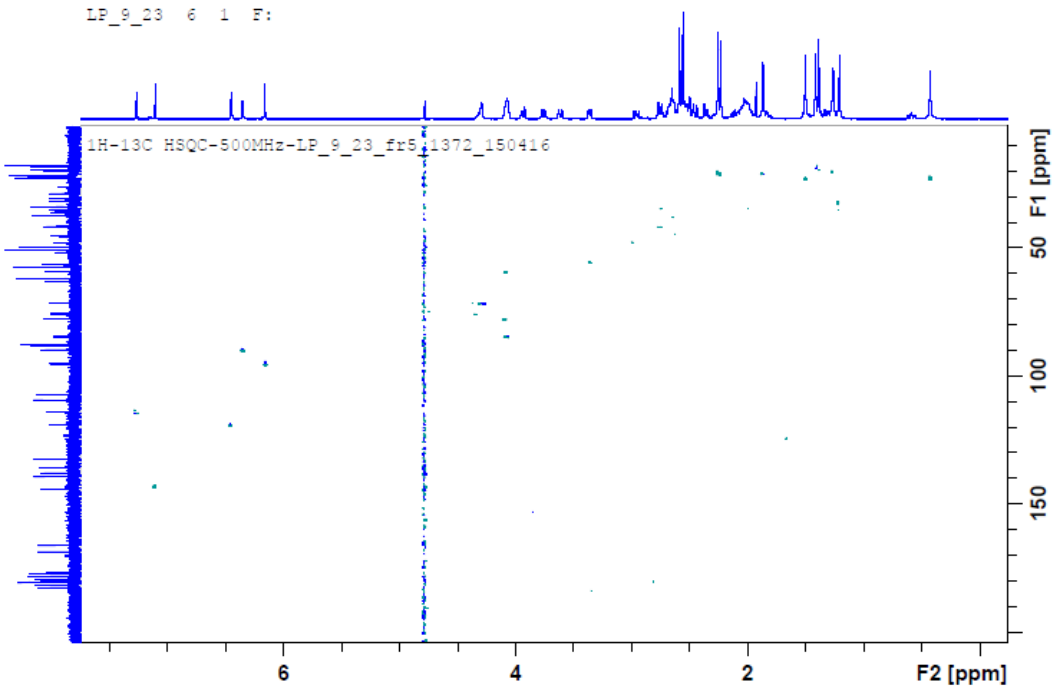

Figure 43. ^{1}H-^{13}C HSQC spectrum of **4**.

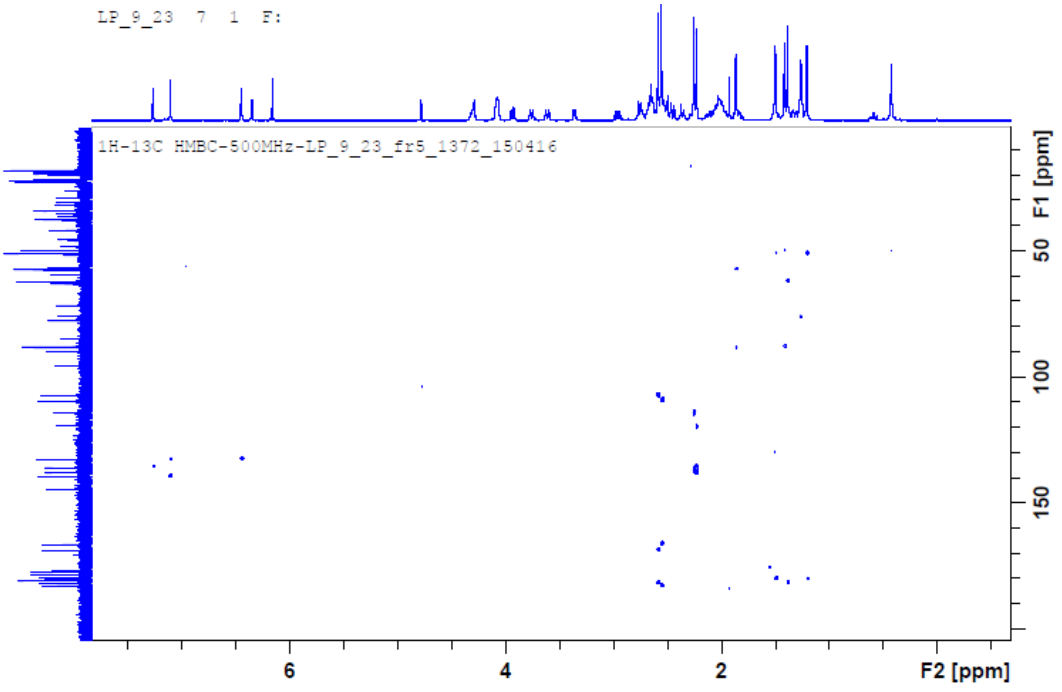

Figure 44. ^{1}H-^{13}C HMBC spectrum of **4**.

^{1}H	δ/ppm		
	1	**4**	**Δδ**
C1	- -	- -	- -
C1A	0.43	0.42	-0.01
C2	- -	- -	- -
C2A	1.39	1.41	+0.02
C21	2.39	2.34	-0.05
C22	- -	- -	- -
C3	4.17	4.08	-0.09
C31	1.96	2.00	+0.04
C32	2.48/2.54	2.50	
C33	- -	- -	- -
C4	- -	- -	- -
C5	- -	- -	- -
C51	2.52	2.56	+0.04
C6	- -	- -	- -
C7	- -	- -	- -
C7A	1.85	1.87	+0.02
C71	2.17/2.56	2.01/2.65	-0.16/+0.09
C72	- -	- -	- -
C8	3.46	- -	- -
C81	1.02/2.00	1.33/2.02	+0.31/+0.02
C82	1.00/1.83	0.59/2.02	-0.41/+0.19
C83	- -	- -	- -
C9	- -	- -	- -
C10	6.06	6.16	+0.10
C11	- -	- -	- -
C12	- -	- -	- -
C12A	1.43	1.50	+0.07
C12B	1.17	1.20	+0.03
C13	3.32	3.37	+0.05
C131	1.95/2.02	2.02	
C132	2.61	2.60	-0.01
C133	- -	- -	- -
C14	- -	- -	- -
C15	- -	- -	- -
C151	2.55	2.58	+0.03
C16	- -	- -	- -
C17	- -	- -	- -
C17B	1.37	1.38	+0.01
C171	1.81/2.63	1.82/2.61	+0.01/-0.02
C172	2.09/2.52	2.02/---	
C173	- -	- -	- -
C175	2.94/3.59	2.95/3.62	+0.01/+0.03
C176	4.28	4.31	+0.03
C177	1.24	1.26	+0.02
C18	2.75	2.96	+0.21
C181	2.66/2.74	2.67/2.76	+0.01/+0.02
C182	- -	- -	- -
C19	4.07	4.08	+0.01
C1R	6.33	6.36	+0.03
C2R	4.26	4.08/4.30	
C3R	4.71	4.72	+0.01
C4R	4.04	4.08	+0.04
C5R	3.73/3.91	3.76/3.95	+0.03/+0.04
C2N	7.06	7.11	+0.05
C4N	6.49	6.45	-0.04
C5N	- -	- -	- -
C6N	- -	- -	- -
C7N	7.26	7.27	+0.01
C8N	- -	- -	- -
C9N	- -	- -	- -
C10N	2.24	2.24	0.00
C11N	2.24	2.26	+0.02

^{13}C	δ/ppm		
	1	**4**	**Δδ**
C1	87.9	87.8	-0.1
C1A	21.9	22.6	+0.7
C2	50.1	49.9	-0.2
C2A	19.3	19.9	+0.6
C21	45.3	45.4	+0.1
C22	178.6	178.5	-0.1
C3	58.8	59.3	+0.5
C31	28.5	28.8	+0.3
C32	37.5	37.5	0.0
C33	180.7	180.6	-2
C4	182.8	182.7	-0.1
C5	110.3	109.3	-1.0
C51	18	18.5	+0.5
C6	168.1	166.3	-1.8
C7	54.2	57.4	+3.2
C7A	21.5	21.7	+0.2
C71	45.5	45.9	+0.4
C72	177.9	181.8	+3.9
C8	58.2	88.4	+30.2
C81	28.5	36.1	+7.6
C82	34.2	31.7	-2.5
C83	180.5	180.4	-0.1
C9	176.4	176.7	+0.3
C10	97.5	95.3	-2.2
C11	179.7	179.4	-0.3
C12	50.9	51.0	+0.1
C12A	21.7	21.8	+0.1
C12B	33.8	34.0	+0.2
C13	56.2	56.5	+0.3
C131	30.8	30.6	-0.2
C132	37.2	37.2	0.0
C133	181	180.9	-0.1
C14	168.8	168.6	-0.2
C15	106.9	107.2	+0.3
C151	17.8	17.9	+0.1
C16	181.7	181.7	0.0
C17	62.0	61.9	-0.1
C17B	18.4	19.5	+1.1
C171	34.8	34.9	+0.1
C172	35	35.3	+0.3
C173	177.5	177.5	0.0
C175	47.9	48.0	+0.1
C176	75.5	75.5	0.0
C177	21.6	22.1	+0.5
C18	41.5	41.6	+0.1
C181	34	34.2	+0.2
C182	178.5	178.4	-0.1
C19	77.5	77.4	-0.1
C1R	89.5	89.7	+0.2
C2R	71.4	71.5	+0.1
C3R	75.6	75.7	+0.1
C4R	84.6	84.7	+0.1
C5R	62.9	63.0	+0.1
C2N	144.3	144.3	0.0
C4N	119.0	119.0	0.0
C5N	135.8	135.7	-0.1
C6N	137.9	137.9	0.0
C7N	114.0	114.1	+0.1
C8N	132.8	132.6	-0.2
C9N	139.5	139.4	-0.1
C10N	22.1	21.9	-0.2
C11N	22.1	21.9	-0.2

Table 2. Comparison of NMR chemical shift values for **1**-**4**. Assignments by ^{1}H NMR, ^{13}C NMR, ^{1}H-^{1}H COSY, ^{1}H-^{1}H ROESY, ^{1}H-^{13}C HSQC and ^{1}H-^{13}C HMBC.

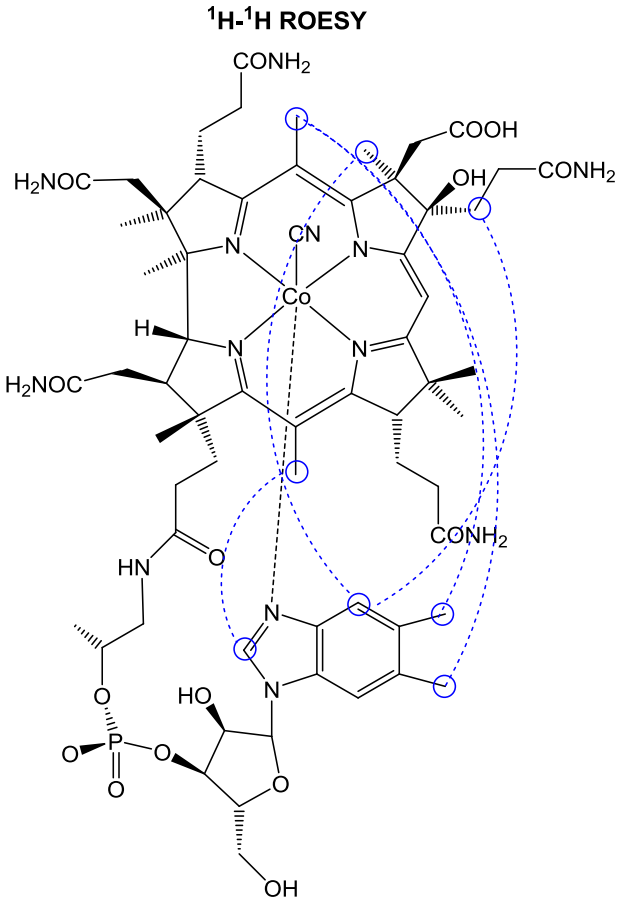

Figure 45. ^{1}H-^{1}H ROESY correlations within **4**.

Co$_\beta$-cyano-Δ^7-dehydro-7-decarboxymethyl-8-decarboxyethyl-cobalamin (**5**):

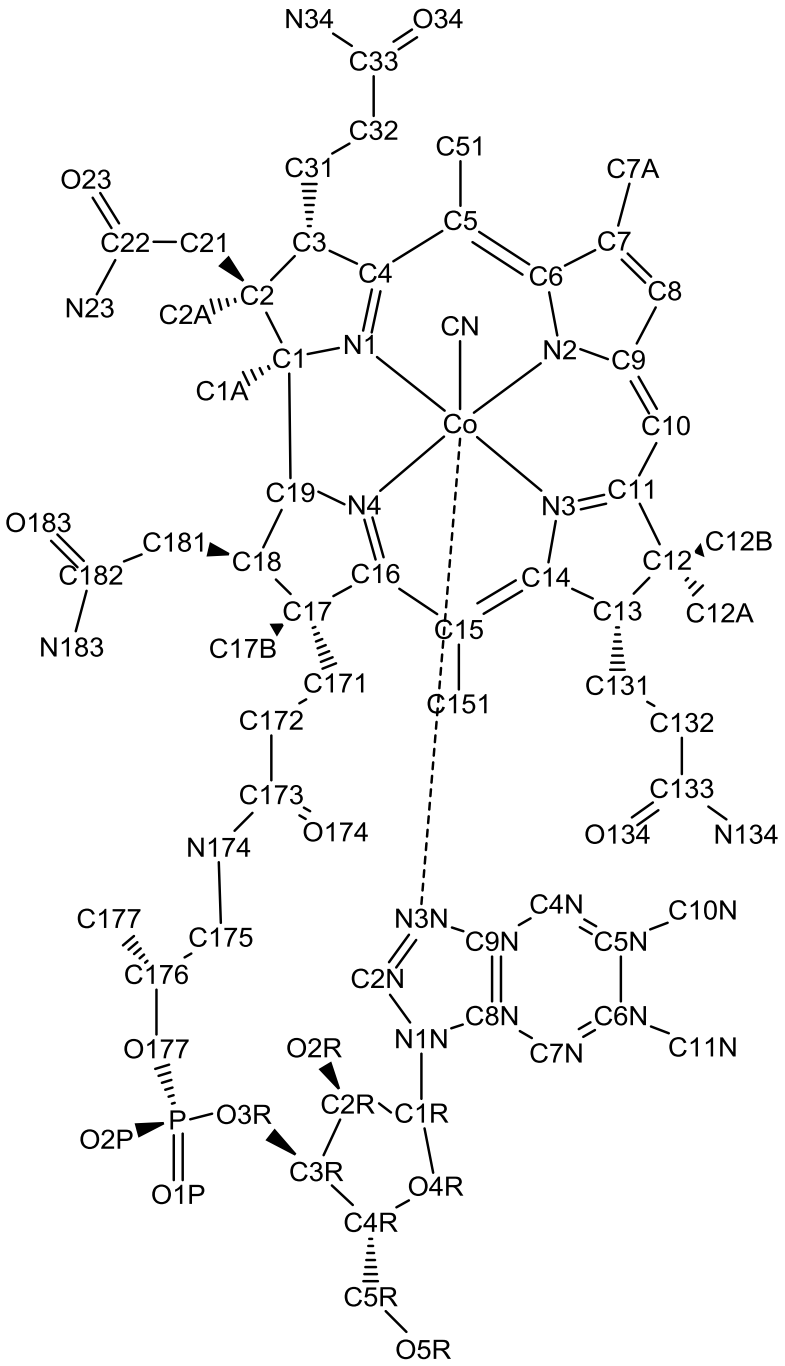

Figure 46. Atom numbering of **5**.

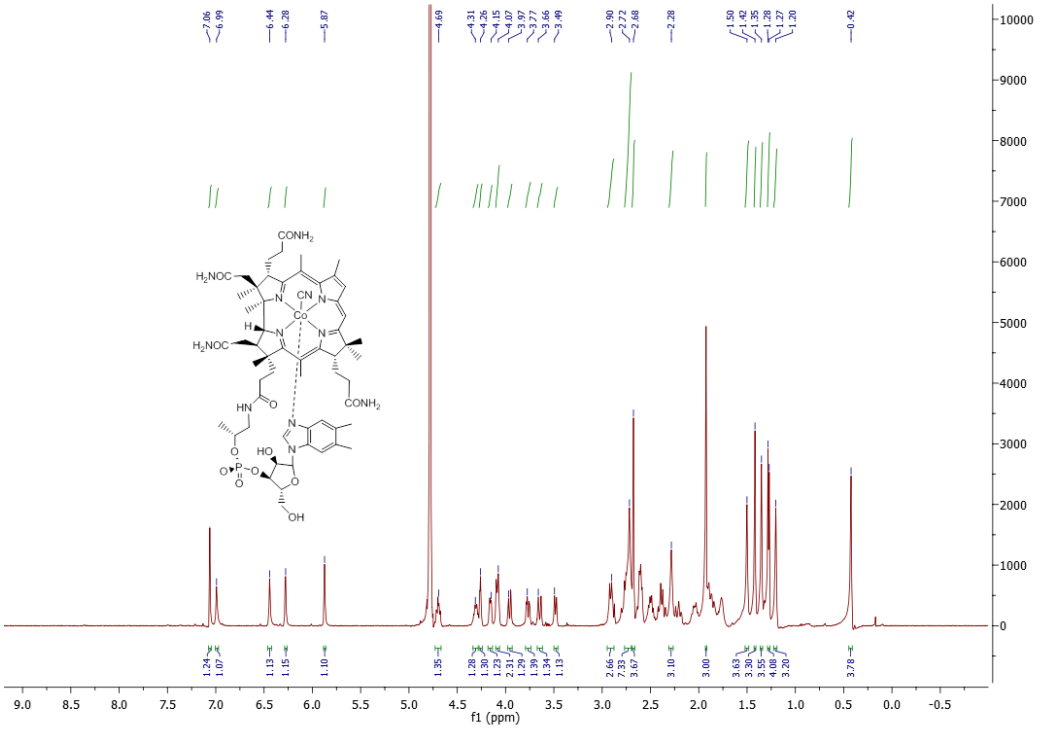

Figure 47. ^{1}H NMR spectrum of **5**.

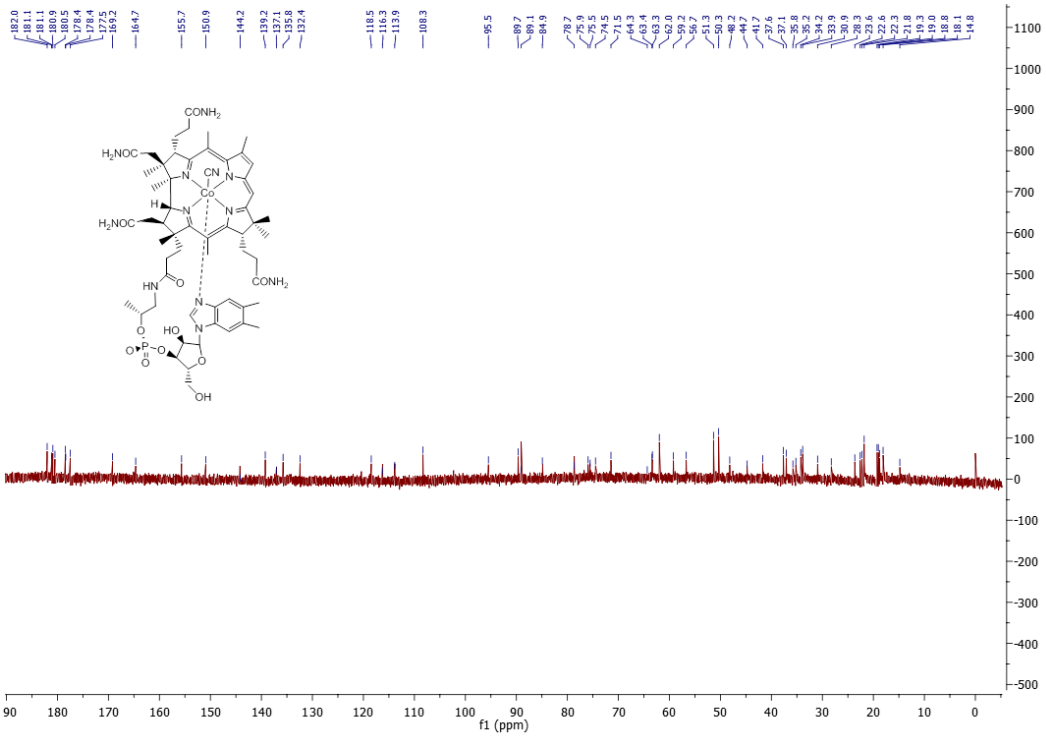

Figure 48**.** ^{13}C NMR spectrum of **5**.

^{13}C	δ/ppm		
	1	**5**	**Δδ**
C1	87.9	89.1	+1.2
C1A	21.9	22.6	+0.7
C2	50.1	50.3	+0.2
C2A	19.3	18.8	-0.5
C21	45.3	44.7	-0.6
C22	178.6	178.4	-0.2
C3	58.8	59.2	+0.4
C31	28.5	28.3	-0.2
C32	37.5	37.6	+0.1
C33	180.7	180.9	+0.2
C4	182.8	182.0	-0.8
C5	110.3	113.9	+3.6
C51	18.0	14.8	-3.2
C6	168.1	155.7	-12.4
C7	54.2	150.9	+96.7
C7A	21.5	23.6	+2.1
C71	45.5	--	--
C72	177.9	--	--
C8	58.2	74.5	+16
C81	28.5	--	--
C82	34.2	--	--
C83	180.5	--	--
C9	176.4	164.7	-11.7
C10	97.5	95.5	-2.0
C11	179.7	180.5	+0.8
C12	50.9	51.3	+0.4
C12A	21.7	22.3	+0.6
C12B	33.8	33.9	-0.1
C13	56.2	56.7	+0.5
C131	30.8	30.9	+0.1
C132	37.2	37.1	-0.1
C133	181.0	181.1	+0.1
C14	168.8	169.2	+0.4
C15	106.9	108.3	+1.4
C151	17.8	18.1	+0.3
C16	181.7	181.1	-0.6
C17	62.0	62.0	0.0
C17B	18.4	19.0	+0.6
C171	34.8	35.2	+0.4
C172	35.0	35.8	+0.8
C173	177.5	177.5	0.0
C175	47.9	48.2	+0.3
C176	75.5	75.5	0.0
C177	21.6	19.3	-2.3
C18	41.5	41.7	+0.2
C181	34.0	34.2	+0.2
C182	178.5	178.4	-0.1
C19	77.5	78.7	+1.2
C1R	89.5	89.7	-0.2
C2R	71.4	71.5	+0.1
C3R	75.6	75.9	+0.3
C4R	84.6	84.9	+0.3
C5R	62.9	64.3	+1.4
C2N	144.3	144.2	-0.1
C4N	119.0	118.5	-0.5
C5N	135.8	135.8	0.0
C6N	137.9	137.1	-0.8
C7N	114.0	116.3	+2.2
C8N	132.8	132.4	-0.4
C9N	139.5	139.2	-0.3
C10N	22.1	21.8	-0.3
C11N	22.1	21.8	-0.3

Table 3. Comparison of ^{13}C NMR chemical shifts of **1** and **5** (tentatively assigned). Co$_\beta$-cyano-8$_\beta$-hydroxy-cobalamin-epi-c-acid (**10**).

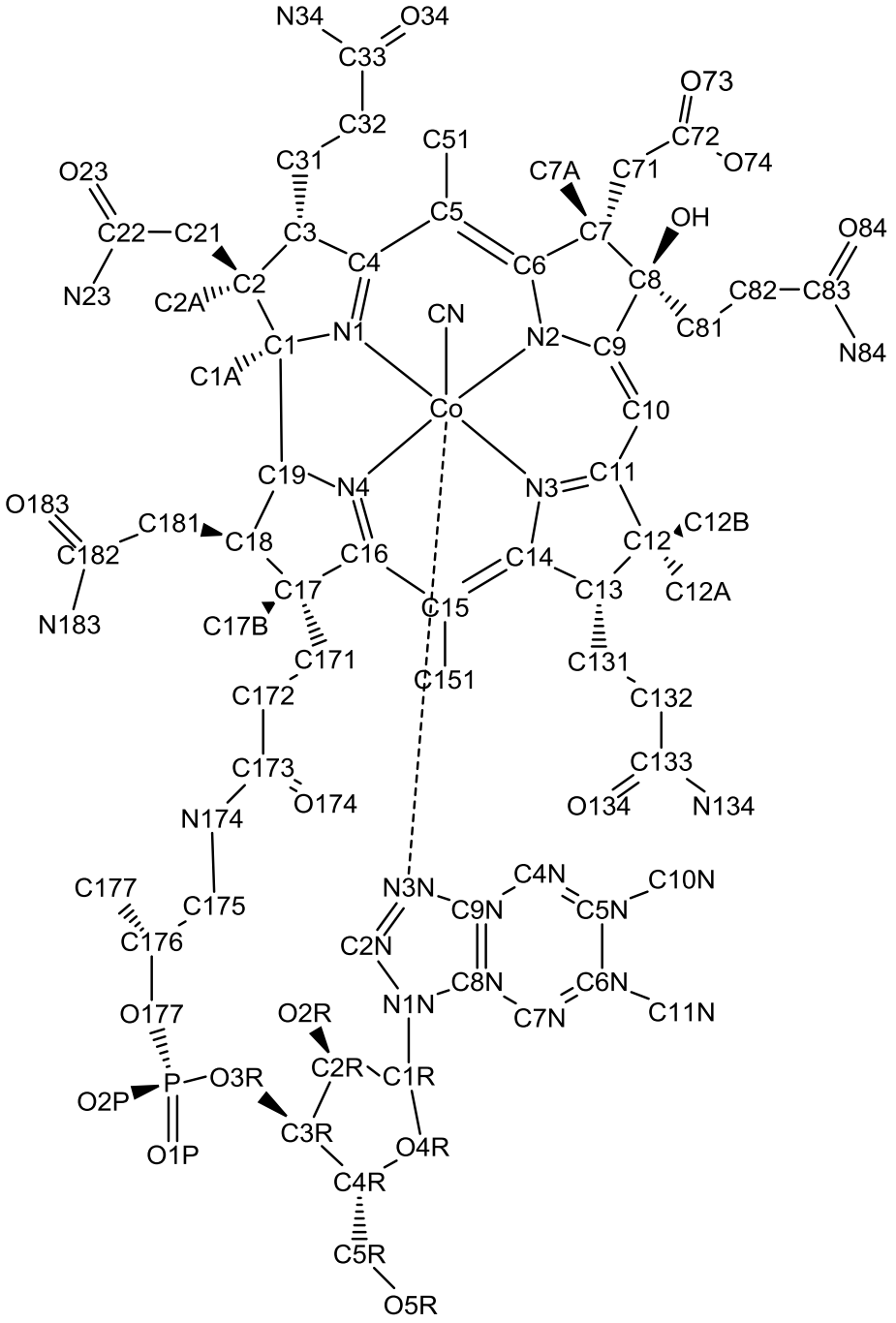

Figure 49. Atom numbering of **10**.

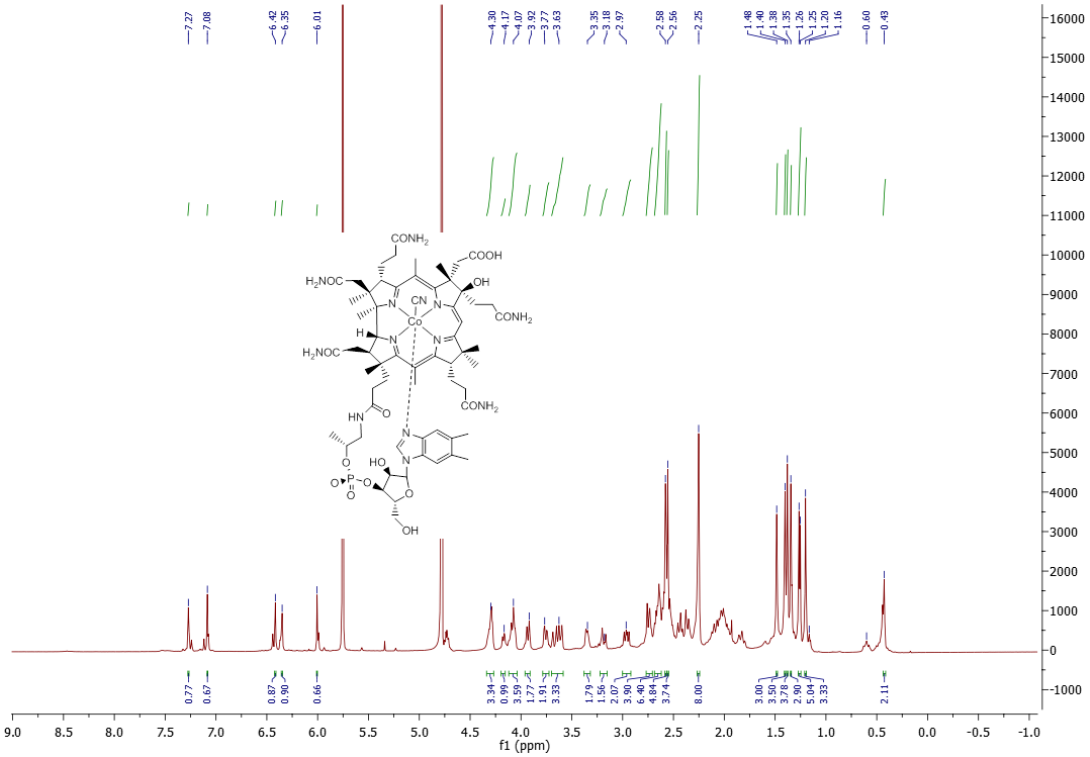

Figure 50. ^{1}H NMR spectrum of **10**.

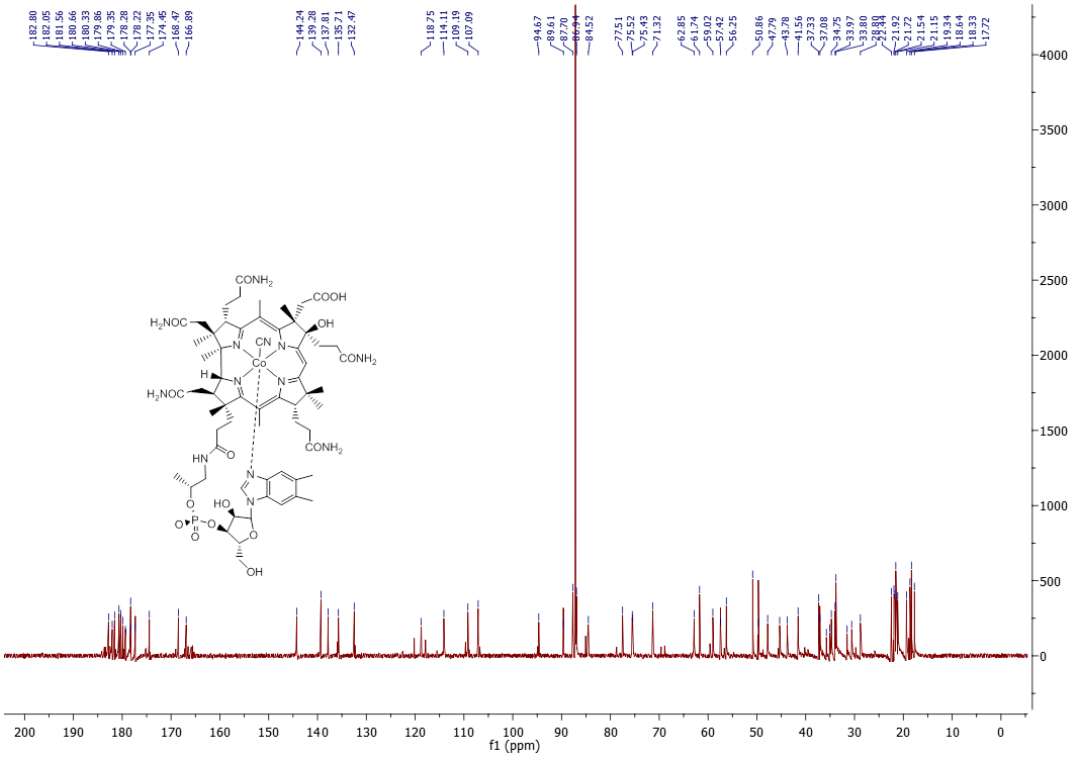

Figure 51. ^{13}C NMR spectrum of **10**.

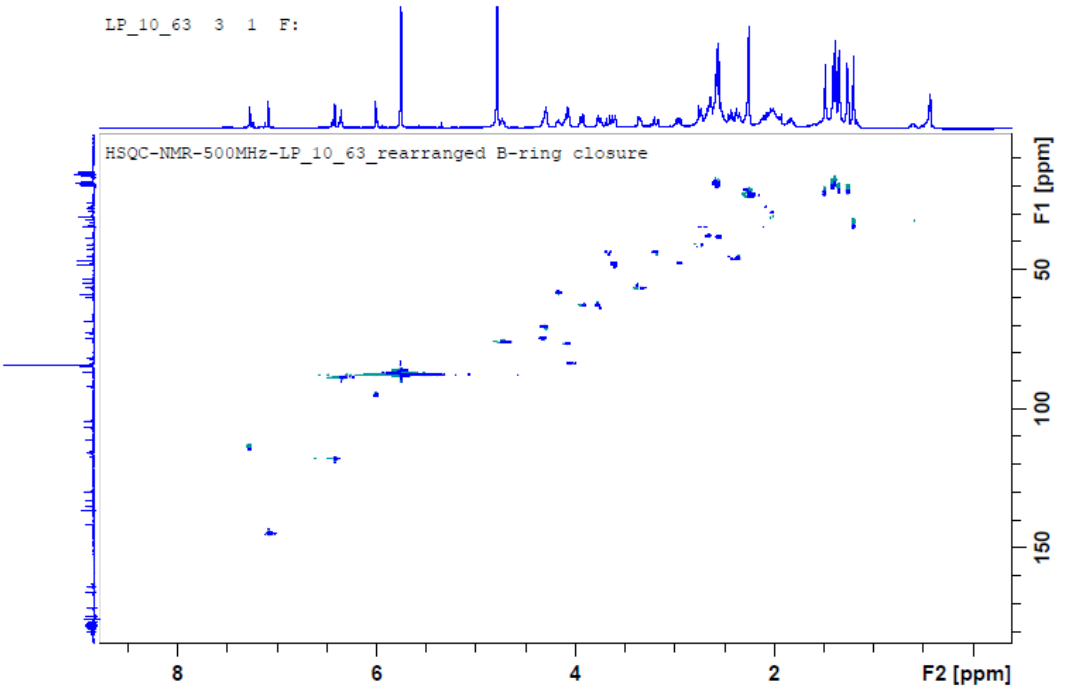

Figure 52. ^{1}H-^{13}C HSQC spectrum of **10**.

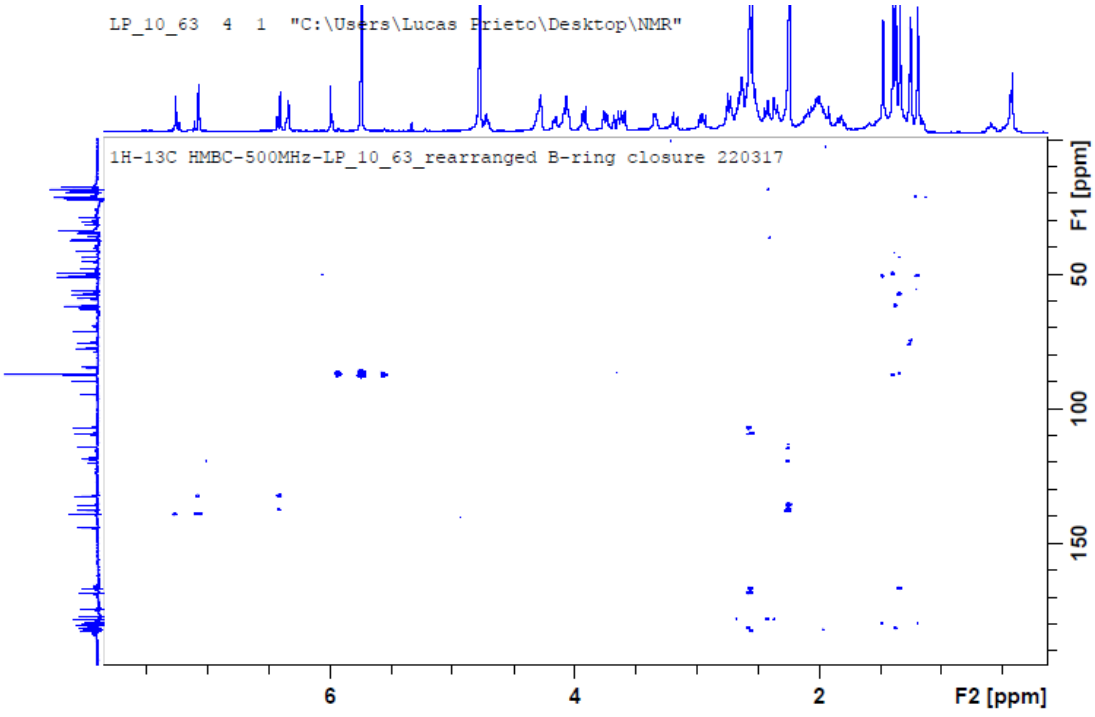

Figure 53. ^{1}H-^{13}C HMBC spectrum of **10**.

^{1}H	δ/ppm		
	8-OH-*epi*-c-acid-CNCbl[100]	**10**	**4**
C1	- -		- -
C1A	0.41	0.43	0.42
C2	- -		- -
C2A	1.39	1.40	1.41
C21	2.34	2.36	2.34
C22	- -	- -	- -
C3	4.14	4.17	4.08
C31	2.00	2.02	2.00
C32	2.49/2.56	2.43	2.50
C33	- -	- -	- -
C4	- -	- -	- -
C5	- -	- -	- -
C51	2.53	2.46	2.56
C6	- -	- -	- -
C7	- -	- -	- -
C7A	1.32	1.26	1.87
C71	3.16/3.65	3.18/3.70	2.01/2.65
C72	- -	- -	- -
C8	3.41	- -	- -
C81	1.02/2.00	1.16/2.02	1.33/2.02
C82	1.00/1.83	0.60/2.02	0.59/2.02
C83	- -	- -	- -
C9	- -	- -	- -
C10	5.98	6.01	6.16
C11	- -	- -	- -
C12	- -	- -	- -
C12A	1.47	1.48	1.50
C12B	1.18	1.20	1.20
C13	3.33	3.35	3.37
C131	1.98/2.06	2.01	2.02
C132	2.56	2.64	2.60
C133	- -	- -	- -
C14	- -	- -	- -
C15	- -	- -	- -
C151	2.55	2.58	2.58
C16	- -	- -	- -
C17	- -	- -	- -
C17B	1.33	1.38	1.38
C171	1.81/2.51		1.82/2.61
C172	2.06/2.60	2.01	2.02
C173	- -	- -	- -
C175	2.93/3.57	2.98/3.63	2.95/3.62
C176	4.28	4.30	4.31
C177	1.23	1.26	1.26
C18	2.75	2.97	2.96
C181	2.66/2.74	2.64/2.75	2.67/2.76
C182	- -	- -	- -
C19	4.06	4.07	4.08
C1R	6.33	6.35	6.36
C2R	4.27	4.07/4.30	4.08/4.30
C3R	4.71	4.73	4.72
C4R	4.05	4.07	4.08
C5R	3.73/3.91	3.77/.3.92	3.76/3.95
C2N	7.06	7.08	7.11
C4N	6.39	6.42	6.45
C5N	- -	- -	- -
C6N	- -	- -	- -
C7N	7.25	7.27	7.27
C8N	- -	- -	- -
C9N	- -	- -	- -
C10N	2.22	2.42	2.24
C11N	2.23	2.37	2.26

^{13}C	δ/ppm		
	8-OH-*epi*-c-acid-CNCbl[100]	**10**	**4**
C1	87.4	86.9	87.8
C1A	21.4	21.5	22.6
C2	49.2	49.7	49.9
C2A	19.2	19.3	19.9
C21	44.8	45.3	45.4
C22	177.8	178.3	178.5
C3	58.7	59.0	59.3
C31	28.2	28.8	28.8
C32	36.4	37.3	37.5
C33	180.0	180.3	180.6
C4	182.4	182.8	182.7
C5	108.6	109.2	109.3
C51	18.4	18.6	18.5
C6	166.2	166.9	166.3
C7	57.6	57.4	57.4
C7A	20.9	21.2	21.7
C71	43.2	43.8	45.9
C72	177.9	182.1	181.8
C8	86.3	87.7	88.2
C81	35.7	35.7	36.1
C82	31.0	31.5	31.7
C83	179.6	179.9	180.4
C9	178.0	174.5	176.7
C10	94.3	94.7	95.3
C11	179.4	179.4	179.4
C12	50.1	50.9	51.0
C12A	21.3	21.9	21.8
C12B	33.2	33.8	34.0
C13	56.0	56.3	56.5
C131	29.8	30.6	30.6
C132	36.5	37.1	37.2
C133	180.2	180.7	180.9
C14	168.8	168.5	168.6
C15	106.7	107.1	107.2
C151	17.5	17.7	17.9
C16	180.9	181.2	181.7
C17	61.1	61.7	61.9
C17B	17.9	18.3	19.5
C171	34.3	34.8	34.9
C172	37.7	35.1	35.3
C173	177.8	177.4	177.5
C175	47.2	47.8	48.0
C176	75.0	75.4	75.5
C177	20.8	21.7	22.1
C18	41.0	41.6	41.6
C181	33.4	34.0	34.2
C182	177.9	178.2	178.4
C19	77.1	77.5	77.4
C1R	89.2	89.6	89.7
C2R	70.9	71.3	71.5
C3R	74.9	75.5	75.7
C4R	84.0	84.5	84.7
C5R	62.5	62.9	63.0
C2N	143.8	144.2	144.3
C4N	118.4	118.8	119.0
C5N	135.1	135.7	135.7
C6N	137.4	137.8	137.9
C7N	113.7	114.1	114.1
C8N	131.8	132.5	132.6
C9N	138.9	139.3	139.4
C10N	21.9	22.4	21.9
C11N	21.7	22.4	21.9

Table 4. Chemical shifts of ^{1}H and ^{13}C NMR spectra of **1**, **4** and **10**. Assignments by ^{1}H NMR, ^{13}C NMR, ^{1}H-^{13}C HSQC and ^{1}H-^{13}C HMBC.

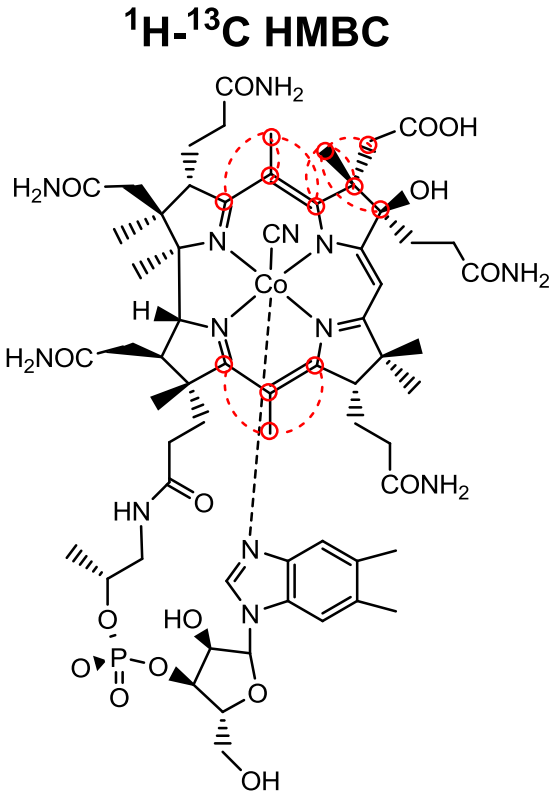

Figure 54. ^{1}H-^{13}C HMBC correlations within **10**.

Co$_\beta$–hydroxo-5,6-diol-cobalamin (**24**):

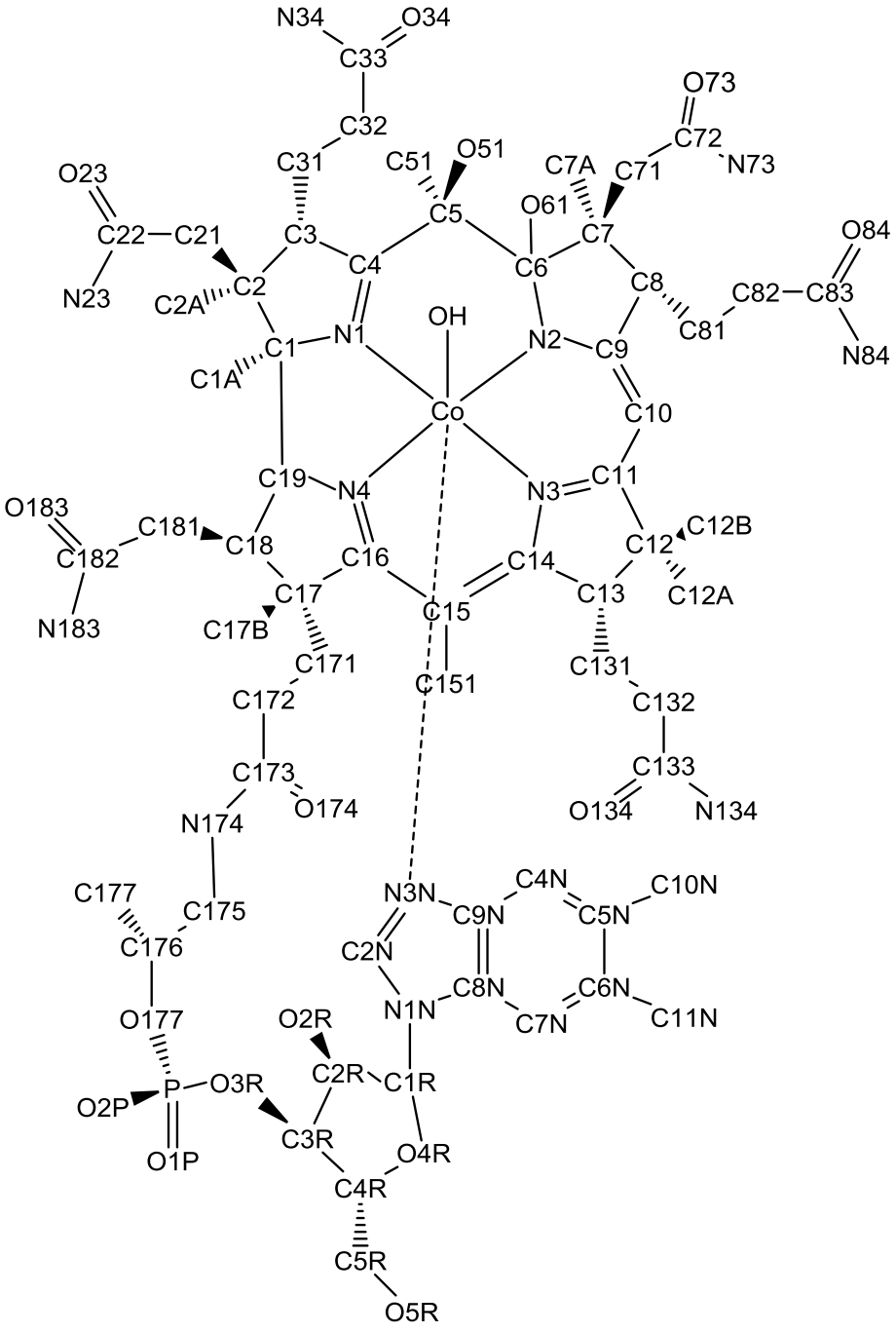

Figure 55. Atom numbering of **24**.

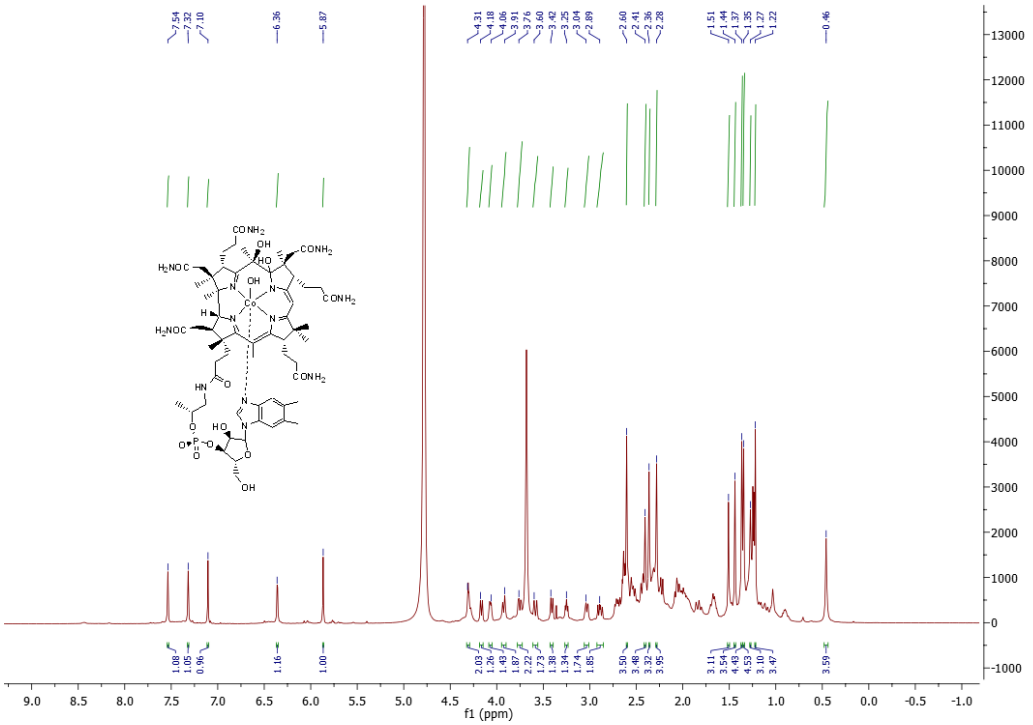

Figure 56. ^{1}H NMR spectrum of **24**.

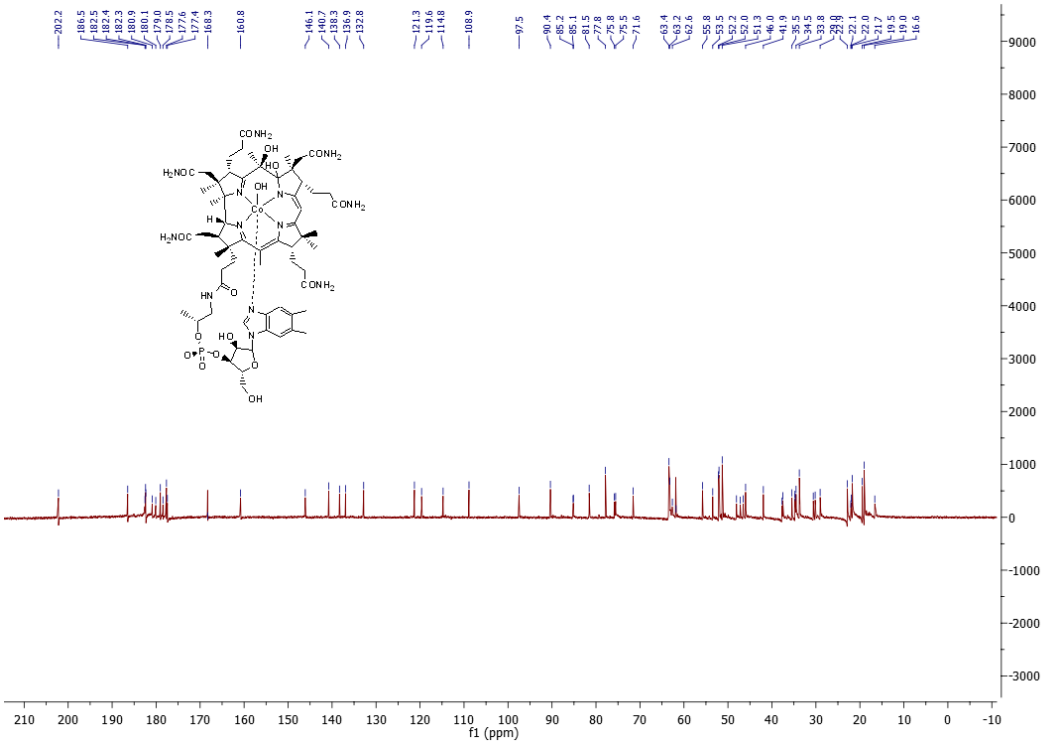

Figure 57. ^{13}C NMR spectrum of **24**.

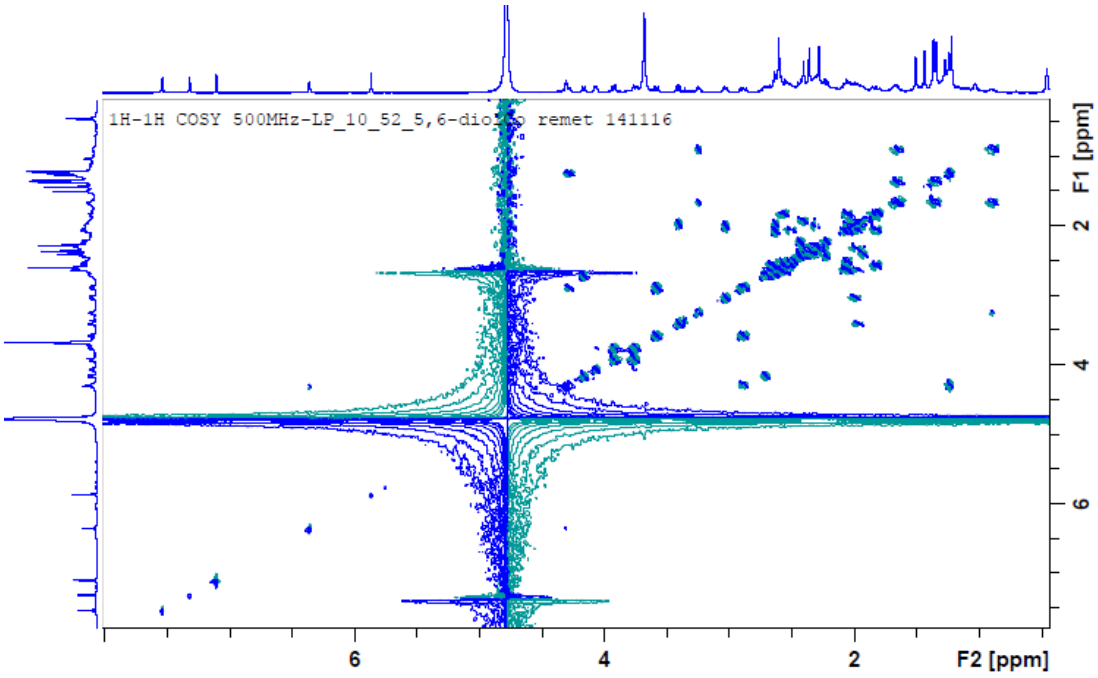

Figure 58. ^{1}H-^{1}H COSY spectrum of **24**.

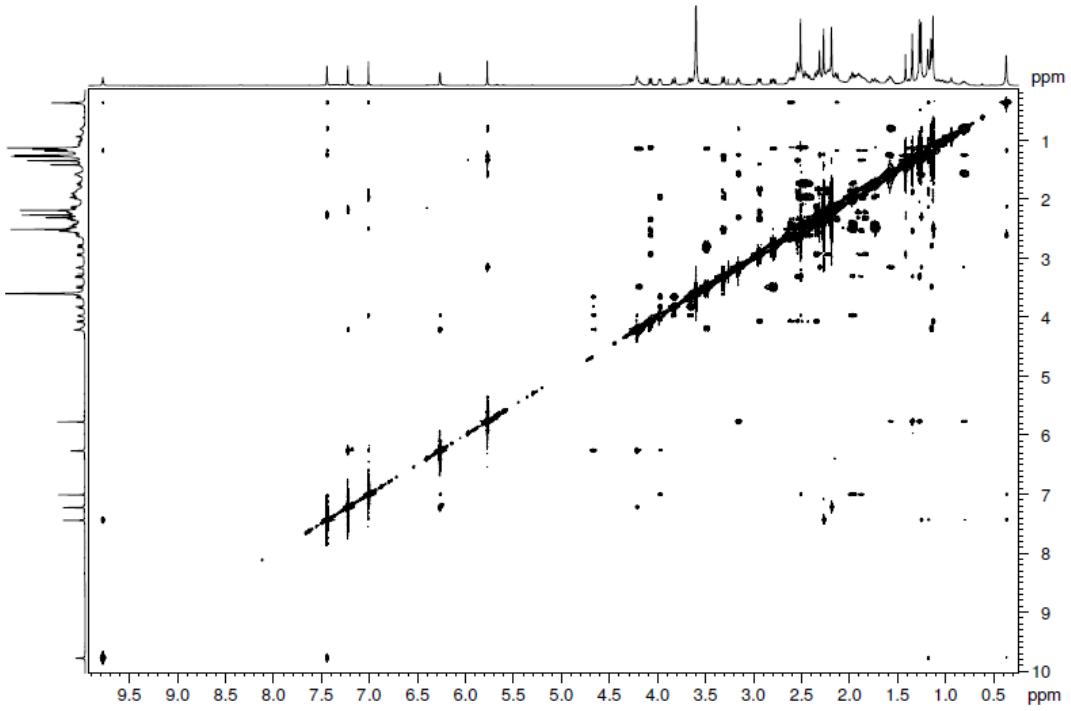

Figure 59. ^{1}H-^{1}H ROESY spectrum of **24**.

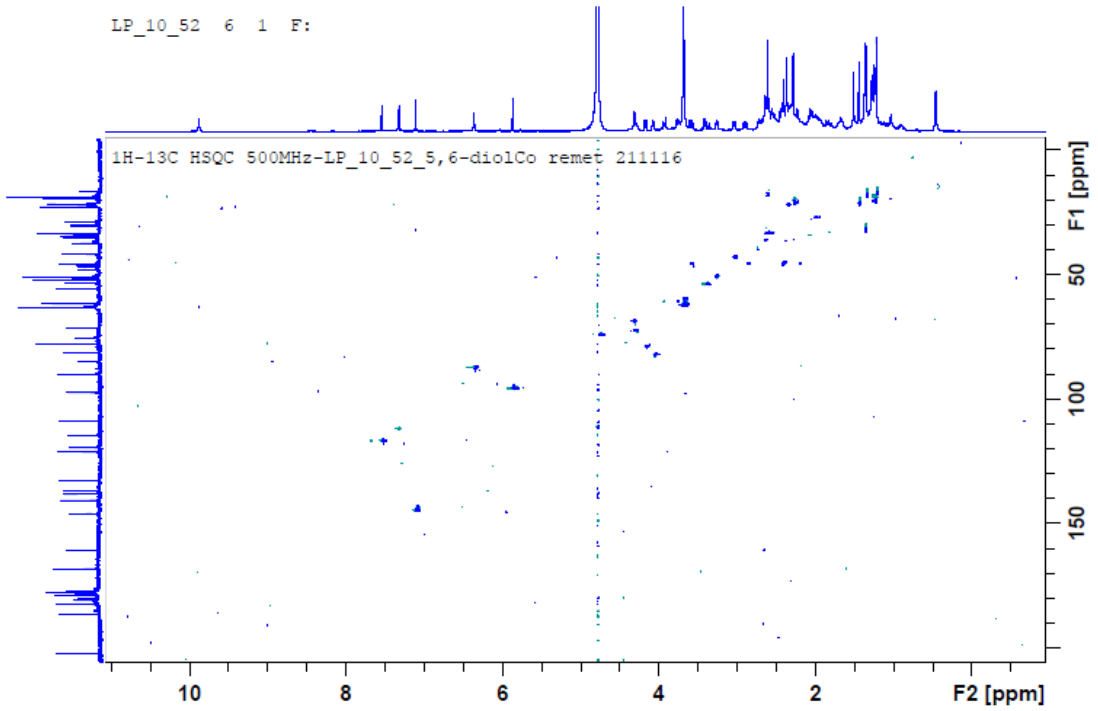

Figure 60. ^{1}H-^{13}C HSQC spectrum of **24**.

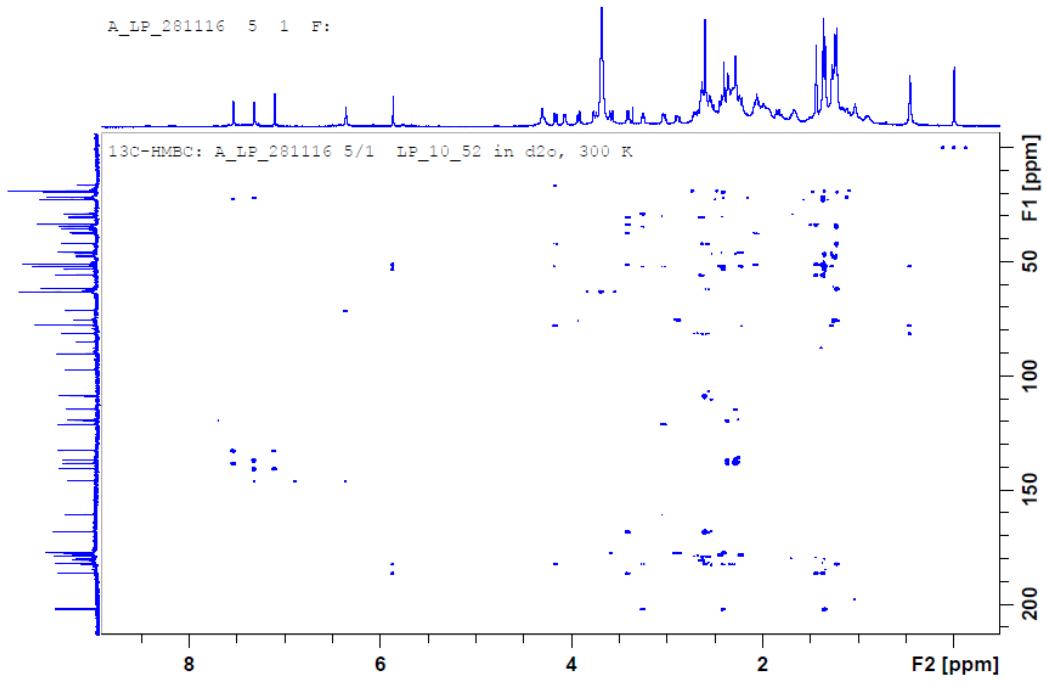

Figure 61. ^{1}H-^{13}C HMBC spectrum of **24**.

^{1}H	δ/ppm		
	1-OH[122]	**24**	**Δδ**
C1	- -	- -	- -
C1A	0.45	0.46	+0.01
C2	- -	- -	- -
C2A	1.47	1.35	-0.12
C21	2.67/2.33	0.92/1.67	
C22	- -	- -	- -
C3	3.99	3.25	-0.74
C31	1.89	0.92	-0.97
C32	2.59/2.54		
C33	- -	- -	- -
C4	- -	- -	- -
C5	- -	- -	- -
C51	2.57	2.41	-0.16
C6	- -	- -	- -
C7	- -	- -	- -
C7A	1.89	1.51	-0.38
C71		- -	
C72	- -	- -	- -
C8	3.43		- -
C81	2.01	1.67/3.04	
C82	1.83/1.01		
C83	- -	- -	- -
C9	- -	- -	- -
C10	6.07	5.87	-0.2
C11	- -	- -	- -
C12	- -	- -	- -
C12A	1.47	1.44	-0.03
C12B	1.30	1.37	+0.07
C13	3.40	3.41	+0.01
C131	2.09	2.00/2.64	
C132	2.66	2.64	-0.02
C133	- -	- -	- -
C14	- -	- -	- -
C15	- -	- -	- -
C151	2.64	2.60	-0.04
C16	- -	- -	- -
C17	- -	- -	- -
C17B	1.40	1.22	-0.18
C171	2.88/2.51		
C172	2.17		
C173	- -	- -	- -
C175	2.96	2.89/3.60	
C176	3.84/3.63	4.31	
C177	1.26	1.27	+0.01
C18			
C181	2.78/2.70	2.89	
C182	- -	- -	- -
C19	4.25	4.18	-0.07
C1R	6.25	6.36	+0.11
C2R			
C3R	4.72	4.31	-0.41
C4R	4.05	4.07	+0.02
C5R	3.93	3.92	+0.01
C2N	6.74	7.10	0.36
C4N	6.50	7.54	+1.04
C5N	- -	- -	- -
C6N	- -	- -	- -
C7N	7.17	7.32	+0.17
C8N	- -	- -	- -
C9N	- -	- -	- -
C10N	2.27	2.36	+0.09
C11N	2.22	2.28	+0.06

^{13}C	δ/ppm		
	1-OH[122]	**24**	**Δδ**
C1	88.0	81.5	-6.5
C1A	22.9	16.6	-6.3
C2	49.9	52.2	+2.3
C2A	20.4	19.5	-0.9
C21	45.8	46.6	+0.8
C22	179.2	182.6	+3.4
C3	59.6	52.0	-7.6
C31	29.3	29.1	-0.2
C32	38.0	34.7	-3.3
C33	180.8	180.1	-0.7
C4	181.9	202.2	+20.3
C5	109.5	121.3	+11.8
C51	18.3	47.2	+28.9
C6	166.8	177.4	+10.6
C7	53.3	63.2	+9.9
C7A	23.1	21.6	-1.5
C71	47.4	46.0	-1.4
C72	178.2	179.0	-0.8
C8	59.2	53.5	5.7
C81	29.1	30.1	+1.0
C82	35.5	37.5	+2.0
C83	180.1	160.8	-19.3
C9	175.8	182.3	+6.5
C10	96.1	97.5	+1.4
C11	179.8	186.5	+6.7
C12	50.4	51.3	+0.9
C12A	22.7	22.1	-0.6
C12B	34.6	33.8	-0.8
C13	56.5	55.8	-0.7
C131	30.7	30.6	-0.1
C132	37.8	37.7	-0.1
C133	181.1	180.9	-0.2
C14	168.0	168.4	+0.4
C15	106.3	108.9	+2.6
C151	18.4	21.7	+3.3
C16	181.2	182.4	+1.2
C17	61.4	61.8	+0.4
C17B	19.6	19.0	-0.6
C171	35.5	34.5	-1.0
C172	34.7	35.5	+0.8
C173	177.8	177.6	-0.2
C175	48.2	48.1	-0.1
C176	75.7	75.5	-0.2
C177	21.9	22.0	+0.1
C18	42.3	41.9	-0.4
C181	34.6	34.8	+0.2
C182	178.8	178.5	-0.3
C19	77.1	77.8	+0.7
C1R	89.9	90.4	+0.5
C2R	71.6	71.6	0.0
C3R	75.8	75.8	0.0
C4R	84.9	85.2	+0.3
C5R	63.2	63.4	+0.2
C2N	145.0	146.1	+1.1
C4N	119.6	119.7	+0.1
C5N	135.7	136.9	+1.2
C6N	137.9	138.3	+0.4
C7N	114.1	114.8	+0.7
C8N	132.4	132.8	+0.4
C9N	139.6	140.7	+1.1
C10N	22.7	22.9	+0.2
C11N	22.1	22.9	+0.8

Table 5. Chemical shifts of ^{1}H and ^{13}C NMR spectra of **1-OH** and **24**. Assignments by ^{1}H NMR, ^{13}C NMR, ^{1}H-^{1}H COSY, ^{1}H-^{1}H ROESY, ^{1}H-^{13}C HSQC and ^{1}H-^{13}C HMBC.

^{1}H-^{13}C HMBC

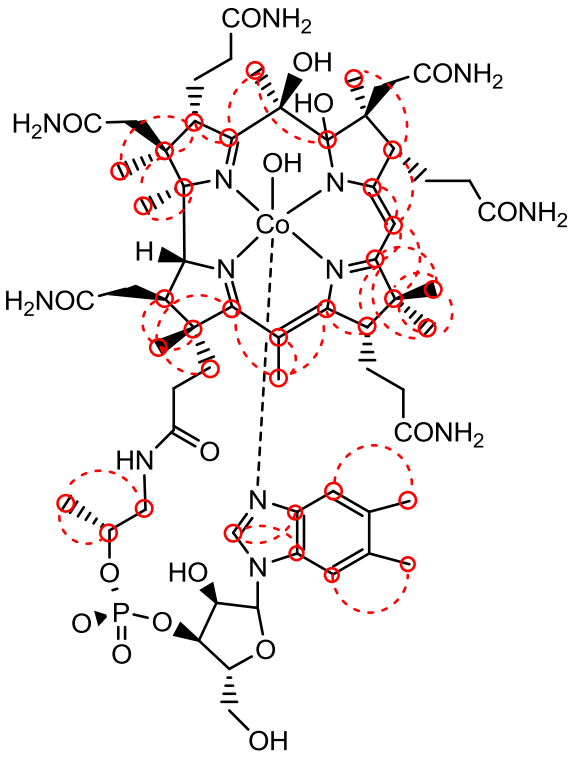

^{1}H-^{1}H ROESY

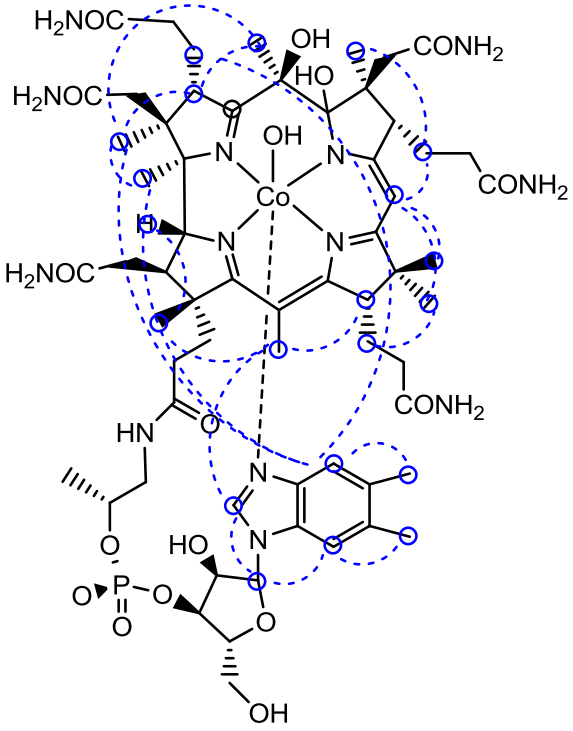

Figure 62. *Top* ^{1}H-^{13}C HMBC correlations within **24**; *Bottom* ^{1}H-^{1}H ROESY correlations within **24**.

^{1}H signal	HMBC	ROESY
C4N	C10N, C8N, C6N	C1A, C2A, C31, C10N
C7N	C11N ,C5N, C9N	C11N, C1R, C3R
C2N	C8N, C9N	C151, C1R
C1R	C2R	C3R, C4R
C10	C8, C9, C11, C12	C81, C12A, C12B
C5R	C3R	
C13	C11, C14	C12B, C151
C3	C2, C21, C22, C31, C32, C4	C2A, C51
C81	C82, C83	C7A
C132	C13, C131, C133	
C151	C15, C14, C16	
C51	C3, C4, C6	C2A
C10N	C4N, C5N, C6N	
C11N	C5N, C6N, C7N	
C7A	C8	
C12A	C11 C12, C12B, C13	
C12B	C11 C12, C12A, C13	
C2A	C21, C3, C4	
C177	C175, C176	
C1A	C1, C2	

Table 6. ^{1}H-^{13}C HMBC and ^{1}H-^{1}H ROESY correlations within **24**.

5,6-diolzincbalalmin (**25**):

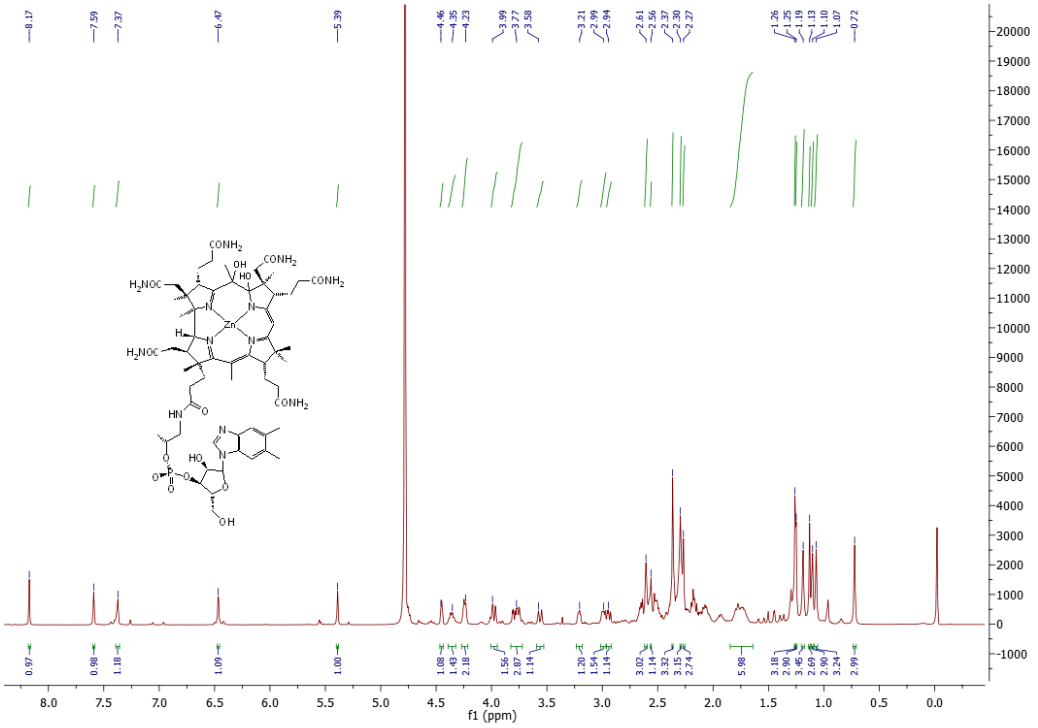

Figure 63. ^{1}H NMR spectrum of 5,6-diol-zincbalamin (**25**).

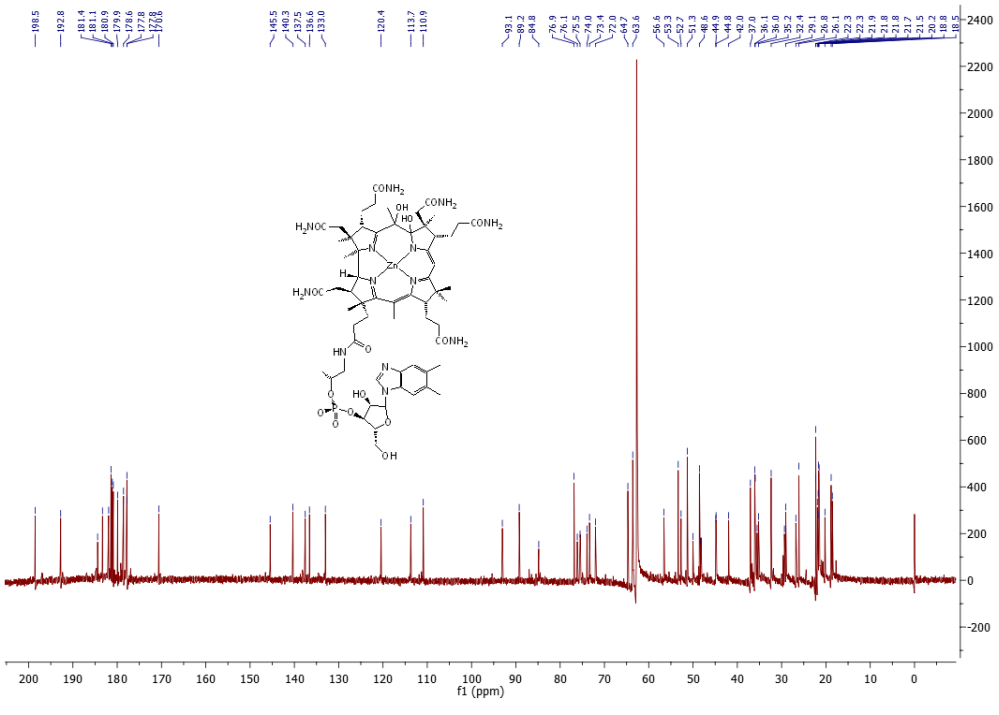

Figure 64. ^{13}C NMR spectrum of 5,6-diol-zincbalamin (**25**).

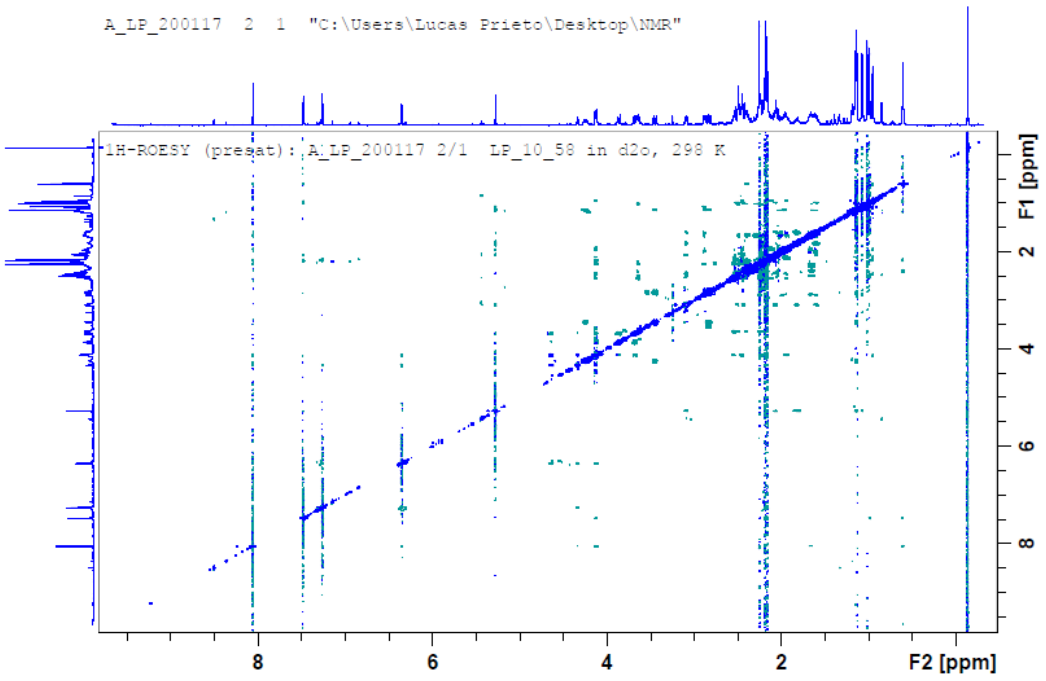

Figure 65. ^{1}H-^{1}H ROESY spectrum of **25**.

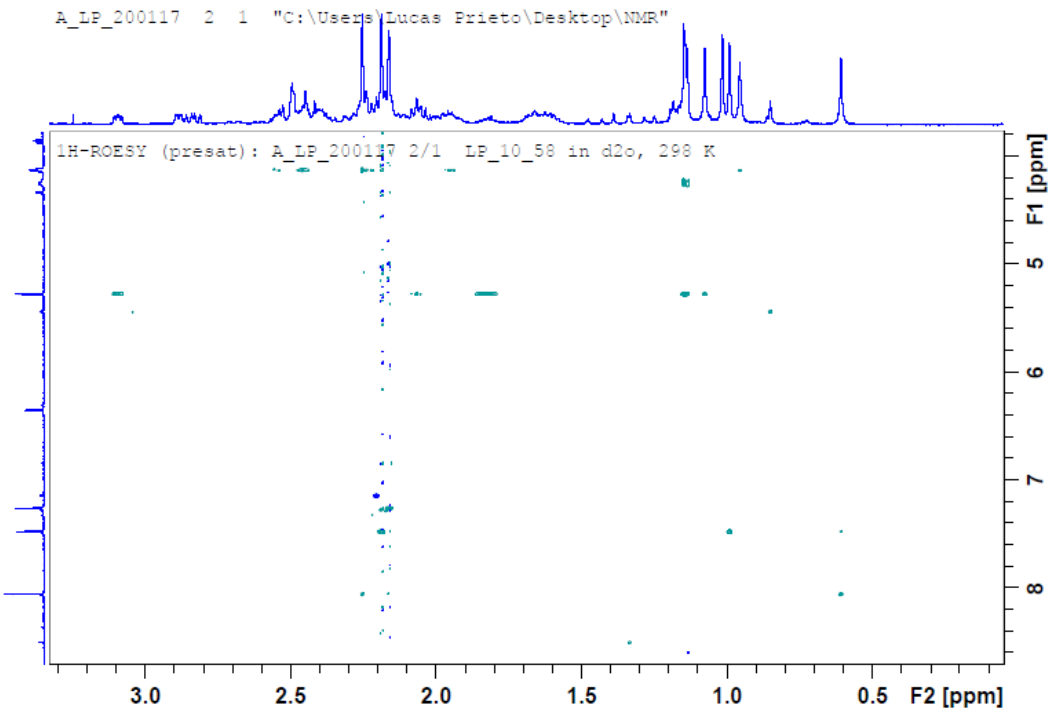

Figure 66. ^{1}H-^{1}H ROESY spectrum of **25** (zoom).

Appendix 1: Modified B_{12} biovectors for the tuneable release of CO[58]

A series of C10 and B ring modified B_{12} derivatives were synthesized during this work according to procedures developed by Wagner et al and by Dr. René Oetterli in our group (Figure 67).[71,98] This includes mainly halogenated B_{12} derivatives and/or B_{12} derivatives containing a c-lactone on the B-ring. As observed by spectroscopic and electrochemical studies, binding electron withdrawing groups (EWG) like halogens to the corrin scaffold affects the electronic properties of the complexes and specifically the redox potential at the Co^{III} center.

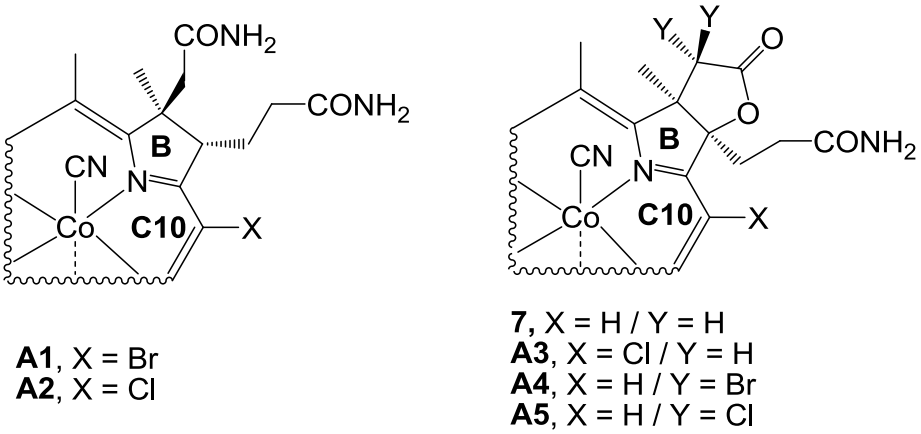

A1, X = Br
A2, X = Cl

7, X = H / Y = H
A3, X = Cl / Y = H
A4, X = H / Y = Br
A5, X = H / Y = Cl

Figure 67. C10 and B-ring modified B_{12} derivatives synthesized for these studies.

The liberation of minute amounts of carbon monoxide (CO) under physiological conditions has benefitial effects under numerous medical conditions.[123-125] Based on previous work by Zobi et al, it is known that vitamin B_{12} can be exploited as a biovector to deliver carbon monoxide releasing molecules (CORMs) based on a 17 electron rhenium (II) complex (Figure 68).[65] CNCbl and $[Et_4N]_2[Re(CO)_2Br_4]$ were connected through a cyanide bridge that ensures electronic communication between the metal centres of both complexes.

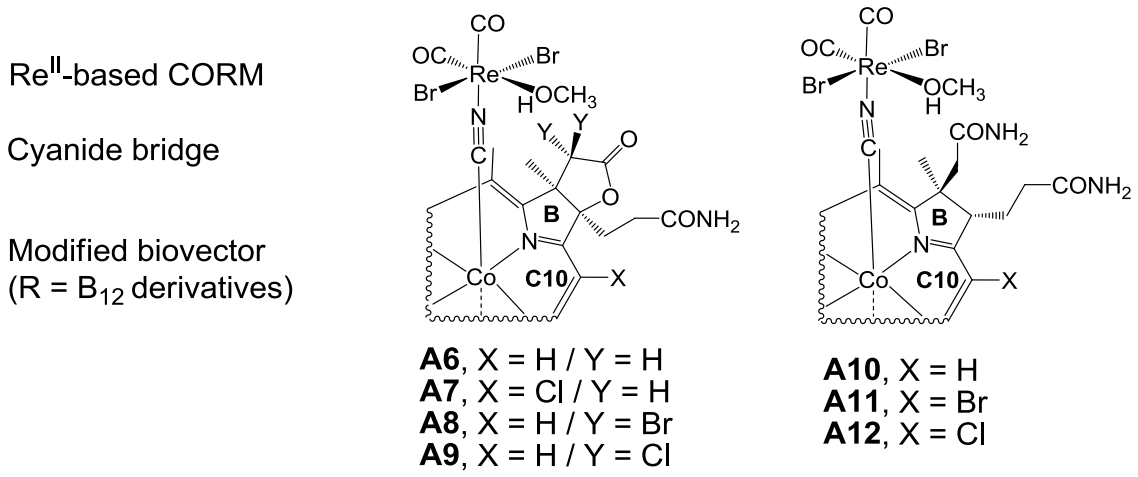

Figure 68. Structures of B_{12}-Re^{II}-CORMs.

Aiming to tune the kinetics of CO release, it was envisaged that changes in the electronic properties of Co^{III} would affect the electronic environment at the Re^{II} complex and consequently modify the CO release. Therefore, the modified B_{12} compounds were synthesized, characterized and sent to our cooperation partner Prof. Fabio Zobi (University of Fribourg, Switzerland), where they were coordinated to the CORM cis-$[Re(CO)_2Br_4]^{2-}$. UV-Vis studies demonstrated that a) aquation of the Re^{II}-core and b) half-life time of CO release within the Co^{III}-CN-Re^{II} complexes were faster the higher $E_{Co(III)/Co(I)}$ values were found. The observed trend may be rationalized considering that an electron deficient Co^{III} ion obtains an enhanced σ-donation from the axial cyanide bridge. As a consequence, the 17-electron Re^{II} complex receives weaker electronic stabilization from the bridging ligand, rendering it more labile towards ligand substitution.

The anti-platelet effect of these B_{12}-Re-CORMS was evaluated by the group of Prof. Chlopicki (Jagiellonian University, Poland), finding that all of them inhibit platelet aggregation. All the investigated compounds avoid the formation of platelets at milimolar range.

Appendix 2: Publications

1) Synthesis of a B-Ring Opened 7,8-*seco*-Vitamin B_{12} Derivative with Grob Fragmentation. R. Oetterli, **L. Prieto**, B. Spingler, F. Zelder, *Org. Lett.*, **2013**, *15*, 4630.

2) Antivitamins for Medicinal Applications. F. Zelder, M. Sonnay, **L. Prieto**, *ChemBioChem*, **2015**, *16*, 1264.

3) Inorganic Cyanide as Protecting Group in the Stereospecific Reconstitution of Vitamin B_{12} from an Artificial Green Secocorrinoid. **L. Prieto**, B. Spingler, F. Zelder, *Org. Lett*, **2016**, *18*, 5292.

4) Modified Biovectors for the Tuneable Activation of Anti-platelet Carbon Monoxide Release**. L. Prieto**, J. Rossier, K. Derszniak, J. Dybas, R. Oetterli, E. Kottelat, S. Chlopicki, F. Zelder, F. Zobi, *Chem Commun*, **2017**, *53*, 6840.

5) A $CoCp_2$ Mediated Demetallation/C-C Bond Forming Reaction: Formation of a Ni^{II}-Containing Vitamin B_{12} Derivative with a Cofactor-F430-Type π-system from a Secocorrin. **L. Prieto**, R. Otterli, F. Zelder, in preparation.

ORGANIC LETTERS

2013
Vol. 15, No. 18
4630–4633

Synthesis of a B Ring Opened 7,8-*seco*-Vitamin B_{12} Derivative with Grob Fragmentation

René M. Oetterli, Lucas Prieto, Bernhard Spingler, and Felix Zelder*

Institute of Inorganic Chemistry, University of Zurich, Winterthurerstrasse 190, 8057 Zurich, Switzerland

zelder@aci.uzh.ch

Received June 4, 2013

ABSTRACT

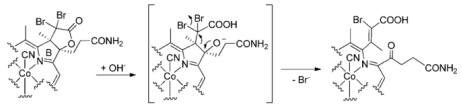

A synthetic route toward B ring opened *7,8-seco*-cyanocobalamins is described. Hydrolysis of a novel *c*-lactone vitamin B_{12} (B_{12}) derivative generates a cobalamin (Cbl) with a β-bromo alcoholate subunit that reacts *in situ* via Grob fragmentation to the secocorrin.

In 2011, Fedosov, Kräutler and co-workers reported a remarkable new 'blue corrinoid' that was produced by hydrolysis of vitamin B_{12} (B_{12}) with aqueous bicarbonate (Scheme 1A).[1] This 7,8-*seco*-cyanocobalamin (7,8-*s*CNCbl) has large parts of homology with its natural precursor, but exhibits an unprecedented structural change at the B-ring of the pseudotetrapyrrolic cobalt(III) corrin macrocycle. Thorough NMR and crystallographic studies revealed cleavage of the peripheral C−C bond at positions 7 and 8 and the formation of a double bond (C7, C71) as well as a keto functionality (C8). The severe structural change in the chromophoric region compared to B_{12} explains the red shift in the absorption spectrum as well as the altered binding to B_{12} transporting proteins.[1] Therapeutic applications as a drug carrier molecule have been proposed for B ring modified B_{12} derivatives,[1,2] but new opportunities as biomimetic catalysts or chemosensors can also be envisaged.[3] However, access toward this new class of compounds is mainly limited by its low yield (3−6%) and long reaction time (3 weeks). The underlying mechanism of this "puzzling partial degradation"[4] is also not yet understood.

We report in this communication a concise and straightforward synthetic route toward this class of corrinoids using Grob fragmentation.[5] A *c*-(α,α-dibromo)-lactone cyanocobalamin (**1**) converts under basic conditions quantitatively and within seconds to the novel 7,8-*s*CNCbl **2** (Scheme 1B). As outlined in Scheme 2, our retrosynthetic analysis of **2** connects C7 and C8 and introduces a β-bromo alcoholate subunit between positions C8 of the B ring and C71 of the *c*-side chain of intermediate **3**. This structural feature is required for the proposed Grob fragmentation of **3** to **2**. We assumed that intermediate **3** is easily accessible by hydrolysis of the double brominated *c*-lactone **1**.

Cyclization at the B ring of B_{12} under formation of a *c*-lactone subunit can be achieved by the treatment of B_{12} with *N*-bromosuccinimide (NBS) at room temperature.[6] We expected to realize concurrent double bromination in the α-position of the carbonyl moiety by slight modifications of this procedure considering the studies by Movassaghi and Jacobsen.[7]

(1) Fedosov, S. N.; Ruetz, M.; Gruber, K.; Fedosova, N. U.; Kräutler, B. *Biochemistry* **2011**, *50*, 8090.
(2) (a) Kurcon, S.; ó Proinsias, K.; Gryko, D. *J. Org. Chem.* **2013**, *78*, 4115. (b) Zelder, F.; Zhou, K.; Sonnay, M. *Dalton Trans.* **2013**, *42*, 854.
(3) (a) Shimakoshi, H.; Abiru, M.; Izumi, S.; Hisaeda, Y. *Chem. Commun.* **2009**, 6427. (b) Männel-Croise, C.; Zelder, F. *Anal. Methods* **2012**, *4*, 2632. (c) Zelder, F.; Alberto, R. In *The Porphyrin Handbook*; Kadish, K. M., Smith, K. M., Guilard, R., Eds.; Elsevier Science: San Diego, 2012; pp 83−130.
(4) Ruetz, M.; Fedosov, S. N.; Kräutler, B. *Angew. Chem., Int. Ed.* **2012**, *51*, 6780.
(5) Eschenmoser, A.; Frey, A. *Helv. Chim. Acta* **1952**, *35*, 1660.
(6) Wagner, F. *Proc. Roy. Soc.* **1965**, *A288*, 344.
(7) Movassaghi, M.; Jacobsen, E. N. *J. Am. Chem. Soc.* **2002**, *124*, 2456.

10.1021/ol401572j
Published on Web 08/30/2013

Scheme 1. (A) Synthesis of 'Blue Corrinoid' from Vitamin B_{12} as Reported in ref 1; (B) Fragmentation of **1** to 'Green Corrinoid' (**2**); (C) Atom Numbering for **1**[a]

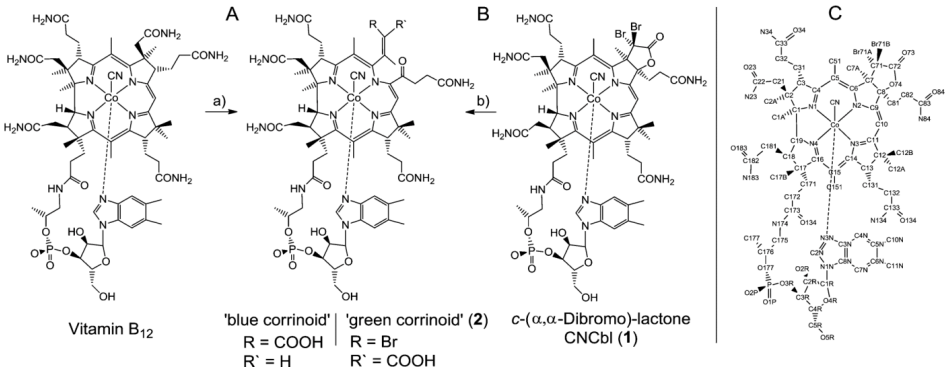

[a] (a) 0.2 M $NaHCO_3$ at pH 9, 50 °C, 3 weeks, 3–6%. (b) pH 11.5, rt, 3 s, 100%.

Scheme 2. Retrosynthetic Analysis of 71-Bromo-7,8-*s*CNCbl (**2**)[a]

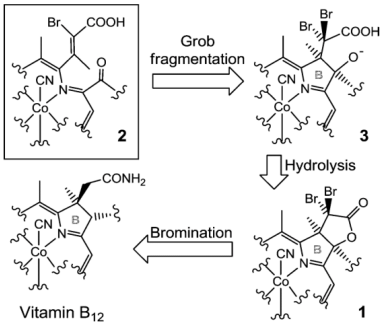

[a] Only the region of the B ring subunit of the B_{12} framework is shown.

Scheme 3. Synthesis of **1**

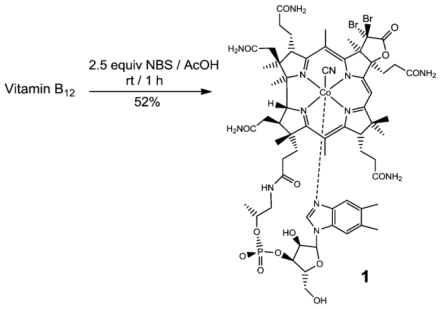

After optimization of the reaction conditions, the synthesis of **1** was performed by treatment of B_{12} with 2.5 equiv of NBS in acetic acid (Scheme 3).[8]

In the high resolution mass spectrum of **1**, an $[M + 2Na]^{2+}$ ion was observed at m/z 778.66763 (m/z_{calc} 778.66762) corresponding to a molecular formula of $C_{63}H_{83}Br_2CoN_{13}O_{15}PNa_2$. This value and the observed isotopic pattern were consistent with the proposed double bromination at C71 of derivative **1**.[8]

The structure of **1** was fully elaborated with two-dimensional homo- and heteronuclear NMR analyses as described in the Supporting Information.[8] Comparison of the ^1H and ^{13}C NMR signals with those of B_{12} indicated diagnostic differences in the B ring area of the corrin macrocycle.[8] The signals in this region show a tendency to shift downfield, which is particularly pronounced for C71 ($\Delta\delta$ = +21.0 ppm) and C8 ($\Delta\delta$ = +37.3 ppm). This behavior is rationalized by the strong deshielding effect of the two electron withdrawing bromo-substituents at C71 as well as the ester functionality at C8, respectively.

The structural identity of **1** was further supported by a crystal structure analysis (Figure 1).[8] Compound **1** crystallized in the orthorhombic space group $P2_12_12_1$ and reassembled those of other Cbl's.[9]

Incubation of **1** for 1 h at pH 9.0 (0.2 M $NaHCO_3$) and 50 °C led to a change of color from red to green and the

(8) Supporting Information.

(9) (a) Zelenka, K.; Brandl, H.; Spingler, B.; Zelder, F. *Dalton Trans.* **2011**, *40*, 9665. (b) Marino, N.; Rabideau, A. E.; Doyle, R. P. *Inorg. Chem.* **2011**, *50*, 220.

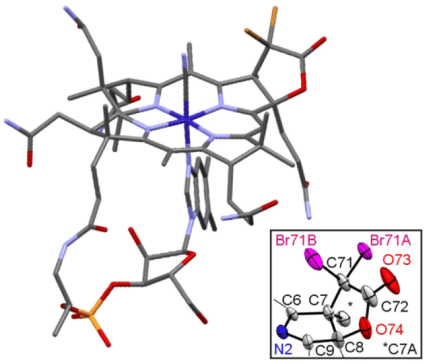

Figure 1. Crystal structure of **1**. *Insert*: details of the B ring and *c*-lactone as ORTEP representation at 50% probability.

quantitative formation of a novel 'green corrinoid' with an absorption maximum (λ_{max}) at 640 nm (Table 1). The red shift ($\Delta\lambda_{max}$ = 60 nm) compared to **1** indicates an alteration of the chromophoric π-system of the corrin macrocycle. A similar trend was observed during the preparation of the 'blue corrinoid' from B_{12}.[1] Control experiments with the unmodified *c*-lactone B_{12} derivative **4** (Table 1; see Scheme S2 for structure)[8] indicated the importance of the bromo leaving group for this type of conversion (Table 1). The kinetics of fragmentation was also followed at pH 10.2 with UV−vis spectroscopy (Figure 2). The conversion of **1** to the 'green corrinoid' obeyed pseudo-first-order kinetics with a rate constant (k_{obs}) of 0.166 min^{-1}.[8] The most convenient approach for the quantitative synthesis of **2** included the conversion of **1** at pH 11.5 within seconds followed by purification with C18-solid phase extraction.

Table 1. Comparison of Rate and Yield of the Fragmentation of *c*-Lactone-B_{12} (**4**)[8] and *c*-(α,α-Dibromo)-lactone-B_{12} (**1**)

entry	*c*-lactone (**4**)	*c*-(α,α-dibromo)-lactone-B_{12} (**1**)
0.2 M $NaHCO_3$ pH 9/50 °C	1d/0%[a]	1 h/100%
pH 11.5/23 °C	1d/0%[a]	3 s/100%

[a] Evaluation of LCMS data indicated quantitative hydrolysis to the corresponding carboxylic acid. For the structure of **4** see Scheme S2.[8]

In addition to UV−vis spectroscopy, the 'structure' of the 'green corrinoid' was fully elucidated as 71-bromo-7,8-*s*CNCbl (**2**) by two-dimensional homo- and heteronuclear NMR analyses, high-resolution mass spectroscopy, and crystal structure analysis.

In the high resolution mass spectrum of **2**, an $[M-H+3Na]^{2+}$ ion was observed at m/z 757.70075 (m/z_{calc} 757.70079) corresponding to a molecular formula of $C_{63}H_{83}BrCoN_{13}O_{16}PNa_3$. This value and the observed isotopic pattern were consistent with the formation of **2** and confirmed the removal of one of the two bromo-substituents at C71 during fragmentation.

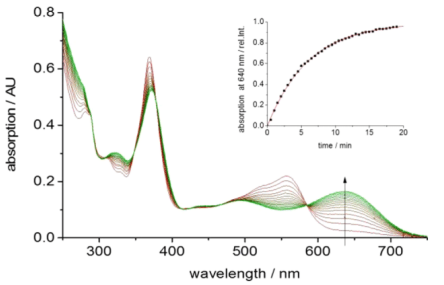

Figure 2. Fragmentation of **1** ($c = 3.99 \times 10^{-5}$ M) at pH 10.2 and 25 °C followed by UV−vis spectroscopy. *Insert:* Change in absorbance at 640 nm for the corresponding reaction.

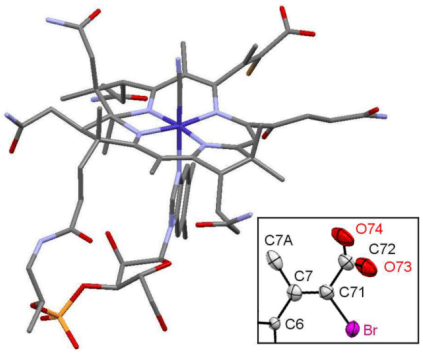

Figure 3. Crystal structure of 'green corrinoid' (**2**). *Insert*: ORTEP representation at 50% probability. Only the major isomer is shown for clarity.

The complete assignments of signals of ^1H and ^{13}C spectra of 'green corrinoid' (**2**) were obtained from $^1H-^1H$-homonuclear (COSY, NOESY) and $^1H-^{13}C$-heteronuclear (HSQC, HMBC) correlations.

Evaluation of the spectra were conducted by comparison with the 'blue corrinoid'[1] as described in the Supporting Information.[8] In brief, the chemical shifts of the green fragmentation product **2** showed the same tendencies as observed for the 'blue corrinoid'[1] under consideration of the residual 71-bromo-substituent and indicated the B ring as the center of structural modification. $^1H-^{13}C$-heteronuclear

multiple bond correlations (HMBC) between H7A and C8 were present in the dibrominated educt **1**, but lacking in the 'green corrinoid' (**2**). This behavior can be explained with the scission of the C7−C8 σ-bond. Furthermore and in agreement with the structure of **2**, the signals of H81 and H82 were downfield shifted. The structural elucidation of the 'green corrinoid' as derivative **2** was further supported by crystal structure analysis[8] and confirmed (i) cleavage of the C7,C8 σ-bond; (ii) formation of a *Z*-configured double bond between C7 and C71 (1.32(1) Å); and (iii) the formation of a keto functionality at C8. Interestingly, the *c*-carboxylic acid functionality showed a strong intermolecular hydrogen bond to a neighboring phosphate group.[8] Derivative **2** crystallized in the uncommon orthorhombic space group $P2_12_12$ with cell dimensions of a = 11.52310(10) Å, b = 52.2227(3) Å, and c = 15.51610(12) Å (Figure 3). There is only one other cobalamin structure known so far that crystallized in the same space group, but with very different cell dimensions of a = 27.2778(17) Å, b = 24.9345(6) Å, and c = 14.0940(14) Å.[10]

Some mechanistic insights into the mode of fragmentation have been obtained from structural comparison between intermediate **3** and product **2**. Based on the *Z*-configuration of the double bond in derivative **2**, we propose Br71A as the leaving group of **3** because of its *anti* orientation to the scissible C7−C8 bond as shown in Scheme 4.[5,11]

In summary we report a concise and convenient two-step procedure for the preparation of 7,8-*seco*-cyanocobalamins. Straightforward synthetic access toward this interesting new class of B_{12} derivatives will facilitate potential applications in the near future.

Scheme 4. Different Views on the C8, C7, C71 Region of the β-Bromo Alcoholate Subunit of Intermediate **3**

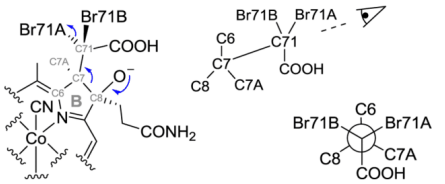

Acknowledgment. This work was financially supported by the Forschungskredit of the University of Zürich. Support by R. Alberto (University of Zurich) and the Institute of Inorganic Chemistry of the University of Zurich is acknowledged. The authors are thankful to L. Bigler (University of Zurich) for recording of the HR-ESI-MS spectra and to DSM Nutritional Products AG (Basel/Switzerland) for a generous gift of vitamin B_{12}.

Supporting Information Available. Preparative procedures and characterizations. NMR assignments of compounds **1** and **2**. Crystal data and structure refinement of compounds **1** and **2**. This material is available free of charge via the Internet at http://pubs.acs.org.

The authors declare no competing financial interest.

(10) Mundwiler, S.; Spingler, B.; Kurz, P.; Kunze, S.; Alberto, R. *Chem.—Eur. J.* **2005**, *11*, 4089.
(11) Prantz, K.; Mulzer, J. *Chem. Rev.* **2010**, *110*, 3741.

ChemPubSoc Europe
DOI: 10.1002/cbic.201500072
CHEMBIOCHEM Reviews

Antivitamins for Medicinal Applications

Felix Zelder,* Marjorie Sonnay, and Lucas Prieto[a]

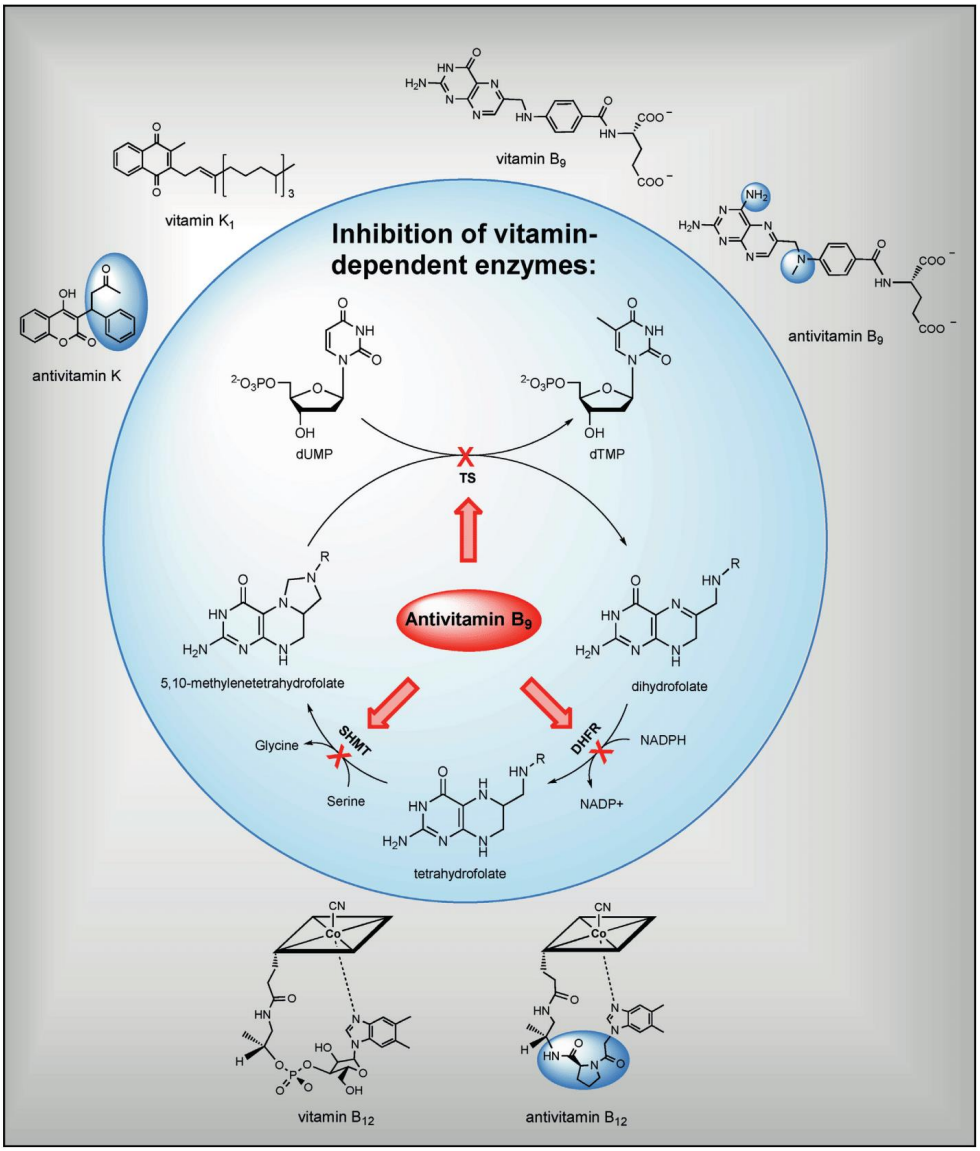

Antivitamins represent a broad class of compounds that counteract the essential effects of vitamins. The symptoms triggered by such antinutritional factors resemble those of vitamin deficiencies, but can be successfully reversed by treating patients with the intact vitamin. Despite being undesirable for healthy organisms, the toxicities of these compounds present considerable interest for biological and medicinal purposes. Indeed, antivitamins played fundamental roles in the development of pioneering antibiotic and antiproliferative drugs, such as prontosil and aminopterin. Their development and optimisation were made possible by the study, throughout the 20th century, of the vitamins' and antivitamins' functions in metabolic processes. However, even with this thorough knowledge, commercialised antivitamin-based drugs are still nowadays limited to antagonists of vitamins B_9 and K. The antivitamin field thus still needs to be explored more intensely, in view of the outstanding therapeutic success exhibited by several antivitamin-based medicines. Here we summarise historical achievements and discuss critically recent developments, opportunities and potential limitations of the antivitamin approach, with a special focus on antivitamins K, B_9 and B_{12}.

Introduction

In 1926, Mellanby reported a dietetic compound of unknown chemical composition that had the ability to counteract the effect of the "calcifying vitamin". He thus called it "toxamin".[1] This observation resulted from animal feeding studies on puppies, which led to the conclusion that, after these animals were fed with cereals, the "calcification of the bones becomes worse, the greater the amount of cereal eaten".[1]

At this time, the structure and mode of action of the vitamin and its counterpart were not yet discovered, but these important pioneering studies marked the starting point of antivitamin research.[2] However, it took almost another decade until vitamin D and phytic acid (Table 1, entry 1) were correctly identified as "calcifying vitamin" and its calcium-binding antagonist.[3,4]

It is possible to cite several other examples, such as scurvy or beriberi,[2] in which diseases and symptoms caused by malnutrition had already been known for centuries without the source being understood. Scurvy, a disease resulting from a diet deficient in vitamin C, was encountered during the Crusades and sieges and caused jaundice, loss of teeth, fever and death. In those days, the cause remained unidentified, but fresh meat and fruits were known to treat these symptoms successfully. The beginning of the 19th century brought advances in physiology, medicine, nutritional science and chemistry, and thus paved the way to determine the cause of this affliction as a vitamin C deficiency.

In this context, beriberi presents another historically revealing example.[2] This disease is due to a vitamin B_1 (thiamine, Table 1, entry 2) deficiency and is associated with severe dysfunctions of the peripheral nervous and cardiovascular systems. It was first described in 1630; however, it took until the end of the 19th century to establish that its cause was diet-related. At that time, the dietary habits of a large number of prisoners in Java were evaluated. It led to the discovery that polished brown rice caused this terrible disease.[2,5] Some years after the essential nutritional effect of unpolished brown rice had been recognised, thiamine was identified by the Dutch physician Christiaan Eijkman as the first essential, exogenous micronutrient in human diet.[2] The importance of this discovery was honoured in 1929 with the Nobel Prize in Physiology or Medicine.[5] In the same period, the lifesaving effects of raw liver extracts were successfully exploited for treating the deadly human disease pernicious anaemia. Whipple, Murphy and Minot were honoured with the 1934 Nobel Prize in Physiology or Medicine for this therapeutic breakthrough. However, the beautiful and elaborate structure of the active compound was not yet known.[6,7] Enormous efforts and developments were then required to isolate this anti-pernicious anaemia cofactor—vitamin B_{12}—and to deduce its structure by X-ray crystallography.[8]

All of these scientific milestones in vitamin research underscore the toxic effects of antivitamins, resulting from the es-

Table 1. Examples of historically important pairs of vitamins and antivitamins: vitamin D and phytic acid (entry 1), thiamine and pyrithiamine (entry 2) and vitamin B_6 (pyridoxine) and deoxypyridoxine (entry 3).

	Vitamin	Antivitamin
1	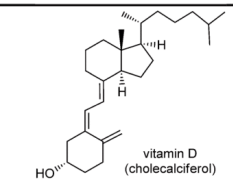 vitamin D (cholecalciferol)	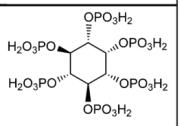 phytic acid
2	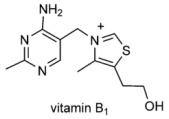 vitamin B_1 (thiamine)	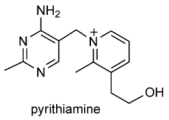 pyrithiamine
3	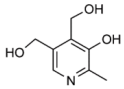 vitamin B_6 (pyridoxine)	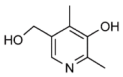 deoxypyridoxine

[a] *Priv. Doz. Dr. F. Zelder, M. Sonnay, L. Prieto*
Institute of Chemistry, University of Zürich
Winterthurerstrasse 190, 8057 Zürich (Switzerland)
E-mail: felix.zelder@chem.uzh.ch

sentiality of vitamins. For this reason, the use of antivitamins to induce a vitamin deficiency would appear to be counterproductive at first sight. However, the administration of antivitamins leads to specific metabolic transformations, and this offers enormous beneficial therapeutic opportunities. Hence, antivitamin metabolic studies have already been successfully exploited for drug development. In this review we intend to focus on important aspects, developments and selected examples of antivitamin research.[2,33–37] In particular, we first give a conceptual overview of antivitamins and classify them on the basis of their modes of action. We then highlight some efforts that led to antivitamin-based drugs, such as warfarin, an antivitamin K acting as anticoagulant, and methotrexate (MTX), an anticancer drug originating from a slight structural modification of vitamin B_9. In this general antivitamin context, antivitamin B_{12} derivatives deserve special attention. Indeed, despite enormous efforts in designing and testing large numbers of potential candidates throughout the years, not a single antivitamin B_{12} derivative has reached the market yet. Nevertheless, the latest observations of inhibitory effects are encouraging and have thus stimulated renewed interest in this research field. The emerging trends in the design, the chemistry and the biology of antivitamin B_{12} derivatives are therefore finally critically discussed.

Felix Zelder obtained his PhD from the University of Heidelberg (Germany) in 2003 and then moved to the Scripps Research Institute for postdoctoral studies. Since 2006, he has been a group leader at the Institute of Chemistry at the University of Zürich. Research in the Zelder group focuses on the development of semiartificial metal complexes for applications in medicinal and analytical chemistry, but also for fundamental studies. F.Z. has been awarded several fellowships and prizes, most recently the Mercator prize (Mercator Foundation, Switzerland) in 2009 and the Venia Legendi for inorganic and bioinorganic chemistry in 2013.

Marjorie Sonnay received an MSc in molecular and biological chemistry from the EPFL (Switzerland) in 2010. She completed her Master's thesis at the University of Edinburgh (UK) in the group of Dr. Paul Lusby. She started her PhD thesis in 2012, under the supervision of F.Z. at the University of Zürich (Switzerland), where she is currently developing new peptide–B_{12} derivatives for biomimetic studies and medicinal applications.

Lucas Prieto studied chemistry at the Universities of Oviedo (Spain) and Vienna (Austria). He moved to Switzerland in 2012 to work on vitamin B_{12} chemistry under the supervision of F.Z. In 2013, he started his PhD at the University of Zürich (Switzerland), where he is currently working on the development of new B_{12} antivitamins.

Antivitamins—Definition and Mode of Action

Antivitamins are molecules that diminish or abolish specific functions of vitamins, as defined by Somogyi and Trautner in 1974.[2] This relatively broad definition is certainly required in order to embrace the large structural and mechanistic diversity of antivitamins. This important diversity is illustrated, among others, by the multiple antivitamins of vitamin B_1 (thiamine). In fact, vitamin B_1 deficiency can be caused by different types of chemical species, ranging from small molecules such as pyrithiamine (Table 1, entry 2) to proteins such as thiaminase. Pyrithiamine is a synthetic, non-functional analogue of thiamine, competing with vitamin B_1 and its derivatives in enzymatic reactions.[38] The same metabolic effect can also be produced by thiaminase, an enzyme present in certain fish and plants, which induces irreversible degradation of the target vitamin.[26,27] Hence, antivitamins exhibit a broad structural and mechanistic complexity, which is sometimes confusing and therefore requires some further classifications. Somogyi arranged antivitamins into two groups, differentiating between structural analogues and structural modifiers.[32] We have kept this valid classification, but have decided to use the description inhibitors instead of structural analogues, emphasising that all of these antivitamins inhibit protein function by competitive binding. Based on this slight modification, our classification focuses solely on the mode of action, and thus distinguishes between inhibitors (class A antivitamins, Table 2, entry 1) and structural modifiers (class B antivitamins, Table 2, entry 2).

Class A antivitamins target proteins involved 1) in the biosynthesis, 2) in the cellular delivery, or 3) in enzymatic transformations of the vitamin (Table 2, entry 1). In contrast to class A, the class B antivitamins (Table 2, entry 2) do not target the participating proteins directly, but convert vitamins into non-functional species. This behaviour is achieved in different ways, either by structurally modifying the vitamin itself or by blocking required additional cofactors such as metal ions. These modifiers include a variety of chemical species ranging from small molecules (e.g., phytic acid) to large proteins (e.g., thiaminase, streptavidin). In a similar manner, but this time targeting the vitamin directly, streptavidin induces the formation of (supramolecular) antivitamin–vitamin complexes, as observed for the streptavidin–biotin dimer.[2] This structural modification impedes any further molecular recognition and cellular uptake of the vitamin. The outstanding binding of the complex ($K_D \approx 10^{-15}$ M) was explored for the development of the biotin/streptavidin technology, which then led to numerous important applications in chemistry and biology.[39,40] However, with

Table 2. Classification of antivitamins.[a]

	Subcategory	Mode of action	Examples	Target	Structural aspect	Medicinal importance	Ref.
1	class A (inhibitors)	A1) inhibitors of the biosynthesis of vitamins	prontosil[b]	dihydropteroate synthetase (DHPS)	non-functional structural analogue of a vitamin building block	antibiotics	[9–11]
		A2) inhibitors of vitamin transportation	OHCbl [*c*-lactam]	target protein has not yet been identified	non-functional structural analogue of the vitamin	antiproliferative activity	[12, 13]
		A3) inhibitors of vitamin-dependent enzymes	1) warfarin[c] 2) methotrexate (MTX)[d]	1) vitamin K epoxide reductase (VKOR) 2) dihydrofolate reductase (DHFR)	non-functional structural analogues of the vitamin	1) anticoagulant drug 2) antiproliferative and antibacterial drugs	[14–18] [19–25]
2	class B (modifiers)	structural modifiers	1) phytic acid 2) thiaminase 3) streptavidin	1) metal ion cofactors (e.g., Ca^{II}, Zn^{II}, Fe^{II}) 2) thiamine 3) biotin	large variety of compounds, ranging from small molecules (1) to proteins (2, 3)	1–3) antinutrients	[3, 4] [26, 27] [28–31]

[a] Refs. [2] and [32]. [b] 4-[(2,4-Diaminophenyl)azo]benzenesulfonamide. [c] (*RS*)-4-Hydroxy-3-(3-oxo-1-phenylbutyl)coumarin. [d] (2*S*)-2-[(4-{[(2,4-Diaminopteridin-6-yl)methyl](methyl)amino}benzoyl)amino]pentanedioic acid.

the exception of streptavidin, class B antivitamins represent important antinutritional factors, but do not play significant roles for medicinal or biological applications. These compounds are thus regarded as antinutrients because they interfere with the absorption of food nutrients.

Relevance and Applications of Antivitamins

Historically, antivitamins have been associated with dangerous and even deadly diseases. Despite this unattractive first assessment, antivitamin research has resulted in significant and exciting developments in both biological and medicinal fields. Indeed, antivitamins and antimetabolites in general have been deeply researched in order to unravel biological riddles such as vitamin-dependent metabolic pathways.

The effects of a deliberately introduced vitamin deficiency were thus explored in bacteria, animals and humans, by feeding the different subjects compounds with known antivitamin activity.[41–44] Such investigations were conducted, among others, on vitamin B_6 deficiency and its effects on humans. This study was performed by administrating deoxypyridoxine (a vitamin B_6 antagonist, Table 1, entry 3) to humans, and this led to the conclusion that significant skin lesions on the face were part of the effects of this deficiency.[43]

The determination of the roles of vitamins in metabolic processes is essential for the development of treatments against vitamin-dependent diseases. Here, again, antivitamins represent a great therapeutic opportunity for such afflictions, and have hence yielded numerous drugs, ranging from anticoagulants to anticancer agents. Among these antivitamin-based drugs, the sulfonamide prontosil (Figure 1) is worth mentioning.[10] It was reported in 1935 by Domagk,[9] who was honoured with a Nobel Prize in Physiology or Medicine for his discovery.[45,46] Prontosil in fact represents the first commercially available antimicrobial agent for humans, and subsequently served as the basis for numerous sulfonamide-based antimicrobial drugs.[47]

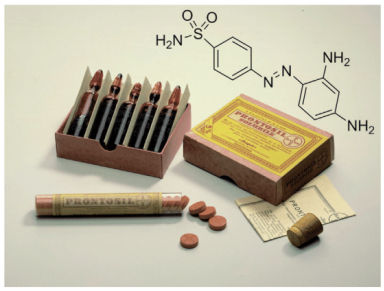

Figure 1. Picture of a historic sample of prontosil, the first commercially available antibiotic. The structure of the drug is depicted on the top right (picture: courtesy of Bayer AG).

Since the discovery of prontosil, numerous antivitamins have been clinically tested and approved as drugs. A search in the Canadian online drug databank (http://www.drugbank.ca) provided abundant examples, a few of which are presented in Table 3. The mode of action of each antivitamin corresponding to the classification in Table 2 is also proposed. As mentioned in the previous chapter, only the class A antivitamins present interesting features for medical applications. Hence, approved antivitamin drugs belong only to class A. Furthermore, Table 3 underscores the importance of vitamins K and B_9 as effective targets for commercially available drug molecules.

Table 3. Examples of vitamin antagonists as approved and clinically tested drugs.[a]

	Name	Vitamin target	Class	Databank code
1	methotrexate	vitamin B_9	A3	DB00563
2	trimetrexate	vitamin B_9	A3	DB01157
3	pemetrexed	vitamin B_9	A3	DB00642
4	dapsone	vitamin B_9	A1	DB00250
5	sulfanilamide	vitamin B_9	A1	DB00259
6	sulfamethoxazole	vitamin B_9	A1	DB01015
7	warfarin	vitamin K	A3	DB00682
8	dicoumarol	vitamin K	A3	DB00266
9	phenindione	vitamin K	A3	DB00498
10	acenocoumarol	vitamin K	A3	DB01418

[a] http://www.drugbank.ca (search from December 2014).

Antivitamin K

After the discovery of vitamin K (Scheme 1) at the beginning of the 20th century by Dam,[48] intense research showed its participation in both bone metabolism[49] and the coagulation cascade.[50,51] The specific role and mechanism of action of vitamin K in those two processes was not unravelled until the discovery in the 1970s of an unusual glutamic acid derivative in the coagulation factor prothrombin (factor II).[52,53]

This so-called carboxyglutamic acid (Scheme 2) turned out to be a product of vitamin K activity.[54] Indeed, vitamin K acts as a cofactor for post-translational carboxylation of glutamic acid moieties in diverse blood clotting proteins (factors II, VII, IX and X; see Scheme 2).[55] This specific modification appears to be of primary importance in the blood clotting process by promoting interaction of the protein with calcium,[56] thus permitting its binding to the phospholipids on the membrane surface, which leads to coagulation.[57–59] The carboxylation of glutamic acid moieties is catalysed by the enzyme γ-carboxylase and requires oxygen, CO_2 and the cofactor vitamin K hydroquinone. In this process, it is proposed that the formation of an elusive, basic vitamin K intermediate[60] (not shown in Scheme 2) initiates the concerted deprotonation of glutamate and coupling with CO_2 to afford the carboxyglutamic acid functionality.[61] Overall, vitamin K hydroquinone undergoes a four-electron oxidation, yielding vitamin K 2,3-epoxide. This then needs to be recycled into the reduced vitamin K hydroquinone by the enzyme vitamin K epoxide reductase (VKOR), in order to be reused (Scheme 2).[62–65] For blood coagulation, this catalytic cycle seems to be of the utmost relevance; indeed, several clotting factors are dependent on this post-translational modification for efficient biological activity.[64] Therefore, deficiencies in this mechanism lead to important clotting troubles, and can be the cause of deadly haemorrhages.[66] In the 1920s, such atrocious bleeding damages mortally affected cattle that ate spoiled hay made from sweet clover.[67] Twenty years of research by Link et al. then established the cause of the "sweet clover disease": dicoumarol (Scheme 1).[16] This compound was found to act as an antivitamin K and was thus later commercialised as an anticoagulant.

Since the discovery of dicoumarol, several other different compounds have been found to display relevant anticoagulant abilities and have therefore been made available on the drug market.[68] Scheme 1 shows two other examples: warfarin and acenocoumarol, each with a "coumarin-like" structure. The

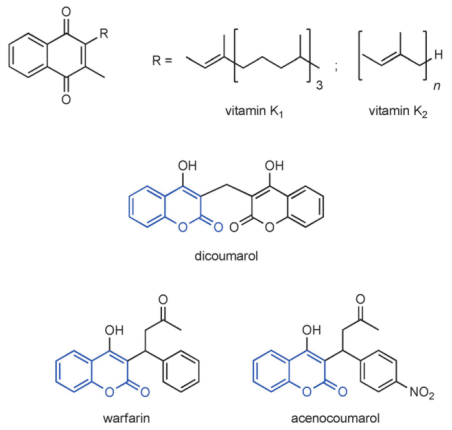

Scheme 1. Vitamins K_1 and K_2 and the commercialised antivitamin K derivatives dicoumarol, warfarin and acenocoumarol (the coumarin subunit is shown in blue).

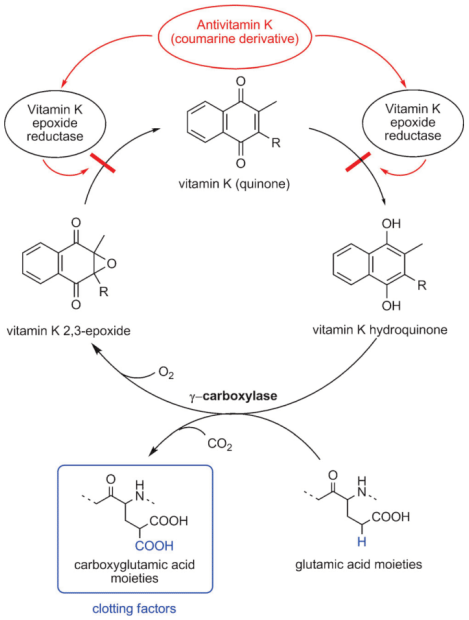

Scheme 2. Vitamin K cycle for the carboxylation of glutamic acid moieties in clotting factors II, VII, IX and X and the site of action of antivitamin K derivatives.

mechanism of action of such antagonists was later discovered to depend on VKOR: this enzyme is indeed inhibited by the antivitamins, thus preventing the reduction of vitamin K for its recycling (Scheme 2).[69–71] Recently, the crystal structure of a bacterial VKOR homologue has been determined and allowed further understanding of the electron-transfer mechanism taking place during the catalysis, as well as of the action of warfarin on such proteins.[72,73] In short, antivitamins K do not antagonise the natural vitamin, but actually obstruct the recycling process by inhibiting the enzyme responsible for vitamin K reduction (VKOR).[25,26] Furthermore, uptake of vitamin K will counteract the antagonist effect and restore natural coagulation activity.[74]

The best-known and most frequently prescribed anticoagulant drug based on an antivitamin is warfarin (Scheme 1). It was discovered in the 1940s[14,15] and was first commercialised as rodent poison, in 1948. However, a few years later, the anticoagulant properties of the substance started to be further studied on humans, due to a regrettable suicide attempt by an army inductee who ingested many tablets of warfarin over several days. After a fortunate change of heart, he was administered with fresh blood and significant amounts of vitamin K, the usual treatment for "sweet clover disease" at this time, and underwent a full recovery. Thanks to this unusual human trial, warfarin demonstrated its interesting characteristics and was thus commercialised as an anticoagulant in 1954.[16]

Warfarin, like all the other coumarin-based antivitamins, is produced and sold as a racemic mixture. However, it has been shown that the *S* isomer is about five times more potent than the *R* isomer. It has been demonstrated to be superior to dicoumarol, due to its broad administration possibilities: indeed, warfarin was the first coumarin-based anticoagulant that could be given orally, intravenously, intramuscularly or rectally, with similar absorption rates for each of these methods.[18] Those criteria propelled warfarin to the forefront of anticoagulant agents for the treatment of thromboembolic disorders and for the prevention of atrial fibrillation, myocardial infraction and stroke.[75,76]

In spite of the applicability of the vitamin K antagonists, their remarkable properties are also undermined by several drawbacks that make these compounds complex to handle in hospital care. They offer only narrow therapeutic windows and show important variations in dose/response relationships, thus requiring constant monitoring in order to avoid bleeding.[77] Numerous factors, such as body mass, diet or alcohol consumption, can influence the response to anticoagulants. Furthermore, the uptake of additional drugs induces various interactions with antivitamin K anticoagulants, thus making the prescription of those drugs more intricate.[78–81] Current research focuses on drugs with more straightforward application, thus facilitating their handling. Such drugs are targeted on inhibiting different coagulation factors, such as thrombin (factor IIa). Diverse approaches have been followed, one of them being direct binding of the inhibitor to the active site of the coagulation factor.[82] Dabigatran represents one of those oral thrombin inhibitors. It presents considerable advantages, such as the reduction of drug–drug interaction and a lack of need for monitoring.[83,84] Other coagulation factors have also been targeted, with excellent results for factor Xa inhibitors such as rivaroxaban. Also for this oral anticoagulant, monitoring is not required.[85] However, antivitamins K have proven to be of great importance throughout the decades and are still nowadays frequently prescribed.

Antivitamin B_9

Folic acid (vitamin B_9, Scheme 3 A) derivatives consist of pteridine, *p*-aminobenzoic acid (PABA) and glutamate building blocks.[86] The reduced forms of this vitamin, such as N^5,N^{10}-methylenetetrahydrofolate (5,10-CH_2-FH4, **1**, Scheme 3 B), act as biological single-carbon sources during nucleotide and amino acid synthesis and are therefore essential for cell growth and replication.[87,88]

For this reason, the uptake of vitamin B_9 antagonists induces cytotoxic effects, and this implies that antivitamin B_9 derivatives have great potential for applications in medicine. Indeed, B_9 antivitamins are currently used to treat a wide range of diseases, ranging from human cancer to bacterial and fungal infections.[11,19–21,23] These types of drugs all belong to the class A antivitamins, according to the classification proposed in Table 2. More precisely, antivitamins B_9 exhibit therapeutic activity in different ways (1–3): 1) by inhibiting folic acid biosynthesis, 2) by impeding cellular uptake, or 3) by inhibiting folate-dependent enzymatic processes. These different biological targets explain their selectivity for different types of organisms as well as their broad therapeutic spectrum. Two prominent drugs based on antivitamin B_9 can be cited as examples:

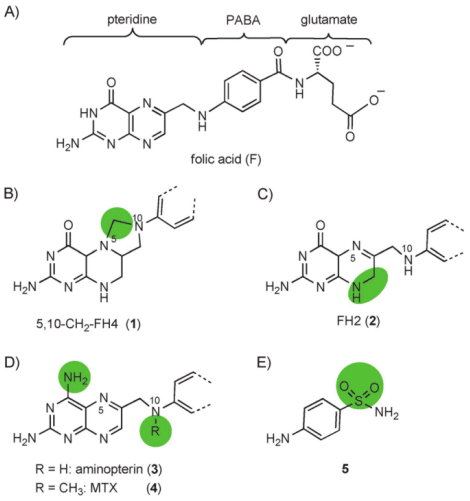

Scheme 3. Chemical structures of A) folic acid (vitamin B_9, F), B) N^5,N^{10}-methylenetetrahydrofolate (5,10-CH_2-FH4, **1**), C) dihydrofolate (FH2, **2**), D) the antivitamins aminopterin (**3**) and methotrexate (MTX, **4**), and E) sulfanilamide (**5**).

methotrexate (MTX, **4**, Scheme 3D)[19,22,34,89] and sulfanilamide (**5**, Scheme 3E).[11] These two drugs, which revolutionised medicinal chemistry as pioneering examples of antibiotic and chemotherapeutic drugs,[10] are discussed.

In 1935, *para*-aminobenzenesulfonamide (**5**, Scheme 3E) was identified as the therapeutically active metabolite of prontosil.[11] This discovery then inspired the search for improved antibacterial drugs belonging to the family of the sulfonamides.[11]

Those drugs are based on a simple concept based on an interesting metabolic difference between mammals and bacteria. Mammals cannot produce folic acid themselves and have to obtain the vitamin from the diet. In contrast, bacteria lack the carrier transport system that is active in mammals. They thus have to synthesise the natural product de novo. Bacterial folate production involves several enzymatic steps, including coupling between 6-hydroxymethyl-7,8-dihydropterin pyrophosphate and PABA, a reaction catalysed by the enzyme dihydropteroate synthetase (DHPS, Scheme 4).[90,91] This biosynthetic step is effectively inhibited by structurally similar *para*-aminosulfonamides, such as sulfanilamide. As a consequence of this inhibition, infectious bacterial cells do not grow or divide any further. Conversely, mammals do not express DHPS and are therefore not targeted by this class of compounds, which explains the target specificity of these drugs.

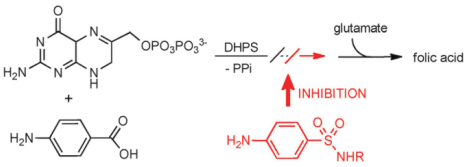

Scheme 4. Coupling of dihydropterin pyrophosphate and PABA, catalysed by dihydropteroate synthetase (DHPS) during bacterial folate biosynthesis.

The drug methotrexate (MTX, **4**) is part of a different group of antivitamins B_9. It inhibits folic-acid-dependent enzymatic transformations directly and is therefore also effective in mammals. To improve understanding of the modes of actions of antivitamin B_9 derivatives, the role of vitamin B_9 in human cell growth processes first needs to be described. Within cells, only the reduced form of folic acid catalyses single-carbon transformations, as depicted in Scheme 5 for the synthesis of thymidylate (dTMP) from deoxyuridylate (dUMP). This reaction is catalysed by the enzyme thymidylate synthase (TS) and requires N^5,N^{10}-methylenetetrahydrofolate (5,10-CH_2-FH4, **1**, Scheme 5A). During this formal methyl-transfer reaction, 5,10-CH_2-FH4 is oxidised to dihydrofolate (FH2), which subsequently has to be reduced to FH4 to restart the catalytic cycle. This transformation is catalysed by dihydrofolate reductase (DHFR), with the aid of nicotinamide adenine dinucleotide phosphate (NADPH) as reductant (Scheme 5B). FH4 is then transformed into the catalytically active 5,10-CH_2-FH4 (**1**) by the enzyme serine hydroxylmethyltransferase (SHMT; Scheme 5C). The proper interplay between all three participating enzymes is required for synthesising dTMP and guaranteeing further cell growth processes.

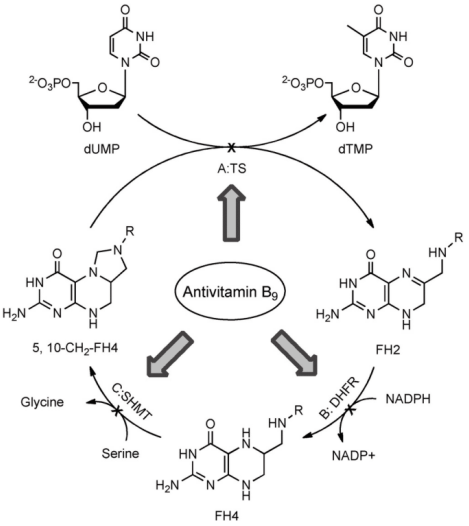

Scheme 5. Requirement for FH4 in the synthesis of 2′-deoxythymidyl-5′-monophosphate (dTMP) from 2′-deoxyuridine-5′-monophosphate (dUMP).

This behaviour explains the attraction of targeting one of these essential metabolic steps for rational design of anticancer drugs. By this approach, the inhibition of thymidylate synthase (TS, approach A) and dihydrofolate reductase (DHFR, approach B) have been successfully explored for the development of commercially available drugs. 5-Fluorouracil represents a prominent example of suicide inhibition targeting TS;[88,92,93] however, this review focuses exclusively on another important class of chemotherapeutics, the inhibitors of DHFR.

In 1948, the therapeutic effect of aminopterin (**3**, Scheme 3D), a compound that induces remissions in pediatric acute leukaemia, was discovered.[19] Shortly afterwards, the structurally related analogue MTX (**4**, Scheme 3D) was introduced because of its superior safety profile.[94–96] Aminopterin and MTX differ only slightly from vitamin B_9, as depicted in Scheme 3D. The two sole structural modifications of MTX are the substitution of an oxo group by an amino group at position 4 of the pteridine ring, together with the replacement of a hydrogen atom by a methyl group at the N10 nitrogen donor moiety. However, it is remarkable that these rather slight modifications induce a 1000-fold higher affinity to the enzyme DHFR.[24] Crystal structure analysis suggests stronger intermolecular interactions between the antagonist and the protein, probably induced by more efficient hydrogen bonding with the protein (Figure 2).[25]

As a consequence of this enhanced affinity, S-phase-dependent cytotoxic effects are observed, including depressed nucleic acid and amino acid syntheses. Unfortunately, these antivita-

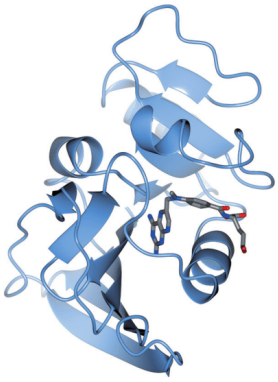

Figure 2. Crystal structure of methotrexate (MTX) bound to the MTX-binding domain of dihydrofolate reductase (DHFT, blue) from *Lactobacillus lactis*.[97]

mins target not only cancer cells, but also other rapidly dividing cells such as bone marrow cells, gastrointestinal mucosa and hair, thus producing severe side effects. Another major drawback of such drugs is the increasing resistance, due to, among other reasons, mutation of the participating transporting proteins. It thus took more than 40 years of intensive research efforts to introduce pemetrexed, an antifolate drug that targets several enzymes, thus allowing the resistance problems to be reduced.[34]

Drawbacks can also be overcome through a conceptually distinct approach: the use of folate bioconjugates for tumour-targeted therapy. This strategy was developed to deliver cytotoxic agents selectively into FR-expressing tumours, instead of directly targeting folate-dependent enzymes such as DHFR.[89,98–102] The development of new non-resistant antivitamin B_9 derivatives is therefore still a key challenge, with the objectives of overcoming current limitations and improving the available therapy.[21,34,35,98,103]

Antivitamin B_{12}

In the previous section the importance of folic acid for DNA synthesis was highlighted, and it was shown that the participating enzymes represent a highly attractive medicinal target for antiproliferative agents. In particular, FH4 is required for catalytic dTMP synthesis, as shown in Scheme 5. Although the natural product is efficiently recycled during turnover, it initially has to be delivered by another cofactor-dependent enzymatic reaction, catalysed by the methylcobalamin-dependent (MeCbl-dependent) methionine synthase (MetH, Scheme 6).[104] For this reason, cell replication is not only dependent on folic acid, but is also directly linked to the metabolism of B_{12}.[88] This dependency explains nicely why rapidly proliferating cells such as cancer cells are much stronger consumers of B_{12} than healthy cells.[105] Hence, B_{12} antivitamins offer enormous medicinal potential for development of antiproliferative agents.

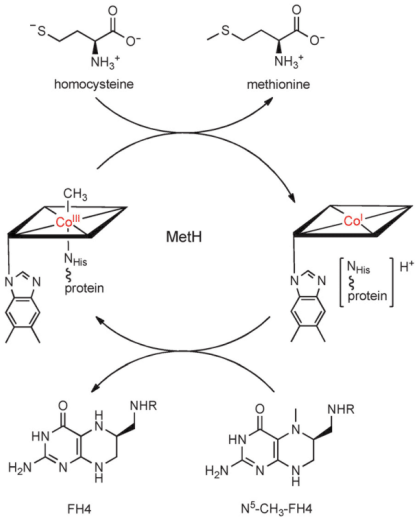

Scheme 6. MetH-catalysed synthesis of methionine from homocysteine and N^5-CH_3-FH4.

However, despite enormous efforts in developing such antivitamins in the 1960s and 1970s, which led to some promising results,[33] not a single antivitamin B_{12} derivative has reached clinical trials yet. As a consequence, this concept vanished almost completely from the literature for three decades. Only recently have some interesting new developments finally revived the scene.[6,105–110] Before discussing B_{12} antivitamins in detail, we will first provide a general overview of the structure, the uptake, the metabolic transformations and the enzymatic reactions of cobalamins (Cbls) in biological systems.[111,112] A Cbl is an octahedral coordination complex that consists of a central cobalt ion, an equatorial tetradentate corrin macrocycle and two axially coordinated ligands. One of these axial ligands is a dimethylbenzimidazole (Dmbz) base, which is intramolecularly appended to the *f*-side chain of the corrin ring through a loop containing an α-ribazole-phosphodiester moiety (Scheme 7). Vitamin B_{12} (CNCbl, abbreviated as "B_{12}") is required by humans in small quantities (≈2–5 μg day^{-1}); however, it is produced only by certain microorganisms.[105] Hence, food is the sole source of B_{12} for mammalians. The uptake of B_{12} from the diet and its subsequent delivery into the cells has been recently reviewed in detail,[113–115] so only some important aspects are briefly presented here.

The first important step is the delivery of the vitamin into the cells, a highly sophisticated process due to the size and the complex structure of the natural product. Therefore, it requires three different binding proteins: intrinsic factor (IF), haptocorrin (HC) and transcobalamin II (TCII).[113,114,116] These proteins combine high affinity with excellent selectivity and fast binding kinetics. Indeed, all transporters bind B_{12} rapidly, with

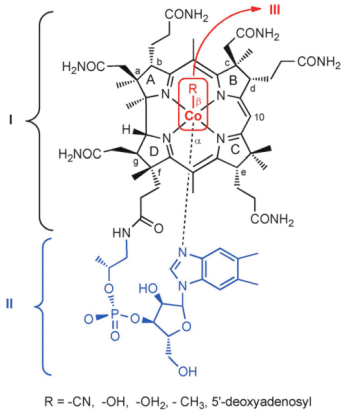

Scheme 7. Structures of Cbls with distinct β-bound ligands R (R = CN for B_{12}, R = OH for hydroxoCbl, R = OH_2 for aquaCbl, R = CH_3 for MeCbl, and R = 5′-deoxyadenosyl for AdoCbl). The classification of molecular subunits into three groups (I–III) is indicated.

k_{on} values between 10^7 and $10^8\ M^{-1}\ s^{-1}$, and exhibit femtomolar dissociation constants (K_d).[116] This extremely efficient mode of binding is achieved by encapsulating the vitamin between the interface of two protein subunits, as revealed by crystal structure analysis of Cbl-TCII, Cbl-HC and Cbl-IF complexes.[116–119] These analysis also revealed that the vitamin is almost completely enclosed by the protein, thus making only two positions of the molecule accessible to the solvent: the β-axially coordinated ligand and the 5′-OH moiety of the ribose unit. Accordingly, it had been demonstrated in earlier cellular uptake studies that B_{12} bioconjugates with structural modifications at those positions were better tolerated.[117, 120, 121] However, except for this specific structural permissiveness, the combination of the three binding proteins ensures that only intact Cbls in their base-on form are transported into the cells.[122]

Within the cells, B_{12} is then metabolised into the catalytically active organometallic cofactors MeCbl and AdoCbl. Each of these two structural modifications requires the prior displacement of the β-bound ligand, a reaction catalysed by the enzyme CblC. When starting with CNCbl, the enzyme catalyses the homolytic cleavage of the cobalt-carbon bond through a reductive mechanism. This process yields to a cyanide group (CN^-) and a cob(II)alamin.[115] Subsequent alkylation of the obtained reduced cobalt species with adenosyltriphosphate (ATP) yields AdoCbl. However, the formation of the cofactor MeCbl requires further reduction of the cobalt to cob(I)alamin, followed by a methyl transfer from S-adenosylmethionine (SAM).[123] The organometallic cofactors AdoCbl and MeCbl can be converted back into cob(II)alamin by the same enzyme CblC, which this time catalyses a nucleophilic displacement.[122] MeCbl and AdoCbl are required as cofactors for the enzymes MetH and methylmalonylCoA mutase (MMCM), respectively.[111] MetH catalyses the methyl-transfer reaction from 5-methyltetrahydrofolate (N^5-CH_3-FH4) to homocysteine, which leads to the formation of tetrahydrofolate (FH4) and methionine. This process requires MeCbl as the catalytically active species, which alkylates homocysteine as shown in Scheme 6.

The amino acid nucleophilically attacks the axial methyl ligand of the cofactor, thus forming methionine and a square-planar Co^I species. In a subsequent oxidative addition, this supernucleophile reacts with N^5-CH_3-FH4 to give MetCbl and FH4.

Interfering with the MetH process therefore leads to a lack of FH4 and impedes DNA synthesis and cell replication, as proposed in the "methylfolate trap hypothesis".[33, 124, 125] This metabolic situation can be principally achieved by protein-targeting antivitamins (Table 2, class A), and can occur in three different ways (1–3): 1) by blocking of the delivery of the vitamin into the cells,[12, 13, 125] 2) by impedance of the transformation of the B_{12} precursor into the organometallic cofactor,[107, 109] or 3) by inhibition of enzymatic functions. It was noted that MetH shows little specificity for structurally modified B_{12} derivatives, thus suggesting that the most attractive and reasonable targets are the proteins involved in the uptake, delivery and metabolism of B_{12}.[126] The major strategy so far pursued for designing B_{12}-based inhibitors is to develop non-functional analogues that are still recognised by their biological targets and show enhanced protein affinity relative to the natural cofactor substrates. However, this situation has not been achieved so far for antivitamins B_{12}. This is somewhat surprising, because B_{12} derivatives with structural modifications at almost any possible position have been synthesised and tested in enzymatic in vitro assays,[33, 106] cell cultures[13] and bacteria,[33, 106, 127, 128] as well as in animal studies.[12, 109] In this context, bacterial growth studies using *Lactobacillus delbrueckii* (formerly known as *L. leichmannii*), *Ochromonas malhamensis* and *E. coli* have been most frequently applied. In these studies, the effectiveness of inhibition is reflected by the inhibition index, "I.I.". This value is defined as the required ratio of inhibitor to vitamin needed to reduce bacterial growth by 50%. A modification of the B_{12} framework can affect the bioactivity of the modified corrinoid in different ways (1–3). The derivative can variously 1) be active, 2) be inactive, or 3) act, as desired, as an antivitamin. It is important to emphasise that a direct comparison of antivitamin activities is only possible for the same biological system; the observed antagonistic effects are not universal. An extrapolation of antivitamin toxicity from one test system to another—that is, from *O. malhamensis* to human tumour sarcoma—is therefore unfortunately meaningless. Pioneering research efforts in this field until 1975 have already been comprehensively reviewed.[33] As this literature is only available in German, we revisit some of the important information here. In this review, we have classified B_{12} antivitamins into three main categories (groups I–III), depending on the location of structural modification: group I contains ring-modified derivatives, group II encompasses the "loop"-modified derivatives, and group III incorporates the metal- and/or upper-axial-ligand-modified derivatives (Scheme 7).

Antivitamins B_{12} of the first category (group I) encompass ring-modified B_{12} derivatives; some are presented in Scheme 8

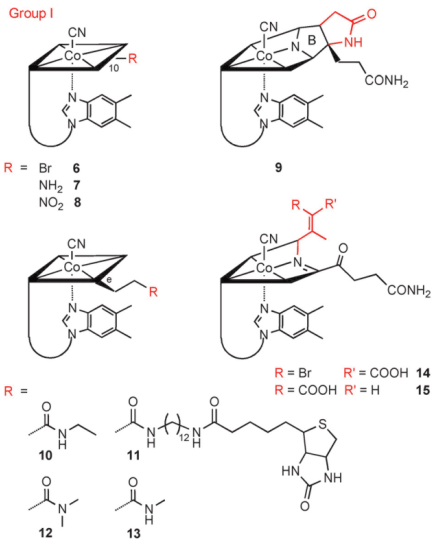

Scheme 8. Structures of the ring-modified antivitamin B_{12} candidates (group I). Modifications of the original B_{12} scaffold are marked in red.

in their cyano forms.[33] A plethora of these straightforwardly accessible compounds with different types of β-axial coordinated ligands have been evaluated for antivitamin activity. For example, the C10-modified analogues CH_3-**6** (i.e., CN-**6** with the CN group replaced by a methyl group, I.I = 9), CN-**7** (I.I = 5) and CH_3-**8** (I.I = 4) were the most powerful antimicrobial antagonists against *L. delbrueckii* (Table 4, entry 1), whereas CN-**10** (I.I = 27), with a modified *e*-side chain, showed the strongest inhibition of *E. coli* 113-3 (Table 4, entry 3).[33] Interestingly, the role of the β-ligand is of importance with regard to the inhibition. For example, derivatives **6** containing either a cyano (CN-**6**) or a methyl (CH_3-**6**) ligand exhibit distinct antivitamin activities ($I.I._{CH_3\text{-}6} = 9$ and $I.I._{CN\text{-}6} = 25$).[33] These data suggest distinct metabolic behaviour of the analogues, but a straightforward analysis based on the available experimental data is not possible. Some decades later, several important in vivo and in vitro studies revealed promising antivitamin activity for the *e*-side chain (**10**–**13**) as well for the *c*-lactam (**9**) modified B_{12} derivatives. In particular, a study with several Cbl analogues of group I revealed that the derivatives with modifications of the *e*-side chain such as the CNCbl [*e*-biotin] conjugate (CN-**11**) are the most potent inhibitors of the growth of BW5147 mouse lymphoma cells, with IC_{50} values between 5 and 15 nM in the presence of 5 nM Cbl and apo-TCII.[125]

In another important in vivo study, the biological effects of 16 different OHCbl analogues were tested on the metabolism of rats. The most pronounced antivitamin activity was observed for the two *e*-side-chain-modified derivatives OHCbl [*e*-dimethylamide] (OH-**12**, Table 4, entry 5), OHCbl [*e*-methylamide] (OH-**13**, Table 4, entry 6) and for the B-ring-modified OHCbl [*c*-lactam] (OH-**9**, Table 4, entry 2). The last two antivitamins decreased the activities of liver L-methylmalonyl coenzyme A mutase and methionine synthase to 66 and 43% of controls, respectively, as indicated by the enhanced serum methylmalonic acid concentration (3200%) and total homocysteine concentration (340%).[12] These studies are in good agreement with in vitro growth tests of leukaemia cells, which show that CNCbl[c-lactam] (CN-**9**) causes methionine deficiency and is cytotoxic to HL60 cells.[13] Most probably, the inhibition effect originates from blocking of the natural intracellular uptake and/or subsequent metabolic conversion of Cbls. In contrast, competitive binding of cofactor **9** to MetH seems to be unlikely, because earlier in vitro studies demonstrated catalytic activity of this analogue in MetH-catalysed reactions.[126]

During the last years, new synthetic strategies have reignited interest in B_{12} antivitamins of group I. Amongst others, our group recently synthesised a new halogenated *c*-lactone B_{12} (structure not shown) that combined two features of positively tested B_{12} antagonists: namely, halogenation at C10 and B-ring lactonisation.[129] This product can be quantitatively converted into **14**, a green 7,8-*seco*-corrinoid, upon Grob fragmentation.[129] Interestingly, Kräutler and co-workers had previously obtained **15**, a structurally similar blue corrinoid with a low affinity for vitamin B_{12} transport proteins ($k_{on} = 10^6\ M^{-1}s^{-1}$).[130,131] Although TCII-mediated transport into human cells can therefore be ruled out, recent results for different B_{12} derivatives that do not bind to TCII suggest the possibility of an alternative uptake mechanism into tumours.[132]

"Loop"-modified Cbls (group II) are rarer than B_{12} antivitamins of group I,[33,106,127,133,134] most probably because of their elaborate synthesis. Aiming at antivitamins of this category, Friedrich and co-workers developed a series of derivatives each containing a structurally modified alkanolamine subunit in the *f*-side chain. An example of these derivatives with rather slight structural modifications is given by **16**, a derivative with a non-natural 2-amino-2-methylpropan-1-ol subunit. This trivial modification induces a remarkable inhibitory effect against *E. coli* 113-3 (CN-**16**, I.I = 3, Table 4, entry 7) and *O. malhamensis* (CN-**16**, I.I = 30). Here, a potential role of the β-axially bound ligand in modulating the inhibitory effects is again suggested. Indeed, the analogue CN-**16** with a β-bound cyanide is slightly more effective in suppressing growth of *E. coli* than the cofactor forms of this derivative (CH_3-**16**, I.I = 5 and Ado-**16**, I.I = 4).[135] Recent efforts in our group yielded new developments in this area. This time, rather radical changes were introduced by substituting the whole *f*-side chain with biomimetic linkers. In particular, the entire α-ribazole-phosphodiester moiety of the loop was substituted in **17** (peptide B_{12}, Figure 3, Table 4, entry 8) by an amino-acid-containing backbone, a modification reminiscent of peptide nucleic acids.[106,136] By this strategy, it was proposed to alter the intrinsic coordination and redox chemistry at the cobalt centre selectively and hence to diminish the metal-centred reactivity of the cofactor. A series of four different peptides B_{12} was thus studied, and it was shown that the redox potentials at the cobalt centre of the modified natural product can indeed be selectively tuned.[137]

Table 4. Examples of antivitamins B_{12}.

	Compound	Modification	Biological test	Inhibition index (I.I.)	Other biological studies	Ref.
1	**6**	I: C10	*L. delbrueckii*	CN-**6** = 25	–	[33]
				CH_3-**6** = 9		
	7			CH_3-**7** = 4	–	
	8			CH_3-**8** = 5	–	
2	**9**	I: B-ring	in vivo studies (infusion in rats)	–	OH-**9**: L-methylmalonyl CoA mutase: 65 %[a] (42 days)	[12]
				–	OH-**9**: methionine synthase: 43 %[a] (14 days) 53 %[a] (42 days)	
				–	OH-**9**: methylmalonic acid: 3200 %[b] (42 days) OH-**9**: homocysteine: 341 %[b] (42 days)	
3	**10**	I: e-side chain	*E. coli*	CN-**10** = 27	–	[33]
4	**11**	I: e-side chain	in vitro mouse lymphoma cells	–	CN-**11**: $IC_{50} \approx 5$–15 nM[125]	
5	**12**	I: e-side chain	in vivo studies (infusion in rats)	–	OH-**12**: L-methylmalonyl CoA mutase: 66 %[a] (14 days)	[12]
				–	OH-**12**: methionine synthase: 52 %[a] (14 days)	
6	**13**	I: e-side chain	in vivo studies (infusion in rats)	–	OH-**13**: L-methylmalonyl CoA mutase: 66 %[a] (14 days)	[12]
				–	OH-**13**: methionine synthase: 57 %[a] (14 days)	
7	**16**	II: propanolamine subunit	*E. coli*	CN-**16** = 3	–	[135]
				Ado-**16** = 4		
				CH_3-**16** = 5		
			O. malhamensis	CN-**16** = 30	–	
8	**17**	II: ribose phosphodiester moiety ("loop")	*Clostridium cochlearium* (glutamate mutase)	–	Ado-**17**: $k_{eff} = 0.26 \times 10^6\ s^{-1}\ M^{-1}$ control with AdoCbl: $k_{eff} = 2.38 \times 10^6\ s^{-1}\ M^{-1}$	[106]
			L. delbrueckii (ribonucleotide reductase)	–	CN-**17**: $IC_{50} = 2\ \mu M$ (10 h)	
9	descobaltocorrin II (D. II, unknown structure)	III: metal-free corrinoid	*L. leichmanii*	n.i.	–	[139]
			E. coli	D. II = 2	–	
			E. gracilis	D. II = 1.5	–	
			A. duodecadis	D. II = 1.8	–	
10	**18**	III: metal-modified corrinoid	*L. leichmanii*	CH_3-**18** = 8	–	[143]
11	**19**	III: β-axial ligand	in vivo studies (infusion in rats)	–	**19**: methylmalonic acid: 336 %[b] (27 days)	[109]
				–	**19**: homocysteine: 147 %[b] (27 days)	
12	**20**	III: β-axial ligand	in vivo studies (infusion in tumour-bearing mice)	–	**20**: 14 % inhibition of tumour growth	[128]

[a] Activity [%] relative to mean control activity. [b] Concentration [%] relative to mean control concentration. n.i.: no inhibition observed.

Subsequently, the biological activity of the prototype CN-**17** was tested, and showed an IC_{50} value of 2 μM in bacterial growth studies with *L. delbrueckii* (Figure 3).[106] This is an important result, from which further advances are expected in the near future.[6]

Group III contains Cbl derivatives with modifications at the Co^{III} centre, either by absence or replacement (metbalamins) of the metal ion, and/or of the "upper" axial ligand. Non-cobalt-containing corrins are only available by biotechnological production and have not so far been synthesised by chemical means. One of the rare examples is represented by Toohey's yellow metal-free corrinoids, which were first obtained from the photosynthetic bacteria *Chromatium vinosum*.[33,138] The antivitamin activities of these "mysterious" pigments were positively tested in *E. coli*, *E. gracilis* and *A. duodecadis*, with I.I. values as low as 1.5 (Table 4, entry 9).[139] Although the identities of these compounds have not yet been exhaustively confirmed by X-ray crystallography, there are excellent indications of an intact intrinsic Cbl structure. Indeed, the insertion of cobalt ions into these species led to the formation of cobalt-containing compounds with several characteristic features of Cbls, including UV/Vis spectra and retention times in paper electrophoresis and chromatography, as well as the growth-promoting character for *L. delbrueckii*. Subsequently, several other metbalamins with metals such as rhodium, iron and zinc were also reported.[140–142] The rhodium-containing pigment was assigned as methylrhodibalamin (CH_3-**18**, Scheme 9, Table 4, entry 10) and showed inhibition of bacterial growth in *L. delbrueckii* (I.I = 8).[143] Despite much promise, this interesting class of compounds was not investigated any further, presumably because of its difficult biosynthetic access and dwindling interest in B_{12} chemistry. In view of advancements in microbiology and biotechnology in recent decades, this class of compounds should nowadays be more accessible, offering new research possibilities in this direction.[144,145]

Apart from metal-free corrinoids and metbalamins, group III also contains antivitamins with unnatural "upper"-axial ligands. The employment of artificial β-coordinating ligands on unmodified B_{12} has indeed revealed fascinating new perspectives.[107,108] The first example worth mentioning is nitrosylcoba-

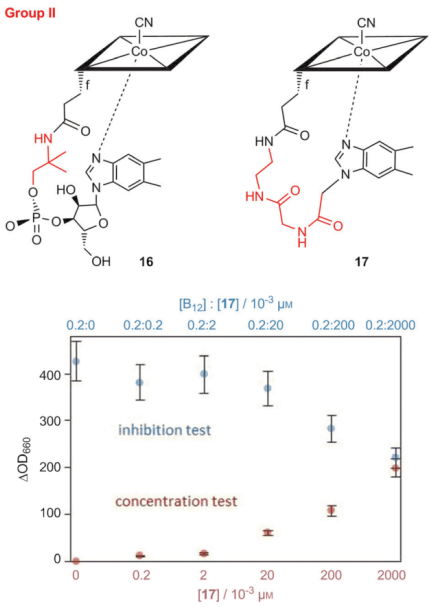

Figure 3. Top: Schematic depiction of two examples of *f*-side-chain-modified B_{12} derivatives of group II (modifications of the original B_{12} scaffold are marked in red). Bottom: Inhibition of bacteria growth of *L. delbrueckii* in the presence of vitamin B_{12} and increasing amounts of **17** (blue). The growth-supporting character of **17** is indicated (red).[106]

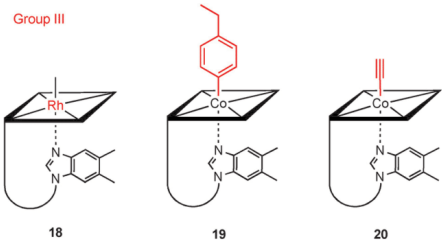

Scheme 9. Structures of some metal-modified and upper-axial-ligand-modified cobalamin antivitamins (group III). Modifications of the natural B_{12} scaffold are marked in red.

lamin (NOCbl).[146,147] This B_{12} derivative represents a catalytically inactive cofactor for MetH and MMCM and is formed, amongst other products, from the reaction of nitric oxide with cob(II)alamins. This B_{12} intermediate is encountered during catalysis (MMCM) or cofactor reactivation (MetH), and its exposure to NO gas leads to the enzymes' inactivation.[148–151]

Kräutler and co-workers also studied the effects of artificial β-ligands for the design of antivitamins. They thus anticipated, in 2013, that a strongly σ-donating 4-ethylphenyl ligand would block the β-position from converting the provitamin to the organometallic cofactors MeCbl and AdoCbl, which would induce vitamin deficiency. They synthesised 4-ethylphenylCbl (**19**) by employing a Co^{II} intermediate in an interesting radical combination reaction. As anticipated for β-modified Cbls, this derivative exhibits high affinity for the transporting proteins IF and TCII, similarly to CNCbl.[108] However, in contrast to its natural counterpart, the antivitamin is no longer converted into the natural cofactors in the CblC-catalysed reaction and should therefore exhibit no catalytic activity.[108] It was indeed shown that this antivitamin induces, as proposed, Cbl deficiency in mice, as indicated by increased methylmalonic acid (MMA) and homocysteine (Hcy) levels in plasma.[109] Surprisingly, despite its TCII-binding properties, treatment with the antivitamin leads to low levels of Cbl in the tissue, but high levels in plasma. The authors proposed "an impaired uptake or an increased export of EtPhCbl" (**19**, Scheme 9, Table 4, entry 11) as a possible explanation.[109] This observation is important because it underscores that TCII affinity for a B_{12} derivative is not necessarily associated with efficient cellular uptake, thus showing once again that the biological behaviour in a complex cellular system cannot be predicted from a single in vitro experiment. In a follow-up study, the structurally similar 2-phenylethynylCbl was introduced as a light-stable potential antivitamin.[107,110] In earlier studies, a structurally related alkynyl-modified B_{12} antivitamin—ethynylCbl (**20**, Scheme 9, Table 4, entry 12)—was also tested. When applied at a daily dose of 1 mg per kg of bodyweight, it exhibited around 14% inhibition in mice with tumour sarcoma.[128] In view of the numerous possibilities for structural variations, further optimisations are expected for this type of antivitamins.

However, despite the on-going progress over the past years, further development is urgently required to push antivitamin B_{12} research to the next level, from academic research into clinical trials. The difficulties encountered so far in designing efficient B_{12}-based inhibitors are probably related to the large and sophisticated complex structure of the natural product, which already translates into highly efficient protein binding. Indeed, structural modifications of Cbls have usually had a counterproductive effect in the past. This unfavourable situation reflects that more detailed structural and mechanistic evaluations are required. It may be expected that such structure–activity relationships will be assisted in the future by computer-based antivitamin design and that new hits will also be obtained from screening structurally more diverse libraries of analogues. Unfortunately, the synthesis of modified B_{12} analogues is a tedious and time-consuming task. For this reason, the development of new, straightforward and short synthetic protocols for B_{12} derivatives with previously unknown types of modifications is of primary importance.[129,152]

In summary, in comparison with the antifolates, the development of antivitamins B_{12} seems still to be in its infancy. However, in view of the renaissance of interest and the recent developments in this area, significant steps forward may be expected for the future.

Summary and Outlook

Pioneering studies and recent advances in the development and application of antivitamins for medicinal applications are reviewed here in detail. After an overview on definitions and classifications of antivitamin research, scientific milestones in the development of pioneering antibiotic, anticancer and anticoagulation drugs are summarised, focusing on antivitamins B_9 and K. With the assistance of selected examples, detailed mechanistic insights into antivitamins' modes of action are proposed. However, despite the long-lasting success, the antivitamin approach has not led to the development of many more examples of approved drugs, with distinct protein targets and modes of action. We have tried to emphasise the difficulties in designing such new therapeutically active compounds through the enormous efforts undertaken in designing antivitamins B_{12}. However, motivated by this scientific challenge and with the potential medicinal impact in mind, a growing number of groups are developing new B_{12} antivitamins for biological purposes and medicinal applications. Nevertheless, until now no analogue compares in efficiency to the antifolates, a successful class of commercially available drugs. Given the limited success of antivitamins B_{12} in the past, the next major breakthrough in this area is difficult to predict but is anticipated in this review, on the basis of a couple of encouraging recent results. Nonetheless, the development of new classes of drugs based on antivitamin B_{12}, with different modes of action, seems to be still far from any real-world application. Therefore, important challenges lie ahead of us. Indeed, because of the urgent need for new drugs with alternative modes of action, the development of antivitamins appears essential. In fact, antivitamins still present enormous potential that has not yet been explored sufficiently.

Acknowledgements

The work of the authors was supported by the Swiss National Science Foundation (grant no. 200021-117822) and a fellowship of the Forschungskredit of the University of Zürich UZH to L.P. F.Z. acknowledges his former students working in this area of research. We also thank our cooperation partners in Marburg (Wolfgang Buckel), Zürich (Helmut Brandl) and Villigen (Eliane Fischer), as well as Bernhard Spingler for creating Figure 2. Support by Roger Alberto and the Institute of Chemistry of the University of Zürich is gratefully acknowledged

Keywords: antivitamins · drugs · enzyme inhibitors · medicinal chemistry · vitamins

[1] E. Mellanby, *J. Physiol.* **1926**, *61*, XXIV.
[2] J. C. Somogyi, K. Trautner in *Vitamine, Vol. 3* (Eds.: R. Ammon, W. Dirscherl), Thieme, Stuttgart, **1974**, pp. 10 – 138.
[3] H. M. Bruce, R. K. Callow, *Biochem. J.* **1934**, *28*, 517 – 528.
[4] D. C. Harrison, E. Mellanby, *Biochem. J.* **1939**, *33*, 1660 – 1680.
[5] C. Eijkman, Nobel Lecture: Antineuritic Vitamin and Beriberi. Nobelprize.org. Nobel Media AB 2014. Web. 2027 Jan 2015. http://www.nobelprize.org/nobel_prizes/medicine/laureates/1929/eijkman-lecture.html.
[6] F. Zelder, K. Zhou, M. Sonnay, *Dalton Trans.* **2013**, *42*, 854 – 862.
[7] G. R. Minot, W. P. Murphy, *JAMA J. Am. Med. Assoc.* **1926**, *87*, 470 – 476.
[8] K. Venkatesan, D. Dale, D. C. Hodgkin, C. E. Nockolds, F. H. Moore, B. H. O'Connor, *Proc. R. Soc. London Ser. A* **1971**, *323*, 455 – 487.
[9] G. Domagk, *Deutsch. Med. Wochenschr.* **1935**, *61*, 829 – 832.
[10] G. Domagk, *Angew. Chem.* **1935**, *48*, 657 – 667.
[11] J. Trefouel, J. Trefouel, F. Nitti, D. Bovet, *C. R. Soc. Biol.* **1935**, *120*, 756 – 758.
[12] S. P. Stabler, E. P. Brass, P. D. Marcell, R. H. Allen, *J. Clin. Invest.* **1991**, *87*, 1422 – 1430.
[13] J. H. Matthews, *Blood* **1997**, *89*, 4600 – 4607.
[14] M. Ikawa, M. A. Stahmann, K. P. Link, *J. Am. Chem. Soc.* **1944**, *66*, 902 – 906.
[15] R. S. Overman, M. A. Stahmann, C. F. Huebner, W. R. Sullivan, L. Spero, D. G. Doherty, M. Ikawa, L. Graf, S. Roseman, K. P. Link, *J. Biol. Chem.* **1944**, *153*, 5 – 24.
[16] K. P. Link, *Circulation* **1959**, *19*, 97 – 107.
[17] G. Tucker, M. Lennard, *Pharmacol. Ther.* **1990**, *45*, 309 – 329.
[18] S. Shapiro, F. E. Ciferri, *JAMA J. Am. Med. Assoc.* **1957**, *165*, 1377 – 1380.
[19] S. Farber, L. K. Diamond, R. D. Mercer, R. F. Sylvester, J. A. Wolff, *N. Engl. J. Med.* **1948**, *238*, 787 – 793.
[20] A. L. Franklin, E. L. R. Stokstad, M. Belt, T. H. Jukes, *J. Biol. Chem.* **1947**, *169*, 427 – 435.
[21] M. P. Pereira, S. O. Kelley, *J. Am. Chem. Soc.* **2011**, *133*, 3260 – 3263.
[22] D. R. Seeger, J. M. Smith, M. E. Hultquist, *J. Am. Chem. Soc.* **1947**, *69*, 2567 – 2567.
[23] N. G. -Dayanandan, J. L. Paulsen, K. Viswanathan, S. Keshipeddy, M. N. Lombardo, W. Zhou, K. M. Lamb, A. E. Sochia, J. B. Alverson, N. D. Priestley, et al., *J. Med. Chem.* **2014**, *57*, 2643 – 2656.
[24] P. T. R. Rajagopalan, Z. Q. Zhang, L. McCourt, M. Dwyer, S. J. Benkovic, G. G. Hammes, *Proc. Natl. Acad. Sci. USA* **2002**, *99*, 13481 – 13486.
[25] D. A. Matthews, R. A. Alden, J. T. Bolin, S. T. Freer, R. Hamlin, N. Xuong, J. Kraut, M. Poe, M. Williams, K. Hoogsteen, *Science* **1977**, *197*, 452 – 455.
[26] C. A. Evans, W. E. Carlson, R. G. Green, *Am. J. Pathol.* **1942**, *18*, 79 – 91.
[27] H. Kündig, J. C. Somogyi, *Int. Z. Vitaminforsch.* **1964**, *34*, 1135 – 1141.
[28] W. G. Bateman, *J. Biol. Chem.* **1916**, *26*, 263 – 291.
[29] M. A. Boas, *Biochem. J.* **1927**, *21*, 712 – 724.
[30] R. E. Eakin, E. E. Snell, R. J. Williams, *J. Biol. Chem.* **1940**, *136*, 801 – 802.
[31] R. Hertz, *Physiol. Rev.* **1946**, *26*, 479 – 494.
[32] J. C. Somogyi in *Ergebnisse der Medizinischen Grundlagenforschung* (Ed.: K. F. Bauer), Thieme, Stuttgart, **1956**, pp. 139 – 188.
[33] W. Friedrich in *Vitamin B12 und Verwandte Corrinoide* (Ed.: W. Friedrich), Thieme, Stuttgart, **1975**, pp. 81 – 87.
[34] M. Visentin, R. Zhao, I. D. Goldman, *Hematol. Oncol. Clin. North Am.* **2012**, *26*, 629 – 648.
[35] E. M. Berman, L. M. Werbel, *J. Med. Chem.* **1991**, *34*, 479 – 485.
[36] A. Ko in *Cancer Management in Man: Chemotherapy, Biological Therapy, Hyperthermia and Supporting Measures, Vol. 13* (Ed.: B. R. Minev), Springer Netherlands, **2011**, pp. 125 – 143.
[37] K. Heidinger, *Pharm. Unserer Zeit* **2004**, *33*, 236 – 243.
[38] E. F. Rogers in *Methods Enzymol., Vol. 18, Part A* (Eds.: B. M. Donald, D. W. Lemuel), Academic Press, **1970**, pp. 245 – 258.
[39] C. M. Dundas, D. Demonte, S. Park, *Appl. Microbiol. Biotechnol.* **2013**, *97*, 9343 – 9353.
[40] T. K. Hyster, L. Knorr, T. R. Ward, T. Rovis, *Science* **2012**, *338*, 500 – 503.
[41] J. M. Ravel, W. Shive, *J. Biol. Chem.* **1946**, *166*, 407 – 415.
[42] W. Shive, *Ann. N.Y. Acad. Sci.* **1950**, *52*, 1212 – 1234.
[43] J. F. Mueller, R. W. Vilter, *J. Clin. Invest.* **1950**, *29*, 193.
[44] W. Hawkins, *Science* **1955**, *121*, 880 – 880.
[45] R. Bentley, *J. Ind. Microbiol. Biotechnol.* **2009**, *36*, 775 – 786.
[46] M. Wainwright, J. E. Kristiansen, *Dyes Pigm.* **2011**, *88*, 231 – 234.
[47] J. Drews, *Science* **2000**, *287*, 1960 – 1964.
[48] H. Dam, *Nature* **1935**, *135*, 652 – 653.
[49] C. Vermeer, K.-S. Jie, M. Knapen, *Annu. Rev. Nutr.* **1995**, *15*, 1 – 21.
[50] B. Furie, B. C. Furie, *Cell* **1988**, *53*, 505 – 518.
[51] E. C. M. Cranenburg, L. J. Schurgers, C. Vermeer, *Thromb. Haemostasis* **2007**, *98*, 120 – 125.
[52] G. L. Nelsestuen, T. H. Zytkovicz, J. B. Howard, *J. Biol. Chem.* **1974**, *249*, 6347 – 6350.
[53] J. Stenflo, P. Fernlund, W. Egan, P. Roepstorff, *Proc. Natl. Acad. Sci. USA* **1974**, *71*, 2730 – 2733.

[54] J. Stenflo, J. W. Suttie, *Annu. Rev. Biochem.* **1977**, *46*, 157 – 172.
[55] B. Furie, B. A. Bouchard, B. C. Furie, *Blood* **1999**, *93*, 1798 – 1808.
[56] P. V. Hauschka, J. B. Lian, P. M. Gallop, *Proc. Natl. Acad. Sci. USA* **1975**, *72*, 3925 – 3929.
[57] G. Nelsestuen, *J. Biol. Chem.* **1976**, *251*, 5648 – 5656.
[58] R. F. Zwaal, P. Comfurius, E. M. Bevers, *Biochim. Biophys. Acta, Rev. Biomembranes* **1998**, *1376*, 433 – 453.
[59] M. Huang, A. C. Rigby, X. Morelli, M. A. Grant, G. Huang, B. Furie, B. Seaton, B. C. Furie, *Nat. Struct. Mol. Biol.* **2003**, *10*, 751 – 756.
[60] M. A. Rishavy, K. W. Hallgren, A. V. Yakubenko, R. L. Shtofman, K. W. Runge, K. L. Berkner, *Biochemistry* **2006**, *45*, 13239 – 13248.
[61] M. A. Rishavy, K. W. Hallgren, K. L. Berkner, *J. Biol. Chem.* **2011**, *286*, 44821 – 44832.
[62] D. W. Stafford, *J. Thromb. Haemostasis* **2005**, *3*, 1873 – 1878.
[63] J. W. Suttie, *Annu. Rev. Biochem.* **1995**, *54*, 459 – 477.
[64] S. R. Presnell, D. W. Stafford, *Thromb. Haemostasis* **2002**, *87*, 937 – 946.
[65] R. B. Silverman, *J. Am. Chem. Soc.* **1981**, *103*, 5939 – 5941.
[66] R. Pauli, J. Lian, D. Mosher, J. Suttie, *Am. J. Hum. Genet.* **1987**, *41*, 566.
[67] F. W. Schofield, *Can. Vet. Record* **1922**, *3*, 73 – 78.
[68] P. Griminger, *J. Nutr.* **1987**, *117*, 1325 – 1329.
[69] A. Zimmermann, J. T. Matschiner, *Biochem. Pharmacol.* **1974**, *23*, 1033 – 1040.
[70] D. Whitlon, J. Sadowski, J. Suttie, *Biochemistry* **1978**, *17*, 1371 – 1377.
[71] L. I. V. Helgeland, *Biochem. Educ.* **1980**, *8*, 66 – 69.
[72] W. Li, S. Schulman, R. J. Dutton, D. Boyd, J. Beckwith, T. A. Rapoport, *Nature* **2010**, *463*, 507 – 512.
[73] S. Liu, W. Cheng, R. F. Grider, G. Shen, W. Li, *Nat. Commun.* **2014**, *463*, 507 – 512.
[74] J. Hanley, *J. Clin. Pathol.* **2004**, *57*, 1132 – 1139.
[75] J. Ansell, J. Hirsh, L. Poller, H. Bussey, A. Jacobson, E. Hylek, *Chest* **2004**, *126*, 204S – 233S.
[76] M. D. Ezekowitz, S. L. Bridgers, K. E. James, N. H. Carliner, C. L. Colling, C. C. Gornick, H. Krause-Steinrauf, J. F. Kurtzke, S. M. Nazarian, M. J. Radford, *N. Engl. J. Med.* **1992**, *327*, 1406 – 1412.
[77] M. N. Levine, G. Raskob, S. Landefeld, C. Kearon, *Chest* **2001**, *119*, 108S – 121S.
[78] A. M. Holbrook, J. A. Pereira, R. Labiris, et al., *Arch. Intern. Med.* **2005**, *165*, 1095 – 1106.
[79] A. Hall, M. Wilkins, *Heart* **2005**, *91*, 563 – 564.
[80] J. Ansell, J. Hirsh, E. Hylek, A. Jacobson, M. Crowther, G. Palareti, *Chest* **2008**, *133*, 160S – 198S.
[81] J. Hollowell, A. Ruigómez, S. Johansson, M.-A. Wallander, L. A. García-Rodríguez, *Br. J. Gen. Pract.* **2003**, *53*, 312 – 314.
[82] J. A. Heit, *Chest* **2003**, *124*, 40S – 48S.
[83] G. J. Hankey, J. W. Eikelboom, *Circulation* **2011**, *123*, 1436 – 1450.
[84] R. D. Hull, M. H. Gersh, *Curr. Med. Res. Opin.* **2014**, 1 – 14.
[85] E. Perzborn, S. Roehrig, A. Straub, D. Kubitza, F. Misselwitz, *Nat. Rev. Drug Discovery* **2011**, *10*, 61 – 75.
[86] R. B. Angier, J. H. Boothe, B. L. Hutchings, J. H. Mowat, J. Semb, E. L. R. Stokstad, Y. Subbarow, C. W. Waller, D. B. Cosulich, M. J. Fahrenbach, et al., *Science* **1946**, *103*, 667 – 669.
[87] W. Shive, W. W. Ackermann, M. Gordon, M. E. Getzendaner, R. E. Eakin, *J. Am. Chem. Soc.* **1947**, *69*, 725 – 726.
[88] L. Stryer in *Biochemistry,* 3 ed., W. H. Freeman and Company, New York, **1988**, pp. 614 – 616.
[89] J. Yang, E. Vlashi, P. Low in *Water Soluble Vitamins, Vol. 56* (Ed.: O. Stanger), Springer Netherlands, **2012**, pp. 163 – 179.
[90] E. L. R. Stokstad, T. H. Jukes, *J. Nutr.* **1987**, *117*, 1335 – 1341.
[91] F. Volpe, M. Dyer, J. G. Scaife, G. Darby, D. K. Stammers, C. J. Delves, *Gene* **1992**, *112*, 213 – 218.
[92] C. Heidelberger, N. K. Chaudhuri, P. Danneberg, D. Mooren, L. Griesbach, R. Duschinsky, R. J. Schnitzer, E. Pleven, J. Scheiner, *Nature* **1957**, *179*, 663 – 666.
[93] D. B. Longley, D. P. Harkin, P. G. Johnston, *Nat. Rev. Cancer* **2003**, *3*, 330 – 338.
[94] J. M. Smith, D. B. Cosulich, M. E. Hultquist, D. R. Seeger, *Trans. N. Y. Acad. Sci.* **1948**, *10*, 82 – 83.
[95] T. H. Jukes, *Cancer Res.* **1987**, *47*, 5528 – 5536.
[96] M. C. Li, R. Hertz, D. B. Spencer, *Proc. Soc. Exp. Biol. Med.* **1956**, *93*, 361 – 366.
[97] J. T. Bolin, D. J. Filman, D. A. Matthews, R. C. Hamlin, J. Kraut, *J. Biol. Chem.* **1982**, *257*, 13650 – 13662.
[98] L. K. Golani, C. George, S. Zhao, S. Raghavan, S. Orr, A. Wallace, M. R. Wilson, Z. Hou, L. H. Matherly, A. Gangjee, *J. Med. Chem.* **2014**, *57*, 8152 – 8166.
[99] C. P. Leamon, I. Pastan, P. S. Low, *J. Biol. Chem.* **1993**, *268*, 24847 – 24854.
[100] Y. J. Lu, E. Sega, P. S. Low, *Int. J. Cancer* **2005**, *116*, 710 – 719.
[101] C. Müller, J. Reber, S. Haller, H. Dorrer, P. Bernhardt, K. Zhernosekov, A. Turler, R. Schibli, *Eur. J. Nucl. Med. Mol. Imaging* **2014**, *41*, 476 – 485.
[102] C. Müller, *Molecules* **2013**, *18*, 5005 – 5031.
[103] C. H. Takimoto, *Oncologist* **1996**, *1*, 68 – 81.
[104] R. G. Matthews in *Chemistry and Biochemistry of B12, Vol. 1, 1st ed.* (Ed.: R. Banerjee), Wiley-Interscience, New York, **1999**, pp. 681 – 706.
[105] F. Zelder, R. Alberto in *The Porphyrin Handbook, Vol. 25* (Eds.: K. M. Kadish, K. M. Smith, R. Guilard), Elsevier Science San Diego, **2012**, pp. 83 – 130.
[106] K. Zhou, R. Oetterli, H. Brandl, F. Lyatuu, W. Buckel, F. Zelder, *ChemBioChem* **2012**, *13*, 2052 – 2055.
[107] M. Ruetz, R. Salchner, K. Wurst, S. Fedosov, B. Kräutler, *Angew. Chem. Int. Ed.* **2013**, *52*, 11406 – 11409; *Angew. Chem.* **2013**, *125*, 11617 – 11620.
[108] M. Ruetz, C. Gherasim, K. Gruber, S. Fedosov, R. Banerjee, B. Kräutler, *Angew. Chem. Int. Ed.* **2013**, *52*, 2606 – 2610; *Angew. Chem.* **2013**, *125*, 2668 – 2672.
[109] E. Mutti, M. Ruetz, H. Birn, B. Kräutler, E. Nexo, *Plos One* **2013**, *8*, e75312.
[110] M. Chrominski, A. Lewalska, D. Gryko, *Chem. Commun.* **2013**, *49*, 11406 – 11408.
[111] B. Kräutler, D. Arigoni, B. Golding, *Vitamin B12 and B12-Proteins*, Wiley-VCH, Weinheim, **1998**.
[112] R. Banerjee, *Chemistry and Biochemistry of B12, Vol. 1*, 1st ed., Wiley-Interscience, New York, **1999**.
[113] A. K. Petrus, T. J. Fairchild, R. P. Doyle, *Angew. Chem. Int. Ed.* **2009**, *48*, 1022 – 1028; *Angew. Chem.* **2009**, *121*, 1040 – 1047.
[114] Z. Schneider in *Comprehensive B12* (Eds.: Z. Schneider, A. Stroinski), Walter de Gruyter, Berlin, New York, **1987**, pp. 17 – 42.
[115] R. Banerjee, C. Gherasim, D. Padovani, *Curr. Opin. Chem. Biol.* **2009**, *13*, 484 – 491.
[116] K. Gruber, B. Puffer, B. Kräutler, *Chem. Soc. Rev.* **2011**, *40*, 4346 – 4363.
[117] J. Wuerges, G. Garau, S. Geremia, S. N. Fedosov, T. E. Petersen, L. Randaccio, *Proc. Natl. Acad. Sci. USA* **2006**, *103*, 4386 – 4391.
[118] E. Furger, D. C. Frei, R. Schibli, E. Fischer, A. E. Prota, *J. Biol. Chem.* **2013**, *288*, 25466 – 25476.
[119] F. S. Mathews, M. M. Gordon, Z. Chen, K. R. Rajashankar, S. E. Ealick, D. H. Alpers, N. Sukumar, *Proc. Natl. Acad. Sci. USA* **2007**, *104*, 17311 – 17316.
[120] P. Siega, J. Wuerges, F. Arena, E. Gianolio, S. N. Fedosov, R. Dreos, S. Geremia, S. Aime, L. Randaccio, *Chem. Eur. J.* **2009**, *15*, 7980 – 7989.
[121] K. Zelenka, H. Brandl, B. Spingler, F. Zelder, *Dalton Trans.* **2011**, *40*, 9665 – 9667.
[122] M. Koutmos, C. Gherasim, J. L. Smith, R. Banerjee, *J. Biol. Chem.* **2011**, *286*, 29780 – 29787.
[123] J. T. Jarrett, D. M. Hoover, M. L. Ludwig, R. G. Matthews, *Biochemistry* **1998**, *37*, 12649 – 12658.
[124] E. L. Smith, *Vitamin B12*, 3 ed., Methuen, London, **1965**.
[125] G. R. McLean, P. M. Pathare, D. S. Wilbur, A. C. Morgan, C. S. Woodhouse, J. W. Schrader, H. J. Ziltener, *Cancer Res.* **1997**, *57*, 4015 – 4022.
[126] J. F. Kolhouse, C. Utley, S. P. Stabler, R. H. Allen, *J. Biol. Chem.* **1991**, *266*, 23010 – 23015.
[127] T. Toraya, A. Ishida, *J. Biol. Chem.* **1991**, *266*, 5430 – 5437.
[128] E. L. Smith, L. Mervyn, P. W. Muggleton, A. W. Johnson, N. Shaw, *Ann. N. Y. Acad. Sci.* **1964**, *112*, 565 – 574.
[129] R. M. Oetterli, L. Prieto, B. Spingler, F. Zelder, *Org. Lett.* **2013**, *15*, 4630 – 4633.
[130] M. Ruetz, S. N. Fedosov, B. Kräutler, *Angew. Chem. Int. Ed.* **2012**, *51*, 6780 – 6784; *Angew. Chem.* **2012**, *124*, 6885 – 6890.
[131] S. N. Fedosov, M. Ruetz, K. Gruber, N. U. Fedosova, B. Kräutler, *Biochemistry* **2011**, *50*, 8090 – 8101.

[132] R. Waibel, H. Treichler, N. G. Schaefer, D. R. van Staveren, S. Mundwiler, S. Kunze, M. Küenzi, R. Alberto, J. Nüesch, A. Knuth, H. Moch, R. Schibli, P. A. Schubiger, *Cancer Res.* **2008**, *68*, 2904 – 2911.
[133] S. Murtaza, M. Ruetz, K. Gruber, B. Kräutler, *Chem. Eur. J.* **2010**, *16*, 10984 – 10988.
[134] T. Toraya in *Vitamin B12 and B12-Proteins* (Eds.: B. Kräutler, D. Arigoni, B. Golding), Wiley-VCH, Weinheim, **1998**, pp. 303 – 320.
[135] W. Friedrich, H. C. Heinrich, E. Königk, P. Schulze, *Ann. N. Y. Acad. Sci.* **1964**, *112*, 601 – 614.
[136] U. Diederichsen, H. W. Schmitt, *Angew. Chem. Int. Ed.* **1998**, *37*, 302 – 305; *Angew. Chem.* **1998**, *110*, 312 – 315.
[137] K. Zhou, F. Zelder, *Angew. Chem. Int. Ed.* **2010**, *49*, 5178 – 5180; *Angew. Chem.* **2010**, *122*, 5305 – 5307.
[138] J. I. Toohey in *Federation Proceedings, Vol. 25*, **1965**, pp. 1628 – 1632.
[139] D. Perlman, J. I. Toohey, *Arch. Biochem. Biophys.* **1968**, *124*, 462 – 465.
[140] R. Bieganowski, W. Friedrich, *FEBS Lett.* **1979**, *97*, 325 – 326.
[141] V. B. Koppenhagen, F. Wagner, J. J. Pfiffner, *J. Biol. Chem.* **1973**, *248*, 7999 – 8002.
[142] V. B. Koppenhagen, J. J. Pfiffner, *J. Biol. Chem.* **1970**, *245*, 5865 – 5867.
[143] V. B. Koppenhagen, B. Elsenhans, F. Wagner, J. J. Pfiffner, *J. Biol. Chem.* **1974**, *249*, 6532 – 6540.
[144] E. Deery, S. Schroeder, A. D. Lawrence, S. L. Taylor, A. Seyedarabi, J. Waterman, K. S. Wilson, D. Brown, M. A. Geeves, M. J. Howard, et al., *Nat. Chem. Biol.* **2012**, *8*, 933 – 940.
[145] S. J. Moore, A. D. Lawrence, R. Biedendieck, E. Deery, S. Frank, M. J. Howard, S. E. J. Rigby, M. J. Warren, *Proc. Natl. Acad. Sci. USA* **2013**, *110*, 14906 – 14911.
[146] L. Hannibal, C. A. Smith, D. W. Jacobsen, N. E. Brasch, *Angew. Chem. Int. Ed.* **2007**, *46*, 5140 – 5143; *Angew. Chem.* **2007**, *119*, 5232 – 5235.
[147] I. G. Pallares, T. C. Brunold, *Inorg. Chem.* **2014**, *53*, 7676 – 7691.
[148] A. Nicolaou, S. H. Kenyon, J. M. Gibbons, T. Ast, W. A. Gibbons, *Eur. J. Clin. Invest.* **1996**, *26*, 167 – 170.
[149] A. Kambo, V. S. Sharma, D. E. Casteel, V. L. Woods, R. B. Pilz, G. R. Boss, *J. Biol. Chem.* **2005**, *280*, 10073 – 10082.
[150] A. Nicolaou, C. J. Waterfield, S. H. Kenyon, W. A. Gibbons, *Eur. J. Biochem.* **1997**, *244*, 876 – 882.
[151] M. Brouwer, W. Chamulitrat, G. Ferruzzi, D. L. Sauls, J. B. Weinberg, *Blood* **1996**, *88*, 1857 – 1864.
[152] K. ó Proinsias, M. Giedyk, D. Gryko, *Chem. Soc. Rev.* **2013**, *42*, 6605 – 6619.

Manuscript received: February 9, 2015
Final article published: May 25, 2015

Organic LETTERS

Letter

pubs.acs.org/OrgLett

Inorganic Cyanide as Protecting Group in the Stereospecific Reconstitution of Vitamin B_{12} from an Artificial Green Secocorrinoid

Lucas Prieto,[†] Markus Neuburger,[‡] Bernhard Spingler,[†] and Felix Zelder*[,†]

[†]Department of Chemistry, University of Zurich, Winterthurerstrasse 190, CH-8057 Zurich, Switzerland

[‡]Department of Chemistry, University of Basel, Spitalstr. 51, CH 4056 Basel, Switzerland

Supporting Information

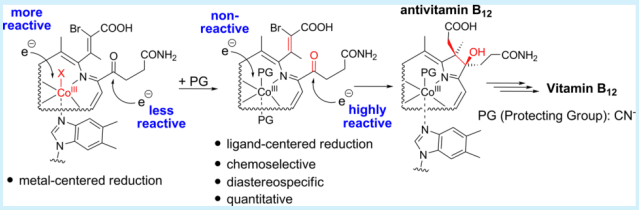

ABSTRACT: The synthesis of vitamin B_{12} in four steps from an artificial green secocorrinoid is presented. The stereospecific reconstitution of the B-ring of the cobalamin involves a quantitative and rapid ligand-centered radical ring closure reaction leading first to a new B_{12} derivative with antivitamin activity that is subsequently converted to the natural product. Chemoselectivity in the one-electron reduction of the macrocycle was achieved by introducing inorganic cyanide as an axially coordinating protecting group of the otherwise reduction-sensitive Co^{III}-ion. The integrity of structure and function of the reconstituted natural product was unequivocally proven by single crystal structural analysis and a microbiological assay using *Lactobacillus leichmannii*.

Vitamin B_{12} ("B_{12}", **1**, Figure 1) and B_{12} cofactors represent the most complex nonpolymeric natural products[1,2] combining uniquely a central cobalt ion with a highly decorated corrin macrocycle.[3] Their nature, structure, chemistry, and enzymology have inspired scientists for decades, and B_{12} research contributed significantly to the advancements in natural sciences in the past century.[2,4,5]

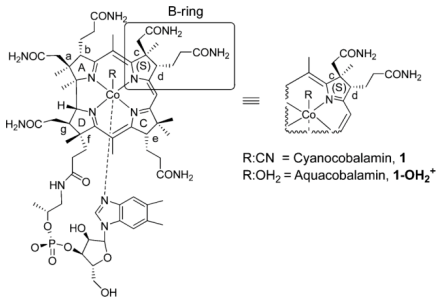

Figure 1. Structural formula of cob(III)alamins: cyanocobalamin (**1**, vitamin B_{12}, R = CN), aquacobalamin (**1-OH$_2^+$**, vitamin B_{12a}, R = H_2O) highlighting the B-ring area (in bracket) and its schematic representation.

The total synthesis of vitamin B_{12} by the groups of Eschenmoser and Woodward is considered a milestone in natural product synthesis for which the development of ingenious novel bond forming reactions and synthetic methodologies were required.[6−11] To name a few, Eschenmoser and his group developed during the first total synthesis of B_{12} the sulfide contraction reaction for joining two halves of the corrin macrocycle together in a metal-templated reaction.[12] Later, photochemical ring closure reactions were introduced for the challenging direct C−C coupling reaction between rings A and D of the corrin macrocycle.[13] Inspired by these important pioneering studies and recent progress in the field,[14] we herein report the unprecedented stereospecific reconstitution of vitamin B_{12} in four steps from an artificial 'green' secocorrinoid[15] with a C−C bond forming radical key reaction using inorganic cyanide as a metal-ion protecting group. In this reaction, the stabilization of the +III oxidation state of the cobalt center with two axially coordinating cyanide ligands was essential for achieving chemoselectivity in the ligand-centered reduction of the Co^{III}-containing octahedral complex.[16,17]

Received: August 31, 2016
Published: October 11, 2016

DOI: 10.1021/acs.orglett.6b02611
Org. Lett. 2016, 18, 5292−5295

The radical C−C bond forming reaction between C8 and C7 of a secocorrinoid was first described by Kräutler and co-workers for converting a 'blue' secocorrinoid[18] into a B_{12} derivative with an intact corrin macrocycle (Scheme 1, top).[14]

Scheme 1. (Top) Schematic Representation of the Conversion of Blue 7,8-*seco*-Corrinoid to Co_{β}-cyano-8_{β}-hydroxy-7-epicobalamin-c-acid; (Bottom) Conversion of Green 7,8-*seco*-Corrinoid to Vitamin B_{12}

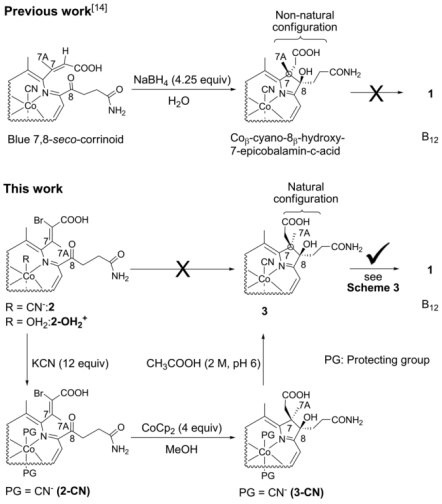

Unfortunately, the configuration of the c-acid side chain at C7 of the reaction product was inverted compared to B_{12}, making further transformations of the epimer to the natural product unfeasible. We speculated whether reconstitution of secocorrinoids to vitamin B_{12} would be principally possible with other derivatives and tested therefore the green 7,8-*seco*-corrinoid **2** (Scheme1, bottom).[15] We were optimistic since $^1H-^1H$ ROESY experiments showed correlations between H_{C7A} and both H_{C4N} and H_{C10N} of this derivative (Scheme 2), suggesting that C7A is directed to the lower (α) site of the secocorrinoid, thus representing the same orientation as observed in B_{12}.[15] For triggering the intended radical ring closure between C7 and C8 of **2**, consisting of a C−C coupling and a subsequent bromine elimination, we applied the one-electron donor cobaltocene ($CoCp_2$, E = −0.750 V vs Ag^+/AgCl in MeOH)[19] in the reaction. However, only metal-centered reduction of Co^{III} to Co^{II} was observed for **2**, leading finally to **2-OH$_2$**$^+$ after reoxidation of the pentacoordinated cob(II)alamin with air (Scheme S1).[20] The observed metal-centered reactivity is in line with the behavior of B_{12} yielding OH_2Cbl (**1-OH$_2$**$^+$) under the same reaction conditions (Scheme S2). In order to achieve chemoselective reduction of the macrocyclic ligand at its C8 position, we transformed **2** with an excess of cyanide to the dicyanospecies **2-CN** (Schemes 1, 2). Advantageously, such an axially coordinating cyanide ligand is easily introduced and can also be selectively removed from the metal center under slightly acidic conditions.[21] Importantly, the dicyano-Co^{III} derivative **2-CN** contains a less reduction-sensitive Co^{III} center compared to **2**. Indeed, the strongly δ-donating cyanide ligand shifts the reduction potential of cob(III)alamins to more negative values (approximately 400 mV) and thus stabilizes the Co^{III}-ion against reduction.[17,22] This behavior should render ligand- instead of metal-centered reductions of **2-CN** more likely, but has not yet been so far exploited for synthetic purposes. In fact, control experiments revealed that violet dicyanoB_{12} (**1-CN**) did not show any color change in the presence of cobaltocene (Scheme S3). After having proven the inertness of Co^{III} in dicyanocob(III)alamins under reductive conditions, the reactivity of **2-CN** was tested in the presence of cobaltocene (Schemes 1, 2, S4). To our delight, the dark green solution turned violet within seconds. The immediate appearance of the typical color of a dicyanocob(III)alamin species suggested reconstution of the corrin macrocycle and excluded any coincidental reduction of the Co^{III} center to a brown Co^{II} derivative.[23] The UV−vis spectrum of **3-CN** closely resembled that of dicyanocob(III)alamin **1-CN**. MS analysis of the reaction mixture suggested conversion of **2-CN** to $Co_{\alpha,\beta}$-dicyano-8_{β}-hydroxy-cobalamin-c-acid (**3-CN**; m/z = 698.4, $[M - H]^{2-}$). ^1H NMR analysis of the crude base-on compound **3** after removal of the cyanide protecting group (Scheme 1, Figure 2) showed excellent agreement with the spectrum of B_{12} (**1**), exhibiting only significant differences in chemical shifts at the B-ring of the macrocycle as well as at C4N of the dimethylbenzimidazole nucleobase (Figures S4−6, Table S1). In particular, **3** lacks a signal at 3.46 ppm of the C8−H proton of **1** and the corresponding ^{13}C signal was shifted downfield by 30 ppm (88.2 ppm in **3** vs 58.2 ppm in **1**). Moreover, the ^1H NMR analysis univocally shows that **3** was formed as a single diastereoisomer in the reaction. The orientation of the c- and d-side chains of **3** was first tentatively assigned based on the reactivity of **3** under acidic conditions. Quantitative conversion to a new species with a pseudo-molecular ion at m/z = 1354.6 ($[M + H]^+$) was observed, that is 18 units less than the molecular mass of **3**. We assumed the formation of a c-lactone between the c-monocarboxylic acid and the 8-hydroxo group of the B-ring for explaining the structural change (Scheme 3). Importantly, such an intramolecular reaction is only possible for steric reasons if both functionalities are pointing toward the same side of the molecule.

Scheme 2. Schematic Representation of the Proposed Radical Triggered Reconstitution of the B-Ring of 3-CN Using Inorganic Cyanide As a Metal-Ion Protecting Group (Intermediate A)[a]

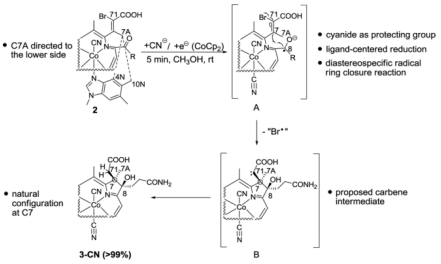

[a]Dotted lines in **2** indicate $^1H-^1H$ ROESY interactions.[15]

DOI: 10.1021/acs.orglett.6b02611
Org. Lett. 2016, 18, 5292−5295

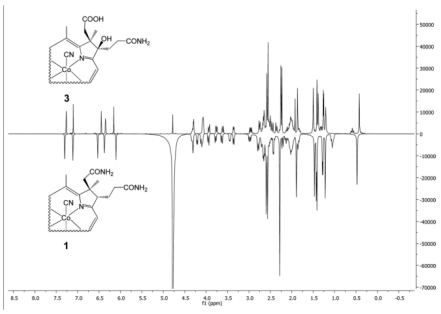

Figure 2. ^{1}H NMR spectra of Co$_{\beta}$-cyano-8$_{\beta}$-hydroxy-cobalamin-c-acid (**3**, top) and cyanocobalamin (B_{12}, **1**, bottom).

Scheme 3. Reconstitution of Vitamin B_{12} (1) from 3

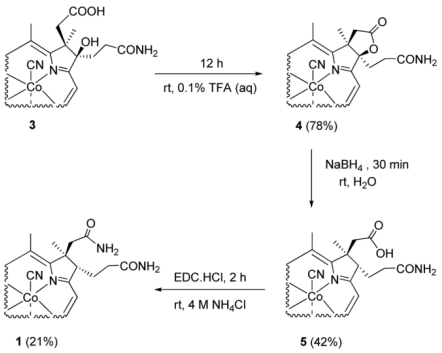

To evaluate the orientation of the c-lactone moiety in the reconstituted compound, we compared its analytical data with those of CNCbl-c-lactone **4** (Figures S7–S9). The latter contains a c-lactone moiety attached to the upper side of the B-ring of the corrin macrocycle and was synthesized independently from B_{12}.[24] In brief, all analytical data for the reconstituted compound and **4** were identical, indicating strikingly that the c-lactone functionalities are directed to the same side of the molecule. In turn, this means for the reconstituted compounds **3** and **4** that the c-acetic acid functionalities at C7 are orientated upward and the propionamide moieties at C8 are orientated to the lower side of the molecule. To our delight, this behavior reveals that the side chains located at the periphery of the B-ring of the reconstituted compounds exhibit the same orientation as in B_{12}. The diastereospecific nature of the ring closure reaction is probably best rationalized by a highly preorganized arrangement of C7, C7A, and C8 in the secocorrinoid **2** for the C–C bond forming reaction (Scheme 2).[15] In particular, the reaction is initiated by the formation of a highly reactive C8 centered radical (intermediate A; Scheme 2) that combines then rapidly and diastereospecifically with the short-distanced C7 under the mild reaction conditions. The existence of intermediate A (Scheme 2) was supported by radical scavenging experiments. Indeed, only starting material was observed by UPLC-MS when the reduction of **2-CN** with cobaltocene was attemped in the presence of the radical scavenger TEMPO (see Supporting Information). However, in the absence of this inhibitor, C–C coupling occurs and it is suggested that this reaction is accompanied by the elimination of a bromine radical from A forming the carbene intermediate B. The latter incorporates finally two hydrogens from MeOH leading to reconstituted **3**.

Having CNCbl-c-lactone (**4**) in hand allowed us to devise a straightforward route to vitamin B_{12} in two steps.[25] Reductive ring opening of **4** with $NaBH_4$ afforded CNCbl-c-acid (**5**) that was finally converted with *N*-(3-(dimethylamino)propyl)-*N*′-ethylcarbodiimide hydrochloride (EDC) and ammonium chloride to CNCbl (**1**) (Scheme 3).

The analytical data of the reconstituted and microbially produced vitamin B_{12} (**1**) are identical. Single crystals of the reconstituted compounds **5** and **1** (both synthesized starting from **2**) were grown by vapor diffusion of acetone into an aqueous solution of either **1** or **5**, and X-ray analysis confirmed the natural configuration of all side chains of the reconstituted products. As the crystals were weakly diffracting on a molybdenum source and X-ray fluorescence using copper radiation was observed, we finally measured both crystals with the help of a gallium source (see Supporting Information for more details). The top portion of Figure 3 shows the overlay of

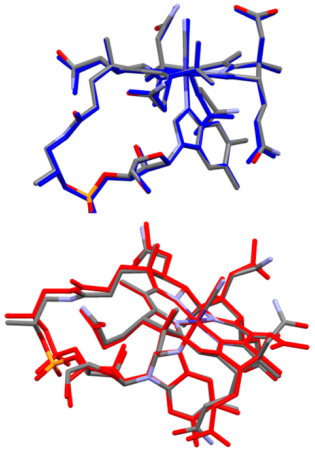

Figure 3. (Top) Overlay of the X-ray structures of **1** (blue) and **5** (normal element colors). (Bottom) Overlay of **1** (normal element colors) and a reference structure of vitamin B_{12} (red).[26]

1 (blue) and **5** (normal element colors), and the bottom portion of Figure 3 is the overlay of **1** (normal element colors) and a reference structure of vitamin B_{12} (red).[26]

With confidence established regarding the structural integrity of reconstituted **1**, its function was evaluated in a microbiological assay using *Lactobacillus leichmannii*.[27] This bacterium requires cofactor B_{12} for ribonucleotide reductase as the only B_{12} dependent enzyme.[27,28] Bacterial cell growth was strongly increased in the presence of nanomolar concentrations

DOI: 10.1021/acs.orglett.6b02611
Org. Lett. 2016, 18, 5292–5295

of reconstituted **1**, and its biological activity was identical to that of the microbially produced natural product (Figure S19).

In contrast, the novel reconstituted Cbl derivative **3** with an acetate functionality at C7 and an alcohol group at C8 behaves differently from B_{12} and shows antivitamin activity in the B_{12}-dependent growth of *L. Leichmannii*. In particular, 50% inhibition was observed with antivitamin **3** (1 μM) in the presence of B_{12} (0.1 nM) (Figure 4).

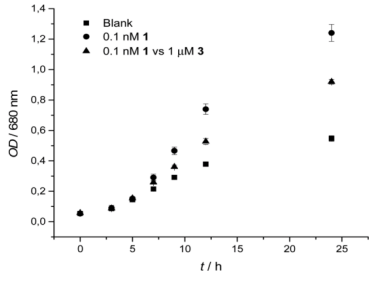

Figure 4. Growth of *Lactobacillus leichmannii* at 37 °C (n = 3) in the presence of B_{12} (0.1 nM) and in the presence and absence of antivitamin B_{12} **3** (1 μM).

These results are inspiring and suggest that this synthetic route can be probably still further exploited for synthesis of even more potent antivitamin B_{12} derivatives, a research field that currently attracts great interest in the community.[3,27,29−32]

In summary, the unprecedented reconstitution of B_{12} from an artificial green secocorrinoid is reported. The key step of the route is a stereospecific radical C−C bond formation for reconstructing the B-ring of the macrocycle. This rapid and quantitative ring closure reaction was initiated by a one-electron ligand-centered reduction of the secocorrinoid and leads first to a novel antivitamin B_{12} derivative that is subsequently converted to the final natural product. Chemoselectivity in this transformation was achieved by reversibly protecting the Co^{III} center of the precursor with inorganic cyanide against undesired metal-centered reduction.

■ ASSOCIATED CONTENT

Supporting Information

The Supporting Information is available free of charge on the ACS Publications website at DOI: 10.1021/acs.orglett.6b02611.

All experimental procedures and complete analytical and biological data of new products (PDF)

■ AUTHOR INFORMATION

Corresponding Author

*E-mail: felix.zelder@chem.uzh.ch.

Notes

The authors declare no competing financial interest.

■ ACKNOWLEDGMENTS

The work of the authors was supported by a fellowship of the Forschungskredit of the University of Zurich (UZH) to L.P. A generous gift of vitamin B_{12} was obtained from DSM Nutritional Products AG (Basel/Switzerland) and Prof. B. Jaun (retired ETH Zurich). We are thankful to PD Dr. L. Bigler (UZH) for the HR-ESI-MS measurements. Assistance from Prof. H. Brandl (Department of Evolutionary Biology and Environmental Studies, UZH) in microbiological assays and Dr. T. Fox (UZH) in NMR measurements and support by Prof. R. Alberto (UZH) and the Department of Chemistry of the University of Zurich are gratefully acknowledged.

■ REFERENCES

(1) Hogenkamp, H. P. C. In *Chemistry and Biochemistry of B12*; Banarjee, R., Ed.; John Wiley and Sons: New York, 1999; pp 3−8.
(2) Kräutler, B. In *Vitamin B 12 and B 12-Proteins*; Kräutler, B., Golding, B. T., Arigoni, D., Eds.; John Wiley and Sons: New York, 2008; pp 3−43.
(3) Zelder, F. *Chem. Commun.* **2015**, *51*, 14004−14017.
(4) Brown, K. L. *Chem. Rev.* **2005**, *105*, 2075−2149.
(5) ó Proinsias, K.; Giedyk, M.; Gryko, D. *Chem. Soc. Rev.* **2013**, *42*, 6605−6619.
(6) Woodward, R. B. *Pure Appl. Chem.* **1973**, *33*, 145−178.
(7) Eschenmoser, A.; Wintner, C. E. *Science* **1977**, *196*, 1410−1420.
(8) Nicolaou, K.; Sorensen, E. *Classics in Total Synthesis* **1996**, 1991.
(9) Riether, D.; Mulzer, J. *Eur. J. Org. Chem.* **2003**, *2003*, 30−45.
(10) Craig, G. W. *J. Porphyrins Phthalocyanines* **2016**, *20*, 1−20.
(11) Eschenmoser, A. *Helv. Chim. Acta* **2015**, *98*, 1483−1600.
(12) Eschenmoser, A. *Q. Rev., Chem. Soc.* **1970**, *24*, 366−415.
(13) Yamada, Y.; Wehrli, P.; Miljkovic, D.; Wild, H.-J.; Bühler, N.; Götschi, E.; Golding, B.; Löliger, P.; Gleason, J.; Pace, B.; Ellis, L.; Hunkeler, W.; Schneider, P.; Fuhrer, W.; Nordmann, R.; Srinivasachar, K.; Keese, R.; Müller, K.; Neier, R.; Eschenmoser, A. *Helv. Chim. Acta* **2015**, *98*, 1921−2054.
(14) Ruetz, M.; Fedosov, S. N.; Kräutler, B. *Angew. Chem., Int. Ed.* **2012**, *51*, 6780−6784.
(15) Oetterli, R. M.; Prieto, L.; Spingler, B.; Zelder, F. *Org. Lett.* **2013**, *15*, 4630−4633.
(16) Lexa, D.; Saveant, J. M. *Acc. Chem. Res.* **1983**, *16*, 235−243.
(17) Sonnay, M.; Fox, T.; Blacque, O.; Zelder, F. *Chem. Sci.* **2016**, *7*, 3836−3842.
(18) Fedosov, S. N.; Ruetz, M.; Gruber, K.; Fedosova, N. U.; Kräutler, B. *Biochemistry* **2011**, *50*, 8090−8101.
(19) Ruiz-Sánchez, P.; König, C.; Ferrari, S.; Alberto, R. *JBIC, J. Biol. Inorg. Chem.* **2011**, *16*, 33−44.
(20) Dereven'kov, I. A.; Salnikov, D. S.; Silaghi-Dumitrescu, R.; Makarov, S. V.; Koifman, O. I. *Coord. Chem. Rev.* **2016**, *309*, 68−83.
(21) Zhou, K.; Zelder, F. *Eur. J. Inorg. Chem.* **2011**, *2011*, 53−57.
(22) Lexa, D.; Sayeant, J. M.; Zickler, J. *J. Am. Chem. Soc.* **1980**, *102*, 2654−2663.
(23) Schindler, O. *Helv. Chim. Acta* **1951**, *34*, 1356−1361.
(24) Bonnett, R. *Chem. Rev.* **1963**, *63*, 573−605.
(25) Brown, K.; Zou, X.; Wu, G.-Z.; Zubkowski, J.; Valente, E. *Polyhedron* **1995**, *14*, 1621−1639.
(26) Mebs, S.; Henn, J.; Dittrich, B.; Paulmann, C.; Luger, P. *J. Phys. Chem. A* **2009**, *113*, 8366−8378.
(27) Zhou, K.; Oetterli, R. M.; Brandl, H.; Lyatuu, F. E.; Buckel, W.; Zelder, F. *ChemBioChem* **2012**, *13*, 2052−2055.
(28) Larsson, K.-M.; Logan, D. T.; Nordlund, P. *ACS Chem. Biol.* **2010**, *5*, 933−942.
(29) Zelder, F.; Sonnay, M.; Prieto, L. *ChemBioChem* **2015**, *16*, 1264−1278.
(30) Kräutler, B. *Chem. - Eur. J.* **2015**, *21*, 11280−11287.
(31) *Vitamin B12 und verwandte Corrinoide*; Friedrich, W., Ed.: Georg Thieme Verlag: Stuttgart, 1975.
(32) Chrominski, M.; Lewalska, A.; Gryko, D. *Chem. Commun.* **2013**, *49*, 11406−11408.

DOI: 10.1021/acs.orglett.6b02611
Org. Lett. 2016, 18, 5292−5295

ChemComm

COMMUNICATION

View Article Online
View Journal | View Issue

Cite this: *Chem. Commun.*, 2017, **53**, 6840

Received 10th May 2017,
Accepted 1st June 2017

DOI: 10.1039/c7cc03642f

rsc.li/chemcomm

Modified biovectors for the tuneable activation of anti-platelet carbon monoxide release†

Lucas Prieto,[a] Jeremie Rossier,[c] Katarzyna Derszniak,[b] Jakub Dybas,[b] René M. Oetterli,[a] Emmanuel Kottelat,[c] Stefan Chlopicki,*[bd] Felix Zelder *[a] and Fabio Zobi *[c]

This communication describes the anti-platelet effects of a new class of *cis*-rhenium(II)-dicarbonyl-vitamin B_{12} complexes (B_{12}-ReCORMs) with tuneable CO releasing properties.

Carbon-monoxide releasing molecules (CORMs) represent an innovative class of compounds which attract interest due to their potential therapeutic utility. Unlike most common drugs whose pharmacological action is dependent on their interaction with a macromolecular target and whose potency is dictated by the stability of the drug-target complex, CORMs exert their therapeutic action *via* the liberated CO molecules.[1–5] However, apart from the common scientific consensus that CORM-based therapy should not lead to significant carboxyhemoglobin (COHb) formation and to the inhibition of respiratory enzymes that are sensitive to CO, it is questionable whether CORMs should release CO slowly or rapidly and what kinetics of CO release is most advantageous for therapeutic applications. There are only few reports clearly showing the advantages of CORMs slowly releasing CO over those releasing CO instantly[6,7] and they relate to the anti-platelet effects of CORMs. Furthermore, it has proved chemically challenging to fine-tune the activation and the rate of CO release within a family of structurally similar CORM compounds. For all of these reasons, versatile classes of CORMs with tuneable release properties affording anti-platelet activity are highly desired for tackling these open questions in systematic structure–activity relationship studies. Such studies will facilitate the development of CORMs with optimal anti-platelet activity.[6–8]

Inspired by our groups' efforts to develop (a) versatile CORMs for biomedical applications[9–12] and (b) vitamin B_{12} derivatives with tuneable coordination and redox properties,[13–15] we envisaged to design and study *cis*-rhenium(II)-dicarbonyl-vitamin B_{12} complexes with adjustable CO releasing properties (Scheme 1) within the range for kinetics of CO release of CORM A1 (Scheme 2a).[16] This molecule exhibits strong anti-platelet and anti-thrombotic activities without a hypotensive effect.[6,7] In particular, for the present prodrug strategy, we started from prototype B_{12}-ReCORM-2[10] (compound **8** in the present study) in which the CORM *cis*-$[Re(CO)_2Br_4]^{2-}$ (**1**) is attached to the axial cyano group of vitamin B_{12}. We speculated whether modifications of the Co^{III}/Co^{I} redox properties of the B_{12} ligand would translate into control of the CO-releasing properties at the opposite Re^{II}-$(CO)_2$ fragment.

This approach seemed to be reasonable because small variations in the coordination sphere of rhenium complexes have profound consequences on the electrochemistry, water stability and CO releasing properties of the dicarbonyl core.[17] B_{12} appeared to be attractive as ligand for the rhenium-based CORM entity mainly because of two reasons: (a) its cellular uptake properties can be exploited to deliver therapeutic agents specifically at disease sites;[18–20] (b) the electronic properties at the cobalt center can be selectively modified by introducing structural modifications at the corrin-π-system.[21–24]

Having the general design of the B_{12}-ReCORMs derivatives in mind (Scheme 1), we synthesized and studied first a series of

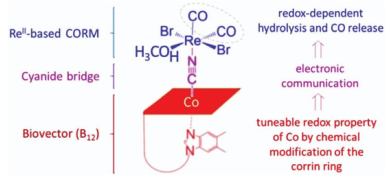

Scheme 1 General design concept for the tuneable activation of CORM-biovectors conjugates.

[a] *University of Zurich, Department of Chemistry, Winterthurerstrasse 190, CH-8057 Zurich, Switzerland. E-mail: felix.zelder@chem.uzh.ch; Web: www.felix-zelder.net; Fax: +41 44 635 6803*
[b] *Jagiellonian Centre for Experimental Therapeutics (JCET), Jagiellonian University, Krakow, Poland*
[c] *Department of Chemistry, University of Fribourg, Chemin du Musée 9, 1700 Fribourg, Switzerland. E-mail: fabio.zobi@unifr.ch*
[d] *Chair of Pharmacology, Jagiellonian University Medical College, Krakow, Poland. E-mail: stefan.chlopicki@jcet.eu*

† Electronic supplementary information (ESI) available. See DOI: 10.1039/c7cc03642f

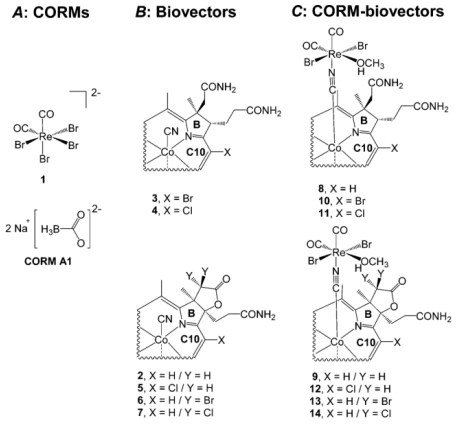

Scheme 2 (A) Re^{II}-Based CORM **1** and CORM A1; (B) modified B_{12}-biovectors **2–7**; (C) CORM-B_{12} complexes **8–14**.

Table 1 Electrochemical and spectroscopic data of vitamin B_{12}, its derivatives (**2–7**)

Compound	E_{red}[a] (mV)	γ band, nm ($\log\varepsilon$)	β/α (π–π^*) bands, nm ($\log\varepsilon$)
$\mathbf{B_{12}}$	−1010	361 (4.4)	519 (3.9)/550 (3.9)
2	−929	359 (4.3)	523 (3.7)/551 (3.7)
3	−798	365 (4.3)	550 (3.7)/576 (3.7)
4	−810	364 (4.2)	551 (3.6)/574 (3.7)
5	−784	363 (4.6)	551 (3.6)/577 (3.6)
6	−710	363 (4.2)	531 (3.7)/559 (3.7)
7	−715	363 (4.2)	531 (3.7)/554 (3.7)

[a] E_{red} data refer to $Co^{III} \rightarrow Co^{I}$ reduction (in 0.1 M Tris buffer at pH 8).

six cobalamins for coordinating them later to **1** (Scheme 2A). In particular, the cobalamin ligands contain structural modifications at C10 and/or at the B ring of the corrin macrocycle (Scheme 2B) and were synthesized according to literature procedures or modifications thereof (see ESI†).[25–28] We examined the electronic properties of compounds **2–7** (Table 1) by spectroscopic (UV-vis) and electrochemical means (cyclovoltammetry). As a general trend, we observed an increase in E_{red} (Co^{III}/Co^{I}) (cathodic reduction potential for the Co^{III} to Co^{I} transition) when electronic withdrawing groups (Br or Cl) and/or a *c*-lactone moiety at the B-ring were introduced in the cobalamin structure. For example, E_{red} (Co^{III}/Co^{I}) was increased by 212 mV compared to B_{12} when one Br is introduced at C10 (**3**) and this effect was further enhanced by 88 mV when an additional dibromolactone moiety was attached to the periphery of the B ring (**6**).

Having demonstrated that chemical modifications of the corrin macrocycle change the overall electronic properties of the cobalamin ligands **2–7**, these biovectors were coordinated to CORM **1** through their axial cyano group (Scheme 2).[29] The formation of a Co–CN–Re bond to afford CORM-biovectors **8–14** (Scheme 2C) was achieved in one single step and was confirmed

Table 2 Half-life ($t_{1/2}$) of stability of **8–14** in water and their CO release

Compound	$t_{1/2}$ hypochromic shift of 410 nm band[a]	$t_{1/2}$ of CO release[a,b]
8	60.1 ± 2.9	33.6 ± 2.3
9	40.2 ± 1.6	24.5 ± 1.8
10	29.5 ± 2.6	25.3 ± 1.8
11	29.6 ± 2.9	22.6 ± 0.7
12	27.3 ± 1.7	24.3 ± 3.0
13	19.1 ± 1.4	20.2 ± 2.9
14	24.9 ± 2.2	16.2 ± 1.2

[a] In H_2O (minutes). [b] Measured from the first order exponential increase of MbCO soret band.

by IR spectroscopy and inductively coupled plasma/optical emission spectrometry (ICP/OES) (see ESI†). With these compounds in hand, we investigated the stability and therefore the CO releasing properties of the Re^{II}-based CORM within the CORM-biovector scaffolds (**8–14**) by UV-vis kinetic experiments. The main difference in the spectra of the biovectors (Scheme 2B, **2–7**) and the CORM-biovectors (Scheme 2C, **8–14**) is the presence of a band at *ca.* 410 nm for the latter compounds. This band is hypsochromically shifted when the bromide ions of the Re^{II} complex undergo aquation. This ligand exchange is the first step towards the aerobic degradation of the Re^{II} core leading to CO release.[10] Therefore, changes in this band in DMSO (see ESI,† Fig. S21) and aqueous solutions (Table 2) over time were monitored.

CORM-biovectors **8–14** show a half-life ($t_{1/2}$) stability in DMSO varying from 1 to >3 hours (see ESI,† Table S1). When this experiment was performed in an aqueous solution, a first order decay behavior was observed. We were delighted to find that $t_{1/2}$ of aquation of the *cis*-$[Re(CO)_2Br_2]^0$ core steadily decreased as E_{red} (Co^{III}/Co^{I}) of the B_{12}-biovector increased (Fig. 1), varying from 60 (**8**) to *ca.* 20 min (**13**). The observed trend may be rationalized considering that an electron deficient Co^{III} ion obtains an enhanced σ-donation from the axial cyanide bridge. As a consequence, the 17-electron Re^{II} complex receives weaker electronic stabilization from the bridging ligand, rendering it more labile towards ligand substitution. Thus, within CORM-biovectors **8–14**, electronic properties of the modified biovectors appear to be the

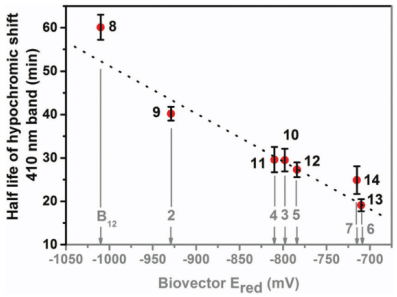

Fig. 1 Plot of $t_{1/2}$ (min) of hypochromic shift of 410 nm band of compounds **8–14** *vs.* $E_{red}(Co^{III}/Co^{I})$ of the same species.

main effect regarding the rate of aquation of the Re^{II}-based CORM. Nonetheless, a slight deviation from linearity (R^2 = 93%) suggests that additional factors might also play a minor role.

Knowing that aquation is the prerequisite for CO release, the relative CO releasing rates of CORM-biovectors **8–14** were determined using the well-known myoglobin (Mb) assay. The apparent rate and amount of CO release were calculated by UV-vis spectroscopy: the formation of carboxy-myoglobin (MbCO) is monitored by an increase in the Soret band of the protein (λ_{max} = 424 nm). Consequently, the $t_{1/2}$ of Soret band shift was taken as a direct measure of $t_{1/2}$ of CO release (Table 2). The $t_{1/2}$ of CO release decreases as a function of E_{red} (Co^{III}/Co^{I}), matching the results obtained for the $t_{1/2}$ of aquation of the Re^{II} CORM within CORM-biovectors **8–14**. Our results point to three defined areas of CO-release within the range of 15–35 min: a $t_{1/2}$ of CO release in a 30–35 min range for cobalamin derivatives with an $E_{red} \leq -1$ V; a 20–25 min range between −0.95 and −0.75 V; a 15–20 min range for Co $E_{red} > -0.75$ V (Fig. 2).

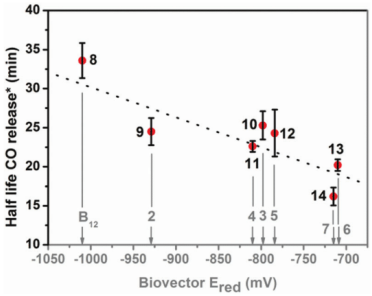

Fig. 2 Plot of $t_{1/2}$ (min) of hyperchromic shift in the MbCO Soret band (λ_{max} = 424 nm) of a Mb solution exposed to compounds **8–14** *vs.* reduction potential of Co^{III} to Co^{I} of the same species. * The $t_{1/2}$ of hyperchromic shift of the 424 nm soret band is taken as a direct measure of $t_{1/2}$ of CO release.

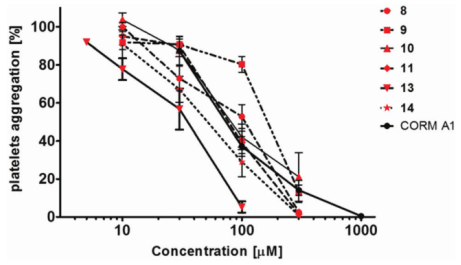

Fig. 3 Inhibition of platelet aggregation by B_{12}-ReCORMs and CORM A1. Results presented as a mean ± SEM (n = 4–22).

These results are important since the modulation of the $t_{1/2}$ of CO release allowed us to study the biological effects on the inhibition of platelet aggregation of various CO-releasing rates within a family of structurally similar CORM compounds in comparison with CORM A1 that has a $t_{1/2}$ of CO release of approximately 20 min.[16] As shown in Fig. 3 and Table 3, all B_{12}-ReCORMs (compounds **8–14**) inhibited platelet aggregation in the concentration range of 10 to 300 μM. In fact, the anti-aggregatory effects of **8** (IC_{50} = 79.64 ± 1.21), **10** (IC_{50} = 87.64 ± 1.13), **11** (IC_{50} = 80.87 ± 1.17) and **14** (IC_{50} = 48.20 ± 1.21) were quite similar to each other and in the same range as observed for CORM A1 (IC_{50} = 77.13 ± 1.17).[6,7] Only B_{12}-CORMs **9** (IC_{50} = 206.2 ± 1.22) and **13** (IC_{50} = 29.39 ± 1.21) deviated significantly from these values (see Table 3). Compounds **8–11**, **14** and CORM A1 inhibited platelet aggregation by more than 80% at 300 μM, while **13** achieved the same effect already at 100 μM. Accordingly, all the presented CORM-biovectors have anti-aggregatory effects relatively close to CORM A1. Only **13** displays a slightly more potent anti-platelet activity than CORM A1 and the other tested B_{12}-ReCORMs.[6–8]

In summary, we have presented a series of B_{12}-ReCORMs with tuneable CO releasing properties. These CORM-biovectors were synthesized by connecting a Re^{II}-dicarbonyl CORM and modified B_{12} derivatives through a cyanide bridge. In this proof-of-concept study it was demonstrated that alterations of the electronic properties at the Co^{III} center of the B_{12}-biovectors translate directly into variations of the CO release kinetics at the Re^{II} metal ion. Although differentiation of the CO releasing kinetics between the different complexes is still relatively small, we demonstrated already that B_{12}-ReCORMs displayed pronounced anti-platelet activity similar or even slightly higher than CORM A1, a compound that affords anti-platelet and anti-thrombotic activities *in vivo* without a hypotensive effect.[7] These findings are encouraging for our future efforts to develop tuneable B_{12}-ReCORMs with further optimized CO-releasing properties to achieve optimal anti-platelet effects for therapeutic applications.

This was supported by National Science Centre grant no. DEC-2013/08/M/MN7/01034 (SCH), the Swiss National Science Foundation Grant no. PP00P2_144700 (FZobi) and a fellowship of the Forschungskredit of the University of Zurich UZH to LP. A generous gift of vitamin B_{12} was obtained from DSM Nutritional Products AG (Basel/Switzerland) and Prof. B. Jaun (retired ETH Zurich).

Table 3 IC_{50} values for anti-aggregatory effects of B_{12}-ReCORMs and CORM A1

COMP.	8	9	10	11	13	14	CORMA1
IC_{50} ± SEM	79.64 ± 1.21	206.20 ± 122	87.64 ± 1.13	80.87 ± 1.17	29.39 ± 1.21	48.20 ± 1.21	77.13 ± 1.17

Notes and references

1 R. Motterlini and L. E. Otterbein, *Nat. Rev. Drug Discovery*, 2010, **9**, 728–743.
2 U. Schatzschneider, *Br. J. Pharmacol.*, 2015, **172**, 1638–1650.
3 S. Garcia-Gallego and G. J. L. Bernardes, *Angew. Chem., Int. Ed.*, 2014, **53**, 9712–9721.
4 S. H. Heinemann, T. Hoshi, M. Westerhausen and A. Schiller, *Chem. Commun.*, 2014, **50**, 3644–3660.
5 F. Zobi, *Future Med. Chem.*, 2013, **5**, 175–188.
6 S. Chlopicki, M. Lomnicka, A. Fedorowicz, E. Grochal, K. Kramkowski, A. Mogielnicki, W. Buczko and R. Motterlini, *Naunyn-Schmiedeberg's Arch. Pharmacol.*, 2012, **385**, 641–650.
7 K. Kramkowski, A. Leszczynska, A. Mogielnicki, S. Chlopicki, A. Fedorowicz, E. Grochal, B. Mann, T. Brzoska, T. Urano, R. Motterlini and W. Buczko, *Arterioscler., Thromb., Vasc. Biol.*, 2012, **32**, 2149–2157.
8 S. Chlopicki, R. Olszanecki, E. Marcinkiewicz, M. Lomnicka and R. Motterlini, *Cardiovasc. Res.*, 2006, **71**, 393–401.
9 H. B. Suliman, F. Zobi and C. A. Piantadosi, *Antioxid. Redox Signaling*, 2016, **24**, 345–360.
10 F. Zobi, O. Blacque, R. A. Jacobs, M. C. Schaub and A. Y. Bogdanova, *Dalton Trans.*, 2012, **41**, 370–378.
11 F. Zobi, L. Quaroni, G. Santoro, T. Zlateva, O. Blacque, B. Sarafimov, M. C. Schaub and A. Y. Bogdanova, *J. Med. Chem.*, 2013, **56**, 6719–6731.
12 E. Kottelat, A. Ruggi and F. Zobi, *Dalton Trans.*, 2016, **45**, 6920–6927.
13 M. Sonnay, T. Fox, O. Blacque and F. Zelder, *Chem. Sci.*, 2016, **7**, 3836–3842.
14 K. Zhou, R. M. Oetterli, H. Brandl, F. E. Lyatuu, W. Buckel and F. Zelder, *ChemBioChem*, 2012, **13**, 2052–2055.
15 K. Zhou and F. Zelder, *Angew. Chem., Int. Ed.*, 2010, **49**, 5178–5180.
16 R. Motterlini, P. Sawle, S. Bains, J. Hammad, R. Alberto, R. Foresti and C. J. Green, *FASEB J.*, 2005, **19**, 284–286.
17 F. Zobi, L. Kromer, B. Spingler and R. Alberto, *Inorg. Chem.*, 2009, **48**, 8965–8970.
18 A. K. Petrus, T. J. Fairchild and R. P. Doyle, *Angew. Chem., Int. Ed.*, 2009, **48**, 1022–1028.
19 F. Zelder, *Chem. Commun.*, 2015, **51**, 14004–14017.
20 J. Rossier, D. Hauser, E. Kottelat, B. Rothen-Rutishauser and F. Zobi, *Dalton Trans.*, 2017, **46**, 2159–2164.
21 K. L. Brown, S. F. Cheng, X. Zou, J. D. Zubkowski, E. J. Valente, L. Knapton and H. M. Marques, *Inorg. Chem.*, 1997, **36**, 3666–3675.
22 S. M. Chemaly, K. L. Brown, M. A. Fernandes, O. Q. Munro, C. Grimmer and H. M. Marques, *Inorg. Chem.*, 2011, **50**, 8700–8718.
23 S. M. Chemaly, M. Florczak, H. Dirr and H. M. Marques, *Inorg. Chem.*, 2011, **50**, 8719–8727.
24 K. ó Proinsias, M. Giedyk and D. Gryko, *Chem. Soc. Rev.*, 2013, **42**, 6605–6619.
25 F. Wagner, *Annu. Rev. Biochem.*, 1966, **35**, 405–434.
26 R. M. Oetterli, L. Prieto, B. Spingler and F. Zelder, *Org. Lett.*, 2013, **15**, 4630–4633.
27 L. Prieto, M. Neuburger, B. Spingler and F. Zelder, *Org. Lett.*, 2016, **18**, 5292–5295.
28 R. Bonnett, J. R. Cannon, V. M. Clark, A. W. Johnson, L. F. J. Parker, E. L. Smith and A. Todd, *J. Chem. Soc.*, 1957, 1158–1168.
29 S. Kunze, F. Zobi, P. Kurz, B. Spingler and R. Alberto, *Angew. Chem., Int. Ed.*, 2004, **43**, 5025–5029.

Appendix 3: Curriculum vitae

Personal data

Name	Lucas Prieto González-Posada
Nationality	Spanish
Date of Birth	10.11.1989

Education

06/2013 – 07/2017	**Ph.D. Studies in Chemistry**, Department of Chemistry, University of Zurich. PD. Dr. Felix Zelder/ Prof. Dr. Roger Alberto.
09/2012-05/2013	**Master Thesis**, Institute of Inorganic Chemistry, University of Zurich. PD. Dr. Felix Zelder.
10/2011 – 07/2012	**Master studies in Chemistry** (Erasmus Exchange Program), University of Vienna (Austria).
2007 – 2012	**"Licenciado en Química" (Diplom in Chemistry)**, University of Oviedo, Oviedo, Spain.

Publications

1) Synthesis of a B-Ring Opened 7,8-*seco*-Vitamin B_{12} Derivative with Grob Fragmentation. R. Oetterli, **L. Prieto**, B. Spingler, F. Zelder, *Org. Lett.*, **2013**, *15*, 4630.

2) Antivitamins for Medicinal Applications. F. Zelder, M. Sonnay, **L. Prieto**, *ChemBioChem*, **2015**, *16*, 1264.

3) Inorganic Cyanide as Protecting Group in the Stereospecific Reconstitution of Vitamin B_{12} from an Artificial Green Secocorrinoid. **L. Prieto**, B. Spingler, F. Zelder, *Org. Lett*, **2016**, *18*, 5292.

4) Modified Biovectors for the Tuneable Activation of Anti-platelet Carbon Monoxide Release**. L. Prieto**, J. Rossier, K. Derszniak, J. Dybas, R. Oetterli, E. Kottelat, S. Chlopicki, F. Zelder, F. Zobi, *Chem Commun*, **2017**, *53*, 6840.

5) A $CoCp_2$ Mediated Demetallation/C-C Bond Forming Reaction: Formation of a Ni^{II}-Containing Vitamin B_{12} Derivative with a Cofactor-F430-Type π-system from a Secocorrin. **L. Prieto**, R. Otterli, F. Zelder, in preparation.

Fellowships

- **Forschungskredit Fellowship 2015**, University of Zurich (08/2015-08/2016). Funding extension for the project: *Metbalamins: a Synthetic Route Towards a New Class of Promising Antivitamin B_{12} candidates.*

- **Forschungskredit Fellowship 2014**, University of Zurich (07/2014-04/2015). Funding for the project: *Metbalamins: a Synthetic Route Towards a New Class of Promising Antivitamin B_{12} candidates.*

Awards

- **CMSZH Travel Award** (2017) to attend the "6th Georgian Bay International Conference on Bioinorganic Chemistry", Parry Sound, Canada.

- **Best Oral Presentation** Award at "Early Researchers Forum" within AsBIC8 (8th Asian Biological Inorganic Chemistry Conference, 2016), Auckland, New Zealand.

- **Student Bursary** (2016) by the Society of Biological Inorganic Chemistry to attend the "8th Asian Biological Inorganic Chemistry Conference".

- **SCS/SCNAT Chemistry Travel Award** (2016) to attend the "8th Asian Biological Inorganic Chemistry Conference".

- **2nd Best Poster Presentation** Prize at ISBOMC 14 (7th International Symposium on Bioorganometallic Chemistry, 2014), Vienna, Austria.

Selected Scientific Contributions

- *Modified Vitamin B_{12} Derivatives for the Tuneable Activation of Anti-platelet CO release,* **Oral Presentation**, "6th Georgian Bay International Conference on Bioinorganic Chemistry" (CanBIC 6), 05/2017, Parry Sound, Canada.

- *A Reversible Route for the Stereospecific Reconstitution of Vitamin B_{12} Using Cyanide as Inorganic Protecting Group,* **Oral Presentation**, Early Researchers Symposium at the 8th Asian Biological Inorganic Chemistry, 12/2016, Auckland, New Zealand.

- *Metal and Ligand Centered Reactivity of Cobalamins*. **Poster Presentation**, 42nd International Conference on Coordination Chemistry (ICCC 2016), 07/2016 Brest, France.

- *Ring-modified Vitamin B_{12} Derivatives as Potential B_{12} Antivitamins*. **Poster Presentation**, 7th International Symposium on Bioorganometallic Chemistry (ISBOMC14), 07/2014, Vienna, Austria.

References

(1) Whipple, G. H.; Hooper, C.; Robscheit, F. *Am. J. Physiol.* **1920**, *53*, 167.

(2) Dawson, A.; Evans, H.; Whipple, G. *Am. J. Physiol.* **1920**, *51*, 232.

(3) Whipple, G.; Hooper, C.; Robscheit, F. *Blood* **1920**, *53*.

(4) Minot, G. R.; Murphy, W. P. *JAMA* **1926**, *87*, 470.

(5) Murphy, W. P.; Monroe, R. T.; Fitz, R. *JAMA* **1927**, *88*, 1211.

(6) Rickes, E. L.; Brink, N. G.; Koniuszy, F. R.; Wood, T. R.; Folkers, K. *Science* **1948**, *107*, 396.

(7) Brink, N. G.; Wolf, D. E.; Kaczka, E.; Rickes, E. L.; Koniuszy, F. R.; Wood, T. R.; Folkers, K. *J. Am. Chem. Soc.* **1949**, *71*, 1854.

(8) Kaczka, E.; Wolf, D. E.; Folkers, K. *J. Am. Chem. Soc.* **1949**, *71*, 1514.

(9) Smith, E. L. *Brit. Med. J.* **1949**, *2*, 1367.

(10) Smith, E. L. *J. Pharm. Pharmacol* **1949**, *1*, 500.

(11) Hodgkin, D. C.; Kamper, J.; Mackay, M.; Pickworth, J.; Trueblood, K. N.; White, J. G. *Nature* **1956**, *178*, 64.

(12) Woodward, R. B. *Pure App. Chem.* **1973**, *33*, 145.

(13) Eschenmoser, A. *Naturwissenschaften* **1974**, *61*, 513.

(14) Eschenmoser, A.; Wintner, C. E. *Science* **1977**, *196*, 1410.

(15) Garibaldi, J. A.; Kosuke, I.; Lewis, J. C.; James, M.; U.S. Patent No. 2576932 A 1951.

(16) Wood, T. R.; David, H.; U.S. Patent No. 2595499 A 1952.

(17) Friedrich, W.; Bernhauer, K. *Angew. Chem.* **1953**, *65*, 627.

(18) Barker, H.; Weissbach, H.; Smyth, R. *Proc. Natl. Acad. Sci. USA* **1958**, *44*, 1093.

(19) Buchanan, J.; Elford, H. L.; Loughlin, R.; McDougall, B.; Rosenthal, S. *Ann. N. Y. Acad. Sci* **1964**, *112*, 756.

(20) Guest, J.; Friedman, S.; Dilworth, M.; Woods, D. *Ann. N. Y. Acad. Sci* **1964**, *112*, 774.

(21) Barker, H.; Suzuki, F.; Iodice, A.; Rooze, V. *Ann. N. Y. Acad. Sci* **1964**, *112*, 644.

(22) Banerjee, R. *Chemistry and Biochemistry of B12*; Wiley, 1999.

(23) Pratt, J. M. *Inorganic chemistry of vitamin B12*; Academic Press Inc. London Ltd., 1972.

(24) Kraatz, H.-B.; Metzler-Nolte, N. *Concepts and models in bioinorganic chemistry*; Wiley-VCh New York, 2006.

(25) Kräutler, B.; Golding, B. T.; Arigoni, D. *Vitamin B12 and B12-Proteins*; Wiley, 2008.

(26) o Proinsias, K.; Giedyk, M.; Gryko, D. *Chem. Soc. Rev.* **2013**, *42*, 6605.

(27) Bridwell-Rabb, J.; Drennan, C. L. *Curr. Opin. Chem. Biol* **2017**, *37*, 63.

(28) Zelder, F.; Sonnay, M.; Prieto, L. *ChemBioChem* **2015**, *16*, 1264.

(29) Zelder, F. *Chem. Commun.* **2015**, *51*, 14004.

(30) Männel-Croise, C.; Zelder, F. *ACS Appl. Mat. Interf.* **2012**, *4*, 725.

(31) Karczewski, M.; Ociepa, M.; Pluta, K.; ó Proinsias, K.; Gryko, D. *Chem. Eur. J.* **2017**, *23*, 7024.

(32) Giedyk, M.; Goliszewska, K.; Gryko, D. *Chem. Soc. Rev.* **2015**, *44*, 3391.

(33) Kräutler, B. J., B. in *Concepts and Models in Bioinorganic Chemistry*; Kraatz, H. B.; Metzler-Nolte N. , Eds., p. 177-212; Wiley-VCH Weinheim, 2006. ; Wiley VCH, Weinheim: 2006.

(34) Brown, K. L.; Hakimi, J. M.; Nuss, D. M.; Montejano, Y. D.; Jacobsen, D. W. *Inorg. Chem.* **1984**, *23*, 1463.

(35) Gruber, K.; Puffer, B.; Kräutler, B. *Chem. Soc. Rev.* **2011**, *40*, 4346.

(36) Battersby, A. R.; Fookes, C. J. R.; Matcham, G. W. J.; McDonald, E. *Nature* **1980**, *285*, 17.

(37) Stich, T. A.; Brooks, A. J.; Buan, N. R.; Brunold, T. C. *J. Am. Chem. Soc.* **2003**, *125*, 5897.

(38) Lexa, D.; Sayeant, J. M.; Zickler, J. *J. Am. Chem. Soc.* **1980**, *102*, 2654.

(39) Zelder, F.; Alberto, R. In *The Porphyrin Handbook*; Kadish, K. M., Smith, K. M., Guilard, R., Eds.; Elsevier Science: San Diego, 2012; Vol. 25, p 83.

(40) Wuerges, J.; Garau, G.; Geremia, S.; Fedosov, S. N.; Petersen, T. E.; Randaccio, L. *Proc. Natl. Acad. Sci. USA* **2006**, *103*, 4386.

(41) Petrus, A. K.; Fairchild, T. J.; Doyle, R. P. *Angew. Chem. Int. Ed.* **2009**, *48*, 1022.

(42) Schneider, Z.; Stroinski, A. *Comprehensive B12: Chemistry, Biochemistry, Nutrition, Ecology, Medicine*; Walter de Gruyter, 1987.

(43) Banerjee, R.; Gherasim, C.; Padovani, D. *Curr Opin Chem Biol* **2009**, *13*, 484.

(44) Jarrett, J. T.; Hoover, D. M.; Ludwig, M. L.; Matthews, R. G. *Biochemistry* **1998**, *37*, 12649.

(45) Mancia, F.; Keep, N. H.; Nakagawa, A.; Leadlay, P. F.; McSweeney, S.; Rasmussen, B.; Diat, O.; Evans, P. R. *Structure* **1996**, *4*, 339.

(46) Drennan, C.; Huang, S.; Drummond, J.; Matthews, R.; Lidwig, M. *Science* **1994**, *266*, 1669.

(47) Stubbe, J. *Science* **1994**, *266*, 1663.

(48) Elschenbroich, C. *Organometallchemie*; Springer-Verlag, 2013.

(49) Friedrich, W. *Vitamin B12 und verwandte Corrinoide*; Thieme Stuttgart, 1975.

(50) McLean, G. R.; Pathare, P. M.; Wilbur, D. S.; Morgan, A. C.; Woodhouse, C. S.; Schrader, J. W.; Ziltener, H. J. *Cancer Res.* **1997**, *57*, 4015.

(51) Guzzo, M. B.; Nguyen, H. T.; Pham, T. H.; Wyszczelska-Rokiel, M.; Jakubowski, H.; Wolff, K. A.; Ogwang, S.; Timpona, J. L.; Gogula, S.; Jacobs, M. R. *PLoS Pathog* **2016**, *12*, e1005949.

(52) Andrès, E.; Loukili, N. H.; Noel, E.; Kaltenbach, G.; Abdelgheni, M. B.; Perrin, A. E.; Noblet-Dick, M.; Maloisel, F.; Schlienger, J.-L.; Blicklé, J.-F. *CMAJ* **2004**, *171*, 251.

(53) Hin, H.; Clarke, R.; Sherliker, P.; Atoyebi, W.; Emmens, K.; Birks, J.; Schneede, J.; Ueland, P. M.; Nexo, E.; Scott, J. *Age and Ageing* **2006**, *35*, 416.

(54) Toh, B.-H.; van Driel, I. R.; Gleeson, P. A. *New. Engl. J. Med.* **1997**, *337*, 1441.

(55) Stryer, L. *Biochemistry*; 3 ed.; W. H. Freeman and Company: New York, 1988.

(56) Pettenuzzo, A.; Pigot, R.; Ronconi, L. *Eur. J. Inorg. Chem.* **2017**, *2017*, 1625.

(57) Kräutler, B. *Chem. Eur. J.* **2015**, *21*, 11280.

(58) Prieto, L.; Rossier, J.; Derszniak, K.; Dybas, J.; Oetterli, R. M.; Kottelat, E.; Chlopicki, S.; Zelder, F.; Zobi, F. *Chem. Commun.* **2017**, *53*, 6840.

(59) Gupta, Y.; Kohli, D. V.; Jain, S. K. *Crit. Rev. Ther. Drug Carrier Syst.* **2008**, *25*, 347.

(60) Siega, P.; Wuerges, J.; Arena, F.; Gianolio, E.; Fedosov, S. N.; Dreos, R.; Geremia, S.; Aime, S.; Randaccio, L. *Chem. Eur. J.* **2009**, *15*, 7980.

(61) Zelenka, K.; Brandl, H.; Spingler, B.; Zelder, F. *Dalt. Trans.* **2011**, *40*, 9665.

(62) Kunze, S.; Zobi, F.; Kurz, P.; Spingler, B.; Alberto, R. *Angew. Chem. Int. Ed.* **2004**, *43*, 5025.

(63) Mundwiler, S.; Spingler, B.; Kurz, P.; Kunze, S.; Alberto, R. *Chem. Eur. J.* **2005**, *11*, 4089.

(64) Shell, T. A.; Shell, J. R.; Rodgers, Z. L.; Lawrence, D. S. *Angew. Chem. Int. Ed.* **2014**, *53*, 875.

(65) Zobi, F.; Blacque, O.; Jacobs, R. A.; Schaub, M. C.; Bogdanova, A. Y. *Dalt. Trans.* **2012**, *41*, 370.

(66) Vortherms, A. R.; Kahkoska, A. R.; Rabideau, A. E.; Zubieta, J.; Andersen, L. L.; Madsen, M.; Doyle, R. P. *Chem. Commun.* **2011**, *47*, 9792.

(67) Somogyi, J. C.; Trautner, K. In *Vitamine*; Ammon, R., Dirscherl, W., Eds.; Georg Thieme: Stuttgart, 1974; Vol. 3, p 10.

(68) Zhou, K.; Oetterli, R. M.; Brandl, H.; Lyatuu, F. E.; Buckel, W.; Zelder, F. *ChemBioChem* **2012**, *13*, 2052.

(69) Mutti, E.; Ruetz, M.; Birn, H.; Kräutler, B.; Nexo, E. *PLoS ONE* **2013**, *8*, e75312.

(70) Stabler, S. P.; Brass, E. P.; Marcell, P. D.; Allen, R. H. *J. Clin. Invest* **1991**, *87*, 1422.

(71) Wagner, F. *Annu. Rev. Biochem* **1966**, *35*, 405.

(72) Zelder, F.; Zhou, K.; Sonnay, M. *Dalt. Trans.* **2013**, *42*, 854.

(73) Smith, E. L.; Mervyn, L.; Muggleton, P.; Johnson, A.; Shaw, N. *Ann. N. Y. Acad. Sci* **1964**, *112*, 565.

(74) Koppenhagen, V. B.; Elsenhans, B.; Wagner, F.; Pfiffner, J. J. *J. Biol. Chem.* **1974**, *249*, 6532.

(75) Helgeland, K.; Jonsen, J.; Laland, S. *Biochem. J.* **1961**, *81*, 260.

(76) Helgeland, K.; Jonsen, J.; Laland, S.; Lygren, T.; Rømcke, O. *Nature* **1963**.

(77) Grüning, B.; Holze, G.; Jenny, T. A.; Nesvadba, P.; Gossauer, A.; Ernst, L.; Sheldrick, W. S. *Helv. Chim. Acta* **1985**, *68*, 1754.

(78) Grüning, B.; Holze, G.; Gossauer, A.; Ernst, L. *Helv. Chim. Acta* **1985**, *68*, 1771.

(79) Holxe, G.; Jenny, T. A.; Nesvadba, P.; Gossauer, A.; Ernst, L.; Keller, W.; Kratky, C. *Helv. Chim. Acta* **1991**, *74*, 1287.

(80) Toohey, J. I. In *Federation proceedings* 1965; Vol. 25, p 1628.

(81) Perlman, D.; Toohey, J. *Nature* **1966**.

(82) Koppenhagen, V.; Pfiffner, J. *J. Biol. Chem.* **1971**, *246*, 3075.

(83) Koppenhagen, V. B.; Wagner, F.; Pfiffner, J. J. *J. Biol. Chem.* **1973**, *248*, 7999.

(84) Widner, F. J.; Lawrence, A. D.; Deery, E.; Heldt, D.; Frank, S.; Gruber, K.; Wurst, K.; Warren, M. J.; Kräutler, B. *Angew. Chem.* **2016**, *128*, 11451.

(85) Eschenmoser, A. *Pure App. Chem.* **1969**, *20*, 1.

(86) Eschenmoser, A. *Q. Rev., Chem. Soc.* **1970**, *24*, 366.

(87) Yamada, Y.; Wehrli, P.; Miljkovic, D.; Wild, H.-J.; Bühler, N.; Götschi, E.; Golding, B.; Löliger, P.; Gleason, J.; Pace, B.; Ellis, L.; Hunkeler, W.; Schneider, P.; Fuhrer, W.; Nordmann, R.; Srinivasachar, K.; Keese, R.; Müller, K.; Neier, R.; Eschenmoser, A. *Helv. Chim. Acta* **2015**, *98*, 1921.

(88) Lewis, N. J.; Pfaltz, A.; Eschenmoser, A. *Angew. Chem. Int. Ed.* **1983**, *22*, 735.

(89) Werthemann, L., PhD Thesis, *Untersuchungen an Kobalt (II)-und Kobalt (III)-Komplexen des Cobyrinsäure-heptamethylesters*, ETH Zurich **1968**.

(90) Lewis, N. J.; Nussberger, R.; Kräutler, B.; Eschenmoser, A. *Angew. Chem.* **1983**, *95*, 744.

(91) Hinze, R. P.; Schiebel, H. M.; Laas, H.; Heise, K. P.; Gossauer, A.; Inhoffen, H. H.; Ernst, L.; Schulten, H. R. *Eur. J. Org. Chem.* **1979**, *1979*, 811.

(92) Kräutler, B. *Helv. Chim. Acta* **1982**, *65*, 1941.

(93) Kräutler, B.; Stepánek, R. *Angew. Chem. Int. Ed.* **1985**, *24*, 62.

(94) Zelder, F. H.; Buchwalder, C.; Oetterli, R. M.; Alberto, R. *Chem. Eur. J.* **2010**, *16*, 6155.

(95) Hinze, R. P.; Wullbrandt, D.; Inhoffen, H. H. *Eur. J. Org. Chem.* **1980**, *1980*, 821.

(96) Ernst, L.; Holze, G.; Inhoffen, H. H. *Eur. J. Org. Chem.* **1981**, *1981*, 198.

(97) Holze, G.; Inhoffen, H. H. *Angew. Chem.* **1985**, *97*, 887.

(98) Oetterli, R. M., PhD Thesis, *A (semi) synthetic Route Towards' Metbalamins'*, University of Zurich, **2013**.

(99) Oetterli, R. M.; Prieto, L.; Spingler, B.; Zelder, F. *Org. Lett.* **2013**, *15*, 4630.

(100) Ruetz, M.; Fedosov, S. N.; Kräutler, B. *Angew. Chem. Int. Ed.* **2012**, *51*, 6780.

(101) Kräutler, B. *Chem. Eur. J.* **2012**, *18*, 9032.

(102) Ruiz-Sánchez, P.; König, C.; Ferrari, S.; Alberto, R. *J. Biol. Inorg. Chem.* **2011**, *16*, 33.

(103) Sonnay, M.; Fox, T.; Blacque, O.; Zelder, F. *Chem. Sci.* **2016**.

(104) Brown, K.; Zou, X.; Wu, G.-Z.; Zubkowski, J.; Valente, E. *Polyhedron* **1995**, *14*, 1621.

(105) Prieto, L.; Neuburger, M.; Spingler, B.; Zelder, F. *Org. Lett.* **2016**, *18*, 5292.

(106) Fedosov, S. N.; Ruetz, M.; Gruber, K.; Fedosova, N. U.; Kräutler, B. *Biochemistry* **2011**, *50*, 8090.

(107) Gossauer, A.; Grüning, B.; Ernst, L.; Becker, W.; Sheldrick, W. S. *Angew. Chem. Int. Ed.* **1977**, *16*, 481.

(108) Bax, A.; Marzilli, L. G.; Summers, M. F. *J. Am. Chem. Soc.* **1987**, *109*, 566.

(109) Prieto, L. M. T., Synthesis of Oxidatively Cleaved 'Incomplete' Corrinoids, University of Zurich, **2013**.

(110) Dobler, M.; Dunitz, J. *Helv. Chim. Acta* **1971**, *54*, 90.

(111) Fürstner, A.; Bogdanović, B. *Angew. Chem. Int. Ed.* **1996**, *35*, 2442.

(112) McMurry, J. E. *Chem. Rev.* **1989**, *89*, 1513.

(113) Girard, P.; Namy, J.; Kagan, H. *J. Am. Chem. Soc.* **1980**, *102*, 2693.

(114) Kagan, H. B. *Tetrahedron* **2003**, *59*, 10351.

(115) Fuchs, J. R.; Mitchell, M. L.; Shabangi, M.; Flowers, R. A. *Tetrahedron Lett.* **1997**, *38*, 8157.

(116) Kishner, N. *J. Russ. Phys. Chem. Soc.* **1911**, *43*, 582.

(117) Wolff, L. *Chem. Liebigs Ann. Chem* **1912**, *384*, 25.

(118) Cram, D. J.; Sahyun, M. R. V. *J. Am. Chem. Soc.* **1962**, *84*, 1734.

(119) Caglioti, L. *Tetrahedron* **1966**, *22*, 487.

(120) Thompson, H.; Dietrich, L.; Elvehjem, C. *J. Biol. Chem.* **1950**, *184*, 175.

(121) Bonnett, R. *Chem. Rev.* **1963**, *63*, 573.

(122) Calafat, A. M.; Marzilli, L. G. *J. Am. Chem. Soc.* **1993**, *115*, 9182.

(123) Alberto, R.; Motterlini, R. *Dalt. Trans.* **2007**, 1651.

(124) García‐Gallego, S.; Bernardes, G. J. *Angew. Chem. Int. Ed.* **2014**, *53*, 9712.

(125) Motterlini, R.; Otterbein, L. E. *Nat. Rev. Drug Discov.* **2010**, *9*, 728.